Wave scattering and refraction from a random rough interface between two elastic solids
by Henry Hemin Yang

A thesis submitted in partial fulfillment of the requirements for the degree of Doctor of Philosophy in Mechanical Engineering
Montana State University

Abstract:
The theory of elastic wave scattering has important industrial applications in non-destructive testing techniques. A problem involving elastic wave scattering from a rough interface (for example, a welding joint of two metal parts) is theoretically studied in this dissertation. The rough interface between two elastic solids is assumed to have a onedimensional random profile with the Gaussian distribution in height and slope of the boundary. In this work, the scattered displacement fields are expressed in a surface integral which contains the scattered fields and also elastic Green's functions. For boundary conditions, the Kirchhoff approximation is applied and the plane reflection coefficients are calculated. The scattered and refracted fields on the boundary are assumed to have the form of the incident wave with plane reflection coefficients. This assumption requires that the radius of curvature of the interface be much larger than the wavelength of the incident wave. The surface integral is calculated numerically.

The results, in terms of scattering coefficients, show that in the specular direction, the scattered fields decrease by a roughness factor as the roughness of the boundary increases. In the case of very rough boundaries, for example, h=0.315 (mm) for the longitudinal wave, and h=0.210 (mm) for the transverse wave, the scattered fields are diffusely scattered, and the maximum value of the scattered field is no longer scattered in the specular direction.

In this dissertation, the restrictions applying the Kirchhoff approximation to this problem are also discussed by giving relations between the roughness of the boundary, the incident frequency, and the incident angle. For typical values of the surface roughness in modern industries, say, fatigue cracks or manufacturing defects, the elastic Kirchhoff approximation requires high frequency incident waves.

WAVE SCATTERING AND REFRACTION FROM A RANDOM ROUGH INTERFACE BETWEEN TWO ELASTIC SOLIDS

by

Henry Hemin Yang

A thesis submitted in partial
fulfillment of the requirements for the degree

of

Doctor of Philosophy

in

Mechanical Engineering

MONTANA STATE UNIVERSITY
Bozeman, Montana

May 1991

APPROVAL

of a thesis submitted by

Henry Hemin Yang

This thesis has been read by each member of the thesis committee and has been found to be satisfactory regarding content, English usage, format, citations, bibliographic style, and consistency, and is ready for submission to the College of Graduate Studies.

5/22/91
Date

R. Jay Conant
Chairperson, Graduate Committee

Approved for the Major Department

5/22/91
Date

Robert J Colwell
Head, Major Department

Approved for the College of Graduate Studies

5/30/91
Date

Henry L Parsons
Graduate Dean

STATEMENT OF PERMISSION TO USE

In presenting this thesis in partial fulfillment of the requirements for a doctoral degree at Montana State University, I agree that the Library shall make it available to borrowers under rules of the Library. I further agree that copying of this thesis is allowable only for scholarly purpose, consistent with "fair use" as prescribed in the U.S. Copyright Law. Requests for extensive copying or reproduction of this thesis should be referred to University Microfilms International, 300 North Zeeb Road, Ann Arbor, Michigan 48106, to whom I have granted "the exclusive right to reproduce and distribute copies of the dissertation in and from microfilm and the right to reproduce and distribute by abstract in any format."

Signature: H. Yang

Date: 5/14/91

ACKNOWLEDGEMENTS

This work was supported by the Department of Interior's Bureau of Mines under Contract No. J0134035 through Department of Energy Contract No. DEAC07-76ID01570. The author would like to thank Idaho National Engineering Laboratory and in particular Dr. K. L. Telschow for his assistance in this project.

I would like to thank Dr. Jay Conant for his guidance and the many useful discussions concerning the project.

I would also like to thank Dr. Michael Wells for his encouragement during my studies at Montana State University.

Finally, I would like to express a special thanks to my wife for her continuous support and encouragement.

TABLE OF CONTENTS

TABLE OF CONTENTS-Continued

LIST OF TABLES

LIST OF FIGURES

LIST OF FIGURES-Continued

LIST OF FIGURES-Continued

LIST OF FIGURES-Continued

LIST OF FIGURES-Continued

LIST OF FIGURES-Continued

LIST OF FIGURES-Continued

LIST OF FIGURES-Continued

LIST OF FIGURES-Continued

ABSTRACT

The theory of elastic wave scattering has important industrial applications in non-destructive testing techniques. A problem involving elastic wave scattering from a rough interface (for example, a welding joint of two metal parts) is theoretically studied in this dissertation. The rough interface between two elastic solids is assumed to have a one-dimensional random profile with the Gaussian distribution in height and slope of the boundary. In this work, the scattered displacement fields are expressed in a surface integral which contains the scattered fields and also elastic Green's functions. For boundary conditions, the Kirchhoff approximation is applied and the plane reflection coefficients are calculated. The scattered and refracted fields on the boundary are assumed to have the form of the incident wave with plane reflection coefficients. This assumption requires that the radius of curvature of the interface be much larger than the wavelength of the incident wave. The surface integral is calculated numerically.

The results, in terms of scattering coefficients, show that in the specular direction, the scattered fields decrease by a roughness factor as the roughness of the boundary increases. In the case of very rough boundaries, for example, h=0.315 (mm) for the longitudinal wave, and h=0.210 (mm) for the transverse wave, the scattered fields are diffusely scattered, and the maximum value of the scattered field is no longer scattered in the specular direction.

In this dissertation, the restrictions applying the Kirchhoff approximation to this problem are also discussed by giving relations between the roughness of the boundary, the incident frequency, and the incident angle. For typical values of the surface roughness in modern industries, say, fatigue cracks or manufacturing defects, the elastic Kirchhoff approximation requires high frequency incident waves.

CHAPTER 1

INTRODUCTION

Examples involving wave scattering from rough surfaces have been found in many areas of study including sound, light, electromagnetics, and others. For instance, in radio astronomy, the roughness properties of the moon's surface are estimated by studying the back-scattered electromagnetic waves from the moon to the earth (Beckmann and Spizzichino, 1963). In acoustics, scattering phenomenon of sound waves from rough surfaces, say, ocean surfaces have been studied (Eckart, 1953). In optics, scattering is associated with the diffraction of light from the rough boundary between two media (Karp, et al., 1966). In seismology, seismic reflection from different layers in the earth have been studied (Brekhouskikh, 1960). A large number of papers on the subject of wave scattering from rough surfaces have been published. The above examples show the variety of wave scattering problems in different areas of applications. However, no matter what the physical properties of the rough surface, the theories for considering this type of problem are almost the same. As Bass and Fuks (1979, p. 1) said, " The methodology of solving this sort of problem is the same regardless of the physical nature of the irregularities". In this dissertation, a brief review of literature on the subject of wave scattering from rough surfaces is given in Chapter 2.

Although the basic theories of wave scattering from rough surfaces are the same, the process of solving practical problems differs according to the involved medium, the nature of equations, and the boundary conditions. The problem dealt with in this dissertation is wave scattering from a rough interface between two elastic solids. This theory has an important application in ultrasonic non-destructive testing techniques. Since these techniques rely on the detection of the signal scattered by defects in a tested material, it is important to understand and predict how a defect will scatter the incident testing signal.

In practice, there is no real interface which is a perfectly smooth plane. A smooth plane is just the limiting case of rough surfaces. If an incident wave is propagating toward a smooth plane interface, a reflected wave and a transmitted wave will be generated according to three main properties: 1) the wavelength or frequency of the incident wave; 2) the angle of the incident wave; 3) the physical properties of the boundary and the media.

However, if the boundary is rough, not smooth, what results will be obtained? Scientists and engineers in various fields have been interested in and have been trying to answer this question for over a century since Rayleigh (1878) conducted the first investigation of the scattering of sound from a rough surface.

The most important difference in the behavior of a smooth boundary and a rough one in wave propagation problems is the fact that a smooth plane will reflect the incident wave in a single direction, and a rough surface will scatter the incident wave in various directions (see Figs. 1 and 2). In the case of the rough surface, certain directions may receive more energy than others. According to this fact, the same surface may be rough for some incident wavelengths and smooth for others; or for the same wavelength, the surface may be either smooth or rough for different incident angles.

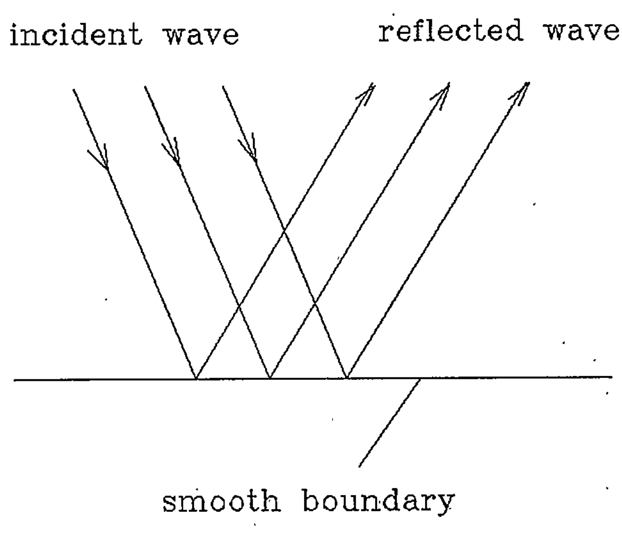

Figure 1. Reflection from a smooth boundary

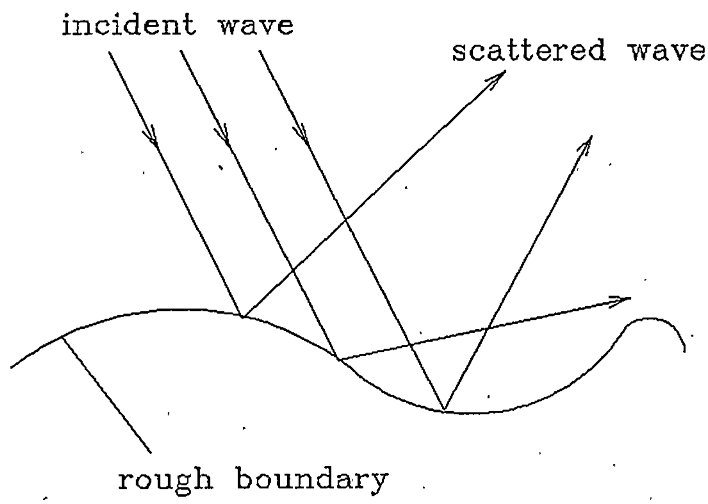

Figure 2. Scattering from a rough boundary

In order to understand the properties of wave scattering from rough surfaces, Rayleigh (1878) suggested a relation involving incident wavelength or wave number, incident angle, and the average amplitude of the height of the surface. In terms of wave number, the relation is given by:

$$R_p = 2kh_o \cos\theta_{inc} \tag{1-1}$$

where k is the wave number; h_o is the average height of the rough surface, and θ_{inc} is the incident angle. Equation (1-1) is commonly known as the Rayleigh's criterion, where R_p is called Rayleigh's parameter. As the Rayleigh's parameter increases, the rough property of the surface increases, and the energy scattered in the specular direction decreases. In this dissertation, we define the specular direction as the direction of the reflected wave in the case of a smooth boundary. It is evident that for certain values of the roughness of the surface and certain values of the incident angle, if the frequency of the incident wave is so low that the wavelength of the incident wave is very large compared with the surface amplitude, then the surface becomes effectively smooth.

Although the subject of wave scattering has been studied in many disciplines for over a century, the consideration of elastic wave scattering from rough random surfaces, especially a rough interface between two elastic solids, is seldom found in earlier reported papers because of its complexity. Therefore, the purpose of this dissertation is to offer a solution to this particular problem involving elastic wave scattering from a rough interface between two solids.

In this dissertation we consider that two elastic media with different material properties are separated by an irregular interface S (see Fig. 3). The height $z=h(x)$ of the interface S is measured from the mean plane $z=0$ in the right-handed x,y,z coordinate system. If it is assumed that a perfect bonding exists along the interface S, the continuity conditions for the displacement and stress components must be satisfied on S, or $z=h(x)$. It is assumed that an incident time-harmonic wave (either pressure or shear) propagates toward the interface S in medium A. When the incident wave reaches the boundary S, two reflected waves (longitudinal and transverse) will be generated in the same medium A, and two refracted waves (longitudinal and transverse) will be generated in the second medium B. Our job is to calculate the distributions of the two scattered fields in region A, and the distributions of the two refracted fields in region B. For a given incident wave, it is easy to calculate the reflected fields and refracted fields if the interface is a plane boundary. In our rough interface case, regular approaches are no longer convenient to use. Therefore the theory of wave scattering from rough surfaces has to be applied.

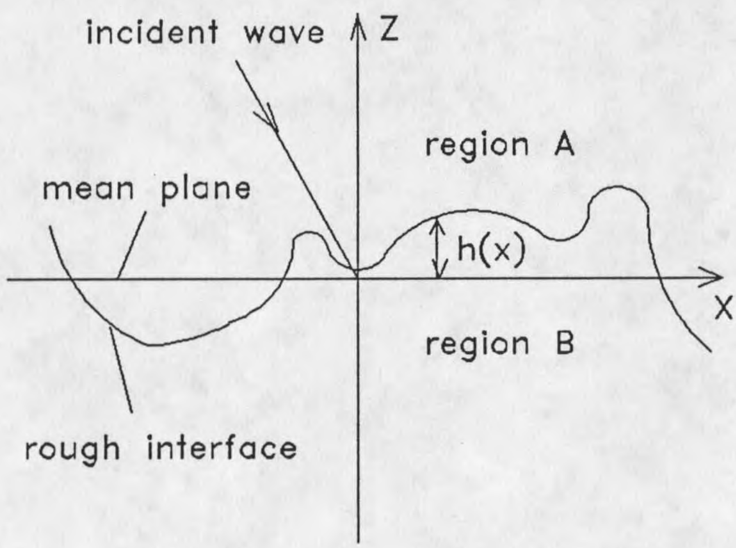

Figure 3. The rough interface between two elastic solids

In Chapter 2, a brief review of this subject is given. The history, different methods, and corresponding discussion of this subject are presented. Some examples of the applications of the wave scattering theory are also given in this chapter.

In Chapter 3, basic assumptions are given to formulate the problem. The scattered fields, including reflected and refracted fields, in terms of displacement components are expressed as surface integrals over the interface S by applying the dynamic elastic reciprocal identity. The surface integrals are the governing equations of this problem. The interface conditions are also given in this chapter. The surface integrals contain the scattered displacement and stress fields on the boundary as well as the elastic Green's functions. These quantities, at this step, are unknown.

In Chapter 4, the Kirchhoff approximation is introduced. The Kirchhoff approximation is based on the assumption that any small domain about a point on the boundary behaves as a locally flat surface. With this assumption, the scattered and the refracted fields on the boundary are expressed in terms of the incident wave and plane reflection coefficients. The plane reflection coefficients are calculated explicitly in this chapter. The restrictions of applying the Kirchhoff approximation are also discussed in this chapter.

In Chapter 5, the elastic Green's functions are calculated by means of Fourier's transform. In order to simplify the calculations, the far-field assumption is made. This assumption requires that the observation point is far away from any point on the rough boundary.

In Chapter 6, the procedures of solving the surface integrals are given. The general solutions of the scattered and the refracted displacement components are given. A dimensionless quantity called the *scattering coefficient* is introduced. In Chapter 6, the characteristics of the random interface are also discussed.

In Chapter 7, the average evaluations of the scattered and refracted fields in both region A and region B are discussed. The interface is considered to have a random rough profile of its surface height. Therefore an average evaluation is performed. To calculate the average values of the scattered and the refracted fields, it is assumed that the distribution densities of the height and the slope of the interface have a Gaussian profile. Some results of roughness factors and integration factors involved in the average evaluation are given and discussed.

The final numerical results and a detailed discussion of the results are given in Chapter 8. The numerical results, in terms of scattering coefficients, show the scattered and the refracted fields from different roughnesses of the rough interface. The incident wave chosen in this work is either compression or shear wave.

From the work in this dissertation, we can conclude that the integral-equation method with the Kirchhoff approximation is a convenient and powerful theoretical method for elastic wave scattering problems. A satisfactory numerical result is obtained from this method. The results show that the scattering coefficients of both scattered and refracted fields decrease as the roughness of the interface increases. The size of the integration domain also affects the results. The scattered and the refracted fields depend also on the incident angle and the frequency of the incident wave.

CHAPTER 2

REVIEW OF THE LITERATURE

Problems involving wave scattering from rough surfaces are of great interest, and have received significant consideration in various fields of physics and engineering. This subject has been studied by scientists and engineers for over a hundred years. Especially in the past few decades, since computer technology has been used as an important tool in science and engineering, the problems of wave scattering from rough boundaries have received more and more detailed attention. Some theoretical methods to solve the problems have been developed, and numerical results have been obtained successfully.

The first mathematical investigation of wave scattering from rough surfaces was conducted by Rayleigh (1878), who discussed the scattering of a normally incident sound wave by a sinusoidal surface. In Rayleigh's work, the scattered field was considered to be a sum of plane waves. Since then, the theory of wave scattering from rough surfaces has been applied in different fields and extended in several directions, including modeling profiles of the rough surface, and developing theoretical approaches.

Modeling Profiles of Rough Surfaces

Modeling the shape of a rough surface has been an important subject in the study of wave scattering problems. In general, studies in this field can be divided into two groups according to whether the surface is a deterministic or a random one.

The deterministic surfaces, such as sinusoidal (Rayleigh, 1878, Vol. 2, p. 89), rectangular (Elliott, 1954), saw-toothed (Proud, Tamarkin and Meecham, 1957), and regular distribution of bosses on a plane (Twersky, 1951, 1953), have been studied extensively. In this case, the surfaces are mostly assumed to have periodic or explicitly given shapes. Historically, this group of rough surfaces was the first to be used, evidently because of the greater simplicity of the non-statistical process. Theoretical approaches for this type of problem include the use of Green's functions, the approximation of the scattered field by an infinite number of plane waves (series approximation), and variational methods.

Surfaces most commonly found in nature, such as the earth, sea, and moon surface, are random rough surfaces. Generally, these surfaces can only be described by their statistical properties since the exact shape of the surfaces are unknown. The theory of stochastic process has been applied to random rough surfaces by Eckart (1953), Ament (1953), Davies (1955), and others. As a result, one of the most common approaches for random rough surfaces is to use the Helmholz formula with some appropriate approximations. For example, the Kirchhoff boundary condition has been used extensively in this approach. Therefore, this approach is called the Kirchhoff theorem, or Kirchhoff method. A good summary and a more detailed explanation of several studies on random rough surfaces can be found in the work by Beckmann and Spizzichino (1963).

Since scholars first turned their attention to the problem of wave scattering from rough surfaces, several theoretical approaches of solving this problem have been developed. These theoretical approaches, in general, are based on Rayleigh's method, the perturbation method, the Kirchhoff method, and their extensions.

Rayleigh's Method

Rayleigh (1878) studied the problem of normal incident sound wave scattering by a rough surface with a sinusoidal profile. Since then, his method has been extended to plane waves of arbitrary incident angles and to scattering by random rough surfaces. Rayleigh assumed that the rough surface had a sinusoidal profile as:

$$h(x) = h_0 \cos(Kx) \tag{2-1}$$

where

$$K=\frac{2\pi}{\Lambda} \tag{2-2}$$

is called the phase constant of the surface; Λ is the wavelength of the surface; and h_o is the amplitude of the surface roughness. Marsh (1961) extended Rayleigh's approach to a random rough surface. However, the central idea of the method is still based on the following assumptions:

1). The scattered field is assumed to be a sum of plane waves. Let p(x,z) denote the total wave field, then

$$p(x,z)=\exp[ik(x\sin\theta_{inc}-z\cos\theta_{inc})]$$

$$+\sum_{m=0}^{\infty}A_m\exp[ik(x\sin\theta_m+z\cos\theta_m)] \tag{2-3}$$

where θ_{inc} is the incident wave angle relative to the mean plane normal of the rough surface, and k is the wave number of the incident wave.

2). This equation holds everywhere on the boundary and in the medium.

3). The scattering field is propagating in the direction θ_m, where

$$\sin\theta_m=\sin\theta_{inc}-\frac{mK}{k}\,(m=0,\pm1,\pm2,\ldots) \tag{2-4}$$

Rayleigh's method was criticized and improved by LaCasace and Tamarkin (1956), Meecham (1956) and others, since Rayleigh only considered the case where the scattering surface has a deterministic shape, and the incident wave propagates normally (in only one direction) on the surface. LaCasace and Tamarkin (1956) extended Rayleigh's method to a case of an arbitrary angle of the incident wave. Meecham (1956) used a variational approach to improve Rayleigh's method for the periodic surface, and applied the method to surfaces with arbitrary shapes. Rayleigh's method was also criticized by Lippmann (1953) and Heeps (1957). Lippmann pointed out that the validity of Rayleigh's second assumption was doubtful for the region between the rough surface and its mean plane. The rough surface is given by $z=h(x)$, where $|h(x)|<h_o$. As Lippmann explained in his paper, Rayleigh expressed the scattered field in terms of plane waves which propagate, or are exponentially damped, in only one direction and away from the grating. This choice for the scattered field is justified for $z>h_o$. However for $z<h_o$, this set of waves does not express the field completely, because at any point in this region the field is composed of waves propagating (or exponentially damped) in both directions. Rayleigh's second assumption was criticized by Heeps (1957) for other reasons. Heeps suspected that if all the reflected energies had the form of undamped plane waves then the surface is necessarily sound absorbing and of pressure significantly different from zero. Thus, in the

neighborhood of a corrugated surface of zero pressure it is necessary to take into account other forms of radiation and such forms play a significant part in satisfying the boundary condition. A more detailed and general criticism of Rayleigh's method can be found in the paper by Fortuin (1970).

Perturbation Method

The perturbation method for wave scattering from rough surfaces has been used in several applications. In this method, restrictions on the height h and the gradient $\underline{\nabla}h$ of the surface exist, i.e.

$$k|h| \ll 1 \tag{2-5}$$

where k is the wave number of the incident wave, and

$$|\underline{\nabla} h| \ll 1 \tag{2-6}$$

It is assumed that if (2-5) and (2-6) are satisfied, and the surface profile slowly varies with no discontinuities, then the field scattered from the rough surface can be expressed by an infinite series, and the total field will be

$$p(\underline{r}) = p^{inc}(\underline{r}) + \sum_{n=0}^{\infty} p_n^{sc}(\underline{r}) \tag{2-7}$$

where $p^{inc}(r)$ is the incident wave field, and $p_n^{sc}(r)$ is the n^{th} order approximation to the scattered field. It is also assumed that if the boundary condition on the rough surfaces has the form

$$f(x,y,z)\,|_{z=h(x,y)}=0 \tag{2-8}$$

then the boundary condition can be expressed in a Taylor series about the mean plane z=0:

$$f(x,y,z)\,|_{z=h(x,y)}=f(x,y,z)\,|_{z=0}+h\frac{\partial f}{\partial z}\,|_{z=0}+\frac{h^2}{2}\,\frac{\partial^2 f}{\partial z^2}\,|_{z=0}+\ldots \tag{2-9}$$

where f(x,y,z) is the pressure for acoustics problems and the stress components for elasticity problems.

In one of the earlier papers (Gilbert and Knopoff, 1960), the perturbation method was used for the surface with arbitrary, but known shape. In this paper the magnitude and slope of the rough surface are small. Tuan and Li (1974) developed Gilbert and Knopoff's work. They tried to remove or reduce the restriction on the slope of the rough surface by introducing a small parameter ϵ. In this way the quantity $\epsilon dh/dx$ can be small without the restriction on dh/dx, the slope of the rough surface. However, the height of the surface is still required to be small. The profile of the surface used in their paper is known.

When the perturbation method is applied to random surfaces, the explicit form for the rough surface is unknown, but certain statistical properties of the rough surface are assumed to be known. Since the surface is random, the scattered field is also random. The average field may be calculated. The reported work on this subject can be found in several papers. For example, Bass and Fuks (1979, p. 84) applied the perturbation method to the problem of wave scattering from a random rough surface. However, due to the restrictions on height and gradient, the range of rough surfaces is limited in the perturbation method.

The Kirchhoff Method

In problems of wave scattering from rough surfaces, the Kirchhoff method provides an approximation for the scattered field on the rough boundary. From the Kirchhoff approximation, the scattered field on the boundary can be expressed in terms of the incident field and the plane wave reflection coefficients. The basic idea for this approximation is as follows: scattering from any point on the rough surface is assumed to behave as if the surface were locally flat. The wave incident at a point on the surface is reflected in the specular direction with a reflection coefficient equal to that of a plane boundary passing through that point and parallel to the local tangent to the surface (see Fig. 4).

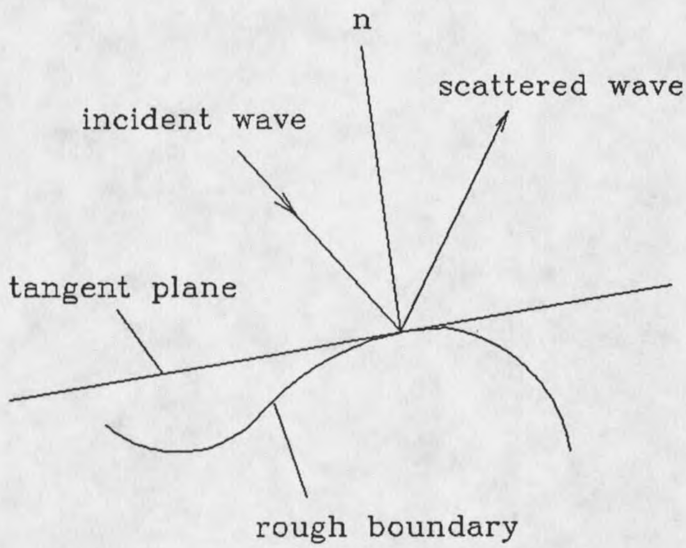

Figure 4. The Kirchhoff approximation

Since this approximation is based on the assumption of local flatness for the surface, it is valid only when the radius of curvature of the surface is much larger than the incident wave length. Therefore the type of rough surface and incident wave must be considered carefully when using the Kirchhoff approximation. Several alternative relations between the rough surface and the incident wave were introduced in earlier papers. In their work, Bechmann and Spizzichino (1963, p. 29) used an inequality which was originally developed by Brekhovskikh (1952). This inequality is based on elementary geometrical considerations and given by

$$4\pi a\cos\theta \gg \lambda \tag{2-10}$$

where a is the radius of the curvature of the surface, θ lies between the local normal and the incident direction and is called "local incident angle", and λ is the wavelength of the incident wave. The inequality (2-10) essentially states that at any distances along the surface from the point of tangency, the tangent plane shall not be appreciably distant from the rough surface. It is clear that the gradient of the surface must have no rapid changes. However, no restrictions on the height or gradient are required in the Kirchhoff method.

Early reported work on wave scattering using the Kirchhoff method can be found in the paper by Eckart (1953). He studied the reflection of sound waves by the sea surface. He expressed the scattered field in terms of a surface integral. In his paper, the sea surface S was assumed as a free boundary (pressure release). Therefore one boundary condition was given as

$$p^{inc}+p^{sc}=0 \qquad \text{on } S \tag{2-11}$$

where p^{inc} and p^{sc} are the incident and scattered pressure fields, respectively. Eckart also assumed that the surface was not too irregular, so that the second boundary condition was given by

$$\frac{\partial p^{inc}}{\partial n} = \frac{\partial p^{sc}}{\partial n} \qquad \text{on } S \qquad (2\text{-}12)$$

where n is the normal to the surface.

Eckart's application of the Kirchhoff method to the problem of wave scattering from the sea surface has been extended to various fields by many others. One of the well developed studies was accomplished by Beckmann and Spizzichino (1963). They generalized and applied the Kirchhoff method to different types of rough surfaces including random ones.

Elastic Wave Scattering

Elastic wave scattering involves the theories of elasticity and wave propagation. The theory of the elastic wave propagation is based upon the linear equations of elastic motion. Many existing approaches to solving the problem of the scattering of elastic waves by an obstacle in an elastic medium are based on the technique of separation of variables. For example, White (1958) considered the displacement wave scattered from an infinitely long cylinder of circular cross-section by expanding the unknown particle displacement in a series of Bessel functions. In White's studies, the obstacle can be either a void, a rigid inclusion, or a cylinder with elastic properties differing from those of its environment. In other papers, for example, the papers by Ying and Truell (1956) and Einspruch and Truell (1960), problems involving elastic wave scattering from a spherical obstacle were studied. In their papers, the technique of separation of variables played an important role in solving the elastodynamic wave equation. Although this method yields results, the applicability of the technique is severely limited, as it can be used only in cases where variables are separable.

Since the elastic wave field contains two parts, a longitudinal and a transverse part, propagating at different speeds, it is rather complicated to solve problems of elastic wave scattering. Hence, the conventional wave equations are not conveniently applied to elastic wave scattering. As Pao and Varatharajulu (1976) said, "Because elastic waves are composed of a longitudinal part and a transverse part, and these two types of waves are coupled at the boundary of a solid, the conventional method of separation of variables and series expansion of wave functions is not effective for problems of scattering of elastic waves".

To overcome the limitation of the method of the separation of variables, Banaugh (1962, 1963) obtained the solution of the wave scattering problem in terms of a set of surface potentials. In Banaugh's study, the particle displacement is written as a sum of two contributions: a contribution due to compressional waves in the form of the gradient of a scalar potential and a contribution due to shear waves in the form of the curl of a vector potential. Indeed

Banaugh eliminated the limitations of the technique of separation of variables. However, in his study, the formulation of the boundary conditions is imposed on the surface potentials which themselves do not correspond directly with elastodynamic physical quantities. From other reported work, for example, by Tan (1975), Pao and Varatharajulu (1976), and others, an integral-equation method, one of the most common methods, has been used in problems of elastic wave scattering. In this method, the particle displacement of the scattered field can be expressed in terms of a surface integral. The integrand in this integral contains the scattered displacement and stress fields on the surface and also elastic Green's functions. However, the calculation of the surface integral is very difficult because these scattered fields are not known. The Kirchhoff approximation has been applied to elastic wave scattering from rough surfaces. By this approximation, the scattered field, say, the displacement field, on the rough surface is expressed as the product of the incident wave and reflection coefficients. The explicit solution of the surface integral has not been found to this author's knowledge. Therefore, a numerical solution must be used in this problem. As an example, Ogilvy (1985, 1986a, and 1986b) successfully studied the problem of the elastic wave scattering and calculated the surface integral by a numerical procedure. Ogilvy obtained the scattered field from rough, crack-like defects. The surface of the defect in Ogilvy's work was considered as a random one.

In most previous work on elastic wave scattering from rough surfaces, the choice of boundary conditions has been considered as a crucial step. Some simpler boundary conditions including free boundary (or pressure release boundary) and rigid boundary have been used in many applications. To this author's knowledge, the study of a random interface between two elastic solids has not been found in earlier reported papers.

CHAPTER 3

FORMULATION OF THE PROBLEM

In this chapter, several basic assumptions regarding elastic material properties, wave propagation and scattering, as well as characteristics of the rough interface are made in order to formulate and solve this problem properly. The governing equations in terms of surface integrals over the interface S, together with interface conditions, are established according to the basic assumptions, the corresponding general equations, and the elastic reciprocal identity.

The problem to be solved in this paper involves a wave propagating in two elastic media, and wave scattering from the rough interface between the two media. Let us consider the two media, A and B, to be elastic solids with different material properties. The interface S between the two elastic solids is rough, and has a random profile in the height of the boundary measured from its mean plane (see Fig. 5). Consider an incident wave propagating in the region A toward the boundary S. When the incident wave reaches the interface S, two scattered waves (longitudinal and transverse) and two refracted waves (longitudinal and transverse) will be generated at the interface S. The two scattered waves will propagate away from the interface in the region A (see Fig. 5) while the two refracted waves will propagate away from the interface in the region B (see Fig. 5).

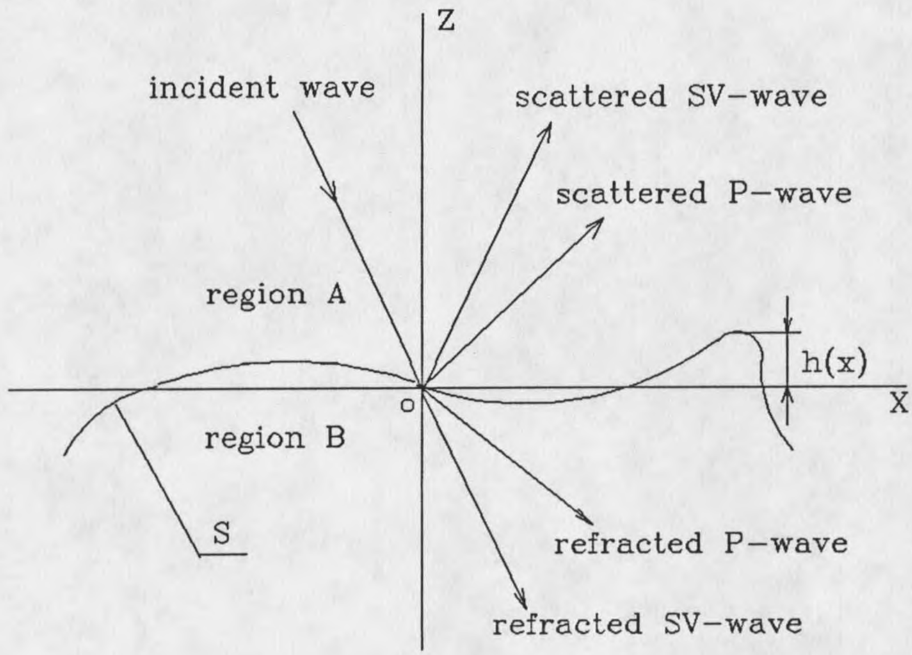

Figure 5. Wave scattering from a rough interface between two elastic solids

For any given incident wave, say, either a longitudinal or a shear wave, the scattered waves in the region A and refracted waves in the region B are the unknown quantities. In this work, we want to obtain the amplitude distributions of the scattered waves in the region A and the refracted waves in the region B. To locate any point in both regions A and B, we employ orthogonal Cartesian coordinates. In this paper we consider a two-dimensional problem, that is, all involved quantities in this problem are assumed to vary in only the x-z plane.

If the interface between the two elastic solids is a smooth plane, all unknowns can be readily determined (see, for example, Achenbach, 1975, p. 168). Since the interface dealt with in this paper is not a smooth plane, but a random rough surface, the usual procedure for solving this problem is no longer applicable. Therefore we need to find an alternative method to formulate and solve this particular problem. In chapter 2, we reviewed several methods to solve the wave scattering problem from rough surfaces from early reported work. Here we will use an integral method along with the Kirchhoff approximation to formulate and solve the problem.

Basic Assumptions and Corresponding Equations

The basic assumptions made in formulating this problem are as follows:

1) The two regions, A and B, in which waves propagate, are elastic solids (for example, copper, steel, or aluminum) with different material properties. Both materials are linear, isotropic, and homogeneous. For the region A, we use symbols E^A, λ^A and μ^A (with superscript A) to denote the Young's mudulus and Lame's elastic constants. For the region B, we use symbols with superscripts B, say, E^B, λ^B and μ^B to denote these constants.

2) The interface between the two regions has a one-dimensional random rough profile in the height z=h(x) measured from its mean line z=0.

3) The two elastic solids are adjoined together, i.e. a perfect bonding is assumed to exist along the interface. Therefore the displacement and stress components are continuous across the interface.

4) Waves involved in this problem are assumed to be plane waves with harmonic time dependence. The incident wave is assumed to be either a longitudinal or shear wave propagating in the region A.

5) The radius of the curvature of the rough interface is taken to be much larger than the wavelength of the incident wave in order to apply the Kirchhoff approximation to this problem. From this assumption, together with the Kirchhoff approximation, the scattered fields on the interface can be expressed as products of the incident wave and the plane reflection coefficients.

6) Far-field assumption is made, that is, the observation point is far away from any point on the rough interface.

7) Shadowing effects and multiple scattering are neglected.

Now we want to formulate and solve this problem from the above assumptions. First let us start with Cauchy's equation (Fung, 1965, pp. 187, 315):

$$\frac{\partial\hat{\tau}_{ij}}{\partial x_i}+\hat{f}_j=\rho\frac{\partial^2\hat{u}_j}{\partial t^2} \tag{3-1}$$

where:

$\hat{\tau}_{ij}$ is stress component;

$\hat{u}_j$ is displacement component;

$\hat{f}_j$ is body force component (per unit volume);

t is time;

ρ is the mass density.

The general stress-strain relation is (Achenbach, 1975, p52)

$$\hat{\tau}_{ij}=C_{ijkl}\hat{\varepsilon}_{ij} \tag{3-2}$$

where $\hat{\varepsilon}_{ij}$ is the strain tensor and the constants C_{ijkl} are

$$C_{ijkl}=C_{klij}=C_{jikl}=C_{ijlk}$$

For linear homogeous isotropic elastic materials, we have

$$C_{ijkl}=\lambda\delta_{ij}\delta_{kl}+\mu(\delta_{ik}\delta_{jl}+\delta_{il}\delta_{jk}) \tag{3-3a}$$

and

$$\hat{\varepsilon}_{ij}=\frac{1}{2}(\hat{u}_{i,j}+\hat{u}_{j,i}) \tag{3-3b}$$

With Eq. (3-3), the relation in Eq. (3-2) can be written as

$$\hat{\tau}_{ij}=\lambda\delta_{ij}\hat{u}_{k,k}+\mu(\hat{u}_{i,j}+\hat{u}_{j,i}) \tag{3-4}$$

where δ_{ij} is the Kronecker delta. λ and μ are Lame' constants which are related to Young's modulus E, Poisson's ratio υ in the following manner:

$$\lambda=\frac{E\nu}{(1+\nu)(1-2\nu)} \tag{3-5}$$

$$\mu=\frac{E}{2(1+\nu)} \tag{3-6}$$

In Eqs. (3-1) and (3-4) the range of the i, j is from 1 to 3, summation is implied by repeated indices, the comma denotes partial differentiation.

The incident displacement wave involved in this problem is considered to be a plane wave propagating with phase velocity c (sometimes called wave speed) in a direction defined by the unit vector $\underline{p}$. It is represented by

$$\underline{\hat{u}}=f(\underline{r}.\underline{p}-ct)\underline{d} \tag{3-7}$$

where $\underline{\hat{u}}$ is the displacement vector of the incident wave; $\underline{d}$ and $\underline{p}$ are unit vectors defining the directions of particle motion and wave propagation, respectively; $\underline{r}$ is the position vector of the particle measured from the coordinate origin.

In an unbounded medium, when the particle motion is parallel to the direction of propagation, the wave is called a longitudinal wave. This type of wave is also often called a pressure wave, or P-wave. In this case, the phase velocity c (or wave speed) equals

$$c=c_p=\left(\frac{\lambda+2\mu}{\rho}\right)^{\frac{1}{2}} \tag{3-8a}$$

When the particle motion is normal to the direction of propagation, the wave is called a transverse wave. This type of wave is also called a shear wave, or S-wave. The phase velocity c (or wave speed), in this case, is:

$$c=c_s=\left(\frac{\mu}{\rho}\right)^{\frac{1}{2}} \tag{3-8b}$$

In elastic wave propagation problems the displacements, stresses and body forces are generally functions of positions and time:

$$\hat{u}_i=\hat{u}_i(\underline{x},t) \tag{3-9a}$$

$$\hat{\tau}_{ij}=\hat{\tau}_{ij}(\underline{x},t) \tag{3-9b}$$

$$\hat{f}_i=\hat{f}_i(\underline{x},t) \tag{3-9c}$$

For time-harmonic waves, the expressions in equation (3-9) can be written as

$$\hat{u}_i=u_i(\underline{x},\omega)\,e^{-i\omega t} \tag{3-10a}$$

$$\hat{\tau}_{ij}=\tau_{ij}(\underline{x},\omega)\,e^{-i\omega t} \tag{3-10b}$$

$$\hat{f}_i=f_i(\underline{x},\omega)\,e^{-i\omega t} \tag{3-10c}$$

where ω is the circular frequency (radians per unit time).

If we substitute Eq. (3-10) into the Eq. (3-1), we have

$$\tau_{ij,j}(\underline{x},\omega)+\rho\omega^2 u_i(\underline{x},\omega)=-f_i(\underline{x},\omega) \tag{3-11}$$

It is clear that the time factor no longer exists in these equations.

Reciprocal Identity for Time-harmonic Motion

The reciprocal theorem is a very useful tool in elastodynamics, and can be used to set up a relation between two distinct elastic states. From this basic relation, the scattered fields in this problem can be consequently expressed by surface integrals over the scattering boundary. The derivation given here is done to Achenbach et. al. (1982, p. 34) Let us consider two different time-harmonic elastic states labeled by superscripts I and II:

$$u_i^I,\tau_{ij}^I,f_i^I$$

and

$$u_i^{II}, \tau_{ij}^{II}, f_i^{II}$$

From Eq. (3-11), we have

$$f_i^I = -(\tau_{ij,j}^I + \rho\omega^2 u_i^I) \tag{3-12a}$$

$$f_i^{II} = -(\tau_{ij,j}^{II} + \rho\omega^2 u_i^{II}) \tag{3-12b}$$

Let the product of Eq. (3-12b) and u_i^I subtract from the product of Eq. (3-12a) and u_i^{II}, we have

$$f_i^{II} u_i^I - f_i^I u_i^{II} = u_i^{II} \tau_{ij,j}^I - u_i^I \tau_{ij,j}^{II} \tag{3-13}$$

Let us now consider the quantity

$$(u_i^{II} \tau_{ij}^I - u_i^I \tau_{ij}^{II})_{,j}$$

which, with expanded, yields

$$(u_i^{II} \tau_{ij}^I - u_i^I \tau_{ij}^{II})_{,j} = (u_i^{II} \tau_{ij,j}^I - u_i^I \tau_{ij,j}^{II}) + (u_{i,j}^{II} \tau_{ij}^I - u_{i,j}^I \tau_{ij}^{II}) \tag{3-14}$$

With the relation in Eq. (3-4), it is easy to show that

$$u_{i,j}^{II} \tau_{ij}^I - u_{i,j}^I \tau_{ij}^{II} = 0$$

Therefore Eq. (3-14) becomes

$$(u_i^{II}\tau_{ij}^{I}-u_i^{I}\tau_{ij}^{II})_{,j}=(u_i^{II}\tau_{ij,j}^{I}-u_i^{I}\tau_{ij,j}^{II})=f_i^{II}u_i^{I}-f_i^{I}u_i^{II} \tag{3-15}$$

Integrating Eq. (3-15) over an arbitrary region V with a boundary S, we have

$$\int_V (u_i^{II}\tau_{ij}^{I}-u_i^{I}\tau_{ij}^{II})_{,j}dv=\int_V (f_i^{II}u_i^{I}-f_i^{I}u_i^{II})\,dv \tag{3-16}$$

From the divergence theorem, the left-hand side of Eq. (3-16) can be written as

$$\int_V (u_i^{II}\tau_{ij}^{I}-u_i^{I}\tau_{ij}^{II})_{,j}dv=\int_S (u_i^{II}\tau_{ij}^{I}-u_i^{I}\tau_{ij}^{II})\,n_j ds \tag{3-17}$$

By substituting Eq. (3-17) into Eq. (3-16), we obtain

$$\int_V (f_i^{II}u_i^{I}-f_i^{I}u_i^{II})\,dv=\int_S (u_i^{II}\tau_{ij}^{I}-u_i^{I}\tau_{ij}^{II})\,n_j ds \tag{3-18}$$

Equation (3-18) is the elastodynamic reciprocal identity for time-harmonic waves. In Eq. (3-18) $\underline{n}$ is the unit vector along the outward normal to the closed boundary S. In order to use the reciprocal identity validly the closed boundary should be large enough to surround all points considered in the problem.

The Integral Expressions for the Scattered Fields

Now we want to apply the reciprocal identity equation (3-18) to derive the governing equations for the fields scattered from a rough interface with random shape.

Let us consider a rough interface S between two regions denoted by V_A and V_B, with different material properties (see Fig. 6).

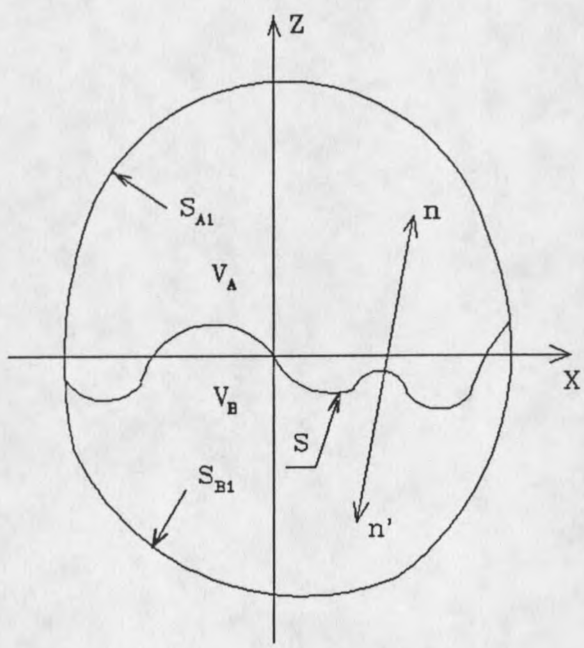

Figure 6. Two regions with their closed boundaries

Let V_A and V_B be bounded regions, and S_A and S_B be their respective boundaries. Each boundary consists of two parts:

$$S_A=S_{A1}+S \tag{3-19a}$$

$$S_B=S_{A1}^B+S \tag{3-19b}$$

If an incident wave in region A reaches the interface S, then a scattered wave will be generated in region A, and a refracted wave in region B. The total displacement fields and stress fields in regions A are given by

$$u_i^{tot/A}=u_i^{inc}+u_i^A \tag{3-20}$$

$$\tau_{ij}^{tot/A}=\tau_{ij}^{inc}+\tau_{ij}^A \tag{3-21}$$

where $u_i^{tot/A}$ and $\tau_{ij}^{tot/A}$ are the total displacement and stress fields; u_i^{inc} and τ_{ij}^{inc} are the displacement and stress fields of the incident wave; u_i^A and τ^A_{ij} are the scattered displacement and stress fields.

Since the incident wave only exists in the region A and the interface, the total displacement fields and the total stress fields in the region B do not include the incident wave, and only contain the refracted displacement fields and the refracted stress fields respectively:

$$u_i^{tot/B}=u_i^B \tag{3-22}$$

$$\tau_{ij}^{tot/B}=\tau_{ij}^{B} \tag{3-23}$$

where $u_i{}^B$ and $\tau^B{}_{ij}$ represent the displacement and stress fields of the refracted wave.

In order to obtain the scattered field, let us first consider the region A. Let the two elastic states in equation (3-18) be

$$\{u_i^I, \tau_{ij}^I, f_i^I\}=\{u_i^A, \tau_{ij}^A, 0\} \tag{3-24a}$$

$$\{u_i^{II}, \tau_{ij}^{II}, f_i^{II}\}=\{u_{ik}^G, \tau_{ijk}^G, \delta_{ik}\delta(\underline{r}'-\underline{r})\} \tag{3-24b}$$

where the scattered field satisfies the wave equation with f_i= 0,

$$\tau_{ij,j}^A+\rho\omega^2 u_i^A=0 \tag{3-25}$$

and $u^G{}_{ik}$ and $\tau^G{}_{ijk}$ are the components of displacement and stress at point Q generated by a unit point load located at point P in direction k (see Fig. 7). In other words, $u^G{}_{ik}$ and $\tau^G{}_{ijk}$ are Green's functions. These satisfy the equation of motion

$$(\tau_{ijk}^G)_{,j}+\rho\omega^2 u_{ik}^G=-\delta_{ik}\delta(\underline{r}'-\underline{r}) \tag{3-26}$$

Put equation (3-24a) and equation (3-24b) into equation (3-18), we have

$$\int_{V_A} [u_i^A(\underline{r}')\,\delta_{ik}\delta(\underline{r}'-\underline{r})]\,dv = \int_{S_A} [u_{ik}^G(\underline{r}'-\underline{r})\,\tau_{ij}^A(\underline{r}') - u_i^A(\underline{r}')\,\tau_{ijk}^G(\underline{r}'-\underline{r})]\,n_j'\,ds(\underline{r}')$$

(3-27)

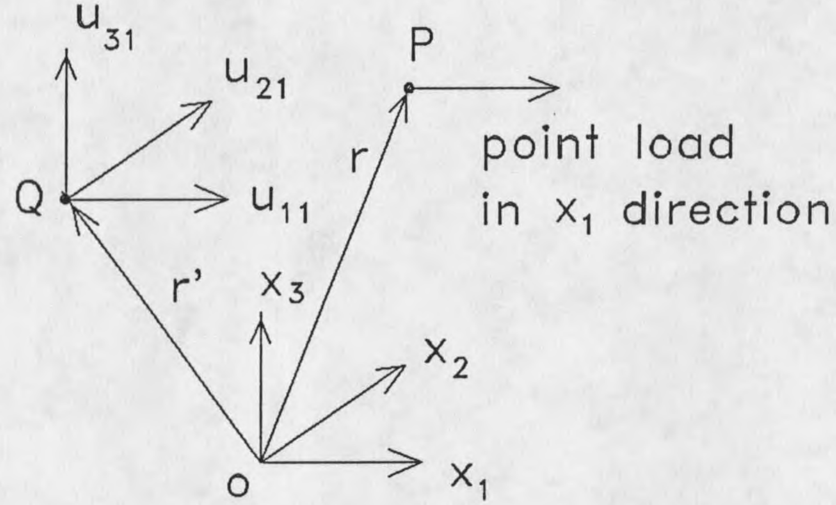

Figure 7. Displacement components generated by a point load in the x_1 direction

Since the delta function has the property

$$\int_V f(\underline{r}')\,\delta(\underline{r}'-\underline{r})\,dv = \begin{cases} f(\underline{r}) & (\ \underline{r} \text{ in V}) \\ 0 & (\ \underline{r} \text{ not in V}) \end{cases}$$

the left-hand side of the equation (3-27) becomes

$$\int_{V_A} u_i^A \delta_{ik} \delta(\underline{r}'-\underline{r})\, dv = u_k^A(\underline{r}) \tag{3-28}$$

where $u_k{}^A(\underline{r})$ is the k_{th} component of the scattered displacement at the point $\underline{r}$.

For convenience in calculation, we want to replace the unit normal $\underline{n}'$ with $\underline{n}$. From Fig. 6, we have

$$n_j = -n_j' \tag{3-29}$$

Therefore the k^{th} component of the scattered displacement can be described in the expression of a surface integral (for more detail, refer to Achenbach 1982)

$$u_k^A(\underline{r}) = \int_{S_A} [u_i^A(\underline{r}')\, \tau_{ijk}^G(\underline{r}'-\underline{r}) - u_{ik}^G(\underline{r}'-\underline{r})\, \tau_{ij}^A(\underline{r}')]\, n_j ds(\underline{r}') \tag{3-30}$$

Also since the boundary of the region A contains two parts, as shown in Eq. (3-19a), the integral given by Eq. (3-30) can be written as

$$\int_{S_A} = \int_{S} + \int_{S_{A1}} \tag{3-31}$$

But the second integral in the right hand side of the Eq. (3-31) does not have any contribution to the scattered field because, owing to the continuity of material properties across S_{A1}, no reflection effect exists on the boundary S_{A1}. Therefore, we finally obtain the expression of the scattered field as

$$u_k^A(\underline{r}) = \int_S [u_i^A(\underline{r}')\tau_{ijk}^G(\underline{r}'-\underline{r}) - u_{ik}^G(\underline{r}'-\underline{r})\tau_{ij}^A(\underline{r}')] n_j ds(\underline{r}') \qquad (3\text{-}32)$$

Similarly we can also obtain the expression of the refracted field in the region B

$$u_k^B = \int_S [\tau_{ij}^B(\underline{r}') u_{ik}^{G/B}(\underline{r}'-\underline{r}) - u_i^B(\underline{r}')\tau_{ijk}^{G/B}(\underline{r}'-\underline{r})] n_j ds(\underline{r}') \qquad (3\text{-}33)$$

where $u^B{}_k$ is the k^{th} component of the refracted displacement field at point $\underline{r}$ in region B, $\underline{r}'$ is any point on the boundary measured from the origin.

The equations (3-32) and (3-33) are the governing equations in this problem. At this step, these two equations are the exact expressions of the scattered displacement fields in both regions. For both of the regions, all related constants, say, Young's modulus E, elastic constants μ and λ, etc. depend on the materials chosen in the problem. In the first region A, we use symbols with superscript A for these constants, say, ρ^A, λ^A, μ^A and etc.. In the second region B, we use superscripts for these constants, for example, ρ^B, λ^B, μ^B, and etc..

Interface Conditions

The interface between the two elastic regions has random irregular shape. At the interface S, a discontinuity in the properties of the medium occurs. We assume that upon crossing the interface S, the mass density and/or the stiffness coefficients jump, at most, by finite amounts.

In this thesis, we assume that the interface is the case of a firm contact, that is, a perfect bonding exists along the interface between the two elastic solids. Therefore the displacement vector $\underline{u}$ and the traction vector $\underline{T}$ must be continuous on the interface S, i.e.

$$\underline{u}^{tot/A} = \underline{u}^{tot/B} \qquad (\text{ on } S) \qquad (3\text{-}34)$$

$$\underline{T}^{tot/A} + \underline{T}^{tot/B} = 0 \qquad (\text{ on } S) \qquad (3\text{-}35)$$

where

$\underline{u}^{tot/A}$ is the total displacement vector in region A;
$\underline{u}^{tot/B}$ is the total displacement vector in region B;
$\underline{T}^{tot/A}$ is the total traction vector in region A;
$\underline{T}^{tot/B}$ is the total traction vector in region B.

Tractions and stresses are related by:

$$T_i^{tot/A} = \tau_{ji}^{tot/A} n_j' \qquad (3\text{-}36)$$

$$T_i^{tot/B} = \tau_{ji}^{tot/B} n_j \qquad (3\text{-}37)$$

Therefore, with Eqs. (3-21), (3-23), and (3-30) substituted in these, and the results used in equation (3-35), we get the following conditions for the stresses on the interface S:

$$\tau_{ji}^{inc}+\tau_{ji}^{A}=\tau_{ji}^{B} \qquad \text{(on S)} \qquad (3\text{-}38a)$$

For the displacement interface condition, with Eqs. (3-20) and (3-22), it is easy to show that

$$u_i^{inc}+u_i^{A}=u_i^{B} \qquad \text{(on S)} \qquad (3\text{-}38b)$$

In elastic wave propagation problem, both displacement and stress fields contain pressure and shear components, i.e.

$$u_i^{A}=u_i^{A/p}+u_i^{A/s} \qquad (3\text{-}39a)$$

$$u_i^{B}=u_i^{B/p}+u_i^{B/s} \qquad (3\text{-}39b)$$

$$\tau_{ij}^{A}=\tau_{ij}^{A/p}+\tau_{ij}^{A/s} \qquad (3\text{-}39c)$$

$$\tau_{ij}^{B}=\tau_{ij}^{B/p}+\tau_{ij}^{B/s} \qquad (3\text{-}39d)$$

Therefore, for a two-dimensional case considered in this particular problem, the Eqs. (3-38) can also be written in terms of components as follows

$$u_1^{inc}+u_1^{A/p}+u_1^{A/s}=u_1^{B/p}+u_1^{B/s} \tag{3-40a}$$

$$u_3^{inc}+u_3^{A/p}+u_3^{A/s}=u_3^{B/p}+u_3^{B/s} \tag{3-40b}$$

$$\tau_{13}^{inc}+\tau_{13}^{A/p}+\tau_{13}^{A/s}=\tau_{13}^{B/p}+\tau_{13}^{B/s} \tag{3-40c}$$

$$\tau_{33}^{inc}+\tau_{33}^{A/p}+\tau_{33}^{A/s}=\tau_{33}^{B/p}+\tau_{33}^{B/s} \tag{3-40d}$$

It is clear that up to four unknowns in this problem can be found from the interface conditions. If the governing equations (3-32) and (3-33), together with the interface conditions (3-40), can be solved explicitly, the solution will be exact. However, since the interface has irregular shape, exact solutions cannot be obtained. An approximate solution for this problem will be discussed in this dissertation.

CHAPTER 4

SOLUTIONS OF THE SCATTERED AND THE REFRACTED FIELDS ON THE ROUGH INTERFACE

The surface integrals, Eqs. (3-32) and (3-33), obtained in Chapter 3 are the exact expressions of the scattered displacement fields at any point in the involved media for this wave scattering problem. However, the integrands in these expressions contain the stress and displacement of the scattered fields and the refracted fields, which are unknown at this step. The integral expressions, Eqs. (3-32) and (3-33), also contain appropriate elastic Green's functions, which need to be determined from the corresponding differential equations. Therefore in order to evaluate these two surface integrals, Eqs. (3-32) and (3-33), we need to obtain the analytical expressions on S for u_i^A, τ^A_{ij}, u_i^B, τ^B_{ij}, u^G_{ijk}, and τ^G_{ijk} first. In this chapter, we will apply the Kirchhoff approximation and the plane reflection coefficient calculation to derive the scattered and refracted fields on the rough boundary. Some restrictions on the Kirchhoff approximation are also discussed in this chapter.

The Kirchhoff Approximation

As mentioned in assumptions in Chapter 3, the boundary is assumed to be a random rough interface, therefore the unknown scattered displacement and stress fields on the boundary can not be obtained by applying regular solution methods. An approximation method has to be used in this case. Several approximation methods for this problem have been considered in wave scattering problems in early reported papers. In this dissertation, we will apply the Kirchhoff, or tangent plane, approximation method. Figure 8 shows the geometrical construction of the Kirchhoff approximation.

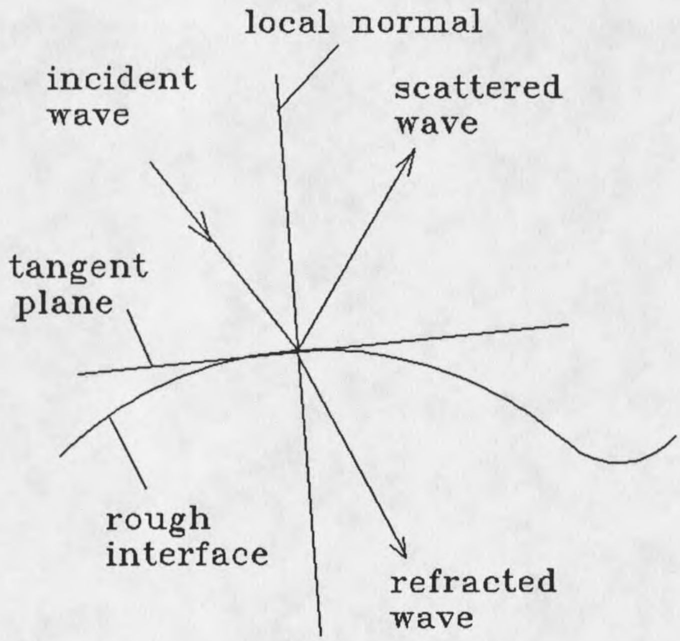

Figure 8. The Kirchhoff approximation for a rough interface problem

The theoretical basis for this approximation is that any point on the rough interface is assumed to behave as if the interface were locally flat and the incident wave at a point on the interface is reflected in the specular direction with a reflection coefficient equal to that of a plane boundary through that point and parallel to the local tangent to the interface (see Fig. 8). In this way, the scattered fields on the boundary can be expressed in terms of the incident wave with plane reflection coefficients.

Let $u_i^{inc/p}$ denote the i^{th} displacement component of the longitudinal wave propagating toward to the interface in region A, then and be given by

$$u_1^{inc/p}=A_{inc}\sin\theta_{inc}\exp[ik_p(x\sin\theta_{inc}-z\cos\theta_{inc})] \tag{4-1a}$$

$$u_2^{inc/p}=0 \tag{4-1b}$$

$$u_3^{inc/p}=-A_{inc}\cos\theta_{inc}\exp[ik_p(x\sin\theta_{inc}-z\cos\theta_{inc})] \tag{4-1c}$$

where A_{inc} is the amplitude of the incident displacement wave; θ_{inc} is the angle of the incident wave relative to the z-axis in the x-z plane (see Fig. 9a); k_p is the longitudinal wave number of the incident wave.

When the incident wave reaches the interface S, scattered waves will be generated in both regions A and B. In region A the scattered displacement P-wave and SV-wave occur at the angles β^A and γ^A with the z-axis, respectively (see Fig. 9a). In region B, the scattered displacement P-wave and SV-wave occur at the angles β^B and γ^B with negative z-axis, respectively (see Fig. 9a).

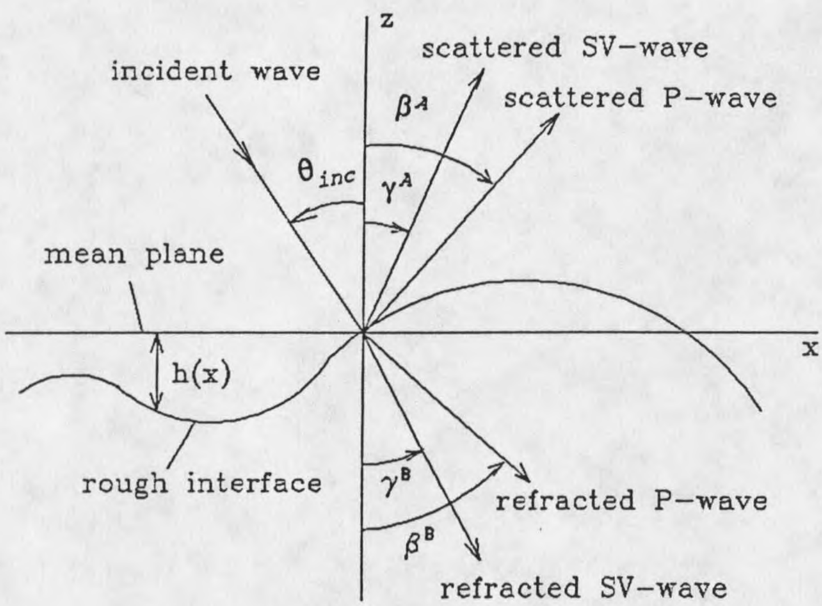

a). All wave fields are in the global coordinates

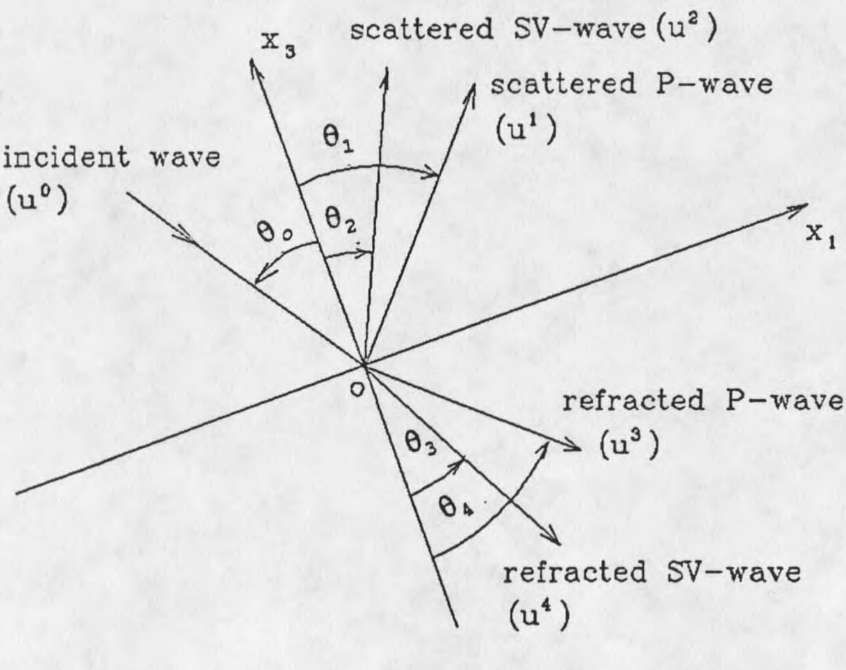

b). All wave fields are in the coordinates with an arbitrary orientation

Figure 9. The incident, scattered, and refracted fields in Cartesian coordinates

Now we want to derive the expressions of the scattered and refracted waves on the interface. Let the incident wave as well as the scattered and refracted waves be represented by

$$\underline{u}^n = A_n \underline{d}^n \exp[ik_n(\underline{x}.\underline{p}^n)] \qquad (n=0,1,2,3,4) \qquad (4\text{-}2)$$

where the value of the index n serves to label the different types of waves, i.e., n=0 for incident wave, n=1 for scattered P-wave, n=2 for scattered SV-wave, n=3 for refracted P-wave, and n=4 for refracted SV-wave (see Fig. 9b); A_n is the amplitude of waves; $\underline{p}_n$ and $\underline{d}_n$ are the unit direction vectors of wave propagation and particle motion, respectively.

For the incident P-wave, we have

$$\underline{d}^0 = \underline{p}^0 = \sin\theta_0 \underline{i} - \cos\theta_0 \underline{k} \qquad (4\text{-}3)$$

for the reflected P-wave, we have

$$\underline{d}^1 = \underline{p}^1 = \sin\theta_1 \underline{i} + \cos\theta_1 \underline{k} \qquad (4\text{-}4)$$

for the reflected SV-wave, we have

$$\underline{p}^2 = \sin\theta_2 \underline{i} + \cos\theta_2 \underline{k} \qquad (4\text{-}5a)$$

$$\underline{d}^2 = \cos\theta_2 \underline{i} - \sin\theta_2 \underline{k} \qquad (4\text{-}5b)$$

for the refracted P-wave, we have

$$\underline{d}^3=\underline{p}^3=\sin\theta_3\underline{i}-\cos\theta_3\underline{k} \qquad (4\text{-}6)$$

for the refracted SV-wave, we have

$$\underline{p}^4=\sin\theta_4\underline{i}-\cos\theta_4\underline{k} \qquad (4\text{-}7a)$$

$$\underline{d}^4=-\cos\theta_4\underline{i}-\sin\theta_4\underline{k} \qquad (4\text{-}7b)$$

where $\underline{i}$ and $\underline{k}$ are the unit vectors in x and z directions respectively, and the angles θ_o through θ_4 are defined in Fig. 9b, relative to an arbitrary x_1, x_3 coordinate system.

We note from Eq. (4-2) that, since the $\underline{d}^n$ (n=0, 1, 2, 3, 4) is a unit vector, we have

$$|\underline{u}^n|=A_n \qquad (n=0,\ 1,\ 2,\ 3,\ 4) \qquad (4\text{-}8)$$

Let

$$R_n^P=\frac{|\underline{u}^n|}{|\underline{u}^o|}=\frac{A_n}{A_o} \qquad (n=0,\ 1,\ 2,\ 3,\ 4) \qquad (4\text{-}9)$$

Therefore, we can write Eq. (4-2) as

$$\underline{u}^n=A_oR_n^P\underline{d}^n\exp(i\eta_n) \qquad (n=0,1,2,3,4) \qquad (4\text{-}10)$$

where

$$\eta_n=k_n(\mathbf{x}\cdot\mathbf{p}^n) \qquad (n=0,1,2,3,4) \tag{4-11}$$

From Eq. (3-40), for two-dimensional motion problem, at z=0, the interface conditions in the coordinates with an arbitrary orientation (shown in Fig. 9b) can be written as

$$u_1^0+u_1^1+u_1^2=u_1^3+u_1^4 \tag{4-12a}$$

$$u_3^0+u_3^1+u_3^2=u_3^3+u_3^4 \tag{4-12b}$$

$$\tau_{31}^0+\tau_{31}^1+\tau_{31}^2=\tau_{31}^3+\tau_{31}^4 \tag{4-12c}$$

$$\tau_{33}^0+\tau_{33}^1+\tau_{33}^2=\tau_{33}^3+\tau_{33}^4 \tag{4-12d}$$

By sustituting Eq. (4-10) and Eqs. (4-3)-(4-7) into Eqs. (4-12a)-(4-12d), we get

$$\begin{aligned}&\sin\theta_o\exp(i\eta_o)+R_1^p\sin\theta_1\exp(i\eta_1)+R_2^p\cos\theta_2\exp(i\eta_2)\\&=R_3^p\sin\theta_3\exp(i\eta_3)-R_4^p\cos\theta_4\exp(i\eta_4)\end{aligned} \tag{4-13a}$$

$$\begin{aligned}&\cos\theta_o\exp(i\eta_o)-R_1^p\cos\theta_1\exp(i\eta_1)+R_2^p\sin\theta_2\exp(i\eta_2)\\&=R_3^p\cos\theta_3\exp(i\eta_3)+R_4^p\sin\theta_4\exp(i\eta_4)\end{aligned} \tag{4-13b}$$

$$\sin 2\theta_o \exp(i\eta_o) - R_1^p \sin 2\theta_1 \exp(i\eta_1) - R_2^p \kappa^A \cos 2\theta_2 \exp(i\eta_2)$$

$$= R_3^p \frac{\mu^B c_p^A}{\mu^A c_p^B} \sin 2\theta_3 \exp(i\eta_3) - R_4^p \frac{\mu^B c_p^A}{\mu^A c_s^B} \cos 2\theta_4 \exp(i\eta_4) \tag{4-13c}$$

$$(\kappa^A)^2 \cos 2\theta_o \exp(i\eta_o) + R_1^p (\kappa^A)^2 \cos 2\theta_1 \exp(i\eta_1) - R_2^p \kappa^A \sin 2\theta_2 \exp(i\eta_2)$$

$$= R_3^p (\kappa^B)^2 \frac{\mu^B c_p^A}{\mu^A c_p^B} \cos 2\theta_3 \exp(i\eta_3) + R_4^p \frac{\mu^B c_p^A}{\mu^A c_s^B} \cos 2\theta_4 \exp(i\eta_4) \tag{4-13d}$$

We note from Eq. (4-11) that the quantity η_n is a function of $\underline{x}$. However, Eqs. (4-13) must be true for all values of $\underline{x}$ on the interface. Therefore, we must require that

$$\eta_o = \eta_1 = \eta_2 = \eta_3 = \eta_4 = \eta \tag{4-14}$$

From Eqs. (4-10) and (4-14), we can express the scattered and refracted waves on the interface in terms of the incident wave quantities A_o and η_o, and the reflection coefficient R_n.

Now we are ready to write out the explicit expressions of the scattered and refracted fields on the interface. Since the scattered and refracted fields contain pressure and shear components as shown in Eq. (3-39), these fields, from Eqs. (4-10) and (4-14), can be written as

$$\underline{u}^A = A_o [R_1^p \underline{d}^1 + R_2^p \underline{d}^2] e^{i\eta_o} \tag{4-15}$$

and with Eqs. (4-4) and (4-5b) we get the scattered displacement components as

$$u_1^A=A_o[R_1^P\sin\theta_1+R_2^P\cos\theta_2]\,e^{i\eta_o} \tag{4-16a}$$

$$u_2^A=0 \tag{4-16b}$$

$$u_3^A=A_o[R_1^P\cos\theta_1-R_2^P\sin\theta_2]\,e^{i\eta_o} \tag{4-16c}$$

Similarly we can get the refracted displacement components as

$$u_1^B=A_o[R_3^P\sin\theta_3-R_4^P\cos\theta_4]\,e^{i\eta_o} \tag{4-17a}$$

$$u_2^B=0 \tag{4-17b}$$

$$u_3^B=-A_o[R_3^P\cos\theta_3+R_4^P\sin\theta_4]\,e^{i\eta_o} \tag{4-17c}$$

We note that in the global coordinates (x-z system), the angles θ_o, θ_1, θ_2, θ_3, and θ_4 will be θ_{inc}, β^A, γ^A, β^B, and γ^B, respectively (see Fig. 9). The amplitude A_o will be replaced by A_{inc}. We also note that on the interface, we have $z=h(x)$ so that with Eqs. (4-14), (4-11) and (4-3) we have:

$$\eta_o=\eta=k_p[x\sin\theta_{inc}-h(x)\cos\theta_{inc}] \tag{4-18}$$

Therefore, with Eqs. (3-39), (4-16) and (4-18), the scattered and refracted fields on the interface, in terms of displacement components in the global coordinates, can be written as

$$u_1^A = (R_1^p \sin\beta^A + R_2^p \cos\gamma^A) A_{inc} \exp[ik_p(x sin\theta_{inc} - h(x)\cos\theta_{inc})] \tag{4-19a}$$

$$u_2^A = 0 \tag{4-19b}$$

$$u_3^A = (R_1^p \cos\beta^A - R_2^p \sin\gamma^A) A_{inc} \exp[ik_p(x sin\theta_{inc} - h(x)\cos\theta_{inc})] \tag{4-19c}$$

and

$$u_1^B = (R_3^p \sin\beta^B - R_4^p \cos\gamma^B) A_{inc} \exp[ik_p(x sin\theta_{inc} - h(x)\cos\theta_{inc})] \tag{4-20a}$$

$$u_2^B = 0 \tag{4-20b}$$

$$u_3^B = -(R_3^p \cos\beta^B + R_4^p \sin\gamma^B) A_{inc} \exp[ik_p(x sin\theta_{inc} - h(x)\cos\theta_{inc})] \tag{4-20c}$$

Eqs. (4-19a) - (4-20c) are the general expressions of the scattered and the refracted displacement components on the interface obtained by applying the Kirchhoff approximation. Since the surface integrals also contain unknown scattered and refracted stress fields on the interface, we need to replace these unknowns by given quantities. According to the stress-displacement relation, Eq. (3-4), we can obtain the stress components of the scattered and the refracted fields on the interface

$$\tau_{33}^{A}=iA_{inc}k_p[\lambda^A(R_1^P\sin\beta^A+R_2^P\cos\gamma^A)(\sin\theta_{inc}) - (\lambda^A+2\mu^A)(R_1^P\cos\beta^A-R_2^P\sin\gamma^A)(\cos\theta_{inc})]\exp(i\eta) \tag{4-21a}$$

$$\tau_{13}^{A}=\tau_{31}^{A}=iA_{inc}k_p\mu^A[(R_1^P\sin\beta^A+R_2^P\cos\gamma^A)(-\cos\theta_{inc}) + (R_1\cos\beta-R_2\sin\gamma)(\sin\theta_{inc})]\exp(i\eta) \tag{4-21b}$$

$$\tau_{33}^{B}=iA_{inc}k_p[\lambda^B(R_3^P\sin\beta^B-R_4^P\cos\gamma^B)\sin\theta_{inc} + (\lambda^B+2\mu^B)(R_3^P\cos\beta^B+R_4^P\sin\beta^B)\cos\theta_{inc}]\exp(i\eta) \tag{4-22a}$$

$$\tau_{13}^{B}=\tau_{31}^{B}=-iA_{inc}k_p\mu^B[(R_3^P\sin\beta^B-R_4^P\cos\gamma^B)\cos\theta_{inc} + (R_3^P\cos\beta^B+R_4^P\sin\gamma^B)\sin\theta_{inc}]\exp(i\eta) \tag{4-22b}$$

Reflection Coefficients

Expressions of displacement and stress components of the scattered and refracted fields on the rough interface involve plane reflection coefficients R_1^P, R_2^P, R_3^P, and R_4^P which need to be determined explicitly.

Let's consider the incident wave as well as the scattered and refracted waves in the local coordinates (x'-z' system, see Fig. 10). Applying the interface conditions again we can obtain the reflection coefficients. But we note that in the local coordinates, the angles θ_o, θ_1, θ_2, θ_3, and θ_4 involved in the unit vectors $\underline{d}$ and $\underline{p}$ will be α, α_p, α_s, $\alpha_p{}^B$, and $\alpha_s{}^B$, respectively (see Fig. 10).

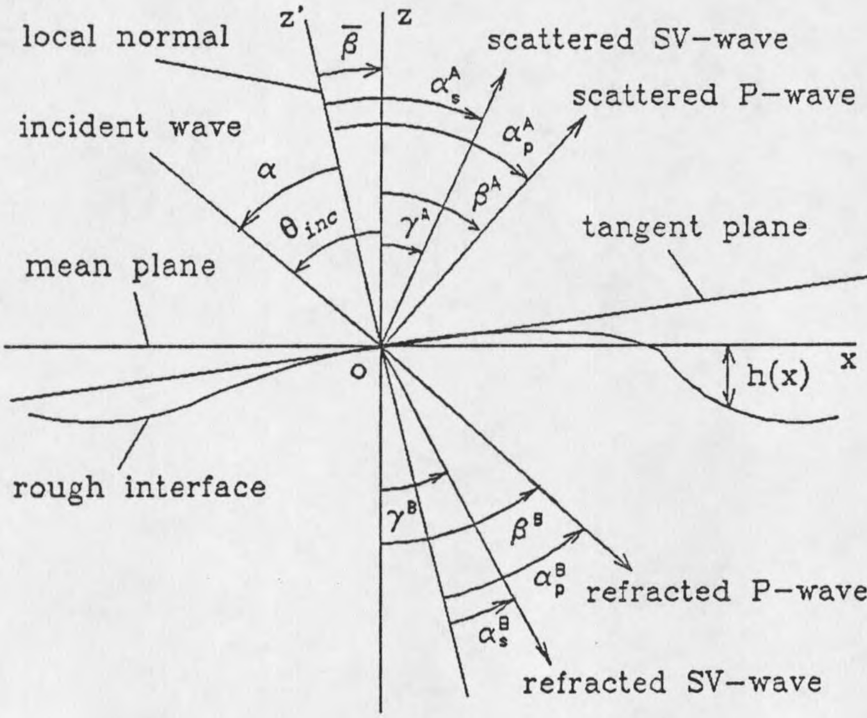

Figure 10. The incident, scattered and refracted fields in the both global and local coordinates

Applying the interface conditions, Eqs. (4-12a) through (4-12d), in the local coordinates, the coefficients $R_1{}^p$, $R_2{}^p$, $R_3{}^p$, and $R_4{}^p$ can be obtained. Since z'=0 on the tangent plane, from Eqs. (4-11), (4-3)-(4-7) and (4-14) we get

$$k_p \sin\alpha = k_p^A \sin\alpha_p^A = k_s^A \sin\alpha_s^A = k_p^B \sin\alpha_p^B = k_s^B \sin\alpha_s^B \qquad (4\text{-}23)$$

If the incident angle α and wave number k_p and k_s are given, the other angles and wave numbers can thus be obtained from these relations. Eqs. (4-12a) through (4-12d) also form a system of four equations for the amplitudes of different waves. In terms of matrix notation the system can be written as

$$\begin{pmatrix} -\sin\alpha_p^A & \cos\alpha_s^A & \sin\alpha_p^B & -\cos\alpha_s^B \\ \cos\alpha_p^A & -\sin\alpha_s^A & \cos\alpha_p^B & \sin\alpha_s^B \\ \sin 2\alpha_p^A & \kappa^A\cos 2\alpha_s^A & T_p\sin 2\alpha_p^B & -T_s\cos 2\alpha_s^B \\ -\cos 2\alpha_s^A & \sin 2\alpha_s^A/\kappa^A & T_pT_\kappa\cos 2\alpha_s^B & T_s\sin 2\alpha_s^B/(\kappa^A)^2 \end{pmatrix}\begin{Bmatrix} R_1^p \\ R_2^p \\ R_3^p \\ R_4^p \end{Bmatrix}=\begin{Bmatrix} \sin\alpha_p^A \\ \cos\alpha_p^A \\ \sin 2\alpha_p^A \\ \cos 2\alpha_s^A \end{Bmatrix} \tag{4-24}$$

where

$$T_p=\frac{\mu^B c_p^A}{\mu^A c_p^B} \tag{4-25a}$$

$$T_s=\frac{\mu^B c_p^A}{\mu^A c_s^B} \tag{4-25b}$$

$$T_\kappa=\frac{\kappa^B}{\kappa^A} \tag{4-25c}$$

and

$$\kappa^q=\frac{c_p^q}{c_s^q}=\frac{k_s^q}{k_p^q} \qquad (q=A,\ B) \tag{4-26}$$

The solution to Eq.(4-24) is

$$R_1^p=\frac{D_1^p}{D^p} \tag{4-27}$$

$$R_2^p=\frac{D_2^p}{D^p} \tag{4-28}$$

$$R_3^p=\frac{D_3^p}{D^p} \tag{4-29}$$

$$R_4^p=\frac{D_4^p}{D^p} \tag{4-30}$$

where

$$\begin{aligned} D^p=&P_1^p\,[Q_2^p\,(V_3^pW_4^p+V_4^pW_3^p)+Q_3^p\,(V_2^pW_4^p+V_4^pW_2^p)+Q_4^p\,(V_3^pW_2^p-V_2^pW_3^p)\,] \\ &+P_2^p\,[Q_1^p\,(V_3^pW_4^p+V_4^pW_3^p)+Q_3^p\,(V_4^pW_1^p-V_1^pW_4^p)+Q_4^p\,(V_1^pW_3^p+V_3^pW_1^p)\,] \\ &+P_3^p\,[Q_1^p\,(V_2^pW_4^p+V_4^pW_2^p)+Q_2^p\,(V_1^pW_4^p-V_4^pW_1^p)+Q_4^p\,(V_1^pW_2^p+V_2^pW_1^p)\,] \\ &+P_4^p\,[Q_1^p\,(V_2^pW_3^p-V_3^pW_2^p)+Q_2^p\,(V_1^pW_3^p+V_3^pW_1^p)+Q_3^p\,(V_1^pW_2^p+V_2^pW_1^p)\,] \end{aligned} \tag{4-31}$$

$$\begin{aligned} D_1^p=-\Big\{&P_1^p\,[Q_2^p\,(V_3^pW_4^p+V_4^pW_3^p)+Q_3^p\,(V_2^pW_4^p+V_4^pW_2^p)+Q_4^p\,(V_3^pW_2^p-V_2^pW_3^p)\,] \\ &+P_2^p\,[Q_1^p\,(-V_3^pW_4^p-V_4^pW_3^p)+Q_3^p\,(V_1^pW_4^p+V_4^pW_1^p)+Q_4^p\,(V_3^pW_1^p-V_1^pW_3^p)\,] \\ &+P_3^p\,[Q_1^p\,(-V_2^pW_4^p-V_4^pW_2^p)+Q_2^p\,(-V_1^pW_4^p-V_4^pW_1^p)+Q_4^p\,(V_2^pW_1^p-V_1^pW_2^p)\,] \\ &+P_4^p\,[Q_1^p\,(V_3^pW_2^p-V_2^pW_3^p)+Q_2^p\,(V_3^pW_1^p-V_1^pW_3^p)+Q_3^p\,(V_2^pW_1^p-V_1^pW_2^p)\,]\Big\} \end{aligned} \tag{4-32}$$

$$D_2^p=2\{P_1^p[Q_1^p(-V_3^pW_4^p-V_4^pW_3^p)+Q_3^pV_1^pW_4^p-Q_4^pV_1^pW_3^p]$$

$$+P_3^p[Q_1^pV_4^pW_1^p+Q_4^pV_1^pW_1^p]+P_4^p[Q_3^pV_1^pW_1^p-Q_1^pV_3^pW_1^p]\} \qquad (4\text{-}33)$$

$$D_3^p=2\{P_1^p[Q_1^p(V_2^pW_4^p+V_4^pW_2^p)+Q_2^pV_1^pW_4^p+Q_4^pV_1^pW_2^p]$$

$$+P_2^p[Q_1^pV_4^pW_1^p+Q_4^pV_1^pW_1^p]+P_4^p[Q_1^pV_2^pW_1^p+Q_2^pV_1^pW_1^p]\} \qquad (4\text{-}34)$$

$$D_4^p=2\{P_1^p[Q_1^p(V_3^pW_2^p-V_2^pW_3^p)-Q_2^pV_1^pW_3^p-Q_3^pV_1^pW_2^p]$$

$$+P_2^p[Q_1^pV_3^pW_1^p-Q_3^pV_1^pW_1^p]+P_3^p[Q_1^pV_2^pW_1^p+Q_2^pV_1^pW_1^p]\} \qquad (4\text{-}35)$$

and

$$P_1^p=\sin\alpha \qquad (4\text{-}36a)$$

$$P_2^p=\cos\alpha_s^A \qquad (4\text{-}36b)$$

$$P_3^p=\sin\alpha_p^B \qquad (4\text{-}36c)$$

$$P_4^p=\cos\alpha_s^B \qquad (4\text{-}36d)$$

$$Q_1^p=\cos\alpha \qquad (4\text{-}37a)$$

$$Q_2^p=\sin\alpha_s^A \qquad (4\text{-}37b)$$

$$Q_3^p=\cos\alpha_p^B \qquad (4\text{-}37c)$$

$$Q_4^p=\sin\alpha_s^B \qquad (4\text{-}37d)$$

$$V_1^p=\sin 2\alpha \qquad (4\text{-}38a)$$

$$V_2^p=\kappa^A\cos 2\alpha_s^A \tag{4-38b}$$

$$V_3^p=\frac{\mu^B C_p^A}{\mu^A C_p^B}\sin 2\alpha_p^B \tag{4-38c}$$

$$V_4^p=\frac{\mu^B C_p^A}{\mu^A C_s^B}\cos 2\alpha_s^B \tag{4-38d}$$

$$W_1^p=\cos 2\alpha_s^A \tag{4-39a}$$

$$W_2^p=\frac{1}{\kappa^A}\sin 2\alpha_s^A \tag{4-39b}$$

$$W_3^p=\frac{\mu^B C_p^A(\kappa^B)^2}{\mu^A C_p^B(\kappa^A)^2}\cos 2\alpha_s^B \tag{4-39c}$$

$$W_4^p=\frac{\mu^B C_p^A}{\mu^A C_s^B(\kappa^A)^2}\sin 2\alpha_s^B \tag{4-39d}$$

Equations (4-27)-(4-39) are the explicit expressions for the plane reflection coefficients in terms of the angular quantities shown in Fig. 10. Expressions of the amplitude ratio A_1/A_o, etc. for a smooth interface problem are also given by Ewing et al (1957, p. 87). Substitution of Eqs. (4-27)-(4-39) into Eqs. (4-19)-(4-22) gives the unknown scattered and refracted fields on the rough interface in terms of the given incident waves and the plane reflection coefficients.

Since the height h of the rough interface varies along x-direction, ie. h is a function of x, the orientation of the local normal is also a function of x and is given by

$$\overline{\beta}=\arctan[h'(x)] \tag{4-40}$$

If the height function h(x) is determined, the local normal becomes known. Therefore all angles involved in the scattered and refracted fields can be explicitly expressed in terms of the known local normal and the given incident angle. From Fig. 10, we have

$$\alpha=\theta_{inc}-\overline{\beta} \tag{4-41}$$

Since the incident wave is a P-wave and in region A, wave numbers of the incident wave and the scattered P-wave, k_p and $k_p{}^A$, are equal. From Eq. (4-23), we have

$$\alpha_p^A=\alpha \tag{4-42}$$

$$\sin\alpha_s^A=\frac{k_p^A}{k_s^A}\sin\alpha \tag{4-43}$$

$$\sin\alpha_p^B=\frac{k_p^A}{k_p^B}\sin\alpha \tag{4-44}$$

$$\sin\alpha_s^B=\frac{k_p^A}{k_s^B}\sin\alpha \tag{4-45}$$

From Fig. 10, we have

$$\beta^A=\alpha_p^A-\overline{\beta} \tag{4-46}$$

$$\gamma^A=\alpha_s^A-\overline{\beta} \tag{4-47}$$

$$\beta^{B}=\alpha_{p}^{B}+\overline{\beta} \tag{4-48}$$

$$\gamma^{B}=\alpha_{s}^{B}+\overline{\beta} \tag{4-49}$$

For a smooth boundary, which is a special case of the rough interface, the height function h(x) and its gradient h'(x) vanish. Therefore the local normal is always parallel to z-axis. In this special case, we have

$$\overline{\beta}=0 \tag{4-50}$$

$$\alpha_{p}^{A}=\alpha=\theta_{inc} \tag{4-51}$$

The above solutions are due to the incident pressure wave. The solutions due to the shear wave are discussed in next section.

<u>The Case of the Incident Shear Wave</u>

The incident wave used in this dissertation is either compression or shear wave. For the case of the incident shear wave, the incident wave can be written as

$$u_1^{inc/s}=-A_{inc}\cos\theta_{inc}\exp[ik_s(x\sin\theta_{inc}-z\cos\theta_{inc})] \tag{4-52a}$$

$$u_2^{inc/s}=0 \tag{4-52b}$$

$$u_3^{inc/s}=-A_{inc}\sin\theta_{inc}\exp[ik_s(x\sin\theta_{inc}-z\cos\theta_{inc})] \tag{4-52c}$$

where A_{inc} is the amplitude of the incident displacement wave; θ_{inc} is the angle of the incident wave relative to the z-axis in the x-z plane; k_s is the wave number of the incident shear wave.

From the Kirchhoff approximation, in the similar way of the incident pressure wave case, the scattered and refracted displacement waves on the interface, in terms of components, can be expressed by the following equations:

in region A,

$$u_1^A = (R_1^s \sin\beta^A + R_2^s \cos\gamma^A) A_{inc} \exp[ik_s(x\sin\theta_{inc} - h(x)\cos\theta_{inc})] \quad (4\text{-}53a)$$

$$u_2^A = 0 \quad (4\text{-}53b)$$

$$u_3^A = (R_1^s \cos\beta^A - R_2^s \sin\gamma^A) A_{inc} \exp[ik_s(x\sin\theta_{inc} - h(x)\cos\theta_{inc})] \quad (4\text{-}53c)$$

in region B,

$$u_1^B = (R_3^s \sin\beta^B - R_4^s \cos\gamma^B) A_{inc} \exp[ik_s(x\sin\theta_{inc} - h(x)\cos\theta_{inc})] \quad (4\text{-}54a)$$

$$u_2^B = 0 \quad (4\text{-}54b)$$

$$u_3^B = -(R_3^s \cos\beta^B + R_4^s \sin\gamma^B) A_{inc} \exp[ik_s(x\sin\theta_{inc} - h(x)\cos\theta_{inc})] \quad (4\text{-}54c)$$

where R_1^s, R_2^s, R_3^s, and R_4^s are the plane reflection coefficients for the case of an incident shear wave.

According to the stress-displacement relation shown in Eq. (3-4), we can obtain the stress components of the scattered and the refracted fields on the interface

$$\tau_{33}^{A}=iA_{inc}k_s[\lambda^A(R_1^s\sin\beta^A+R_2^s\cos\gamma^A)(\sin\theta_{inc}) - (\lambda^A+2\mu^A)(R_1^s\cos\beta^A-R_2^s\sin\gamma^A)(\cos\theta_{inc})]\exp(i\eta^s) \tag{4-55a}$$

$$\tau_{13}^{A}=\tau_{31}^{A}=iA_{inc}k_s\mu^A[(R_1^s\sin\beta^A+R_2^s\cos\gamma^A)(-\cos\theta_{inc}) + (R_1^s\cos\beta^A-R_2^s\sin\gamma^A)(\sin\theta_{inc})]\exp(i\eta^s) \tag{4-55b}$$

$$\tau_{33}^{B}=iA_{inc}k_s[\lambda^B(R_3^s\sin\beta^B-R_4^s\cos\gamma^B)\sin\theta_{inc} + (\lambda^B+2\mu^B)(R_3^s\cos\beta^B+R_4^s\sin\beta^B)\cos\theta_{inc}]\exp(i\eta^s) \tag{4-56a}$$

$$\tau_{13}^{B}=\tau_{31}^{B}=-iA_{inc}k_s\mu^B[(R_3^s\sin\beta^B-R_4^s\cos\gamma^B)\cos\theta_{inc} + (R_3^s\cos\beta^B+R_4^s\sin\gamma^B)\sin\theta_{inc}]\exp(i\eta^s) \tag{4-56b}$$

where

$$\eta^s=k_s[x\sin\theta_{inc}-h(x)\cos\theta_{inc}] \tag{4-57}$$

Expressions of displacement and stress components of the scattered and refracted fields on the rough boundary involve plane reflection coefficients R_1^s, R_2^s, R_3^s, and R_4^s which can be obtained from plane interface conditions.

In the similar way of the incident pressure wave case, the reflection coefficients due to the incident shear wave can be expressed as

$$R_1^s = \frac{D_1^s}{D^s} \tag{4-58}$$

$$R_2^s = \frac{D_2^s}{D^s} \tag{4-59}$$

$$R_3^s = \frac{D_3^s}{D^s} \tag{4-60}$$

$$R_4^s = \frac{D_4^s}{D^s} \tag{4-61}$$

In Eqs. (4-58)-(4-61) the quantities D^s and D_n^s (n=1,2,3,4) are functions of P_n^s, Q_n^s, V_n^s and W_n^s (n=1,2,3,4). The relationships are given in Eqs. (4-31)-(4-35) with the superscript p replaced by s. The quantities P_n^s, Q_n^s, V_n^s and W_n^s (n=1,2,3,4) are expressed as

$$P_1^s = \sin\alpha \tag{4-62a}$$

$$P_2^s = -\cos\alpha_p^A \tag{4-62b}$$

$$P_3^s = \cos\alpha_p^B \tag{4-62c}$$

$$P_4^s = -\cos\alpha_s^B \tag{4-62d}$$

$$Q_1^s = \cos\alpha \tag{4-63a}$$

$$Q_2^s = -\sin\alpha_p^A \tag{4-63b}$$

$$Q_3^s = -\sin\alpha_p^B \tag{4-63c}$$

$$Q_4^s = \sin\alpha_s^B \tag{4-63d}$$

$$V_1^s = \sin 2\alpha \tag{4-64a}$$

$$V_2^s = -\kappa^A \cos 2\alpha_p^A \tag{4-64b}$$

$$V_3^s = \frac{\mu^B C_s^A}{\mu^A C_p^B} (\kappa^B)^2 \cos 2\alpha_p^B \tag{4-64c}$$

$$V_4^s = \frac{\mu^B C_s^A}{\mu^A C_s^B} \sin 2\alpha_s^B \tag{4-64d}$$

$$W_1^s = \cos 2\alpha \tag{4-65a}$$

$$W_2^s = \frac{1}{\kappa^A} \sin 2\alpha_p^A \tag{4-65b}$$

$$W_3^s = \frac{\mu^B C_s^A}{\mu^A C_p^B} \sin 2\alpha_p^B \tag{4-65c}$$

$$W_4^s = \frac{\mu^B C_s^A}{\mu^A C_s^B} \cos 2\alpha_s^B \tag{4-65d}$$

The definitions of all angles in these equations are shown in the Fig. 10. It is clear that all angles involved in the reflection coefficients are related to the incident angle and the angle of the local normal which is given by Eq. (4-40).

In the case of incident shear wave the relations between angles as well as wave numbers in Eq. (4-23) becomes, in local coordinates,

$$k_s \sin\alpha = k_p^A \sin\alpha_p^A = k_s^A \sin\alpha_s^A = k_p^B \sin\alpha_p^B = k_s^B \sin\alpha_s^B \tag{4-66}$$

If the height function h(x) is determined, the local normal becomes known. Therefore all angles involved in the scattered and refracted fields can be explicitly expressed in terms of the known local normal and the given incident angle, ie..

$$\alpha = \theta_{inc} - \overline{\beta} \tag{4-67}$$

$$\alpha_s^A = \alpha \tag{4-68}$$

$$\sin\alpha_p^A = \frac{k_s^A}{k_p^A} \sin\alpha \tag{4-69}$$

$$\sin\alpha_p^B = \frac{k_s^A}{k_p^B} \sin\alpha \tag{4-70}$$

$$\sin\alpha_s^B = \frac{k_s^A}{k_s^B} \sin\alpha \tag{4-71}$$

So far we replaced the unknown scattered and the refracted displacement and stress fields on the boundary by the known incident wave field and the plane reflection coefficients. It is clear that the scattered and the refracted fields on the boundary depend on the properties of the rough boundary, in addition to the given incident wave. Therefore to solve the problem numerically, we need to determine the properties of the rough interface which will be discussed in later chapters.

Restrictions of the Kirchhoff Approximation

When the Kirchhoff approximation is applied to problems of wave scattering from a rough surface, some corresponding restrictions on this approximation must be considered (Ogilvy 1985). The basic assumptions of the Kirchhoff approximation are as follows:

a) scattering from any point on the rough interface is assumed to be the same as from a surface that is locally flat;

b) shadowing effects and multiple scattering are both neglected.

First let us consider the assumption a). The validity of this assumption will be very good when the radius of the curvature of the rough boundary is large compared with the wave length of the incident wave. But the validity will break down if the roughness includes sharp edges or sharp points, i.e. the radius of any curvature of the rough boundary is small. Figure 11 shows these two limiting cases.

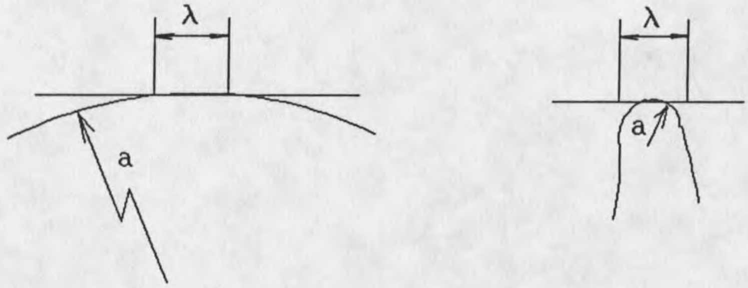

i). a >> λ (a is large)

ii). a < λ (a is small)

Figure 11. Two types of rough surfaces
a is the radius of curvature;
λ is the wave length of incident wave.

To describe the assumption quantitatively, let us assume that the radius of curvature of the rough boundary is at least m times larger than the wave length of the incident wave. This can be expressed as:

$$m\lambda \leq a \tag{4-72}$$

where a is the local radius of curvature at any point; λ is the wave length of the incident wave; m is a positive number and greater than 1 ($m > 1$).

For the two-dimensional problem considered in this paper, the definition of the radius of the curvature of the rough boundary denoted by h(x) can be described by the following equation:

$$a=-\frac{\left[1+\left(\dfrac{\partial h(x)}{\partial x}\right)^2\right]^{3/2}}{\dfrac{\partial^2 h(x)}{\partial x^2}} \tag{4-73}$$

If the function h(x) is given, the radius of the curvature can be easily obtained from Eq.(4-73). Here we use both cases (i.e. h(x) is given and h(x) is random) to set up the restriction about the wavelength of the incident wave and the roughness of the boundary.

If h(x) is given and has, for example, the sinusoidal profile

$$h(x)=h_o\cos px \tag{4-74}$$

the radius of the curvature can be written as:

$$a=\frac{\left(1+h_o^2p^2\sin^2px\right)^{3/2}}{h_op^2\cos px} \tag{4-75}$$

To find the strictest condition on the radius of the curvature and the wavelength, we need to determine the minimum radius of the curvature. From equation (4-75), this is given by

$$a_{\min}=\frac{1}{h_o p^2} \tag{4-76}$$

Therefore the restriction (4-72) becomes

$$m\lambda \le \frac{1}{h_o p^2} \tag{4-77}$$

If we describe the incident wave in terms of frequency and wave speed, the restriction in (4-77) can be written as

$$F \ge m c h_o p^2 \tag{4-78}$$

where c is the wave speed of the incident wave; F is the frequency of the incident wave.

For a random boundary, properties of the curvature can be described by the standard deviation σ, and the correlation length λ_o. If we replace h_o and p in Eq.(4-78) with σ and $1/\lambda_o$, respectively, the restriction for the random case of a rough boundary, from the basic idea discussed above, can be expressed as

$$F \ge \frac{m\sigma c}{\lambda_o^2} \tag{4-79}$$

If the values of the roughness (denoted by h_o and p or σ and λ_o), the wave speed c, and the factor m are given, we can have the exact value for the frequency needed in this restriction from Eqs. (4-78) or (4-79).

In many practical examples of rough surfaces in modern industries, for instance, fatigue cracks or manufacturing defects, the typical values of the roughness (Billy, et al 1980), in terms of the root mean square height and the correlation length, are

$$\sigma \approx 0.12\,(mm) \tag{4-80a}$$

$$\lambda_o \approx 0.65\,(mm) \tag{4-80b}$$

Waves propagate at different speeds in different materials. Therefore the corresponding values of frequencies in the restriction (4-78) or (4-79) vary. For some typical materials (say steel, copper, and aluminum), if the value of the factor m is chosen, for example, m=3 (Ogilvy, 1985), the values of the required frequencies for the restriction can be determined. Table 1 shows the values of compression wave speeds, factor m, and corresponding frequencies.

Table 1. Values of required frequencies for the Kichhoff approximation

material	p-wave speed (m/sec)	frequency (MHz)	
		m=3	m=4
steel	5900	5.027	6.703
copper	4600	3.920	5.226
aluminum	6300	5.368	7.157

From these values of the frequencies listed in Table 1, it is clear that the Kirchhoff approximation is a high frequency approximation.

Now let us consider the second assumption in the Kirchhoff approximation. Since shadowing effects (see Fig. 12) and multiple scattering (see Fig. 13) are both neglected in this assumption, the incident angle measured from the normal to the mean plane must be small enough such that this assumption is acceptable. It is obvious that there is more chance for the shadowing effects and the multiple scattering to occur as the incident angle increases. The problem of shadowing and multiple scattering is quite complicated. Therefore exact restrictions on this subject can be hardly obtained. Here we discuss an approximated method for this restriction. A description for this restriction can be obtained through a geometrical construction (see Fig. 14).

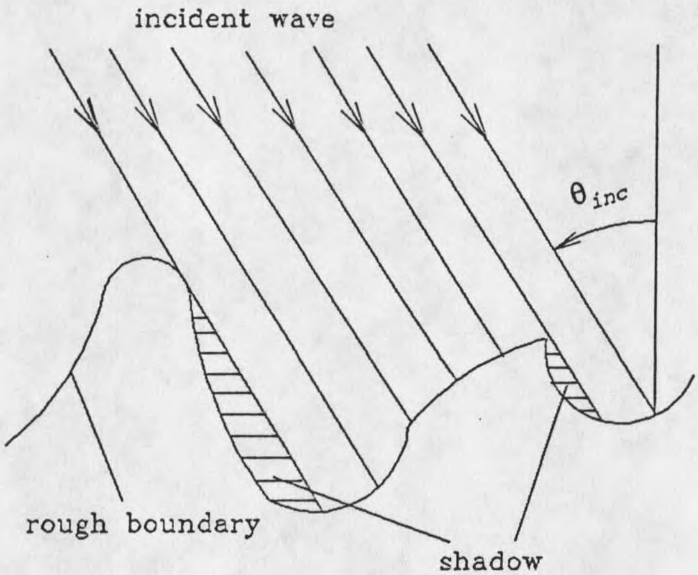

Figure 12. Shadowing effects

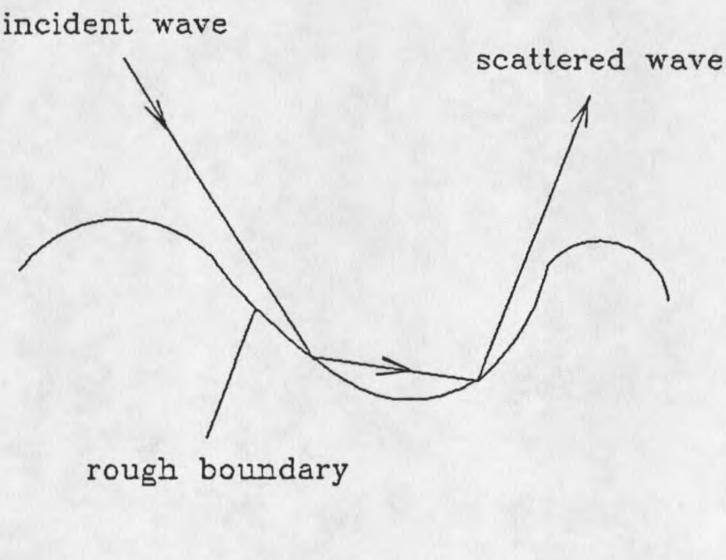

Figure 13. Multiple scattering

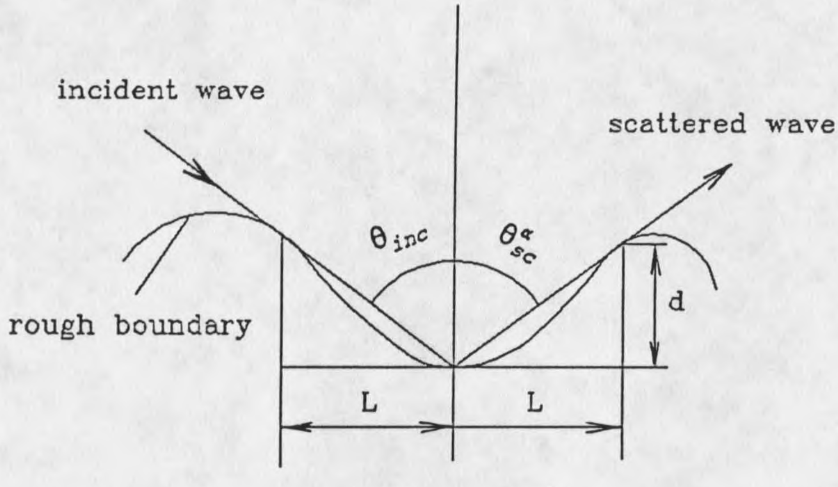

Figure 14. Restriction on shadowing effects and multiple scattering

In this approximated method, the most important consideration of the restriction on shadowing effects and multiple scattering should focus on the incident angle as well as the highest points and the lowest points on the rough boundary, because these high points block the path of the incident wave and the reflected wave. If the incident angle is very large, some form of shadowing effects or multiple scattering will occur. Therefore to satisfy the assumption on the shadowing and multiple scattering, we need to consider the following inequalities (Ogilvy 1985):

$$\theta_{inc}<\theta_{cr} \tag{4-81a}$$

$$\theta^{\alpha}_{sc}<\theta_{cr}\ ,\ \alpha=p,s \tag{4-81b}$$

where θ^{p}_{sc} and θ^{s}_{sc} are the angles of the scattered P-wave and

SV-wave, respectively; θ_{cr} is the critical angle, and given by

$$\theta_{cr}=\arctan\frac{L}{d} \tag{4-82}$$

For a real rough surface, the values of the d and L vary along x-axis. Here we just consider the average case of the roughness. This leads to

$$\theta_{cr}=\arctan\frac{\lambda_o}{\sigma} \tag{4-83}$$

Using the previously given values of σ and λ_o, the critical angle will be $\theta_{cr}=80^o$. It is clear that if σ increases or λ_o decreases, the restriction on the incident angle is more severe.

For a given incident wave, the angles θ^p_{sc} and θ^s_{sc} are different because of their different wavenumbers. For example, for an incident P-wave with the angle $\theta_{inc}=80^o$, from Eqs. (4-41)-(4-43), we have $\theta^p_{sc}=80^o$ and $\theta^s_{sc}=33^o$. For an incident SV-wave with the angle $\theta_{inc}=33^o$, from Eqs. (4-67)-(4-69), we have $\theta^p_{sc}=80^o$ and $\theta^s_{sc}=33^o$. Therefore, in order to satisfy the inequalities in Eq. (4-81), we need the restriction on the incident angle as follows:

$$\theta_{inc}<80^o \qquad \text{for P-wave}$$

$$\theta_{inc}<33^o \qquad \text{for SV-wave}$$

CHAPTER 5

SOLUTIONS OF THE ELASTIC GREEN'S FUNCTIONS

In Chapter 3, we derived the general expressions of the scattered and the refracted fields described by surface integrals, given by Eqs. (3-32) and (3-33). In the surface integrals, the remaining unknown quantities which need to be determined are the elastic Green's functions for displacement and stress components. In order to evaluate the surface integrals, the Green's functions must to be determined explicitly. The governing equation used for this is given in Eq. (3-26). The relation between the Green's displacement tensor and the Green's stress tensor is

$$\tau^{G}_{ijk}=c_{ijlm}(u^{G}_{lk})_{,m} \tag{5-1}$$

In the present paper, we assume that the material is homogenous and isotropic. Therefore c_{ijlm} is given by (3-3a). Put this into Eq. (3-26), together with Eq. (3-4), we get

$$\mu(u^{G}_{ik})_{,jj}+(\lambda+\mu)(u^{G}_{ik})_{,ij}+\rho\omega^2 u_{ik}=-\delta_{ik}\delta(\underline{r}'-\underline{r}) \tag{5-2}$$

The solution to Eq. (5-2) is given by Achenbach, Gautesen, and McMaken (1982, p. 24) as

$$u_{ik}^{G}=\left(\frac{1}{\mu}\right)\left\{\delta_{ik}F(k_sR)+\frac{1}{k_s^2}[F(k_sR)-F(k_pR)]_{,ik}\right\} \tag{5-3}$$

With Eq. (3-4)

$$\tau_{ijk}^{G}=\left\{\frac{2}{k_s^2}[F(k_sR)-F(k_pR)]_{,ijk}+\delta_{ik}F(k_sR)_{,j}\right.$$

$$\left.+\delta_{jk}F(k_sR)_{,i}+\delta_{ij}\left(1-\frac{2k_p^2}{k_s^2}\right)F(k_pR)_{,k}\right\} \tag{5-4}$$

where

$$F(k_\alpha R)=\frac{\exp(ik_\alpha R)}{4\pi R} \qquad \alpha=p,\ s \tag{5-5}$$

and

$$R=|\underline{r}'-\underline{r}| \tag{5-6}$$

Equations (5-3) and (5-4) are the Green's functions of the displacement and the stress components in region A. Similarly we can obtain the solutions of the Green's functions of the displacement and stress components in region B. The solutions for region B have the same form as the solutions for region A, and the only difference is that material properties of region B are different from region A. Therefore all parameters, related to material properties, involved in the solutions should be written with either superscripts B or subscripts B, for example, μ^B, λ^B, etc.

For most practical applications, the far-field approximation is considered as a convenient way to simplify the calculation and performed as follows (Achenbach, Gautesen, and McMaken 1982, p25). Assume that the distance between the observation point P and the origin is much larger than the distance between any point Q on the boundary and the origin (see Fig. 15).

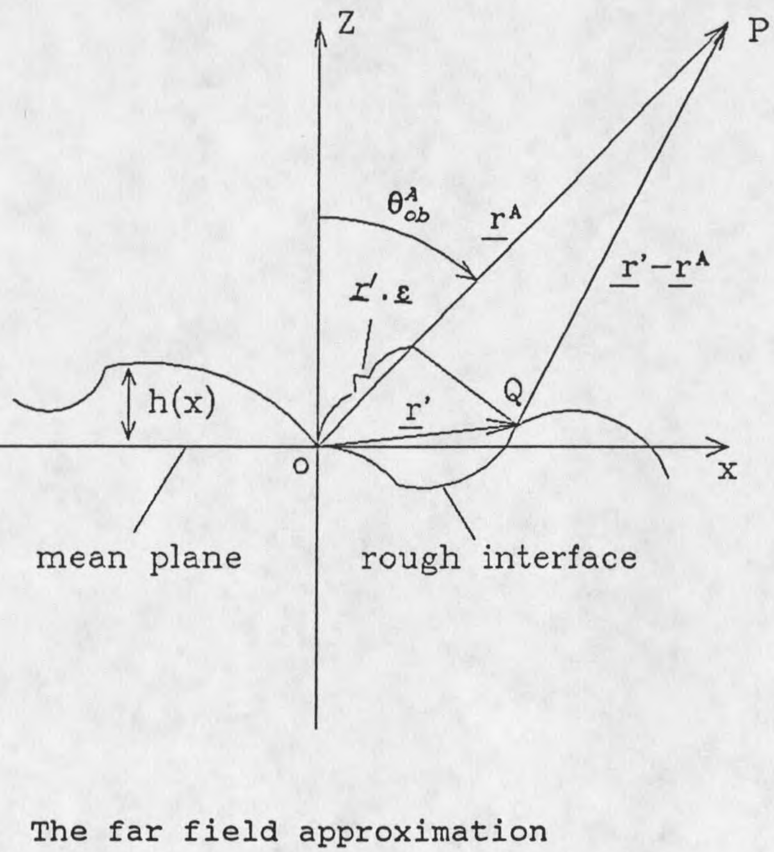

Figure 15. The far field approximation

Therefore we have

$$|\underline{r}| \gg |\underline{r}'| \tag{5-7}$$

$$R=|\underline{r}'-\underline{r}| \approx r-\underline{r}'.\underline{\varepsilon} \tag{5-8}$$

where $\underline{\epsilon}$ is a unit vector in the direction of $\underline{r}$, and can be written as

$$\underline{\varepsilon}=\frac{\underline{r}}{|\underline{r}|} \tag{5-9}$$

and

$$r=|\underline{r}|=(x^2+y^2+z^2)^{\frac{1}{2}} \tag{5-10}$$

In Eq. (5-8) the vector $\underline{r}$' denotes the position of any point on the interface, and can be written as

$$\underline{r}'=x\underline{i}+h(x)\underline{k} \tag{5-11}$$

With Eq. (5-8), Eq. (5-5) becomes

$$F(k_\alpha R)=\frac{\exp(ik_\alpha R)}{4\pi R} \approx \frac{\exp[ik_\alpha(r-\underline{r}'.\underline{\varepsilon})]}{4\pi r} \qquad \alpha=p,s \tag{5-12}$$

From the far field approximation and appropriate derivatives of the terms $F(k_\alpha R)$ Eqs. (5-3) and (5-4) can be written as

$$u_{ik}^{G}=u_{ik}^{G/p}+u_{ik}^{G/s} \tag{5-13}$$

$$\tau_{ijk}^{G}=\tau_{ijk}^{G/p}+\tau_{ijk}^{G/s} \tag{5-14}$$

The displacement and the stress components in Eqs. (5-13) and (5-14) show that both contain two parts, the longitudinal part and the transverse part.

By taking the derivative of Eqs. (5-3) and (5-4), the longitudinal and transverse components of the Green's functions can be written as (Achenbach, Gautesen, and McMaken 1982, p. 25)

$$u_{ik}^{G/p}=A_{ik}^{p}G(k_p r) \tag{5-15}$$

$$u_{ik}^{G/s}=A_{ik}^{s}G(k_s r) \tag{5-16}$$

$$\tau_{ijk}^{G/p}=iH_{ijk}^{p}G(k_p r) \tag{5-17}$$

$$\tau_{ijk}^{G/s}=iH_{ijk}^{s}G(k_s r) \tag{5-18}$$

where

$$G(k_p r)=\frac{e^{ik_p r}}{4\pi r}e^{-ik_p r'\cdot\underline{x}} \tag{5-19a}$$

$$G(k_s r) = \frac{e^{ik_s r}}{4\pi r} e^{-ik_s \underline{r}'\cdot\underline{\varepsilon}} \tag{5-19b}$$

and

$$A_{ik}^{p} = \frac{1}{\lambda^A + 2\mu^A} \varepsilon_i \varepsilon_k \tag{5-20}$$

$$A_{ik}^{s} = \frac{1}{\mu^A} (\delta_{ik} - \varepsilon_i \varepsilon_k) \tag{5-21}$$

$$H_{ijk}^{p} = k_p [2\kappa^{-2} \varepsilon_i \varepsilon_j + (1 - 2\kappa^{-2}) \delta_{ij}] \varepsilon_k \tag{5-22}$$

$$H_{ijk}^{s} = k_s [\delta_{ik} \varepsilon_j + \delta_{jk} \varepsilon_i - 2\varepsilon_i \varepsilon_j \varepsilon_k] \tag{5-23}$$

The symbols ϵ_i, ϵ_j and ϵ_k denote the components of the unit vector defined in Eq. (5-9). The symbol κ is defined in Eq. (4-26).

In region A, the unit vector and its components have the forms

$$\underline{\varepsilon}^A = \sin\theta_{ob}^A \underline{i} + \cos\theta_{ob}^A \underline{k} \tag{5-24}$$

$$\varepsilon_1^A = \sin\theta_{ob}^A \tag{5-25a}$$

$$\varepsilon_2^A = 0 \tag{5-25b}$$

$$\varepsilon_3^A=\cos\theta_{ob}^A \qquad (5\text{-}25c)$$

where $\theta^A{}_{ob}$ is called the observation angle as shown in Fig. 15. Similarly, In region B, we have

$$\underline{\varepsilon}^B=\sin\theta_{ob}^B\underline{i}-\cos\theta_{ob}^B\underline{k} \qquad (5\text{-}26)$$

$$\varepsilon_1^B=\sin\theta_{ob}^B \qquad (5\text{-}27a)$$

$$\varepsilon_2^B=0 \qquad (5\text{-}27b)$$

$$\varepsilon_3^B=-\cos\theta_{ob}^B \qquad (5\text{-}27c)$$

Therefore the parameters $A^p{}_{ik}$, $A^s{}_{ik}$, $H^p{}_{ijk}$, and $H^s{}_{ijk}$ involved in solutions of Green's functions can be expressed in terms of the observation angle. When Eqs. (5-24), (5-25) are substituted into Eqs. (5-20)-(5-23) we get

$$A_{11}^{p/A}=\frac{1}{\lambda^A+2\mu^A}\sin^2\theta_{ob}^A \qquad (5\text{-}28a)$$

$$A_{11}^{s/A}=\frac{1}{\mu^A}\cos^2\theta_{ob}^A \qquad (5\text{-}28b)$$

$$A_{31}^{p/A}=\frac{1}{\lambda^A+2\mu^A}\sin\theta_{ob}^A\cos\theta_{ob}^A \qquad (5\text{-}28c)$$

$$A_{31}^{s/A}=-\frac{1}{\mu^A}\sin\theta_{ob}^A\cos\theta_{ob}^A \tag{5-28d}$$

$$H_{111}^{p/A}=k_p^A\left[1-2\frac{(k_p^A)^2}{(k_s^A)^2}\right]\sin\theta_{ob}^A+2\frac{(k_p^A)^3}{(K_s^A)^2}\sin^3\theta_{ob}^A \tag{5-29a}$$

$$H_{111}^{s/A}=2k_s^A\sin\theta_{ob}^A\cos^2\theta_{ob}^A \tag{5-29b}$$

$$H_{131}^{p/A}=2\frac{(k_p^A)^3}{(k_s^A)^2}\sin^2\theta_{ob}^A\cos\theta_{ob}^A \tag{5-29c}$$

$$H_{131}^{s/A}=k_s^A\cos\theta_{ob}^A(1-2\sin^2\theta_{ob}^A) \tag{5-29d}$$

$$H_{331}^{p/A}=k_p^A\left[1-2\frac{(k_p^A)^2}{(k_s^A)^2}\right]\sin\theta_{ob}^A+2\frac{(k_p^A)^3}{(k_s^A)^2}\sin\theta_{ob}^A\cos^2\theta_{ob}^A \tag{5-29e}$$

$$H_{331}^{s/A}=-2k_s^A\sin\theta_{ob}^A\cos^2\theta_{ob}^A \tag{5-29f}$$

In our two-dimensional problem the second component, the component in y-direction, vanishes. The parameters of the component in z-direction are

$$A_{13}^{p/A}=\frac{1}{\lambda^A+2\mu^A}\sin\theta_{ob}^A\cos\theta_{ob}^A \tag{5-30a}$$

$$A_{13}^{s/A}=-\frac{1}{\mu^A}\sin\theta_{ob}^A\cos\theta_{ob}^A \tag{5-30b}$$

$$A_{33}^{p/A}=\frac{1}{\lambda^A+2\mu^A}\cos^2\theta_{ob}^A \tag{5-30c}$$

$$A_{33}^{s/A}=\frac{1}{\mu^A}\sin^2\theta_{ob}^A \tag{5-30d}$$

$$H_{113}^{p/A}=k_p^A\left[1-2\frac{(k_p^A)^2}{(k_s^A)^2}\right]\cos\theta_{ob}^A+2\frac{(k_p^A)^3}{(k_s^A)^2}\sin^2\theta_{ob}^A\cos\theta_{ob}^A \tag{5-31a}$$

$$H_{113}^{s/A}=-2k_s^A\sin^2\theta_{ob}^A\cos\theta_{ob}^A \tag{5-31b}$$

$$H_{133}^{p/A}=2\frac{(k_p^A)^3}{(k_s^A)^2}\sin\theta_{ob}^A\cos^2\theta_{ob}^A \tag{5-31c}$$

$$H_{133}^{s/A}=k_s^A\sin\theta_{ob}^A(1-2\cos^2\theta_{ob}^A) \tag{5-31d}$$

$$H_{333}^{p/A}=k_p^A\left[1-2\frac{(k_p^A)^2}{(k_s^A)^2}\right]\cos\theta_{ob}^A+2\frac{(k_p^A)^3}{(k_s^A)^2}\cos^3\theta_{ob}^A \tag{5-31e}$$

$$H_{333}^{p/A}=2k_s^A\sin^2\theta_{ob}^A\cos\theta_{ob}^A \tag{5-31f}$$

In region B, with Eqs. (5-26), (5-27) the parameters of the Green's functions have the similar form. The non-zero components are

$$A_{11}^{p/B}=\frac{1}{\lambda^B+2\mu^B}\sin^2\theta_{ob}^B \tag{5-32a}$$

$$A_{11}^{s/B}=\frac{1}{\mu^B}\cos^2\theta_{ob}^B \tag{5-32b}$$

$$A_{31}^{p/B}=-\frac{1}{\lambda^B+2\mu^B}\sin\theta_{ob}^B\cos\theta_{ob}^B \tag{5-32c}$$

$$A_{31}^{s/B}=\frac{1}{\mu^B}\sin\theta_{ob}^B\cos\theta_{ob}^B \tag{5-32d}$$

$$H_{111}^{p/B}=k_p^B\left[1-2\frac{(k_p^B)^2}{(k_s^B)^2}\right]\sin\theta_{ob}^B+2\frac{(k_p^B)^3}{(k_s^B)^2}\sin^3\theta_{ob}^B \tag{5-33a}$$

$$H_{111}^{s/B}=2k_s^B\sin\theta_{ob}^B\cos^2\theta_{ob}^B \tag{5-33b}$$

$$H_{131}^{p/B}=-2\frac{(k_p^B)^3}{(k_s^B)^2}\sin^2\theta_{ob}^B\cos\theta_{ob}^B \tag{5-33c}$$

$$H_{131}^{s/B}=k_s^B\cos\theta_{ob}^B(2\cos^2\theta_{ob}^B-1) \tag{5-33d}$$

$$H_{331}^{p/B}=k_p^B\left[1-2\frac{(k_p^B)^2}{(k_s^B)^2}\right]\sin\theta_{ob}^B+2\frac{(k_p^B)^3}{(k_s^B)^2}\sin\theta_{ob}^B\cos^2\theta_{ob}^B \tag{5-33e}$$

$$H_{331}^{s/B}=-2k_s^B\sin\theta_{ob}^B\cos^2\theta_{ob}^B \tag{5-33f}$$

$$A_{13}^{p/B}=\frac{1}{\lambda^{B}+2\mu^{B}}\sin\theta_{ob}^{B}\cos\theta_{ob}^{B} \tag{5-34a}$$

$$A_{13}^{s/B}=\frac{1}{\mu^{B}}\sin\theta_{ob}^{B}\cos\theta_{ob}^{B} \tag{5-34b}$$

$$A_{33}^{p/B}=\frac{1}{\lambda^{B}+2\mu^{B}}\cos^{2}\theta_{ob}^{B} \tag{5-34c}$$

$$A_{33}^{s/B}=\frac{1}{\mu^{B}}\sin^{2}\theta_{ob}^{B} \tag{5-34d}$$

$$H_{113}^{p/B}=-k_{p}^{B}\left[1-2\frac{(k_{p}^{B})^{2}}{(k_{s}^{B})^{2}}\right]\cos\theta_{ob}^{B}+2\frac{(k_{p}^{B})^{3}}{(k_{s}^{B})^{2}}\sin^{2}\theta_{ob}^{B}\cos\theta_{ob}^{B} \tag{5-35a}$$

$$H_{113}^{s/B}=2k_{s}^{B}\sin^{2}\theta_{ob}^{B}\cos\theta_{ob}^{B} \tag{5-35b}$$

$$H_{133}^{p/B}=2\frac{(k_{p}^{B})^{2}}{(k_{s}^{B})^{2}}\sin\theta_{ob}^{B}\cos^{2}\theta_{ob}^{B} \tag{5-35c}$$

$$H_{133}^{s/B}=k_{s}^{B}\sin\theta_{ob}^{B}(1-2\cos^{2}\theta_{ob}^{B}) \tag{5-35d}$$

$$H_{333}^{p/B}=-k_{p}^{B}\left[1-2\frac{(k_{p_{B}})^{2}}{(k_{s}^{B})^{2}}\right]\cos\theta_{ob}^{B}+2\frac{(k_{p}^{B})^{3}}{(k_{s}^{B})^{2}}\cos^{3}\theta_{ob}^{B} \tag{5-35e}$$

$$H_{333}^{s/B}=-2k_{s}^{B}\sin^{2}\theta_{ob}^{B}\cos\theta_{ob}^{B} \tag{5-35f}$$

Finally, with Eqs. (5-11), (5-24) and (5-26) we have

$$\underline{r}' \cdot \underline{\varepsilon}^{A} = x\sin\theta_{ob}^{A} + h(x)\cos\theta_{ob}^{A} \tag{5-36}$$

$$\underline{r}' \cdot \underline{\varepsilon}^{B} = x\sin\theta_{ob}^{B} - h(x)\cos\theta_{ob}^{B} \tag{5-37}$$

CHAPTER 6

THE GENERAL SOLUTIONS OF DISPLACEMENT COMPONENTS OF THE SCATTERED AND THE REFRACTED FIELDS

Now we are able to derive the general solutions of the scattered and refracted fields. Notice that with Eqs. (4-19) and (4-20), the scattered and the refracted fields on the rough boundary can be written in terms of the known incident field, and that from Chapter 5 the Green's functions are also known. Therefore the surface integrals Eqs. (3-32) and (3-33) can be evaluated.

However, Eqs. (3-32) and (3-33) also contain quantities related to the rough interface, for example, the unit normal of the rough surface, differential element ds, and etc. Therefore we want to discuss the characteristics of the rough interface before deriving the general solutions of the displacement components.

The Characteristics of the Rough Interface

The expression of the scattered and refracted fields contain the form of the unit normal $\underline{n}$ of the rough surface. From the height function $z = h(x)$, we can find the surface normal as

$$\underline{n}=\frac{\nabla F}{|\nabla F|} \tag{6-1}$$

where $F = z - h(x) = 0$

$$\nabla F=\frac{\partial F}{\partial x}\underline{i}+\frac{\partial F}{\partial Z}\underline{k}=-h'(x)\,\underline{i}+\underline{k} \qquad (6\text{-}2)$$

$$|\nabla F|=\left\{\left(\frac{\partial F}{\partial x}\right)^2+\left(\frac{\partial F}{\partial z}\right)^2\right\}^{\frac{1}{2}}$$

$$=\left[1+h'^2(x)\right]^{\frac{1}{2}} \qquad (6\text{-}3)$$

therefore

$$\underline{n}=\frac{1}{\left[1+h'^2(x)\right]^{\frac{1}{2}}}\left[-h'(x)\,\underline{i}+\underline{k}\right] \qquad (6\text{-}4)$$

and

$$n_1=n_x=\frac{-h'(x)}{\left[1+h'(x)\right]^{\frac{1}{2}}} \qquad (6\text{-}5a)$$

$$n_2=n_y=0 \qquad (6\text{-}5b)$$

$$n_3=n_z=\frac{1}{\left[1+h'^2(x)\right]^{\frac{1}{2}}} \qquad (6\text{-}5c)$$

In terms of the angle ß between the surface normal and the z-axis (see Figure 10), the surface normal can also be written as

$$\underline{n}=-\sin\bar{\beta}\,\underline{i}+\cos\bar{\beta}\,\underline{k} \qquad (6\text{-}6)$$

where

$$\bar{\beta}=\arctan[h'(x)] \tag{6-7}$$

Then

$$n_1=n_x=\frac{-h'(x)}{[1+h'^2(x)]^{\frac{1}{2}}}=-\sin\bar{\beta} \tag{6-8a}$$

$$n_2=n_y=0 \tag{6-8b}$$

$$n_3=n_z=\frac{1}{[1+h'^2(x)]^{\frac{1}{2}}}=\cos\bar{\beta} \tag{6-8c}$$

In terms of the height function h(x), the differential element ds can be written as

$$ds=\frac{dx}{\cos\bar{\beta}}=[1+h'^2(x)]^{\frac{1}{2}}dx \tag{6-9}$$

Therefore we have

$$n_1 ds=-h'(x)\,dx \tag{6-10}$$

$$n_3 ds=dx \tag{6-11}$$

The limits of integration in the x-direction are set as $(L_1,\ L_2\ )$.

The General Solutions Due to An Incident P-wave

In this work, both incident pressure wave and incident shear wave are considered. First let us look at the general solutions due to the incident pressure wave.

In terms of components, the general solutions for displacement given by equations (3-32) and (3-33), can be written as

$$u_1^A(\underline{r}) = \int_s [u_1^A \tau_{111}^G n_1 + u_1^A \tau_{131}^G n_3 + u_3^A \tau_{311}^G n_1 + u_3^A \tau_{331}^G n_3$$

$$- u_{11}^G \tau_{11}^A n_3 - u_{11}^G \tau_{13} n_3 - u_{31}^G \tau_{31}^A n_1 - u_{31}^G \tau_{33} n_3]\, ds(\underline{r}') \qquad (6\text{-}12a)$$

$$u_2^A(\underline{r}) = 0 \qquad (6\text{-}12b)$$

$$u_3^A(\underline{r}) = \int_s [u_1^A \tau_{113}^G n_1 + u_1^A \tau_{133}^G n_3 + u_3^A \tau_{313}^G n_1 + u_3^A \tau_{333}^G n_3$$

$$- u_{13}^G \tau_{11}^A n_1 - u_{13}^G \tau_{13}^A n_3 - u_{33}^G \tau_{31}^A n_1 - u_{33}^G \tau_{33}^A n_3]\, ds(\underline{r}') \qquad (6\text{-}12c)$$

and

$$u_1{}^B(\underline{r}) = \int_s [\tau_{11}^B u_1{}^G n_1 + \tau_{13}^B u_{11}^G n_3 + \tau_{131}^B u_{31}^G n_1 + \tau_{33}^B u_{31}^G n_3$$

$$- u^{1\,B} \tau_{111}^G n_1 - u_1{}^B \tau_{131}^G n_3 - u_3{}^B \tau_{311}^G n_1 - u_3{}^B \tau_{331} n_3]\, ds(\underline{r}') \qquad (6\text{-}13a)$$

$$u_2{}^B(\underline{r}) = 0 \qquad (6\text{-}13b)$$

$$u_3^B(\underline{r}) = \int_S [\tau_{11}^B u_{13}^G n_1 + \tau_{13}^B u_{13}^G n_3 + \tau_{31}^B u_{33}^G n_1 + \tau_{33}^B u_{33}^G n_3$$

$$- u_1^B \tau_{113}^G n_1 - u_1^B \tau_{133}^G n_3 - u_3^B \tau_{313}^G n_1 - u_3^B \tau_{333}^G n_3]\, ds(\underline{r}') \qquad (6\text{-}13c)$$

In Eqs. (6-12) and (6-13) $u^G{}_{ik}$, $\tau^G{}_{ijk}$ are given by Eqs. (5-13)-(5-16), and $u^A{}_i$, $\tau^A{}_{ik}$, $u^B{}_i$, $\tau^B{}_{ik}$, are given by Eqs. (4-19)-(4-22). Note that from Eqs. (5-13)-(5-16) and Eqs. (5-28)-(5-31) the general functions for displacement and stress are zero whenever the subscripts i,j or k have a value of 2.

To evaluate the integral expressions of the scattered and refracted fields, we need to substitute Eqs. (4-19a)-(4-22b) and (5-15a)-(5-16b) into Eqs. (6-12) and (6-13). However, this will result in long and complicated formulas. Now we want to simplify the formulas. First let us rewrite the scattered and refracted fields of the displacement and stress components on the interface, Eqs. (4-19)-(4-22), as

$$u_1^A = f_1^{A/p} \exp(i\eta) \qquad (6\text{-}14a)$$

$$u_3^A = f_3^{A/p} \exp(i\eta) \qquad (6\text{-}14b)$$

$$\tau_{33}^A = i f_{33}^{A/p} \exp(i\eta) \qquad (6\text{-}14c)$$

$$\tau_{13}^A = i f_{13}^{A/p} \exp(i\eta) \qquad (6\text{-}14d)$$

For region B, we have

$$u_1^B = f_1^{B/p}\exp(i\eta) \tag{6-15a}$$

$$u_3^B = f_3^{B/p}\exp(i\eta) \tag{6-15b}$$

$$\tau_{33}^B = i f_{33}^{B/p}\exp(i\eta) \tag{6-16a}$$

$$\tau_{13}^B = i f_{13}^{B/p}\exp(i\eta) \tag{6-16b}$$

where η is given by Eq. (4-18), and

$$f_1^{A/p} = A_{inc}\left[R_1^p \sin\beta^A + R_2^p \cos\gamma^A\right] \tag{6-17a}$$

$$f_3^{A/p} = A_{inc}\left[R_1^p \cos\beta^A - R_2^p \sin\gamma^A\right] \tag{6-17b}$$

$$f_{11}^{A/p} = A_{inc}k_p\left\{R_1^p\left[(\lambda^A+2\mu^A)\sin\theta_{inc}\sin\beta^A - \lambda\cos\theta_{inc}\cos\beta^A\right]\right.$$

$$\left. + R_2^p\left[(\lambda^A+2\mu^A)\sin\theta_{inc}\cos\gamma^A + \lambda^A\cos\theta_{inc}\sin\gamma^A\right]\right\} \tag{6-17c}$$

$$f_{13}^{A/p} = f_{31}^{A/p} = A_{inc}k_p\mu^A\left[R_1^p(\sin\theta_{inc}\cos\beta^A - \cos\theta_{inc}\sin\beta^A)\right.$$

$$\left. - R_2^p(\sin\theta_{inc}\sin\gamma^A + \cos\theta_{inc}\cos\gamma^A)\right] \tag{6-17d}$$

$$f_{33}^{A/p} = A_{inc}k_p\left\{R_1^p\left[\lambda^A\sin\theta_{inc}\sin\beta^A - (\lambda^A+2\mu^A)\cos\theta_{inc}\cos\beta^A\right.\right.$$

$$\left. + R_2^p\left[\lambda^A\sin\theta_{inc}\cos\gamma^A + (\lambda^A+2\mu^A)\cos\theta_{inc}\sin\gamma^A\right]\right\} \tag{6-17e}$$

For region B, we have

$$f_1^{B/p}=A_{inc}(R_3^p\sin\beta^B-R_4^p\sin\gamma^B) \tag{6-18a}$$

$$f_3^{B/p}=-A_{inc}(R_3^p\cos\beta^B+R_4^B\sin\gamma^B) \tag{6-18b}$$

$$f_{11}^{B/p}=A_{inc}k_p\{R_3^p[(\lambda^B+2\mu^B)\sin\theta_{inc}\sin\beta^B+\lambda^B\cos\theta_{inc}\cos\beta^B$$

$$+R_4^p[\lambda^B\cos\theta_{inc}\sin\gamma^B-(\lambda^B+2\mu^B)\sin\theta_{inc}\sin\gamma^B]\} \tag{6-18c}$$

$$f_{13}^{B/p}=f_{31}^{B/p}=A_{inc}k_p\mu^B[R_3^{B/p}(\cos\theta_{inc}\sin\beta^B+\sin\theta_{inc}\cos\beta^B)$$

$$+R_4^p(\sin\theta_{inc}\sin\gamma^B-\cos\theta_{inc}\sin\gamma^B)] \tag{6-18d}$$

$$f_{33}^{B/p}=A_{inc}k_p\{R_3^p[(\lambda^B+2\mu^B)\cos\theta_{inc}\cos\beta^B+\lambda^B\sin\theta_{inc}\sin\beta$$

$$+R_4^p[(\lambda^B+2\mu^B)\cos\theta_{inc}\sin\gamma^B-\lambda^B\sin\theta_{inc}\sin\gamma^B]\} \tag{6-18e}$$

By substitution of Eqs. (5-11), (5-12) and (6-14a)-(6-15d) into Eqs. (6-12a)-(6-13c), the scattered and refracted fields of the displacements can be written as

$$u_1^A=i\int_S e^{i\eta}\{n_1[G(k_pr)(H_{111}^{p/A}f_1^{A/p}+H_{131}^{p/A}f_3^{A/p}-A_{11}^{p/A}f_{11}^{A/p}-A_{31}^{p/A}f_{31}^{A/p})$$

$$+G(k_sr)(H_{111}^{s/A}f_1^{A/p}+H_{131}^{s/A}f_3^{A/p}-A_{11}^{s/A}f_{11}^{A/p}-A_{31}^{s/A}f_{31}^{A/p})]$$

$$+n_3[G(k_pr)(H_{131}^{p/A}f_1^{A/p}+H_{331}^{p/A}f_3^{A/p}-A_{11}^{p/A}f_{13}^{A/p}-A_{31}^{p/A}f_{33}^{A/p})$$

$$+G(k_sr)(H_{131}^{s/A}f_1^{A/p}+H_{331}^{s/A}f_3^{A/p}-A_{11}^{s/A}f_{13}^{A/p}-A_{31}^{s/A}f_{33}^{A/p})]\}ds \tag{6-19a}$$

$$u_2^A=0 \tag{6-19b}$$

$$u_3^A=i\int_S e^{i\eta}\{n_1[G(k_p r)\,(H_{113}^{p/A}f_1^{A/p}+H_{133}^{p/A}f_3^{A/p}-A_{13}^{p/A}f_{11}^{A/p}-A_{33}^{p/A}f_{31}^{A/p})$$

$$+G(k_s r)\,(H_{113}^{s/A}f_1^{A/p}+H_{133}^{s/A}f_3^{A/p}-A_{13}^{s/A}f_{11}^{A/p}-A_{33}^{s/A}f_{31}^{A/p})$$

$$+n_3[G(k_p r)\,(H_{133}^{p/A}f_1^{A/p}+H_{333}^{p/A}f_3^{A/p}-A_{13}^{p/A}f_{13}^{A/p}-A_{33}^{p/A}f_{33}^{A/p})$$

$$+G(k_s r)\,(H_{133}^{s/A}f_1^{A/p}+H_{333}^{s/A}f_3^{A/p}-A_{13}^{s/A}f_{13}^{A/p}-A_{33}^{s/A}f_{33}^{A/p})]\}ds \tag{6-19c}$$

For region B, we have

$$u_1^B=i\int_S e^{i\eta}\{n_1[G(k_{p/B}r)\,(H_{111}^{p/B}f_1^{B/p}+H_{131}^{p/B}f_3^{B/p}-A_{11}^{p/B}f_{11}^{B/p}-A_{31}^{p/B}f_{31}^{B/p})$$

$$+G(k_{s/B}r)\,(H_{111}^{s/B}f_1^{B/p}+H_{131}^{s/B}f_3^{B/p}-A_{11}^{s/B}f_{11}^{B/p}-A_{31}^{s/B}f_{31}^{B/p})]$$

$$+n_3[G(k_{p/B}r)\,(H_{131}^{p/B}f_1^{B/p}+H_{331}^{p/B}f_3^{B/p}-A_{11}^{p/B}f_{13}^{B/p}-A_{31}^{p/B}f_{33}^{B/p})$$

$$+G(k_{s/B}r)\,(H_{131}^{s/B}f_1^{B/p}+H_{331}^{s/B}f_3^{B/p}-A_{11}^{s/B}f_{13}^{B/p}-A_{31}^{s/B}f_{33}^{B/p})]\}ds \tag{6-20a}$$

$$u_2^B=0 \tag{6-20b}$$

$$u_3^B=i\int_S e^{i\eta}\{n_1[G(k_{p/B}r)\,(H_{113}^{p/B}f_1^{B/p}+H_{133}^{p/B}f_3^{B/p}-A_{13}^{p/B}f_{11}^{B/p}-A_{33}^{p/B}f_{31}^{B/p})$$

$$+G(k_{s/B}r)\,(H_{113}^{s/B}f_1^{B/p}+H_{133}^{s/B}f_3^{B/p}-A_{13}^{s/B}f_{11}^{B/p}-A_{33}^{s/B}f_{31}^{B/p})$$

$$n_3[G(k_{p/B}r)\,(H_{133}^{p/B}f_1^{B/p}+H_{333}^{p/B}f_3^{B/p}-A_{13}^{p/B}f_{13}^{B/p}-A_{33}^{p/B}f_{33}^{B/p})$$

$$+G(k_{s/B}r)\,(H_{133}^{s/B}f_1^{B/p}+H_{333}^{s/B}f_3^{B/p}-A_{13}^{s/B}f_{13}^{B/p}-A_{33}^{s/B}f_{33}^{B/p})]\}ds \tag{6-20c}$$

With Eqs. (5-18), (5-36) and (5-37) we can write

$$e^{i\eta}G(k_p r) = \frac{e^{ik_p r}}{4\pi r} e^{i[D_{p/A}x + E_{p/A}h(x)]} \tag{6-21a}$$

$$e^{i\eta}G(k_s r) = \frac{e^{ik_s r}}{4\pi r} e^{i[D_{s/A}x + E_{s/A}h(x)]} \tag{6-21b}$$

and for region B

$$e^{i\eta}G(k_{p/B} r) = \frac{e^{ik_{p/B} r}}{4\pi r} e^{i[D_{p/B}x + E_{p/B}h(x)]} \tag{6-22a}$$

$$e^{i\eta}G(k_{s/B} r) = \frac{e^{ik_{s/B} r}}{4\pi r} e^{i[D_{s/B}x + E_{s/B}h(x)]} \tag{6-22b}$$

where

$$D_{p/A} = k_p(\sin\theta_{inc} - \sin\theta_{ob}^A) \tag{6-23a}$$

$$E_{p/A} = -k_p(\cos\theta_{inc} + \cos\theta_{ob}^A) \tag{6-23b}$$

$$D_{s/A} = k_p\sin\theta_{inc} - k_s\sin\theta_{ob}^A \tag{6-23c}$$

$$E_{s/A} = -(k_p\cos\theta_{inc} + k_s\cos\theta_{ob}^A) \tag{6-23d}$$

and

$$D_{p/B} = k_p\sin\theta_{inc} - k_{p/B}\sin\theta_{ob}^B \tag{6-24a}$$

$$E_{p/B} = -(k_p\cos\theta_{inc} - k_{p/B}\cos\theta_{ob}^B) \tag{6-24b}$$

$$D_{s/B}=k_p\sin\theta_{inc}-k_{s/B}\sin\theta_{ob}^{B} \tag{6-24c}$$

$$E_{s/B}=-(k_p\cos\theta_{inc}-k_{s/B}\cos\theta_{ob}^{B}) \tag{6-24d}$$

After replacing all terms involved in the integrands of integrals (6-19) and (6-20) with equations (6-21) and (6-22) we have

$$u_1^A=\frac{ie^{ik_pr}}{4\pi r}\int_{L_1}^{L_2}\Big[-h(x)\,(H_{111}^{p/A}f_1^{A/p}+H_{131}^{p/A}f_3^{A/p}-A_{11}^{p/A}f_{11}^{A/p}-A_{31}^{p/A}f_{31}^{A/p})$$

$$+(H_{131}^{p/A}f_1^{A/p}+H_{331}^{p/A}f_3^{A/p}-A_{11}^{p/A}f_{13}^{A/p}-A_{31}^{s/A}f_{33}^{A/p})\Big]e^{i[D_{p/A}x+E_{p/A}h(x)]}dx$$

$$+\frac{ie^{ik_sr}}{4\pi r}\int_{L_1}^{L_2}\Big[-h(x)\,(H_{111}^{s/A}f_1^{A/p}+H_{131}^{s/A}f_3^{A/p}-A_{11}^{s/A}f_{11}^{A/p}-A_{31}^{s/A}f_{31}^{A/p})$$

$$+(H_{131}^{s/A}f_1^{A/p}+H_{331}^{s/A}f_3^{A/p}-A_{11}^{s/A}f_{13}^{A/p}-A_{31}^{s/A}f_{33}^{A/p})\Big]e^{i[D_{s/A}x+E_{s/A}h(x)]}dx \tag{6-25a}$$

$$u_2^A=0 \tag{6-25b}$$

$$u_3^A=\frac{ie^{ik_pr}}{4\pi r}\int_{L_1}^{L_2}\Big[-h'(x)\,(H_{113}^{p/A}f_1^{A/p}+H_{133}^{p/A}f_3^{A/p}-A_{13}^{p/A}f_{11}^{A/p}-A_{33}^{p/A}f_{31}^{A/p})$$

$$+(H_{133}^{p/A}f_1^{A/p}+H_{333}^{p/A}f_3^{A/p}-A_{13}^{p/A}f_{13}^{A/p}-A_{33}^{p/A}f_{33}^{A/p})\Big]e^{i[D_{p/A}x+E_{p/A}h(x)]}dx$$

$$+\frac{ie^{ik_s r}}{4\pi r}\int_{L_1}^{L_2}\Big[-h'(x)\,(H_{113}^{s/A}f_1^{A/p}+H_{133}^{p/A}f_3^{A/p}-A_{13}^{s/A}f_{11}^{A/p}-A_{33}^{s/A}f_{31}^{A/p})$$

$$+(H_{133}^{s/A}f_1^{A/p}+H_{333}^{s/A}f_3^{A/p}-A_{13}^{s/A}f_{13}^{A/p}-A_{33}^{s/A}f_{33}^{A/p})\Big]e^{i[D_{s/A}x+E_{s/A}h(x)]}dx \qquad (6\text{-}25c)$$

The equations (6-25a)-(6-25c) are the general solutions of the scattered field of the displacement components in region A.

In the similar way, we obtain the solutions for region B as:

$$u_1^B=\frac{ie^{ik_{p/B}r}}{4\pi r}\int_{L_1}^{L_2}\Big[-h(x)\,(H_{111}^{p/B}f_1^{B/p}+H_{131}^{p/B}f_3^{B/p}-A_{11}^{p/B}f_{11}^{B/p}-A_{31}^{p/B}f_{31}^{B/p})$$

$$+(H_{131}^{p/B}f_1^{B/p}+H_{331}^{p/B}f_3^{B/p}-A_{11}^{p/B}f_{13}^{B/p}-A_{31}^{p/B}f_{33}^{B/p})\Big]e^{i[D_{p/B}x+E_{p/B}h(x)]}dx$$

$$+\frac{ie^{ik_{s/B}r}}{4\pi r}\int_{L_1}^{L_2}\Big[-h'(x)\,(H_{111}^{s/B}f_1^{B/p}+H_{131}^{s/B}f_3^{B/p}-A_{11}^{s/B}f_{11}^{B/p}-A_{31}^{s/B}f_{31}^{B/p})$$

$$+(H_{131}^{s/B}f_1^{B/p}+H_{331}^{s/B}f_3^{B/p}-A_{11}^{s/B}f_{13}^{B/p}-A_{31}^{s/B}f_{33}^{B/p})\Big]e^{i[D_{s/B}x+E_{s/B}h(x)]}dx$$

(6-26a)

$$u_2^B=0 \qquad (6\text{-}26b)$$

$$u_3^B=\frac{ie^{ik_{p/B}r}}{4\pi r}\int_{L_1}^{L_2}\Big[-h'(x)\,(H_{113}^{p/B}f_1^{B/p}+H_{133}^{p/B}f_3^{B/p}-A_{13}^{p/B}f_{11}^{B/p}-A_{33}^{p/B}f_{31}^{B/p}$$

$$+\left(H_{133}^{p/B}f_1^{B/p}+H_{333}^{p/B}f_3^{B/p}-A_{13}^{p/B}f_{13}^{B/p}-A_{33}^{p/B}f_{33}^{B/p}\right)\Big]e^{i[D_{p/B}x+E_{p/B}h(x)]}dx$$

$$+\frac{ie^{ik_{s/B}r}}{4\pi r}\int_{L_1}^{L_2}\Big[-h'(x)\left(H_{113}^{s/B}f_1^{B/p}+H_{133}^{s/B}f_3^{B/p}-A_{13}^{s/B}f_{11}^{B/p}-A_{33}^{s/B}f_{31}^{B/p}\right)$$

$$+\left(H_{133}^{s/B}f_1^{B/p}+H_{333}^{s/B}f_3^{B/p}-A_{13}^{s/B}f_{13}^{B/p}-A_{33}^{s/B}f_{33}^{B/p}\right)\Big]e^{i[D_{s/B}x+E_{s/B}h(x)]}dx \qquad (6\text{-}26c)$$

The equations (6-26a)-(6-26c) are the general solutions of the refracted fields of the displacement components in region B.

The General Solutions Due to An Incident SV-wave

For the case of an incident shear wave, the general solutions of the displacement components of the scattered and the refracted fields can be obtained in the similar way applied for the case of the incident compression wave. In this case, the expression (6-16) in the section above becomes

$$\eta^s=k_s[x\sin\theta_{inc}-h(x)\cos\theta_{inc}] \qquad (6\text{-}27)$$

and

$$f_1^{A/s}=A_{inc}[R_1^s\sin\beta^A+R_2^s\cos\gamma^A] \qquad (6\text{-}28a)$$

$$f_3^{A/s}=A_{inc}[R_1^s\cos\beta^A-R_2^s\sin\gamma^A] \qquad (6\text{-}28b)$$

$$f_{11}^{A/s}=A_{inc}k_s\{R_1^s[(\lambda^A+2\mu^A)\sin\theta_{inc}\sin\beta^A-\lambda^A\cos\theta_{inc}\cos\beta^A$$

$$+R_2^s[(\lambda^A+2\mu^A)\sin\theta_{inc}\cos\gamma^A+\lambda^A\cos\theta_{inc}\sin\gamma^A]\} \qquad (6\text{-}28c)$$

$$f_{13}^{A/s}=f_{31}^{A/s}=A_{inc}k_s\mu^A[R_1^s(\sin\theta_{inc}\cos\beta^A-\cos\theta_{inc}\sin\beta^A)$$

$$-R_2^s(\sin\theta_{inc}\sin\gamma^A+\cos\theta_{inc}\cos\gamma^A)] \qquad (6\text{-}28d)$$

$$f_{33}^{A/s}=A_{inc}k_s\{R_1^s[\lambda^A\sin\theta_{inc}\sin\beta^A-(\lambda^A+2\mu^A)\cos\theta_{inc}\cos\beta^A$$

$$+R_2^s[\lambda^A\sin\theta_{inc}\cos\gamma^A+(\lambda^A+2\mu^A)\cos\theta_{inc}\sin\gamma^A]\} \qquad (6\text{-}28e)$$

For region B, we have

$$f_1^{B/s}=A_{inc}(R_3^s\sin\beta^B-R_4^s\sin\gamma^B) \qquad (6\text{-}29a)$$

$$f_3^{B/s}=-A_{inc}(R_3^s\cos\beta^B+R_4^s\sin\gamma^B) \qquad (6\text{-}29b)$$

$$f_{11}^{B/s}=A_{inc}k_s\{R_3^s[(\lambda^B+2\mu^B)\sin\theta_{inc}\sin\beta^B+\lambda^B\cos\theta_{inc}\cos\beta^B$$

$$+R_4^s[\lambda^B\cos\theta_{inc}\sin\gamma^B-(\lambda^B+2\mu^B)\sin\theta_{inc}\sin\gamma^B]\} \qquad (6\text{-}29c)$$

$$f_{13}^{B/s}=f_{31}^{B/s}=A_{inc}k_s\mu^B[R_3^s(\cos\theta_{inc}\sin\beta^B+\sin\theta_{inc}\cos\beta^B)$$

$$+R_4^s(\sin\theta_{inc}\sin\gamma^B-\cos\theta_{inc}\sin\gamma^B)] \qquad (6\text{-}29d)$$

$$f_{33}^{B/s}=A_{inc}k_s\{R_3^s[(\lambda^B+2\mu^B)\cos\theta_{inc}\cos\beta^B+\lambda^B\sin\theta_{inc}\sin$$

$$+R_4^s[(\lambda^B+2\mu^B)\cos\theta_{inc}\sin\gamma^B-\lambda^B\sin\theta_{inc}\sin\gamma^B]\} \qquad (6\text{-}29e)$$

Again for the case of the incident shear wave, the parameters expressed by Eqs. (6-23a) - (6-24d) become

$$D^s_{p/A}=k_s\sin\theta_{inc}-k_p\sin\theta^A_{ob} \tag{6-30a}$$

$$E^s_{p/A}=-k_s(\cos\theta_{inc}+\cos\theta^A_{ob}) \tag{6-30b}$$

$$D^s_{s/A}=k_s(\sin\theta_{inc}-\sin\theta^A_{ob}) \tag{6-30c}$$

$$E^s_{s/A}=-k_s(\cos\theta_{inc}+\cos\theta^A_{ob}) \tag{6-30d}$$

and for region B

$$D^s_{p/B}=k_s\sin\theta_{inc}-k_{p/B}\sin\theta^B_{ob} \tag{6-31a}$$

$$E^s_{p/B}=-(k_s\cos\theta_{inc}-k_{p/B}\cos\theta^B_{ob}) \tag{6-31b}$$

$$D^s_{s/B}=k_s\sin\theta_{inc}-k_{s/B}\sin\theta^B_{ob} \tag{6-31c}$$

$$E^s_{s/B}=-(k_s\cos\theta_{inc}-k_{s/B}\cos\theta^B_{ob}) \tag{6-31d}$$

Scattering Coefficients

In order to obtain the general solutions in the form of dimensionless quantities, let us introduce a new term, the scattering coefficient which is expressed as

$$Cf^{A}_{pp}=\frac{u^{A/p}}{u^{o/p}} \tag{6-32a}$$

$$Cf^{A}_{ps}=\frac{u^{A/s}}{u^{o/s}} \tag{6-32b}$$

where $u^{A/p}$ is the scattered displacement of P-wave in region A; $u^{A/s}$ is the scattered displacement of SV-wave in region A; $u^{o/p}$ is the reflected displacement of P-wave in the specular direction in region A for a smooth boundary; $u^{o/s}$ is the reflected displacement of SV-wave in the specular direction in region A for a smooth boundary.

For region B, we have

$$Cf^{B}_{pp}=\frac{u^{B/p}}{u^{o/p}_{B}} \tag{6-33a}$$

and

$$Cf^{B}_{ps}=\frac{u^{B/s}}{u^{o/s}_{B}} \tag{6-33b}$$

The definition of all terms in Eqs. (6-33a) and (6-33b) are the same as region A.

CHAPTER 7

AVERAGE EVALUATION OF THE SCATTERED AND REFRACTED FIELDS

Equations (6-25) and (6-26) are the explicit solutions of the scattered and refracted fields in this problem. However, these equations contain the shape of the rough interface through the height function h(x) and its derivative h'(x). Therefore, at this step, to carry out the integration in Eqs. (6-25) and (6-26), we need to know either the explicit expression for the height function h(x) if the rough interface has a given shape, or the probability properties of the rough interface if the interface has a random profile. In this work, we deal with the random rough interface. Since the height function of the random rough interface does not have an explicit expression, the exact results of the scattered and refracted fields cannot be obtained. An average evaluation of the scattered and refracted fields is considered in this paper. The performance of the average evaluation requires that the height distribution density of the rough boundary have a known profile. In this chapter we will discuss the probability properties of the rough boundary and the average evaluation.

Probability Properties of the Rough Boundary

The rough interface, as mentioned above, is described by height function h(x). For a random case of the rough interface, the properties are described by the distribution density of the height. In this work, we chose the height distribution to be a Gaussian profile. It is generally accepted that machine treated surfaces have a Gaussian distribution in the surface roughness (Whitehouse and Archard, 1970). If we chose the mean value of the height as zero, i.e., $\langle h(x)\rangle = 0$, the Gaussian distribution of the height has the form as (Beaumont, 1986, p. 113)

$$p[h(x)]=\frac{1}{\sigma\sqrt{2\pi}}\exp\left\{\frac{-[h(x)]^2}{2\sigma^2}\right\} \tag{7-1}$$

where σ is variance of the random height, also called standard deviation. The square of the variance is given by

$$\sigma^2=\langle[h(x)-\langle h(x)\rangle]^2\rangle \tag{7-2}$$

If the mean value of the height $\langle h(x)\rangle=0$, then the square of the variance becomes

$$\sigma^2=\langle[h(x)]^2\rangle \tag{7-3}$$

σ is also called root mean square (r. m. s.).

It can be shown that if a random rough surface has a Gaussian distribution of the surface height, then the distribution of the slope of the rough surface also has a Gaussian profile (Adler, 1981, p. 31), and is given by

$$p[h'(x)] = \frac{1}{\sigma_g\sqrt{2\pi}} \exp\left\{\frac{-[h'(x)]^2}{2\sigma_g^2}\right\} \qquad (7\text{-}4)$$

where σ_g is root mean square of the gradient of the height:

$$\sigma_g^2 = \langle [h'(x)]^2 \rangle \qquad (7\text{-}5)$$

The root mean square of h(x) and h'(x) can not describe the rough surface completely because they can only tell us some information about the height of the hills and valleys of the surface, they cannot tell us whether these hills and valleys are crowded close together or whether they are far apart. Therefore another function, the correlation function or autocorrelation function, needs to be considered.

The correlation function of a random surface gives a measure of the degree of correlation between two points on the surface. For our surface, whose roughness variation is in one direction only, we therefore have the correlation function given by

$$c(L) = \langle h(x+L)h(x) \rangle \qquad (7\text{-}6)$$

where L is the "separation parameter" between two points x_1 and $x_2=x_1+L$ on the rough surface. Let $h_1=h(x_1)$ and $h_2=h(x_2)$. If L is large, then x_1 and x_2 are far away from each other, and h_1 and h_2 will be independent. If L is small, then x_1 and

x_2 are near each other, and h_1 and h_2 will be correlated. If L=0, we have

$$c(0)=\langle h^2(x)\rangle \tag{7-7}$$

The normalized correlation function, or autocorrelation function, C_N (L), is defined by

$$C_N(L)=\frac{\langle h(x+L)\,h(x)\rangle}{\langle h^2(x)\rangle} \tag{7-8}$$

The important properties of $C_N(L)$

$$C_N(0)=1 \tag{7-9}$$

$$C_N(L) \to 0 \quad \text{as} \quad L \to \infty \tag{7-10}$$

Now we need to specify a form of the correlation function to further characterize the rough surface. One of the most commonly used forms of the function is (Maradudin and Mills, 1976).

$$C(L)=C(0)\,e^{-\frac{L^2}{2T_0^2}} \tag{7-11}$$

in which T_0 is defined to be the correlation length over which C(L) falls by a factor of $e^{-1/2}$. It can also be shown that

$$\sigma_g^2=-C''(0)=\frac{\sigma^2}{T_0^2} \tag{7-12}$$

So far we have obtained the parameters σ, σ_g and T_0 which define the defect roughness of the random rough interface.

Average Values of the Scattered Fields

Each component of the scattered and refracted fields in expressions (6-25) and (6-26) contains two parts (P-wave and SV-wave) as indicated by Eqs. (3-39). Before we take average evaluation of these expressions, let us have some rules about random variables. If x is a random variable, and f(x) is a function of x, we have a rule for averaging as (Beaumont, 1986, p. 234)

$$\left\langle \int_a^b f(x)\,dx \right\rangle = \int_a^b \langle f(x) \rangle\,dx \qquad (7\text{-}13)$$

and if x_1 and x_2 are independent, we have

$$\langle p(x_1)\,q(x_2) \rangle = \langle p(x_1) \rangle \langle q(x_2) \rangle \qquad (7\text{-}14)$$

Take the average of Eqs. (6-25a)-(6-26c) term by term, with Eqs. (7-13) and (7-14), we have the average value of the scattered fields in region A:

$$\langle u_1^{A/p} \rangle = \frac{i e^{ik_p r}}{4\pi r} \int_{L_1}^{L_2} [\langle -h'(x) \rangle \langle \xi_1^p \rangle + \langle \zeta_1^p \rangle] \langle e^{i[D_{p/A}x + E_{s/A}h(x)]} \rangle\,dx \qquad (7\text{-}15a)$$

$$\langle u_1^{A/s} \rangle = \frac{i e^{ik_s r}}{4\pi r} \int_{L_1}^{L_2} [\langle -h'(x) \rangle \langle \xi_1^s \rangle + \langle \zeta_1^s \rangle] \langle e^{i[D_{s/A}x + E_{s/A}h(x)]} \rangle\,dx \qquad (7\text{-}15b)$$

$$\langle u_3^{A/p}\rangle = \frac{ie^{ik_p r}}{4\pi r}\int_{L_1}^{L_2}[\langle -h'(x)\rangle\langle\xi_3^p\rangle + \langle\zeta_3^p\rangle]\langle e^{i[D_{p/A}x+E_{p/A}h(x)]}\rangle dx \qquad (7\text{-}15c)$$

$$\langle u_3^{A/s}\rangle = \frac{ie^{ik_s r}}{4\pi r}\int_{L_1}^{L_2}[\langle -h'(x)\rangle\langle\xi_3^s\rangle + \langle\zeta_3^s\rangle]\langle e^{i[D_{s/A}x+E_{s/A}h(x)]}\rangle dx \qquad (7\text{-}15d)$$

In equations (7-15a)-(7-15d) ξ_i^{α} and ζ_i^{α} ($i= 1, 3$ and $\alpha=p, s$) are, in complicated way, functions of the gradient of the surface height. The average value of these functions are given by

$$\langle\xi_1^{\alpha}\rangle = H_{111}^{\alpha/A}\langle f_1^{A/p}\rangle + H_{131}^{\alpha/A}\langle f_3^{A/p}\rangle - A_{11}^{\alpha/A}\langle f_{11}^{A/p}\rangle - A_{31}^{\alpha/A}\langle f_{31}^{A/p}\rangle \ , \ \alpha=p, \qquad (7\text{-}16a)$$

$$\langle\xi_3^{\alpha}\rangle = H_{113}^{\alpha/A}\langle f_1^{A/p}\rangle + H_{133}^{\alpha/A}\langle f_3^{A/p}\rangle - A_{13}^{\alpha/A}\langle f_{11}^{A/p}\rangle - A_{33}^{\alpha/A}\langle f_{31}^{A/p}\rangle \ , \ \alpha=p, \qquad (7\text{-}16b)$$

$$\langle\zeta_1^{\alpha}\rangle = H_{131}^{\alpha/A}\langle f_1^{A/p}\rangle + H_{331}^{\alpha/A}\langle f_3^{A/p}\rangle - A_{11}^{\alpha/A}\langle f_{13}^{A/p}\rangle - A_{31}^{\alpha/A}\langle f_{33}^{A/p}\rangle \ , \ \alpha=p, \qquad (7\text{-}16a)$$

$$\langle\zeta_3^{\alpha}\rangle = H_{133}^{\alpha/A}\langle f_1^{A/p}\rangle + H_{333}^{\alpha/A}\langle f_3^{A/p}\rangle - A_{13}^{\alpha/A}\langle f_{13}^{A/p}\rangle - A_{33}^{\alpha/A}\langle f_{33}^{A/p}\rangle \ , \ \alpha=p, \qquad (7\text{-}16b)$$

The explicit expressions of $f_i^{A/p}$ and $f_{ij}^{A/p}$ ($i, j = 1, 3$) are given in Eqs. (6-17a)-(6-17e), and the explicit expressions of H^{α}_{ijk} and A^{α}_{ik} ($i, j, k = 1, 3$ and $\alpha=p, s$) are given in Eqs. (5-28a)-(5-31f).

For region B, we have the average value of the refracted fields

$$\langle u_1^{B/p}\rangle = \frac{ie^{ik_{p/B} r}}{4\pi r}\int_{L_1}^{L_2}[\langle h'(x)\rangle\langle\xi_1^{p/B}\rangle + \langle\zeta_1^{p/B}\rangle]\langle e^{i[D_{p/B}x+E_{p/B}h(x)]}\rangle dx \qquad (7\text{-}17a)$$

$$<u_1^{B/s}>=\frac{ie^{ik_{s/B}r}}{4\pi r}\int_{L_1}^{L_2}[<h'(x)><\xi_1^{s/B}>+<\zeta_1^{s/B}>]<e^{i[D_{s/B}x+E_{s/B}h(x)]}>dx \qquad (7\text{-}17b)$$

$$<U_3^{B/p}>=\frac{ie^{ik_{p/B}r}}{4\pi r}\int_{L_1}^{L_2}[<-h'(x)><\xi_3^{p/B}>+<\zeta_3^{p/B}>]<e^{i[D_{p/B}x+E_{p/B}h(x)]}>dx \qquad (7\text{-}17c)$$

$$<u_3^{B/s}>=\frac{ie^{ik_{s/B}r}}{4\pi r}\int_{L_1}^{L_2}[<-h'(x)><\xi_3^{s/B}>+<\zeta_3^{s/B}>]<e^{i[D_{s/B}x+E_{s/B}h(x)]}>dx \qquad (7\text{-}17d)$$

where

$$<\xi_1^{\alpha/B}>=H_{111}^{\alpha/B}<f_1^{B/p}>+H_{131}^{\alpha/B}<f_3^{B/p}>-A_{11}^{\alpha/B}<f_{11}^{B/p}>-A_{31}^{\alpha/B}<f_{31}^{B/p}> \ , \quad \alpha=j \qquad (7\text{-}18a)$$

$$<\xi_3^{\alpha/B}>=H_{113}^{\alpha/B}<f_1^{B/p}>+H_{133}^{\alpha/B}<f_3^{B/p}>-A_{13}^{\alpha/B}<f_{11}^{B/p}>-A_{33}^{\alpha/B}<f_{31}^{B/p}> \ , \quad \alpha=j \qquad (7\text{-}18b)$$

$$<\zeta_1^{\alpha/B}>=H_{131}^{\alpha/B}<f_1^{B/p}>+H_{331}^{\alpha/B}<f_3^{B/p}>-A_{11}^{\alpha/B}<f_{13}^{B/p}>-A_{31}^{\alpha/B}<f_{33}^{B/p}> \ , \quad \alpha=j \qquad (7\text{-}18a)$$

$$<\zeta_3^{\alpha/B}>=H_{133}^{\alpha/B}<f_1^{B/p}>+H_{333}^{\alpha/B}<f_3^{B/p}>-A_{13}^{\alpha/B}<f_{13}^{B/p}>-A_{33}^{\alpha/B}<f_{33}^{B/p}> \ , \quad \alpha=j \qquad (7\text{-}18b)$$

In Eq. (7-18) the explicit expressions of $f_i^{B/p}$ and $f_{ij}^{B/p}$ (i, j = 1, 3) are given in Eqs. (6-18a)-(6-18e), and the explicit expressions of $H^{\alpha/B}_{ijk}$ and $A^{\alpha/B}_{ik}$ (i, j, k = 1, 3 and α=p, s) are given in Eqs. (5-32a)-(5-35f).

Equations (7-15) through (7-18) are the general expressions of the average evaluation of the scattered and refracted fields. Since the chosen height distribution has Gaussian profile, it is clear that if the mean value of the height vanishes, i.e. <h(x)> = 0, then the mean value of the gradient also vanishes, i.e.

$$\langle h'(x)\rangle = 0 \tag{7-19}$$

Therefore all terms involving <h'(x)> in Eqs. (7-15) through (7-18) will be zero.

The averaging is with respect to h(x). Therefore the exponential terms in the integrands become

$$\langle e^{i[D_{\alpha/A}x+E_{\alpha/A}h(x)]}\rangle = e^{iD_{\alpha/A}x}\langle e^{iE_{\alpha/A}h(x)}\rangle \quad , \quad \alpha=p,s \tag{7-20}$$

and

$$\langle e^{i[D_{\alpha/B}x+E_{\alpha/B}h(x)]}\rangle = e^{iD_{\alpha/B}x}\langle e^{iE_{\alpha/B}h(x)}\rangle \quad , \quad \alpha=p,s \tag{7-21}$$

Putting these results in to the expressions of the scattered and refracted fields, Eqs. (7-15) through (7-18), we have

$$\langle u_1^{A/p}\rangle = q^p(r)\langle\zeta_1^p\rangle\langle e^{iE_{p/A}h(x)}\rangle\int_{L_1}^{L_2} e^{iD_{p/A}x}dx \tag{7-22a}$$

$$\langle u_1^{A/s}\rangle = q^s(r)\langle\zeta_1^s\rangle\langle e^{iE_{s/A}h(x)}\rangle\int_{L_1}^{L_2} e^{iD_{s/A}x}dx \tag{7-22b}$$

$$\langle u_3^{A/p}\rangle = q^p(r)\langle\zeta_3^p\rangle\langle e^{iE_{p/A}h(x)}\rangle\int_{L_1}^{L_2} e^{iD_{p/A}x}dx$$

(7-22c)

$$\langle u_3^{A/s}\rangle = q^s(r)\langle\zeta_3^s\rangle\langle e^{iE_{s/A}h(x)}\rangle\int_{L_1}^{L_2} e^{iD_{s/A}x}dx \tag{7-22d}$$

where

$$q^\alpha(r) = \frac{ie^{k_\alpha r}}{4\pi r} \quad , \quad \alpha=p,s$$

For region B, we have

$$<u_1^{B/p}>=q^{p/B}(r)<\zeta_1^{p/B}><e^{iE_{p/B}h(x)}>\int_{L_1}^{L_2} e^{iD_{p/B}x}dx \tag{7-23a}$$

$$<u_1^{B/s}>=q^{s/B}(r)<\zeta_1^{s/B}><e^{iE_{s/B}h(x)}>\int_{L_1}^{L_2} e^{iD_{s/B}x}dx \tag{7-23b}$$

$$<u_3^{B/p}>=q^{p/B}(r)<\zeta_3^{p/B}><e^{iE_{p/B}h(x)}>\int_{L_1}^{L_2} e^{iD_{p/B}x}dx \tag{7-23c}$$

$$<u_3^{B/s}>=q^{s/B}(r)<\zeta_3^{s/B}><e^{iE_{s/B}h(x)}>\int_{L_1}^{L_2} e^{iD_{s/B}x}dx \tag{7-23d}$$

where

$$q^{\alpha/B}(r)=\frac{ie^{ik_{\alpha/B}r}}{4\pi r}\ , \quad \alpha=p,s$$

The average value of a function with the Gaussian distribution can be expressed as (Crandall, et. al. p44, 1958)

$$<f(z)>=\int_{-\infty}^{\infty} f(z)\frac{1}{\sigma\sqrt{2\pi}}e^{\frac{-z^2}{2\sigma^2}}dz \tag{7-24}$$

Therefore we have

$$<e^{iE_{\alpha/A}h(x)}>=\int_{-\infty}^{\infty} e^{iE_{\alpha/A}h(x)}\frac{1}{\sigma\sqrt{2\pi}}e^{\frac{-[h(x)]^2}{2\sigma^2}}d[h(x)]$$

$$=e^{\frac{-E_{\alpha/A}^2\sigma^2}{2}}\ , \quad \alpha=p,s \tag{7-25}$$

The integral in (7-25) can be found in Gradshteyn and Ryzhik (1980, p. 307). Similarly, for region B, we have

$$<e^{iE_{\alpha/B}h(x)}>=\int_{-\infty}^{\infty} e^{iE_{\alpha/B}h(x)} \frac{1}{\sigma\sqrt{2\pi}} e^{\frac{-[h(x)]^2}{2\sigma^2}} d[h(x)]$$

$$=e^{\frac{-E^2_{\alpha/B}\sigma^2}{2}} \quad , \quad \alpha=p,s \tag{7-26}$$

The results in (7-25) and (7-26) contain the roughness σ, and are called roughness factors. It is clear that these factors are always less than 1.0 if σ is not zero, and equal to 1.0 if $\sigma = 0.0$, i.e.

$$e^{\frac{-E^2_{\alpha/A}\sigma^2}{2}} \leq 1.0 \quad , \quad \alpha=p,s \tag{7-27}$$

For the integrals in Eqs. (7-22) and (7-23), we have

$$\int_{L_1}^{L_2} e^{iD_{\alpha/A}x}dx=\frac{1}{iD_\alpha}(e^{iD_{\alpha/A}L_2}-e^{iD_{\alpha/A}L_1}) \quad , \quad \alpha=p,s \tag{7-28}$$

Taking the real part of the result in (7-28), we have

$$Re\left(\int_{L_1}^{L_2} e^{iD_{\alpha/A}x}dx\right)=\frac{1}{D_{\alpha/A}}(\sin D_{\alpha/A}L_2-\sin D_{\alpha/A}L_1) \quad , \quad \alpha=p,s \tag{7-29}$$

Putting these results into Eqs. (7-22), we have

$$<u_1^{A/\alpha}>=q^{\alpha/A}(r)\, e^{\frac{-E^2_{\alpha/A}\sigma^2}{2}} <\zeta_1^\alpha> g_A^{D/\alpha} \quad , \quad \alpha=p,s \tag{7-30}$$

where

$$g_A^{D/\alpha}=\frac{1}{D_{\alpha/A}}(\sin D_{\alpha/A}L_2-\sin D_{\alpha/A}L_1) \quad , \quad \alpha=p,s \tag{7-31}$$

For Eqs. (7-23), similarly we have

$$\langle u_1^{B/\alpha}\rangle=\eta^{B/\alpha}(r)\,e^{\frac{-E_{\alpha/B}^2\sigma^2}{2}}\langle\zeta_1^{\alpha/B}\rangle g_B^{D/\alpha}\quad,\ \alpha=p,s \tag{7-32}$$

where

$$g_B^{D/\alpha}=\frac{1}{D_{\alpha/B}}(\sin D_{\alpha/B}L_2-\sin D_{\alpha/B}L_1)\quad,\ \alpha=p,s \tag{7-33}$$

To get the dimensionless form of Eqs. (7-31) and (7-33), we can rewrite them as

$$f_\beta^{D/\alpha}=\frac{g_\beta^{D/\alpha}}{L_2-L_1}=\frac{(\sin D_{\alpha/\beta}L_2-\sin D_{\alpha/\beta}L_1)}{D_{\alpha/\beta}(L_2-L_1)}\quad,\ \alpha=p,s\ ;\ \beta=A,B \tag{7-34}$$

The Roughness Factors and the Integration Factors

From the expressions of the average evaluations of the scattered and the refracted fields Eqs. (7-30) and (7-32), we can see that there are two types of factors involved in the results: roughness factors and integration factors. The integration factors denoted by $f_A^{D/\alpha}$ and $f_B^{D/\alpha}$ (α=p,s) are given in Eq. (7-34) in which $D_{\alpha/A}$ and $D_{\alpha/B}$ (α=p,s) are quantities related to the wave number, the incident angle, and the observation angle. The explicit expressions of $D_{\alpha/A}$ and $D_{\alpha/B}$ are given in Eqs. (6-23a)-(6-24d). The plots of the integration factors for different integration domains are shown in Figs. 16-19. From these figures, we can see that the changing of the integration domain affects the profile of the factor for both compression and shear components in both region A and B. As the extent integration domain increases, the number of the side lobes increases. The specular directions of the scattered and refracted fields depend on the incident angle and the wavenumbers, as shown in Eqs. (4-41)-(4-45). For example, if the incident angle is chosen to be 30°, the specular direction for the scattered P-wave as given is 30° (Eqs. (4-41), (4-42)), and 15.7° for the scattered SV-wave (Eq. (4-43)). Figs. 16-19 show that the values of the integration factors in the specular directions do not change as the integration domain changes.

With Eq. (6-23b) and the following relation between the wavenumber k, frequency F, and wavelength λ :

$$k_\alpha=\frac{2\pi F}{C_\alpha}=\frac{2\pi}{\lambda_\alpha}\ , \quad \alpha=p,s \tag{7-35}$$

the roughness factor for the compression component $f^{r/p}$, as an example, can be written as

$$f^{r/p}=e^{-\frac{E^2\sigma^2}{2}}=\exp\left[-S_p\left(\frac{\sigma F}{C_p}\right)^2\right]=\exp\left[-S_p\left(\frac{\sigma}{\lambda_p}\right)^2\right]=\exp\left(-S_p\Gamma_p^2\right) \tag{7-36}$$

where

$$S_p=2\pi^2(\cos\theta_{inc}+\cos\theta_{ob})^2 \tag{7-37}$$

and

$$\Gamma_p=\frac{\sigma}{\lambda_p} \tag{7-38}$$

is the apparent roughness.

Figures 20-23 show the results of the roughness factors versus the apparent roughness Γ for a fixed incident angle

(30^{o}) and observation angle. The fixed observation angle in each of these figures is chosen to be the angle in the specular direction. From these figures, we see that as Γ increases, the roughness factor increases. Figs. 24-27 show the results of the roughness factors versus observation angles. Note that the curves in these figures are normalized by dividing the value of the factor in the specular direction. From these figures, we can see that as Γ increases, angles beyond the specular see significant increase of the roughness factor, while angles less than the specular see slight decrease in the roughness factor.

Similarly, the results of the scattered and the refracted fields due to incident shear wave are related to these factors. The numerical results of these factors due to incident shear wave are listed in Figs. 28-37.

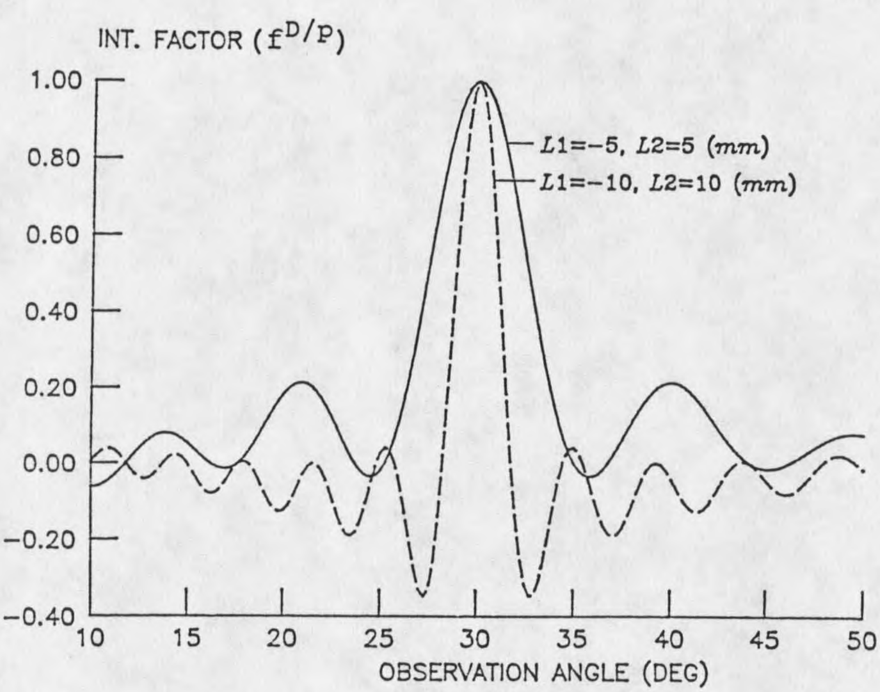

Figure 16. Integration factor for scattered P-wave in region A (σ=0.12 mm)

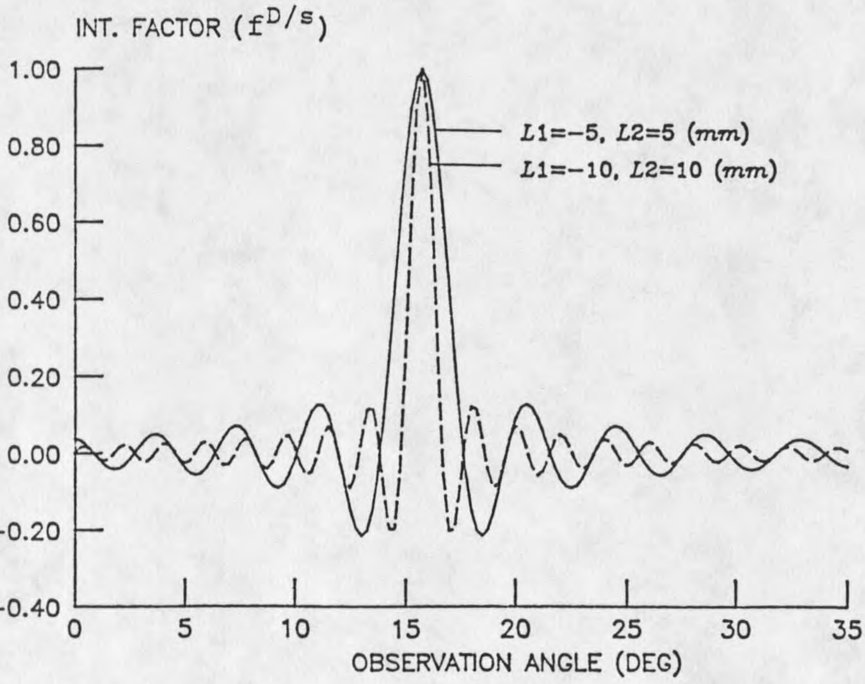

Figure 17. Integration factor for scattered SV-wave in region A (σ=0.12 mm)

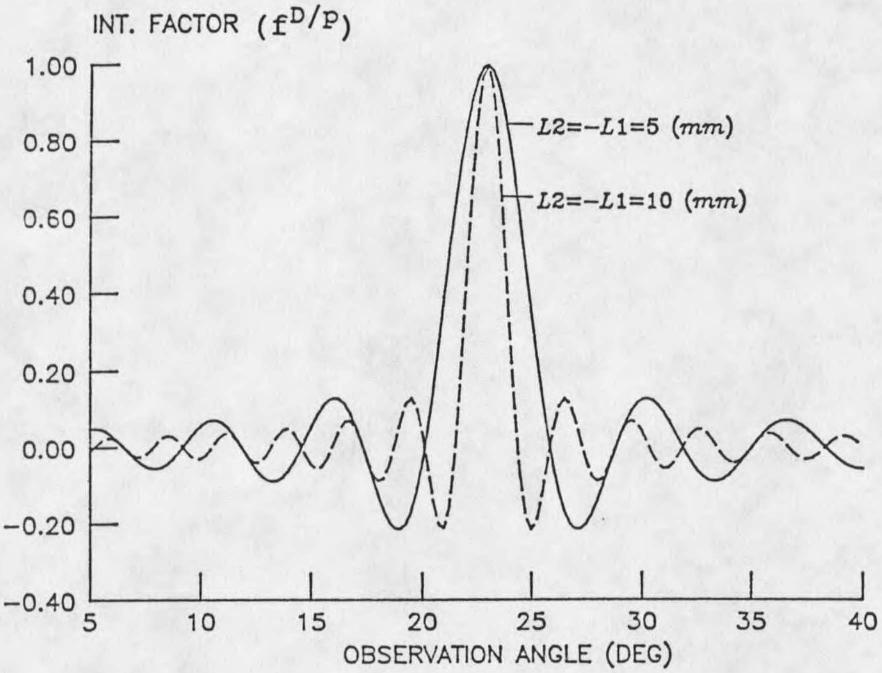

Figure 18. Integration factor for refracted P-wave in region B (σ=0.12 mm)

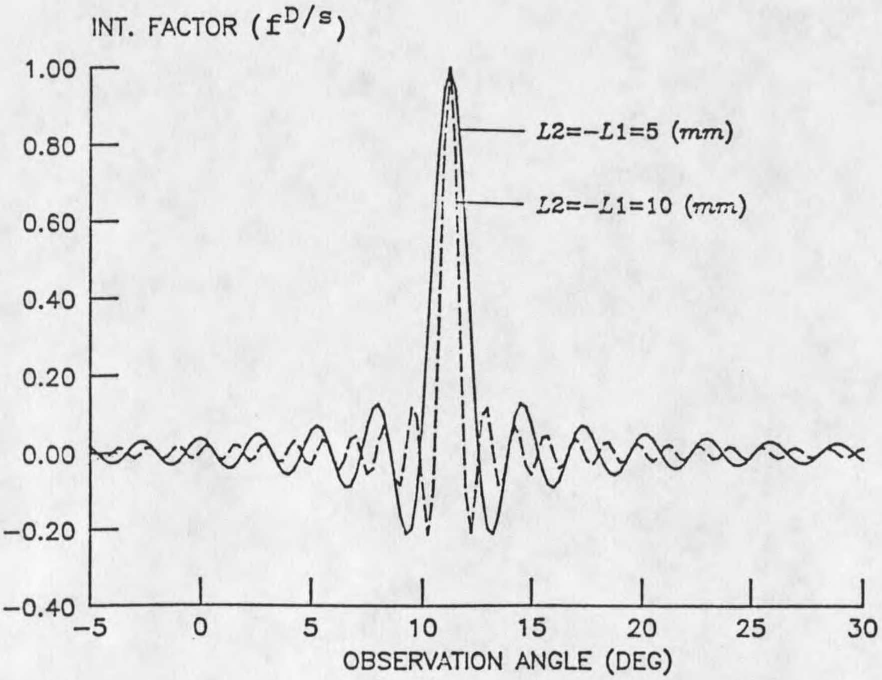

Figure 19. Integration factor for refracted SV-wave in region B (σ=0.12 mm)

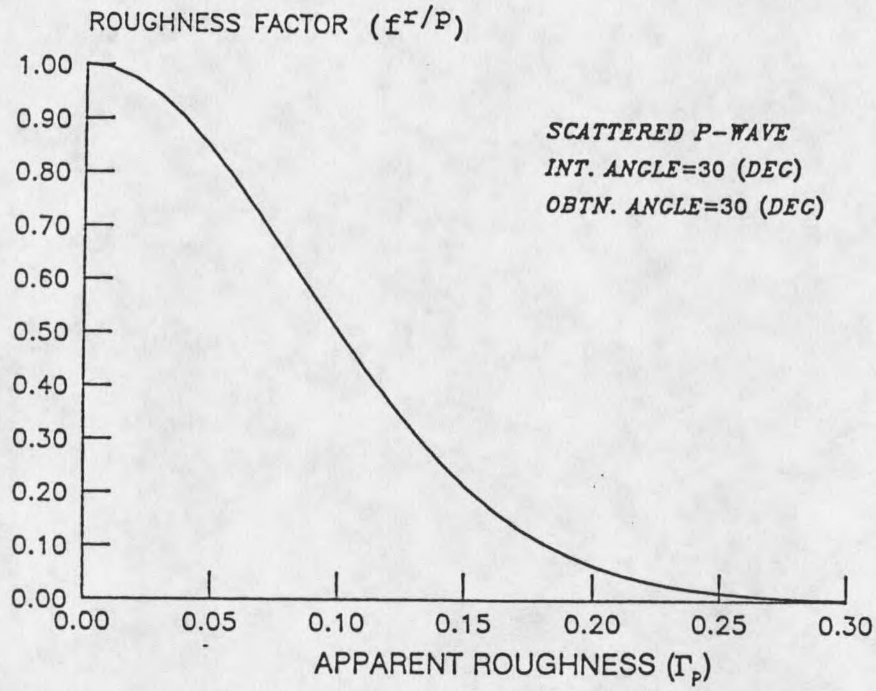

Figure 20. Roughness factor versus the apparent roughness Γ_p (scattered P-wave, $\theta_{ob}=30^{\circ}$)

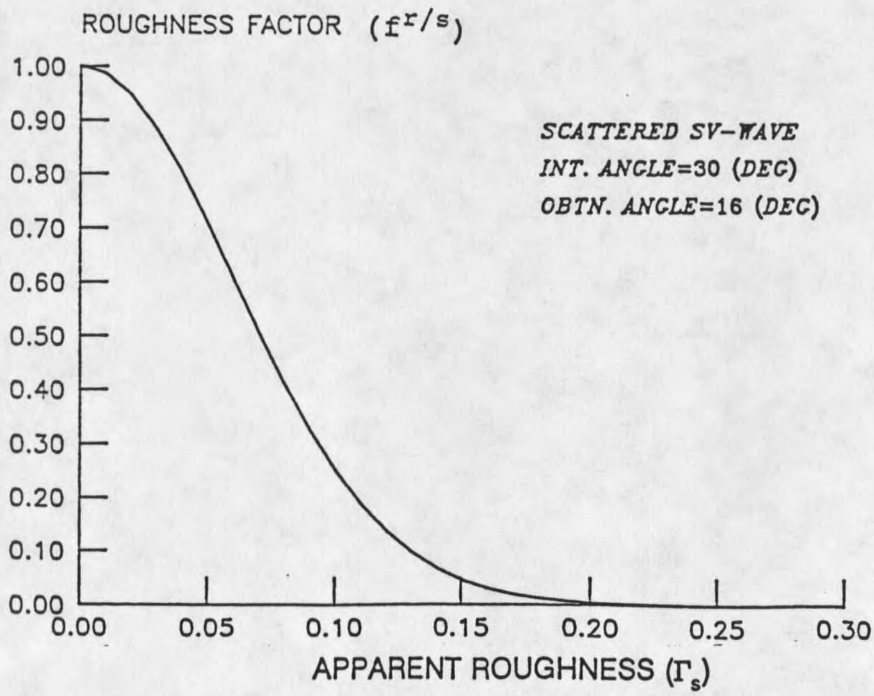

Figure 21. Roughness factor versus the apparent roughness Γ_s (scattered SV-wave, $\theta_{ob}=15.7^{\circ}$)

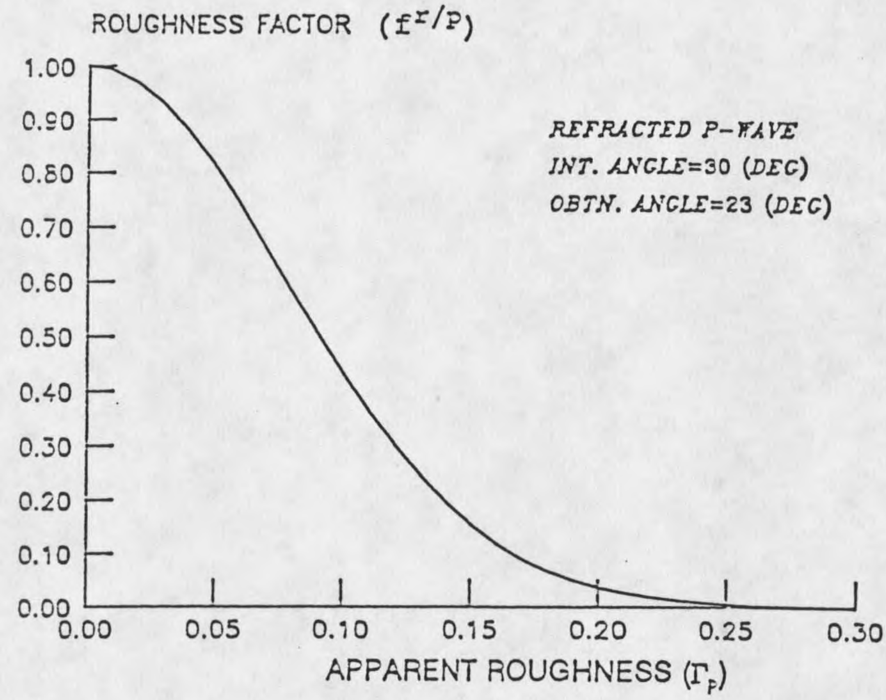

Figure 22. Roughness factor versus the apparent roughness Γ_p (refracted P-wave, θ_{ob}=22.9°)

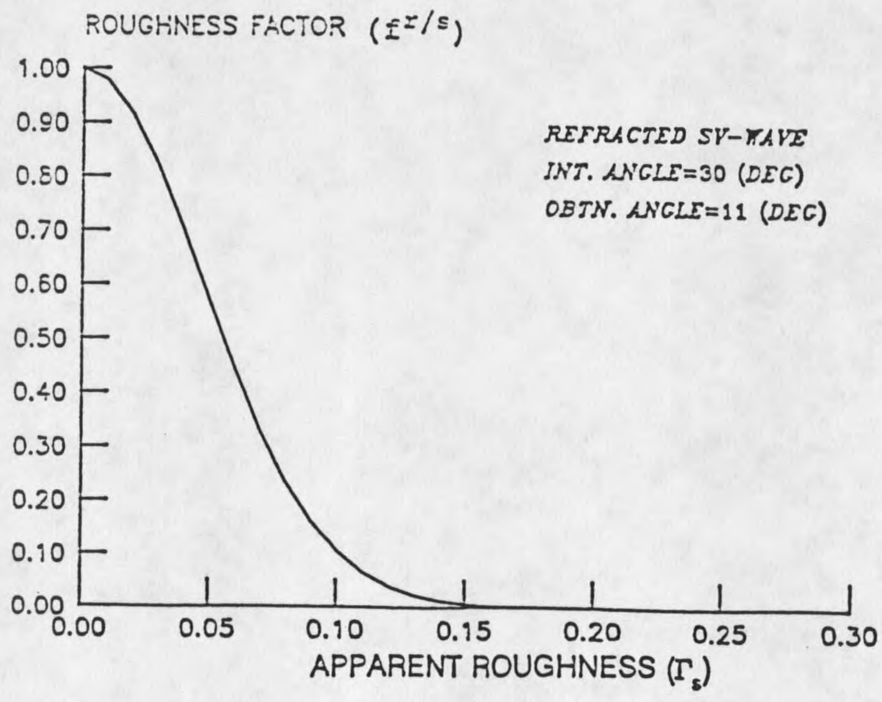

Figure 23. Roughness factor versus the apparent roughness Γ_s (refracted SV-wave, θ_{ob}=11.2°)

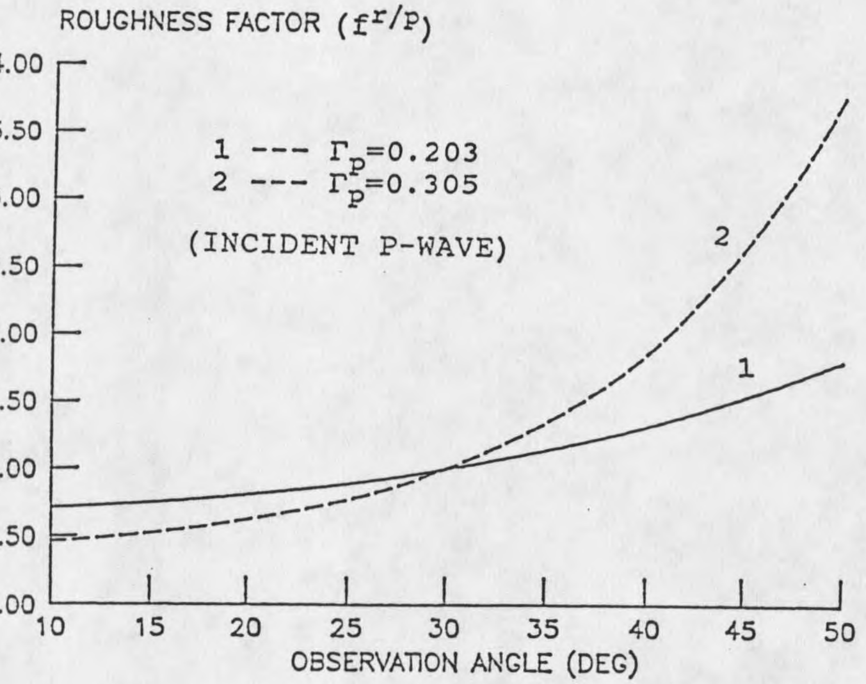

Figure 24. Roughness factor versus observation angle (scattered P-wave)

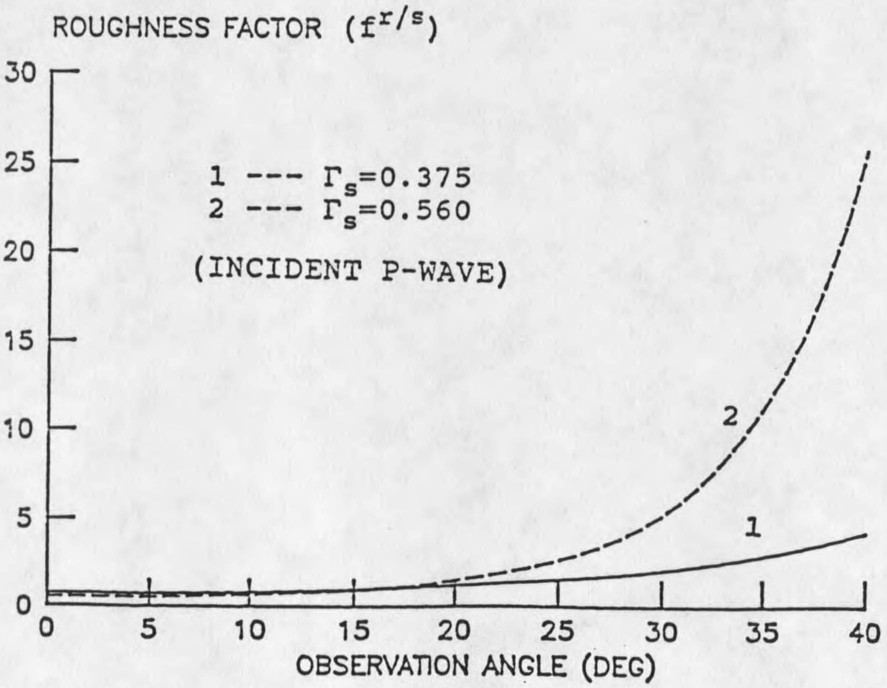

Figure 25. Roughness factor versus observation angle (scattered SV-wave)

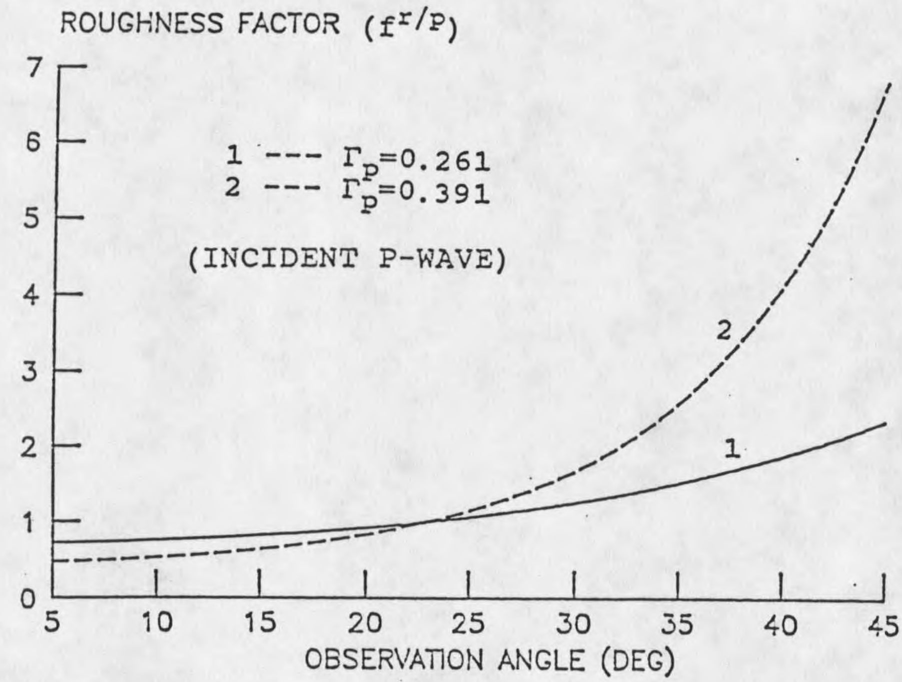

Figure 26. Roughness factor versus observation angle (refracted P-wave)

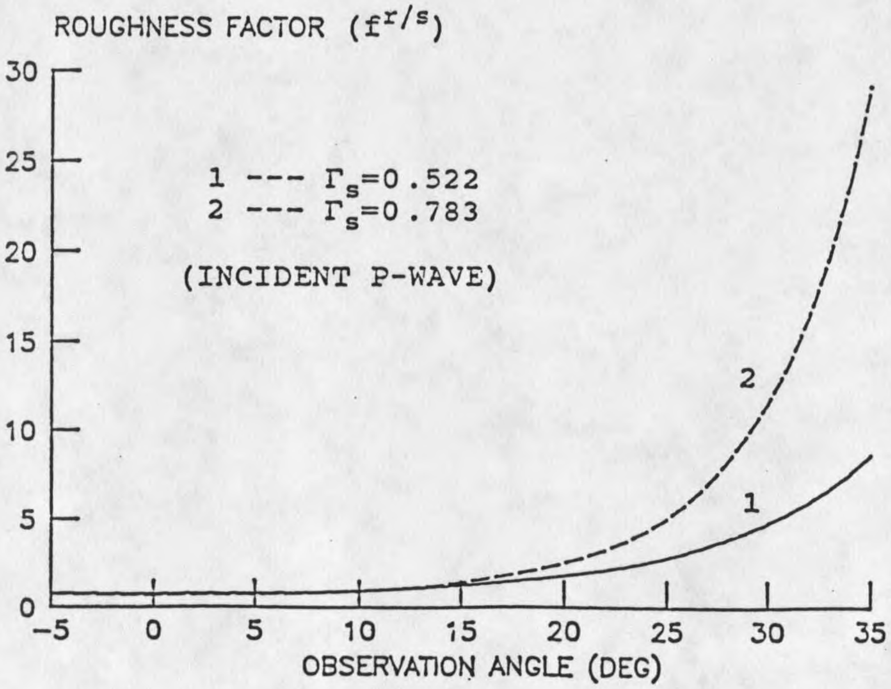

Figure 27. Roughness factor versus observation angle (refracted SV-wave)

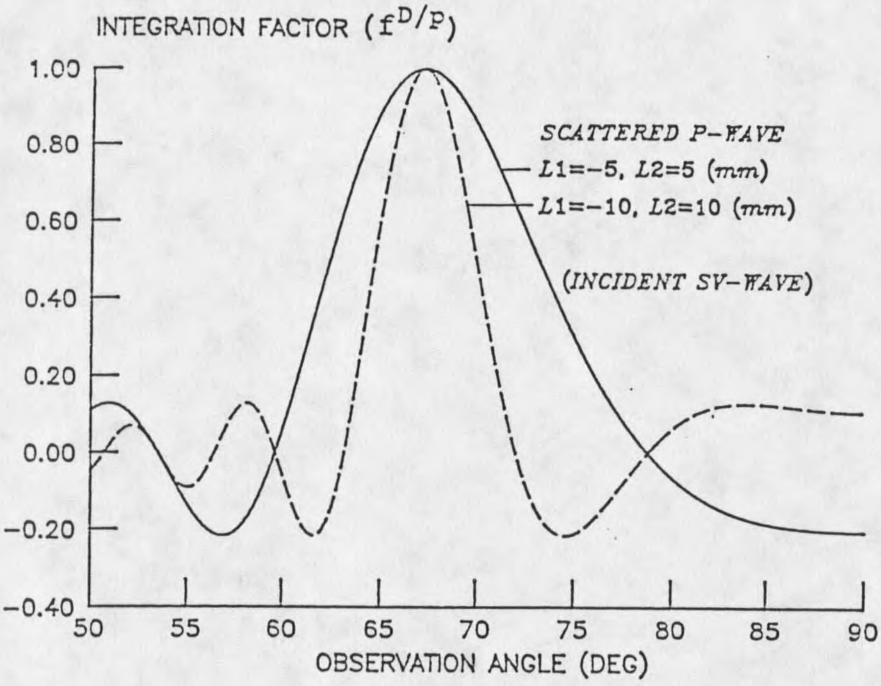

Figure 28. Integration factor for scattered P-wave in region A due to incident SV-wave (σ=0.12 mm)

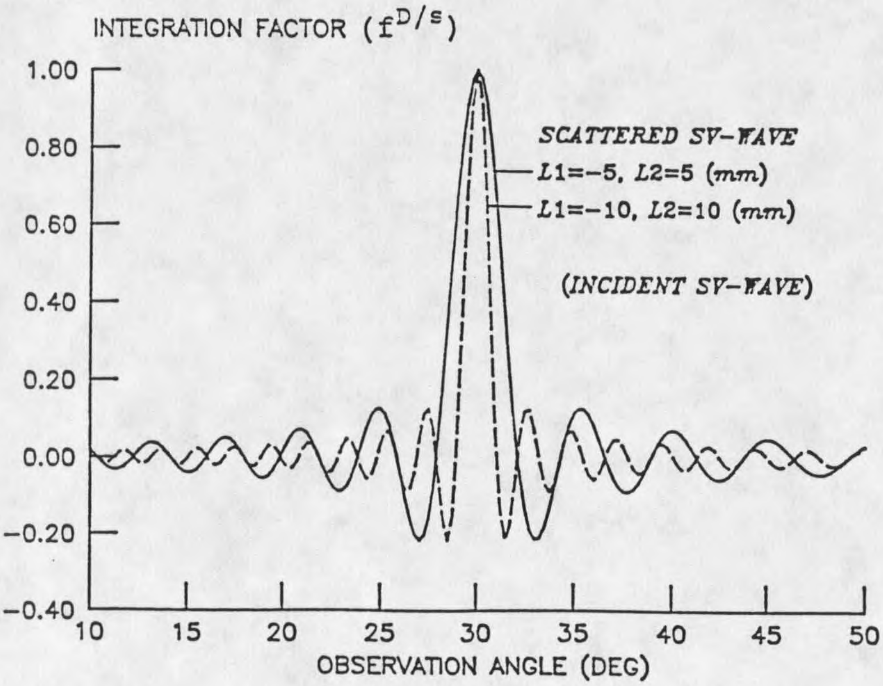

Figure 29. Integration factor for scattered SV-wave in region A due to incident SV-wave (σ=0.12 mm)

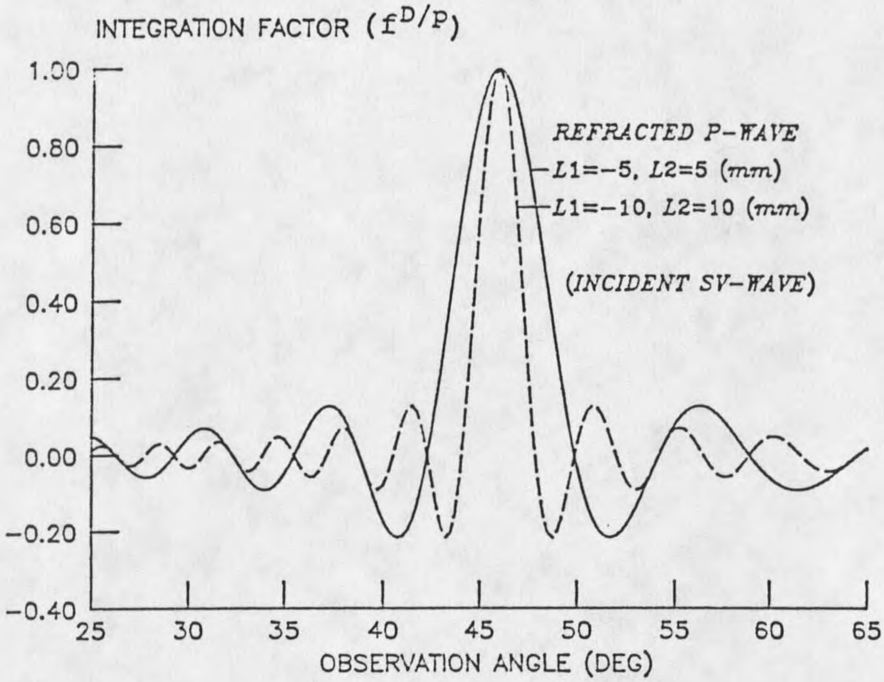

Figure 30. Integration factor for refracted P-wave in region B due to incident SV-wave (σ=0.12 mm)

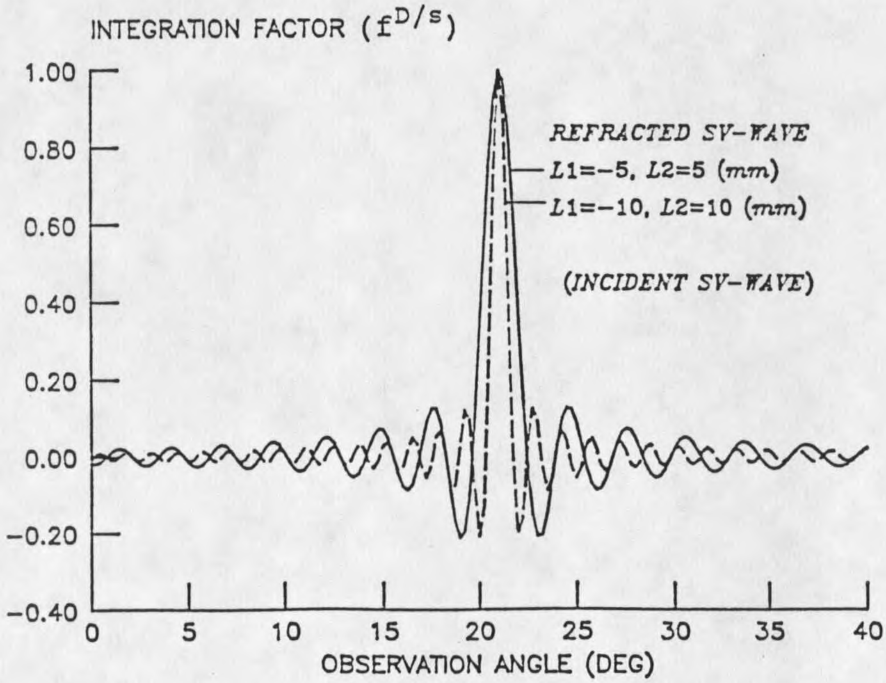

Figure 31. Integration factor for refracted SV-wave in region B due to incident SV-wave (σ=0.12 mm)

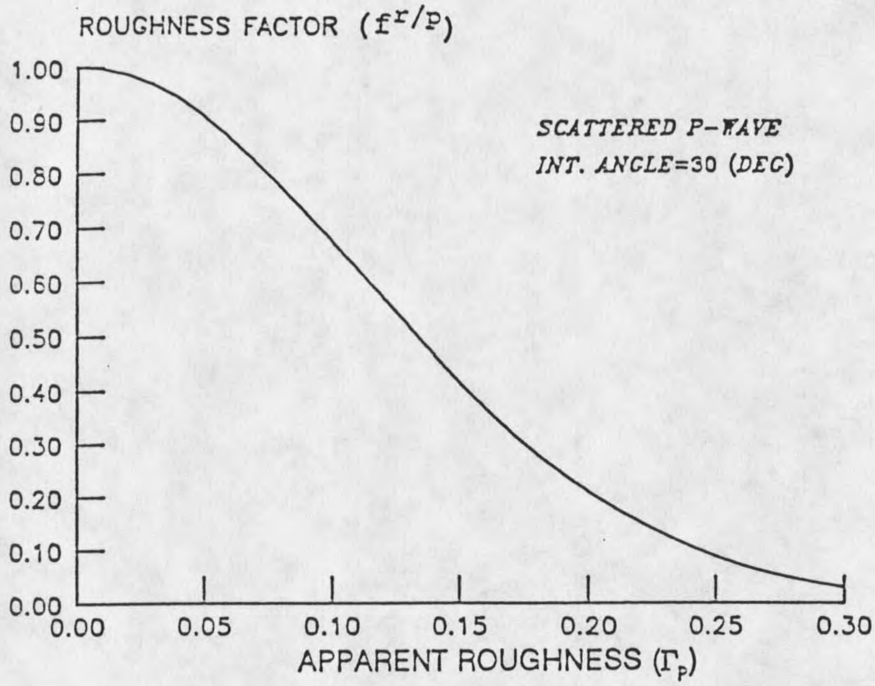

Figure 32. Roughness factor versus Γ_p (scattered P-wave due to incident SV-wave, $\theta_{ob}=67.2°$)

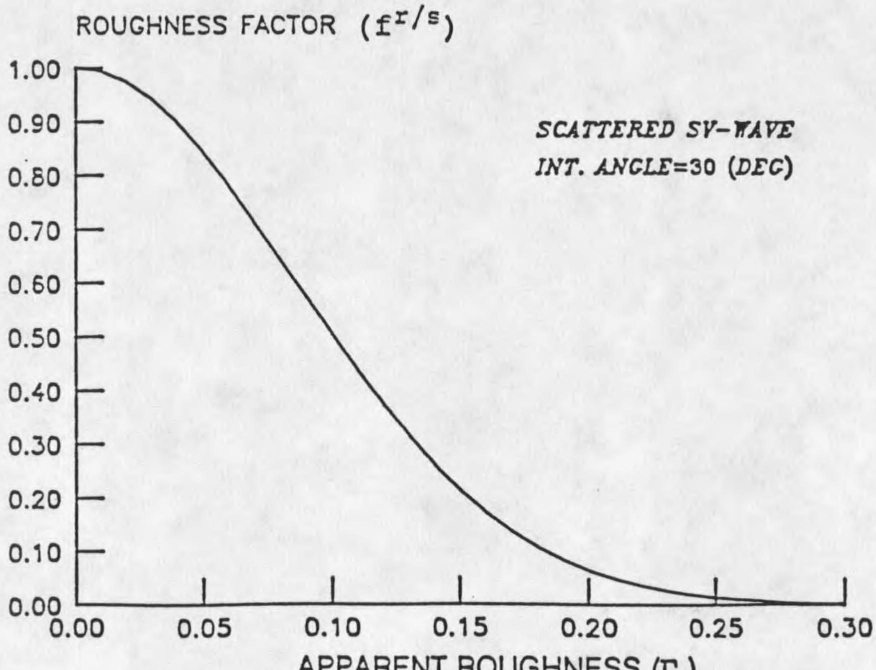

Figure 33. Roughness factor versus Γ_s (scattered SV-wave due to incident SV-wave, $\theta_{ob}=30°$)

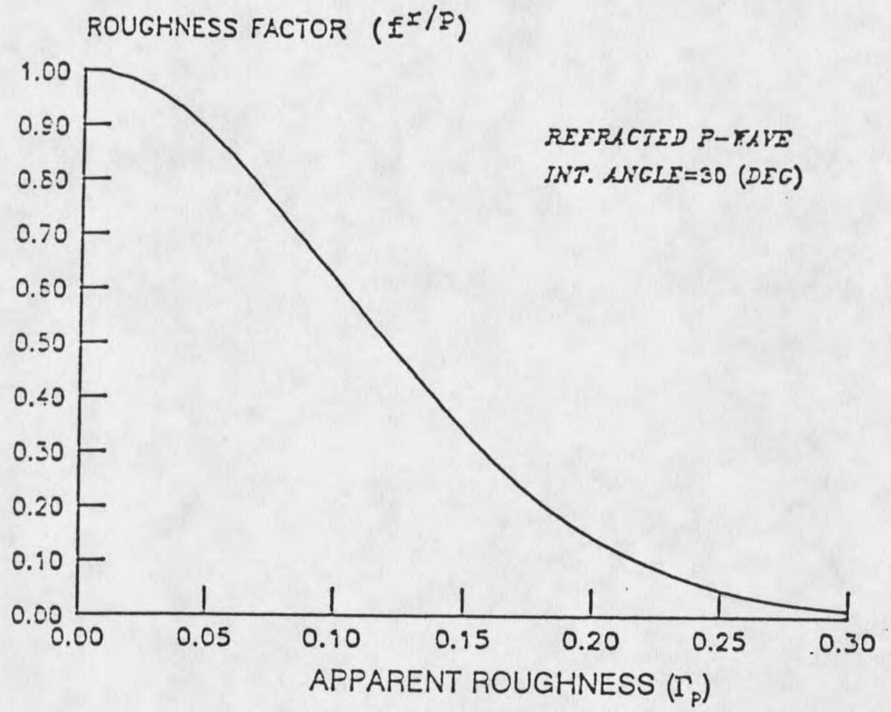

Figure 34. Roughness factor versus Γ_p (refracted P-wave due to incident SV-wave, θ_{ob}=45.9°)

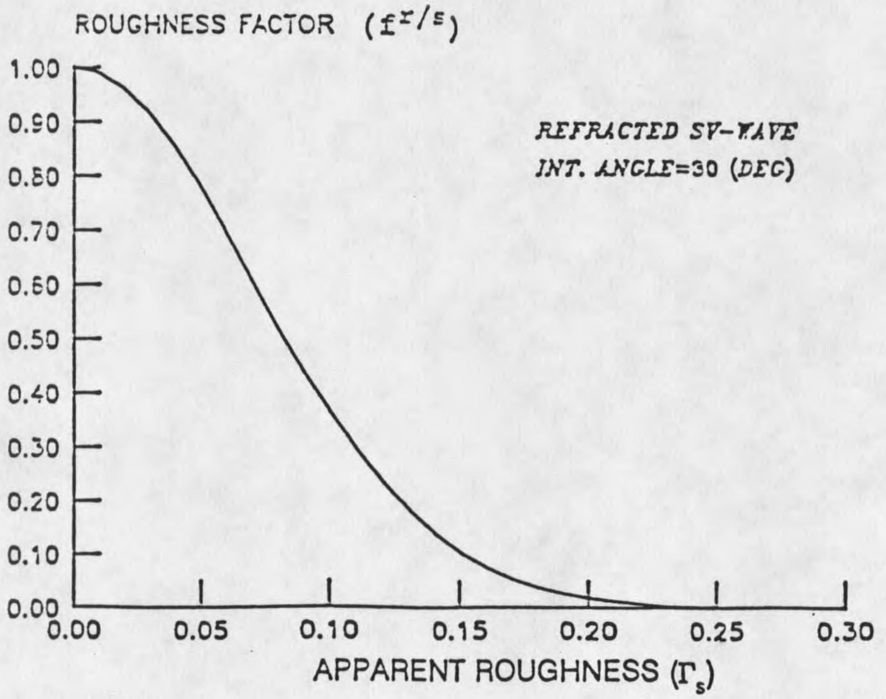

Figure 35. Roughness factor versus Γ_s (refracted SV-wave due to incident SV-wave, θ_{ob}=21.1°)

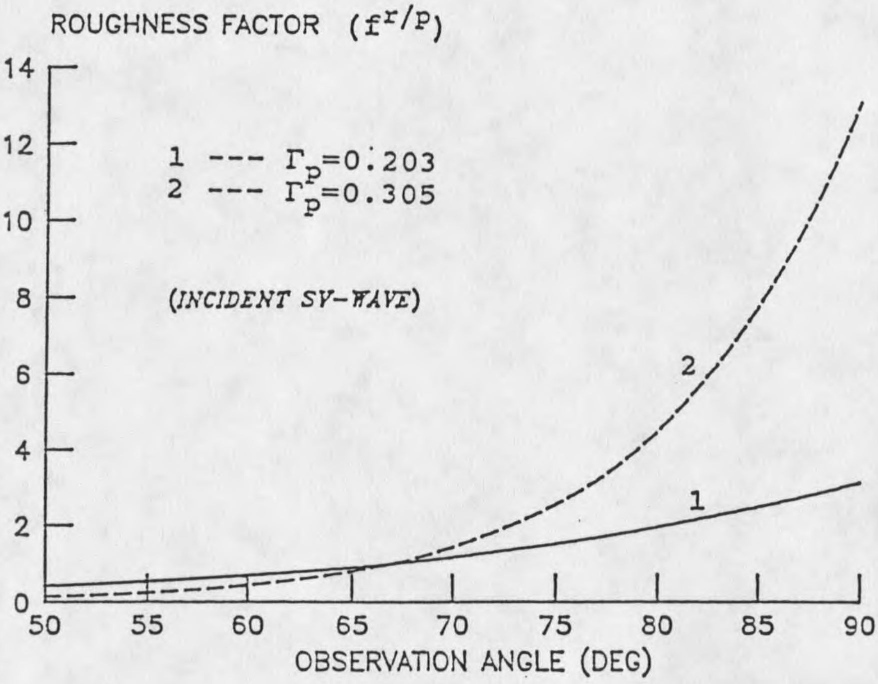

Figure 36. Roughness factor versus observation angle (scattered P-wave due to incident SV-wave)

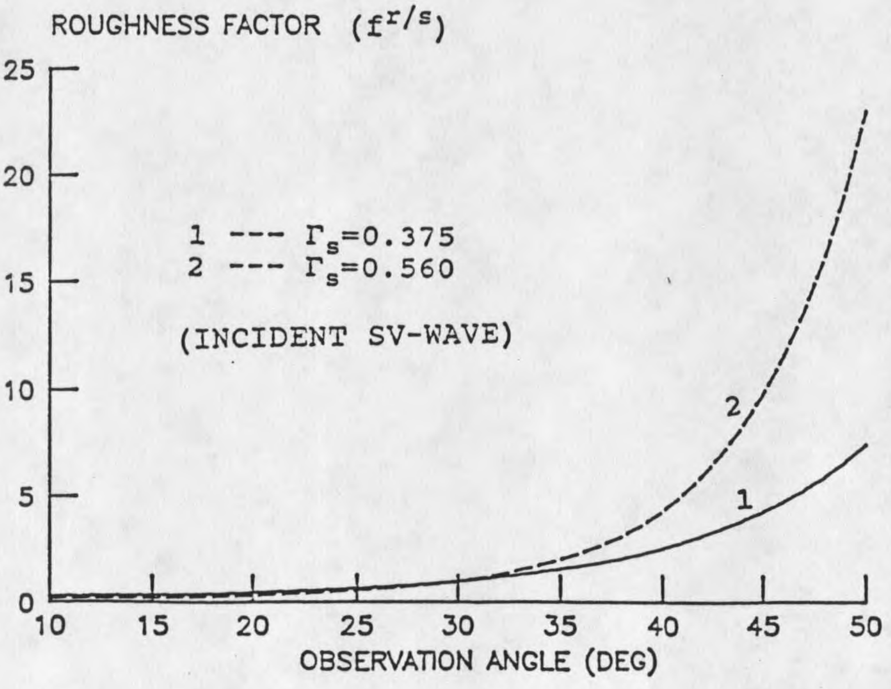

Figure 37. Roughness factor versus observation angle (scattered SV-wave due to incident SV-wave)

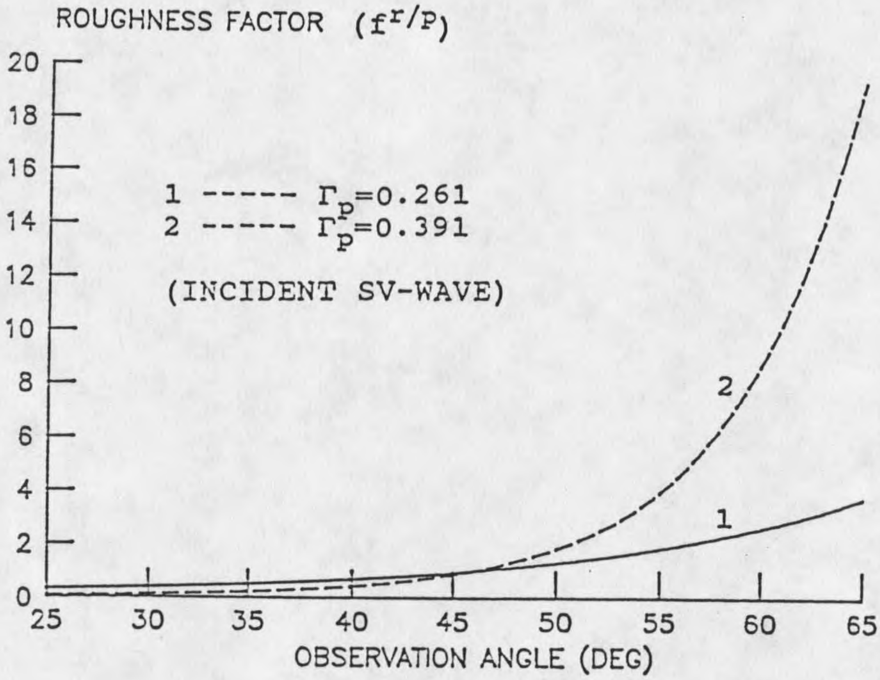

Figure 38. Roughness factor versus observation angle (refracted P-wave due to incident SV-wave)

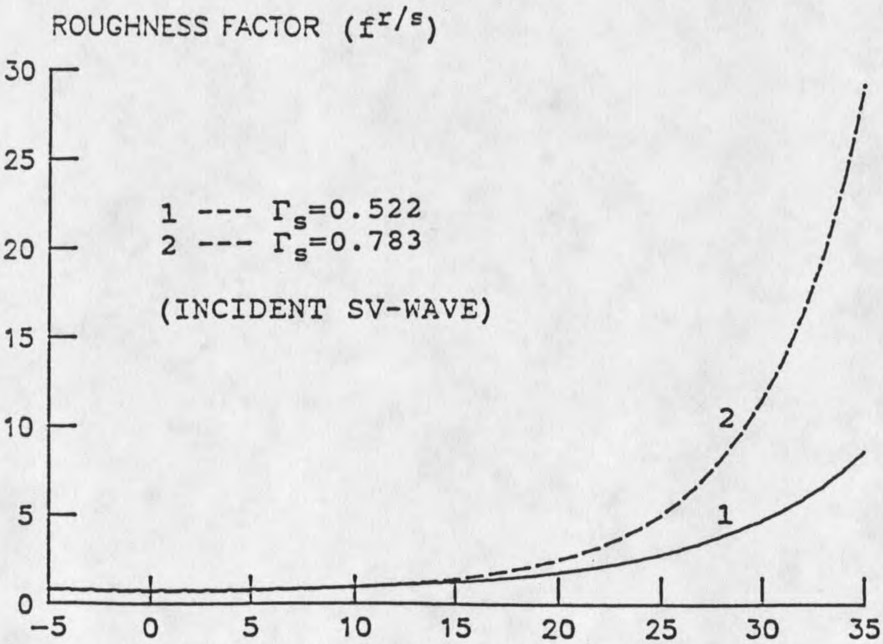

Figure 39. Roughness factor versus observation angle (refracted SV-wave due to incident SV-wave)

CHAPTER 8

RESULTS AND DISCUSSION

The final results of the scattered and refracted fields, in terms of the average values of the scattering and refracting coefficients, are expressed in Chapter 7, by Eqs. (7-30) and (7-32). Since these average evaluations contain complicated functions of the roughness and the gradient of the roughness, the calculations of these equations are very difficult and must be performed numerically. In this chapter, we show the given conditions for numerical computations, the numerical results (see the following figures), and the corresponding discussions.

The Procedure of the Numerical Calculation

In order to obtain the final numerical results of the problem, we need to evaluate the average quantities $<\zeta_i^{\alpha/A}>$ and $<\zeta_i^{\alpha/B}>$ shown in Eqs. (7-30) and (7-32). These two quantities are functions of h'(x) which are shown in Eqs. (7-16), and (7-18). The average evaluation of these two quantities, from Eq. (7-24), will be:

$$<\zeta_i^{\alpha/A}> = \int_{-\infty}^{\infty} \zeta_i^{\alpha/A}[h'(x)] \frac{1}{\sigma\sqrt{2\pi}} e^{\frac{-[h'(x)]^2}{2\sigma^2}} d[h'(x)] \qquad (8\text{-}1)$$

Because the quantity $\zeta_i^{\alpha/A}$ is related to h'(x) in a complicated way, Eq. (8-1) cannot be calculated explicitly and has been evaluated numerically. First lets change the variable in the integration in Eq. (8-1).

Let

$$y^2 = \frac{[h'(x)]^2}{2\sigma^2} \tag{8-2}$$

and then we have

$$d[h'(x)] = \sqrt{2}\,\sigma\,dy \tag{8-3}$$

Putting Eqs. (8-2) and (8-3) into Eq. (8-1) we get

$$\langle \zeta_i^{\alpha/A} \rangle = \int_{-\infty}^{\infty} W(y)\, e^{-y^2} dy \tag{8-4}$$

where

$$W(y) = \frac{1}{\sqrt{\pi}} \zeta_i^{\alpha/A} [h'(x)] \tag{8-5}$$

By applying the Gaussian Quadrature formula (Stroud and Secrest, p217, 1966), the Eq. (8-4) can be easily evaluated. In this work we choose fifteen terms (N=15) in the Gaussian Quadrature formula. We also examined the results for N=6 and N=30. The identity of these three sets of results indicated the accuracy of the numerical results.

<u>The Given Conditions for the Numerical Calculations</u>

a). The elastic materials of the two regions involved in this particular problem are considered to be metals. The region A is assumed to be steel, and region B is assumed to be copper. Values for some material properties of these two metals are listed in Table 2.

Table 2. Values of some material properties of two media in this problem

	region A	region B
material	steel	copper
density (kg/m^3)	7800	8500
Young's modulus (kg/cm^2)	$2.1X10^6$	$1.9X10^6$
Poisson ratio	0.26	0.33
P-wave speed (m/s)	5900	4600
SV-wave speed (m/s)	3200	2300

b). The rough boundary between the two materials is assumed to have a random profile in its height. The roughness of the boundary is measured by the variance or the root mean square of the height (r.m.s.). For common metal manufacturing, the typical value of the variance is about 0.12 (mm). In this paper, we use several different values of the variance, for example, σ=0.0-0.3 (mm). This range of the values denotes the cases from the smooth to very rough boundaries.

c). The domain of the integration is assumed to be arbitrary and from L_1 to L_2. The domain is related to the width of the incident wave as

$$L_2 - L_1 = \frac{W}{\cos\theta_{inc}} \tag{8-6}$$

where W is the width of the incident wave. In this paper, we use different dimensions of the domain on the axis by changing the values of L_1 and L_2, for example, $L_2 = -L_1 = 5$, 10, 15, 20, 30, 50, 100, 200 (mm).

d). The incident wave is assumed to be a time-harmonic compression wave propagating in region A. The frequency of the incident wave used in this dissertation is assumed to be 10 (MHz). The incident angles used here are 0, 10, 20 and 30 (degree) relative to the normal of the mean plane of the rough boundary. For given frequency and wave speed of a wave, the wave number of the wave can be obtained by the following relation

$$k_\alpha = \frac{2\pi F}{c_\alpha}\ ,\quad \alpha = p, s \tag{8-7}$$

where F is the frequency of the wave (Hz); k_α is the wave number; c_α is the wave speed. Table 3. shows the values of the wave numbers and the wave speeds of the waves involved in this work.

Table 3. The values of wave numbers and wave speeds (frequency F=10 MHz)

	wave speed (m/s)	wavenumber (1/mm)
P-wave in region A	5900	10.6495
SV-wave in region A	3200	19.6350
P-wave in region B	4600	13.6591
SV-wave in region B	2300	27.3182

Results of the Scattered and Refracted Fields due to Incident Compression Wave

In this dissertation, we first calculated the numerical results of the scattered P-wave and SV-wave components in both region A and region B due to the incident compression wave. All results due to the incident compression wave are listed in Figs. 40-75. In examining of these figures, we want to discuss several points about the results.

a). Results in specular directions

For a rough boundary, the incident wave is reflected in several directions. The specular direction is defined as the direction in which the wave is reflected from a smooth boundary. In this paper, we consider the specular directions of the scattered P-wave and SV-wave components in region A, as well as the specular directions of the refracted P-wave and

SV-wave components in region B. For a certain roughness of the boundary, most energy is still reflected in the specular direction even though the boundary scatters the wave into several different directions. Therefore the investigation of the result of the scattered fields (in region A) and the refracted fields (in region B) in the specular directions is very important. As the incident angle and the wave number change, the specular directions vary. For given materials, the corresponding wave numbers are constant, and the specular directions depend only on the incident angle. The explicit relations between the specular directions and the incident angle were given by Eqs. (4-42)-(4-46). Table 4 shows the values of the corresponding specular directions for different incident angles. Figures 40-49 show the results of the scattered compression and shear waves in terms of scattering coefficients. Figures 50-59 show the results of the compression and shear components of the refracted wave. From these figures, we can see that for certain values of roughnesses of the interface (for example, $\sigma<0.315$ mm for the scattered P-wave, $\sigma<0.210$ for the scattered SV-wave, $\sigma<0.275$ for the refracted P-wave, and $\sigma<0.170$ for the refracted SV-wave), the maximum values (peak values) of the distributions of the compression and shear components of both scattered and refracted waves still occur in the specular directions. From these figures we can also see that the values in the specular directions of all the waves decrease as the roughness increases.

Table 4. Values of specular directions (degree) for different incident angles due to incident P-wave with frequency f=10 MHz

incident angle (degree)	scattered P-wave (region A)	scattered SV-wave (region A)	refracted P-wave (region B)	refracted SV-wave (region B)
10	10	5.405	7.782	3.883
20	20	10.693	15.467	7.664
30	30	15.738	22.946	11.243
45	45	22.556	33.460	16.005
60	60	28.021	42.475	19.737

b). The general angular distribution of the results

From Figs. 40-49 and 50-59, we can see the general angular distributions of the compression and shear components of both scattered and refracted waves respectively. The basic profile of the angular distribution versus the observation angle is similar for different component and different roughness. The reason for this fact is the dimension and the shape of the rough boundary over which the integration is carried out. As we mentioned in Chapter 7, we introduce a factor (called integration factor in this paper) $f^{D/\alpha}$ (α = p, s) which is given by Eq. (7-31). It is just this integration factor which affects the basic profile of the angular distributions of the scattered P-wave and SV-wave components of both the scattered and refracted fields except the case of very rough interfaces.

c). The roughness effects in the results

From these figures, we can see that the roughness of the interface affects the overall scattering coefficients of the scattered and the refracted fields in two ways. First, as the roughness increases, the values of the overall scattering coefficients of both scattered and refracted fields decrease. This is due to the roughness factors which are given and discussed in Chapter 7. Second, the overall scattering coefficients not only decrease as the roughness increases, but also are affected in the side lobes by the roughness. From Figs. 40-44, we can see that as the roughness increases, the size of the side lobes (relative to the result in the specular direction) in the region of the smaller observation angle is getting smaller, and the size of the side lobes in the region of the larger observation angle is getting larger. This is due to the angular effects of the roughness factor. Figures 24-27 in Chapter 7 show the results of the angular effects. Figures 40-59 also show the difference between the shear components and the compression components in the effects by roughness. By comparing Figs. 40, 41 with Figs. 45, 46 and Figs. 50, 51 with Figs. 55, 56, we note that for both scattered and refracted waves, the changing of the results from a smooth interface to a certain rough interface for the shear components is considerably greater than that for the compression components.

This is due to the shorter shear wavelength.

d). The effects by integration domain in the results

The size of the integration domain, which depends on the width of the incident wave, affects the results of both scattered and refracted fields. Figures 60-71 show the effects. From these figures, it is clear that for both compression and shear wave components of the scattered and refracted waves, the size of the integration domain affects the distribution of the results. As the size of the integration domain increases, the number of the side lobes increases, and the amplitude of the side lobes decreases. The width of lobe in the specular direction decreases as the size of the integration domain increases. However the amplitude of the lobe in the specular direction does not change for different integration domains. From these results, we can see that the larger the size of the integration domain, the more scattered energy concentrates in the specular direction.

e). Diffusely scattering and refracting

Figures 44, 49, 54 and 59 show the results of the diffusely scattering and refraction for both compression and shear waves. From these figures, we can see that the diffuse scattering and refraction occurs for the case of very rough interface. However for different waves, the diffusing occurs at different roughness. The shear components of both scattered and refracted waves diffuse at smaller values of the roughness than the compression components do. For example, in the scattered fields, diffusion occurs at σ=0.210 (mm) for the shear component and σ=0.315 (mm) for the compression component. In refracted fields, diffusion occurs at σ=0.170 for the shear component and σ=0.275 for the compression component. This is because the wave numbers of the shear waves are larger than those of the compression waves. The expressions of the roughness factors, Eq. (7-36), show that the roughness factors are dependent on the wave numbers.

f). Diffraction effects in the wave scattering problem

From Figs. 40, 45, 50 and 55 we note that scattering from a smooth surface exists in this problem. This is because of the diffraction. Since the size of the scattering surface, which is related to the size of the width of the incident wave, is assumed to be finite, the diffraction effects occur. For more detail about diffraction effects, refer to the papers by Achenbach and Gaustesen (1977) and Banaugh and Goldsmith (1963). In order to investigate the diffraction effects involved in this problem, we studied a special case of the scattering from a smooth surface for one material only (the second region is assumed to be vacuum). The results for different size of the smooth surface are calculated and shown in Figs. 72-77. From these figures we can see that the diffraction effects decrease as the size of the integration domain increases. For a large size of the smooth surface, for example, L=200 (mm), the plot (Fig. 77) shows that diffraction effect is very small and can be ignored.

g). Effect of varying roughness for large size surface

Figures 78-81 show that for different roughness, the scattering coefficients from a large size surface have different distributions. As the roughness increases, the value of the scattering coefficient decreases. For a very rough surface, for example σ=0.315 (mm), the overall distribution of the scattered field changes considerably. Since the diffraction effect is very small in the case of a large size surface, the results in Figs. 78-81 show the "pure" effect of the wave scattering form a rough surface.

h). Comparison of results for different incident angles

In this work the results of scattered fields for different incident angles, for example, θ_{inc}=0, 10, 20, 30 (degree), are also calculated and shown in Figures (82-85). From these figures we can see that the incident angle affects the over all distribution of the scattered field. For the normal incident wave, the scattered field has a symmetrical distribution about the specular direction (see Fig. 82). If the incident angle is changed from the normal direction, say θ_{inc}=10 (degree), the scattered field has no longer a symmetrical distribution about the specular direction (see Fig. 83). From the figure we see that the scattered field at the region beyond the specular direction has larger values than those at the region less than the specular direction. The figure presents a uneven distribution. As the incident angle increases, the uneven distribution increases (see

Figs. 84, 85).

The Results due to Incident Shear Wave

For incident shear wave, the specular directions of all scattered and refracted waves are different from those due to the incident compression wave. Table 5. shows the values of the specular directions due to the incident shear wave.

Table 5. Values of specular directions (degree) for different incident angles due to incident SV-wave

incident angle (degree)	scattered P-wave (region A)	scattered SV-wave (region A)	refracted P-wave (region B)	refracted P-wave (region B)
30	67.2016	30	45.9515	21.0619

The numerical results for the case of the incident shear wave, in terms of scattering coefficient, are listed in Figs. 86-111. From these figures we can see that the results of the scattered and refracted fields due to the incident shear wave have similar properties as the case of incident compression wave does.

Figures 86-99 show that both scattered and refracted fields due to incident shear wave decrease as the roughness increases. Figures 89, 93, 96 and 99 show the results of the diffusely scattering and refraction for both compression and shear waves. From these figures, we can see that the diffusely scattering and refraction occur for the case of very rough interface. However for different waves, the diffusing occurs at different roughness. The shear components of both scattered and refracted waves diffuse at smaller values of the roughness than the compression components do. For example, in the scattered fields, the diffusion occurs at σ=0.170 (mm) for the shear component and σ=0.220 (mm) for the compression component. In refracted fields, the diffusion occurs at σ=0.150 for the shear component and σ=0.220 for the compression component. This is because the wavelength of the shear wave is larger than that of the compression wave. The expressions of the roughness factors, Eq. (7-36), show that the roughness factors are dependent to the wave numbers.

Figures 100-111 show that the size of the integration domain, which depends on the width of the incident wave, affects the results of both scattered and refracted fields. From these figures we can see that for both compression and shear wave components of the scattered and refracted waves, the size of the integration domain affects the distribution of the results. As the size of the integration domain increases, the number of the side lobes increases, and the amplitude of the side lobes decreases. The width of lobe in the specular direction decreases as the size of the integration domain increases. However the amplitude of the lobe in the specular direction does not change for different integration domains.

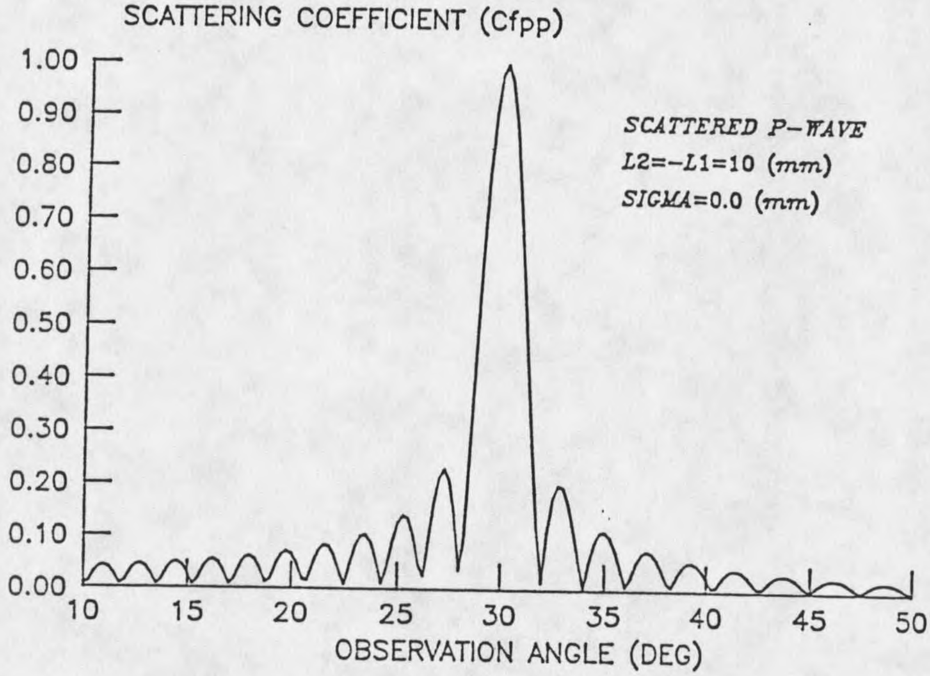

Figure 40. Scattering coefficient for scattered P-wave in region A due to incident P-wave (σ=0.0 mm)

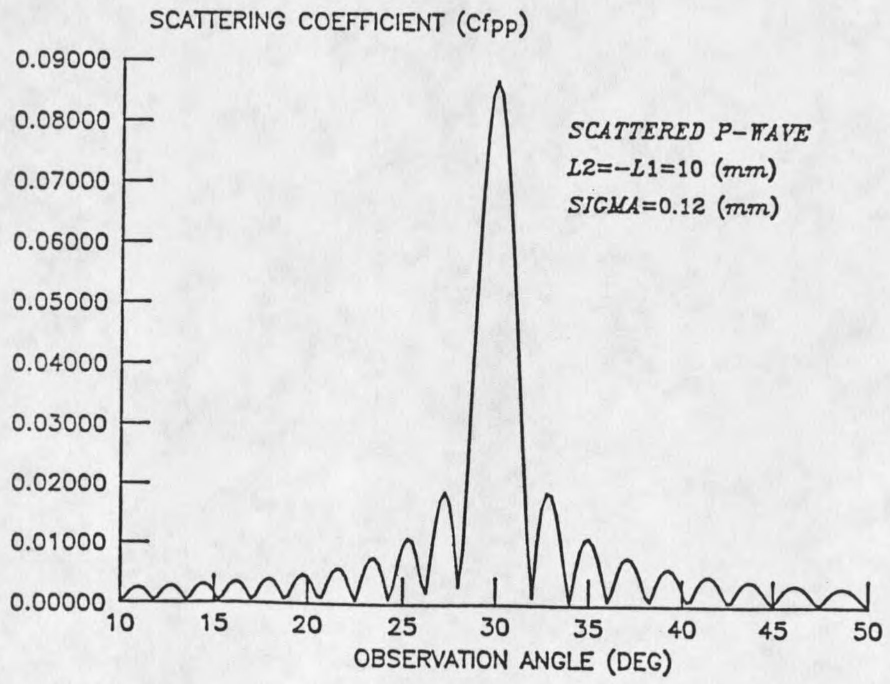

Figure 41. Scattering coefficient for scattered P-wave in region A due to incident P-wave (σ=0.12 mm)

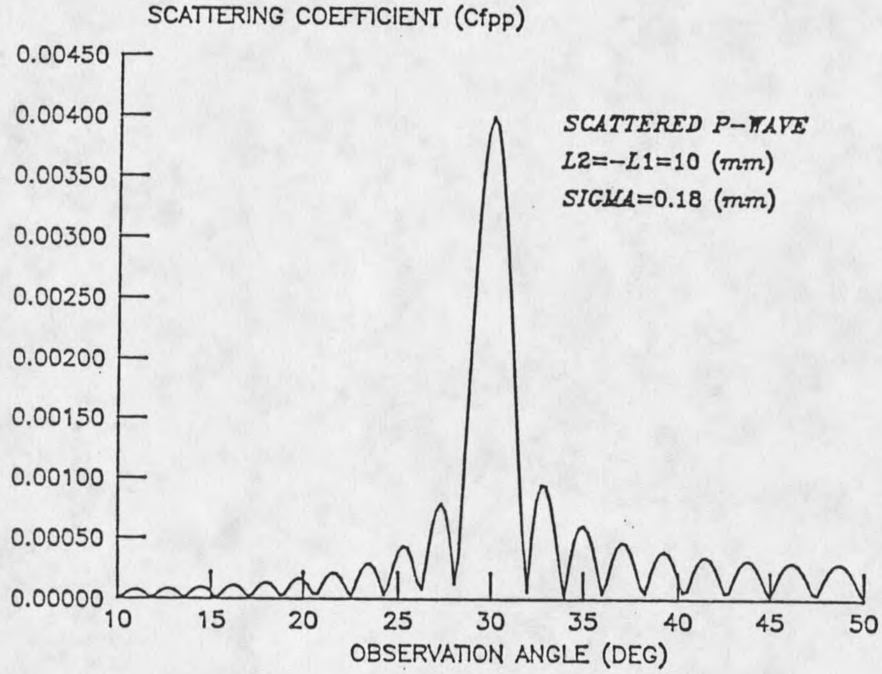

Figure 42. Scattering coefficient for scattered P-wave in region A due to incident P-wave (σ=0.18 mm)

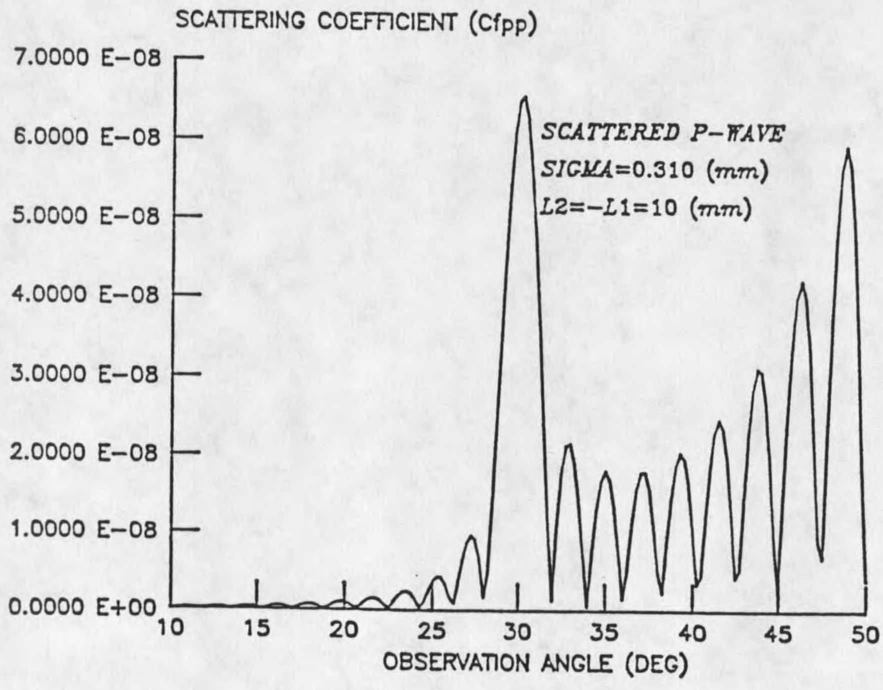

Figure 43. Scattering coefficient for scattered P-wave in region A due to incident P-wave (σ=0.310 mm)

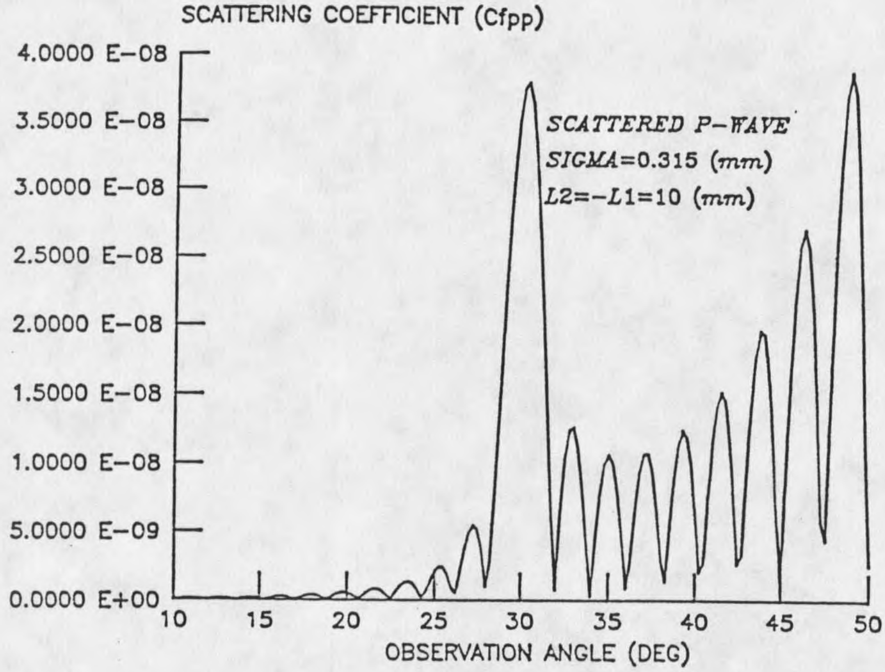

Figure 44. Scattering coefficient for scattered P-wave in region A due to incident P-wave (σ=0.315 mm)

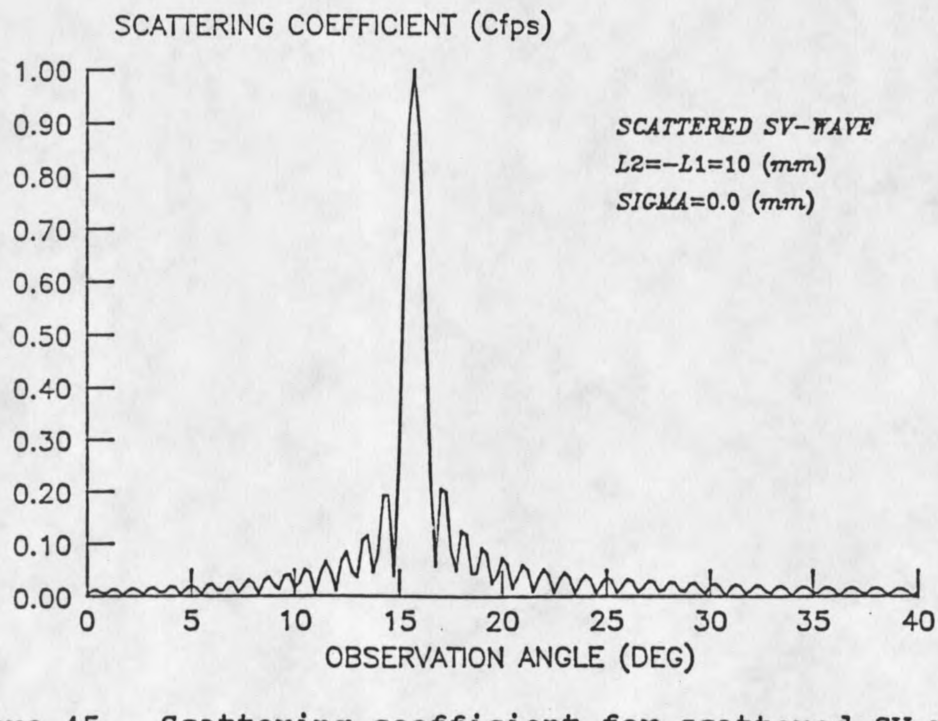

Figure 45. Scattering coefficient for scattered SV-wave in region A due to incident P-wave (σ=0.0 mm)

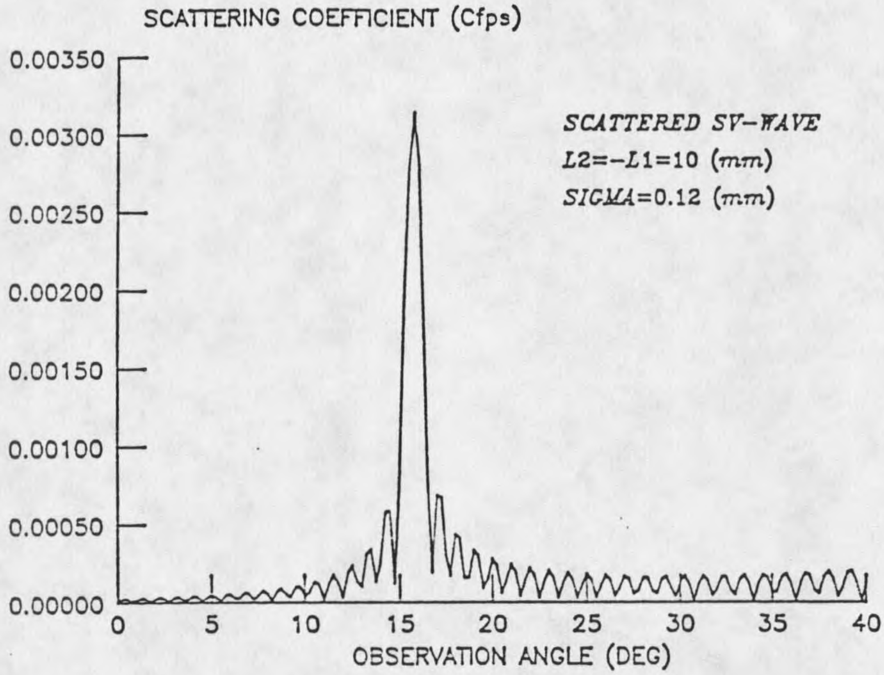

Figure 46. Scattering coefficient for scattered SV-wave in region A due to incident P-wave (σ=0.12 mm)

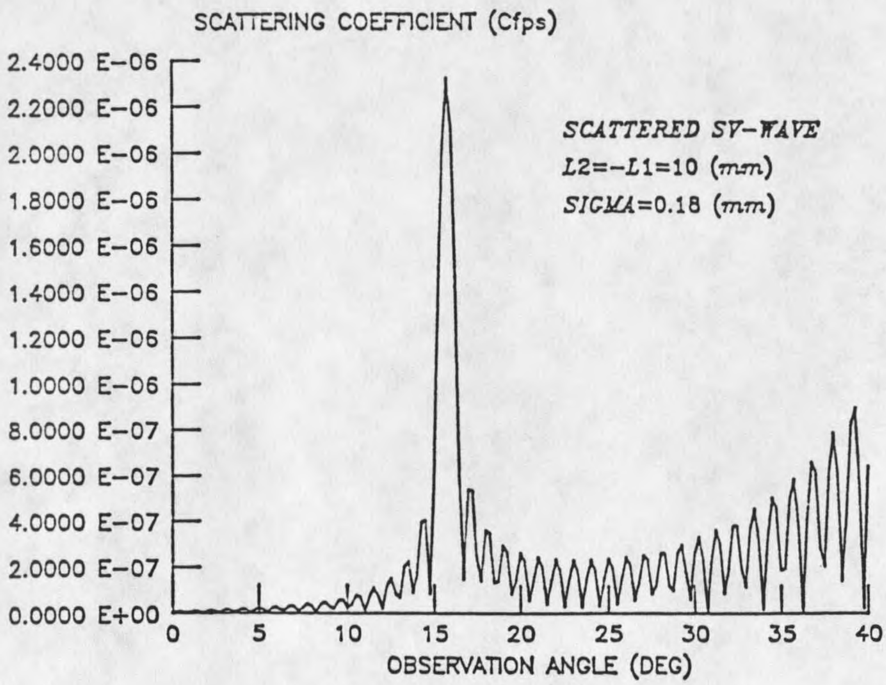

Figure 47. Scattering coefficient for scattered SV-wave in region A due to incident P-wave (σ=0.18 mm)

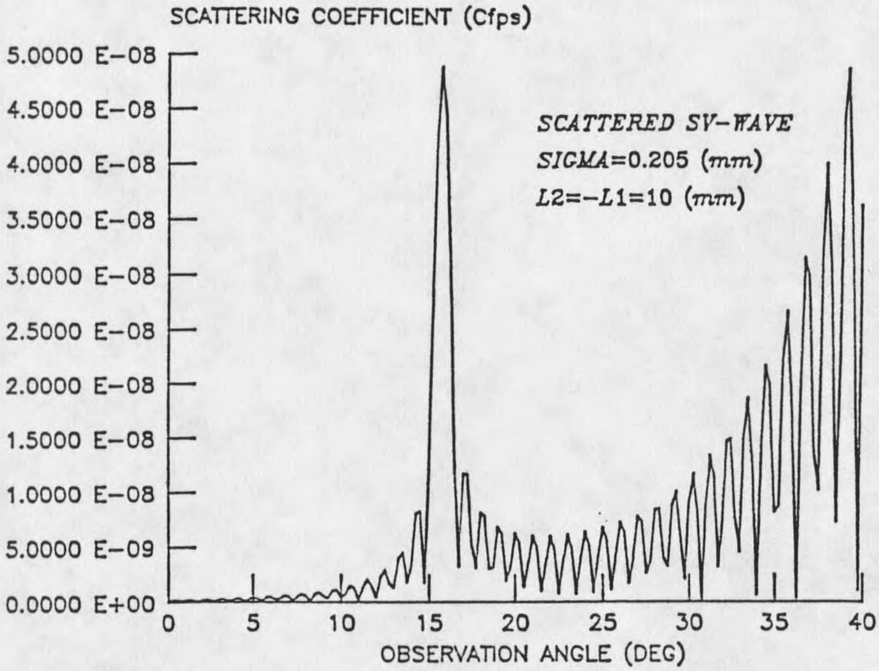

Figure 48. Scattering coefficient for scattered SV-wave in region A due to incident P-wave (σ=0.205 mm)

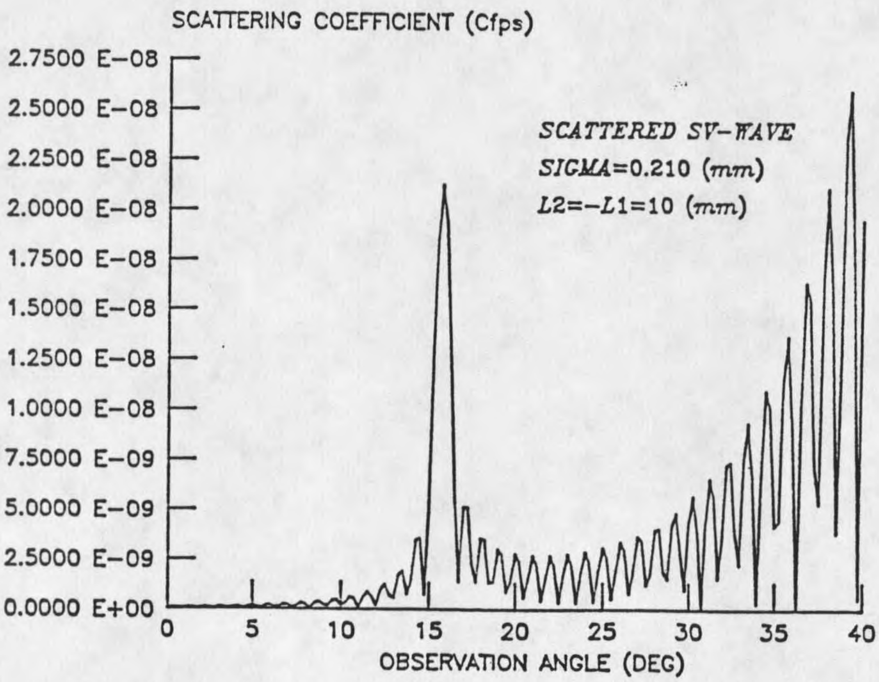

Figure 49. Scattering coefficient for scattered SV-wave in region A due to incident P-wave (σ=0.210 mm)

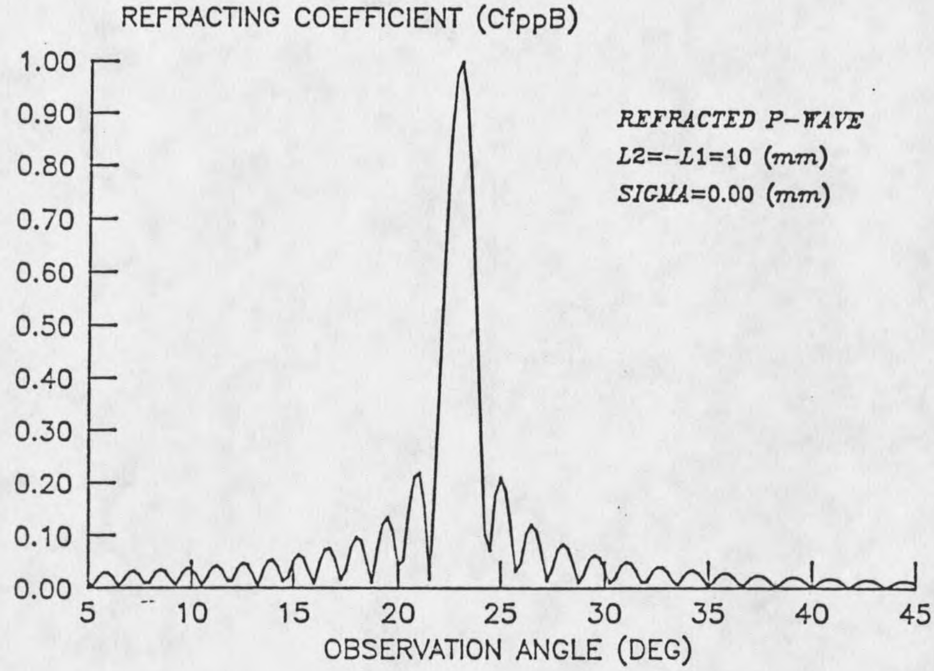

Figure 50. Scattering coefficient for refracted P-wave in region B due to incident P-wave (σ=0.0 mm)

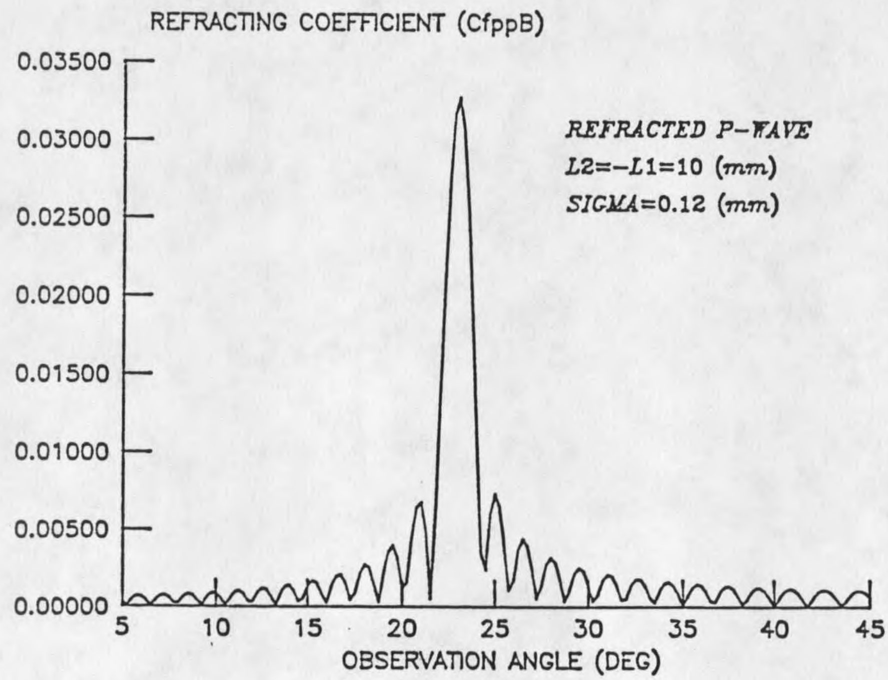

Figure 51. Scattering coefficient for refracted P-wave in region B due to incident P-wave (σ=0.12 mm)

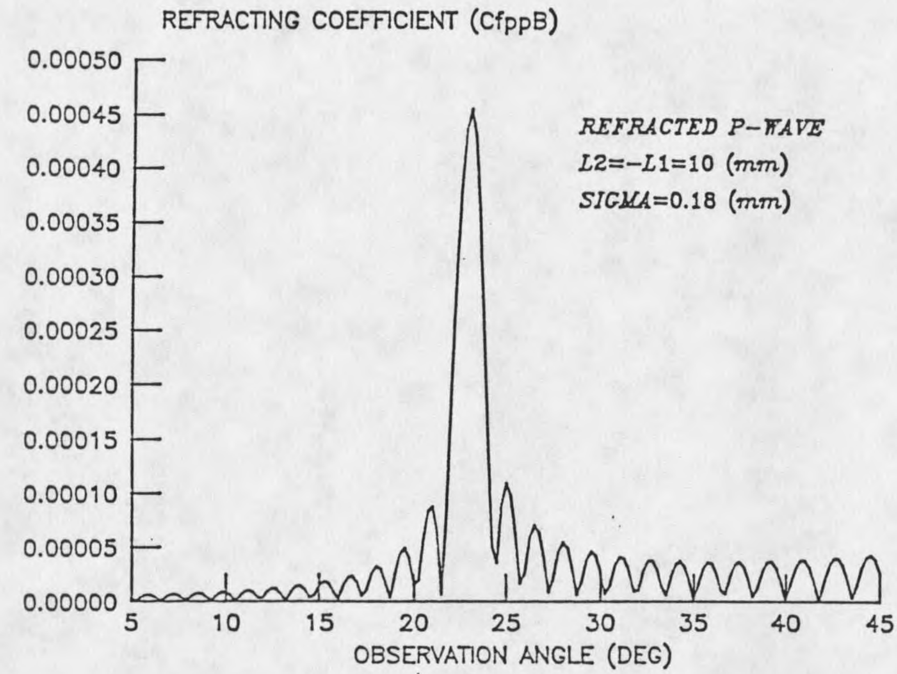

Figure 52. Scattering coefficient for refracted P-wave in region B due to incident P-wave (σ=0.18 mm)

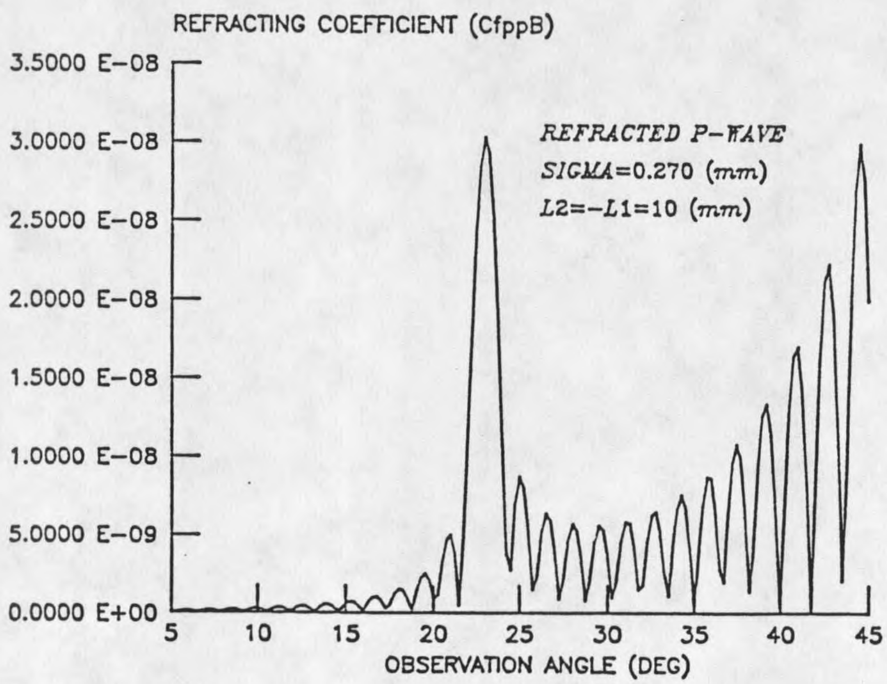

Figure 53. Scattering coefficient for refracted P-wave in region B due to incident P-wave (σ=0.270 mm)

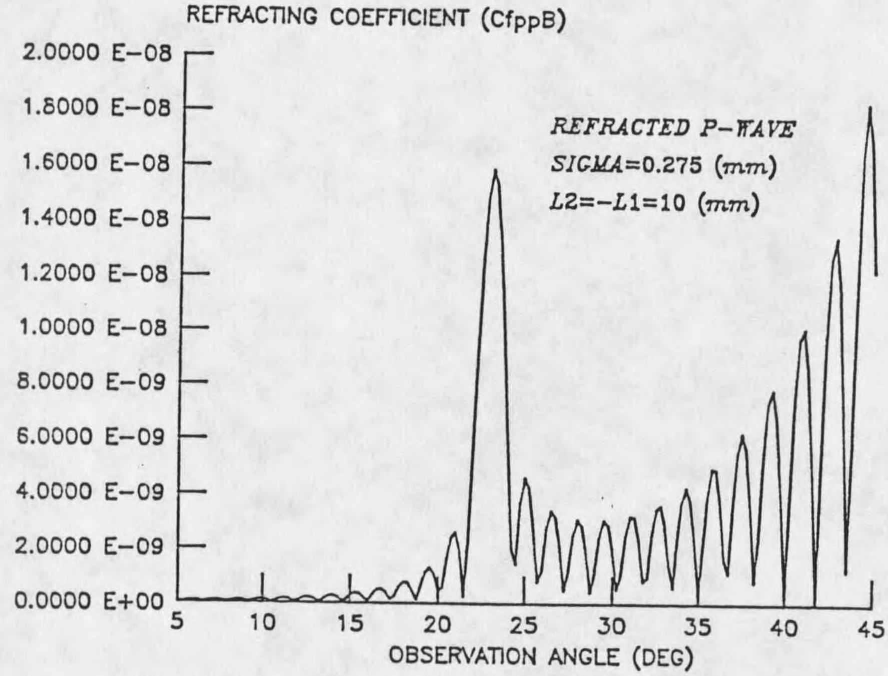

Figure 54. Scattering coefficient for refracted P-wave in region B due to incident P-wave (σ=0.275 mm)

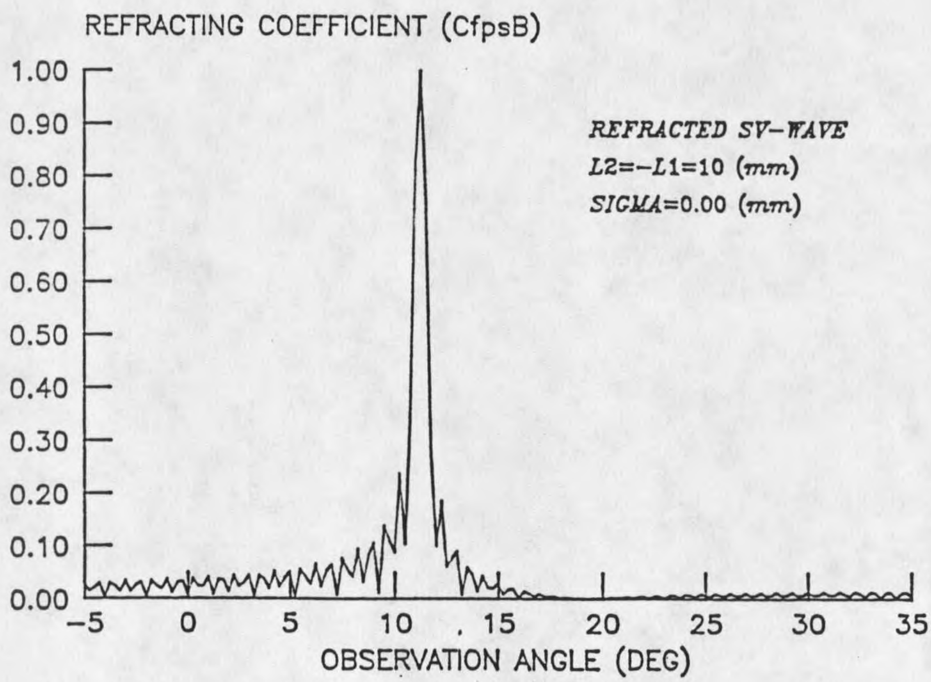

Figure 55. Scattering coefficient for refracted SV-wave in region B due to incident P-wave (σ=0.0 mm)

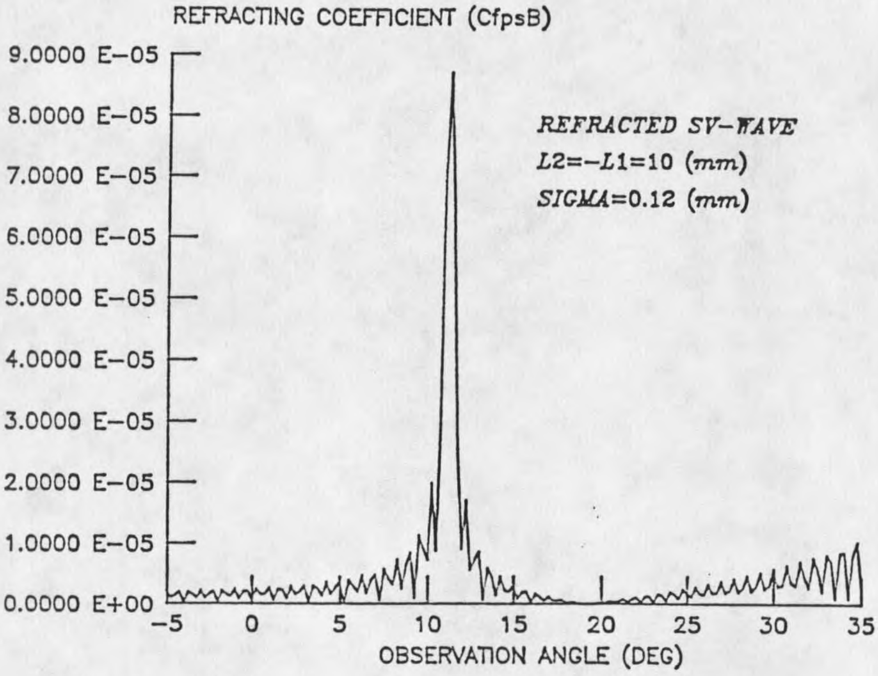

Figure 56. Scattering coefficient for refracted SV-wave in region B due to incident P-wave (σ=0.12 mm)

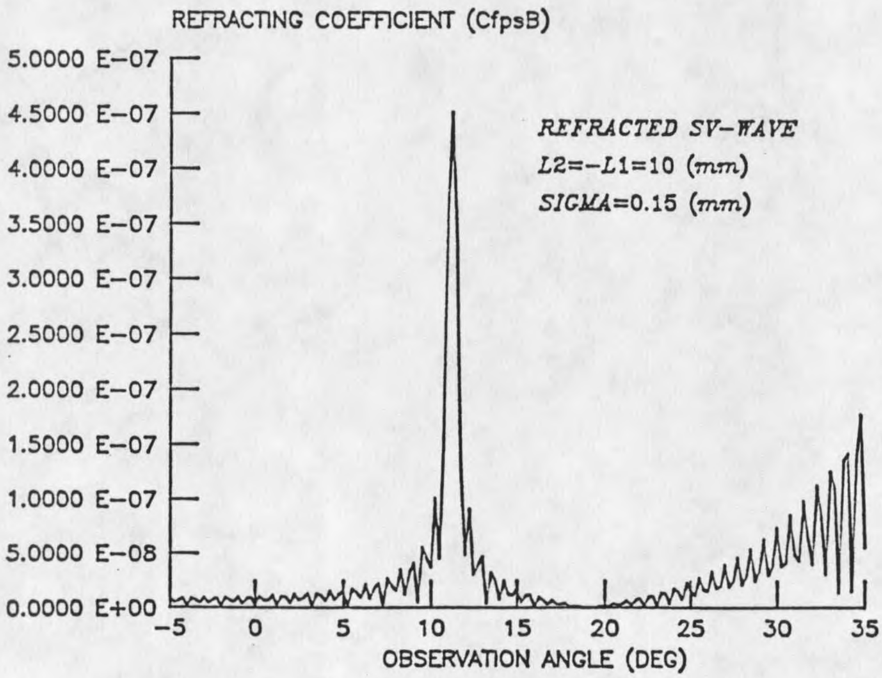

Figure 57. Scattering coefficient for refracted SV-wave in region B due to incident P-wave (σ=0.15 mm)

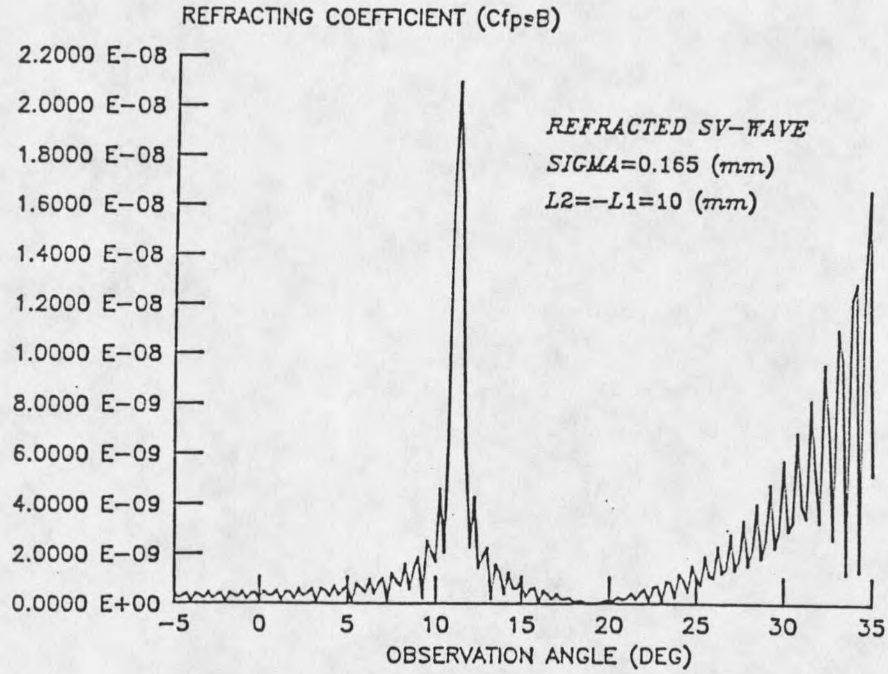

Figure 58. Scattering coefficient for refracted SV-wave in region B due to incident P-wave (σ=0.165 mm)

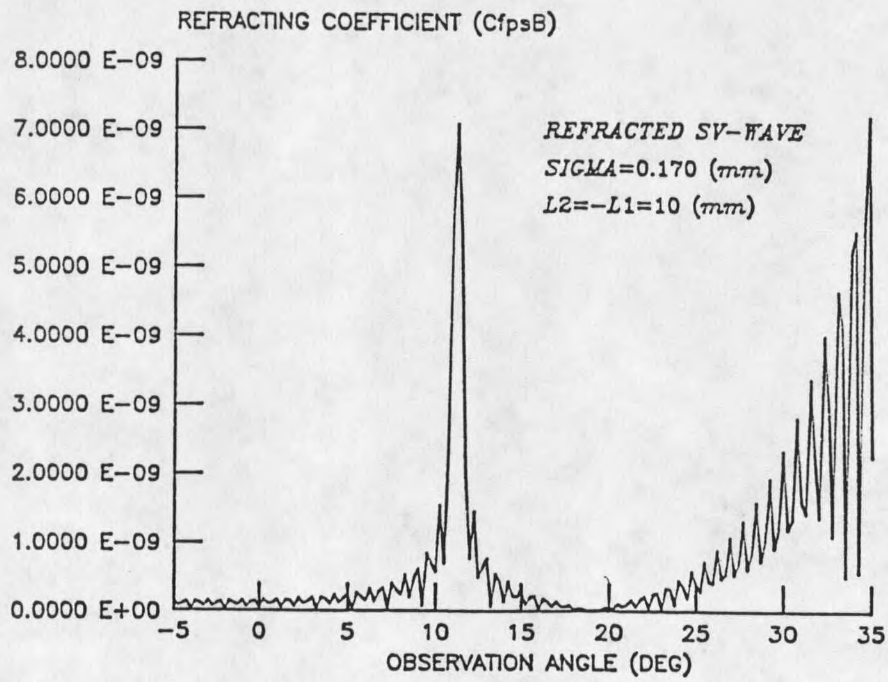

Figure 59. Scattering coefficient for refracted SV-wave in region B due to incident P-wave (σ=0.170 mm)

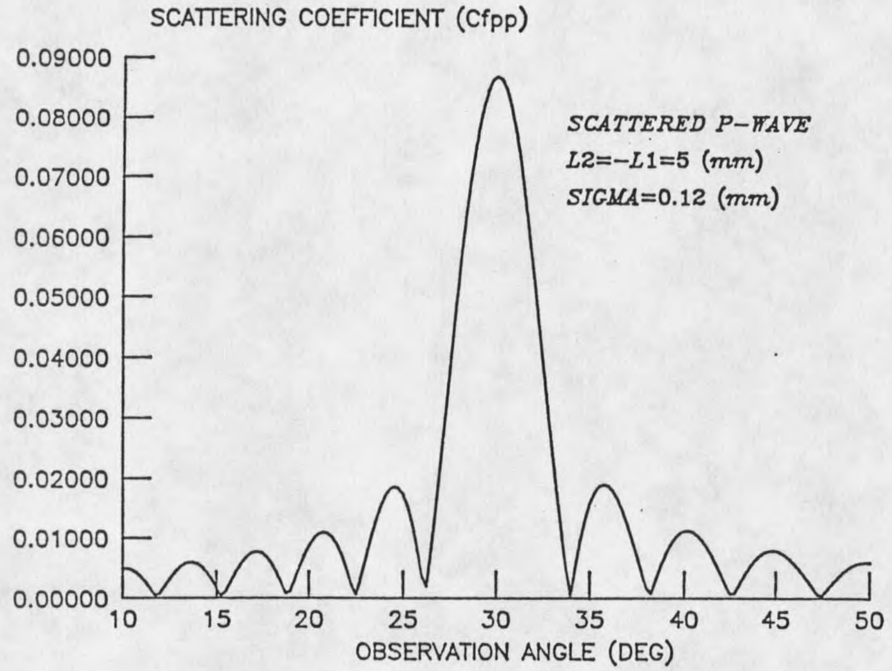

Figure 60. Scattering coefficient for scattered P-wave in region A due to incident P-wave (L_2=$-L_1$=5 mm)

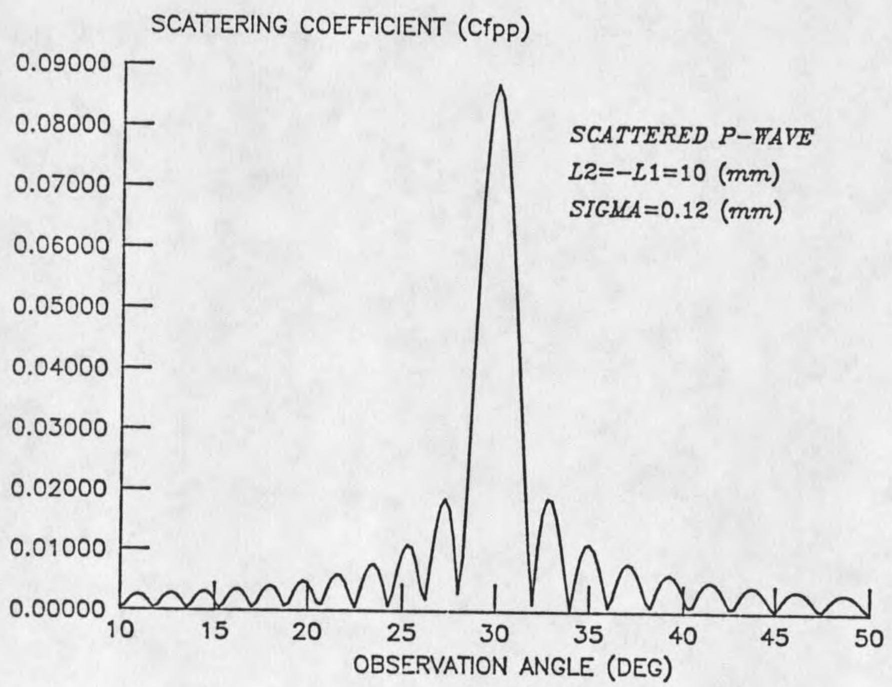

Figure 61. Scattering coefficient for scattered P-wave in region A due to incident P-wave (L_2=$-L_1$=10 mm)

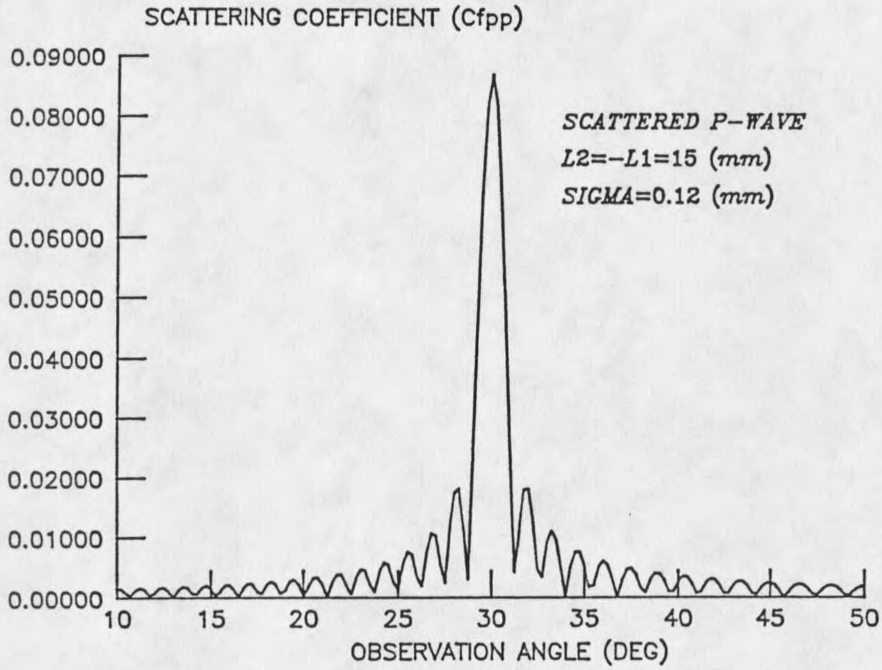

Figure 62. Scattering coefficient for scattered P-wave in region A due to incident P-wave (L_2=-L_1=15 mm)

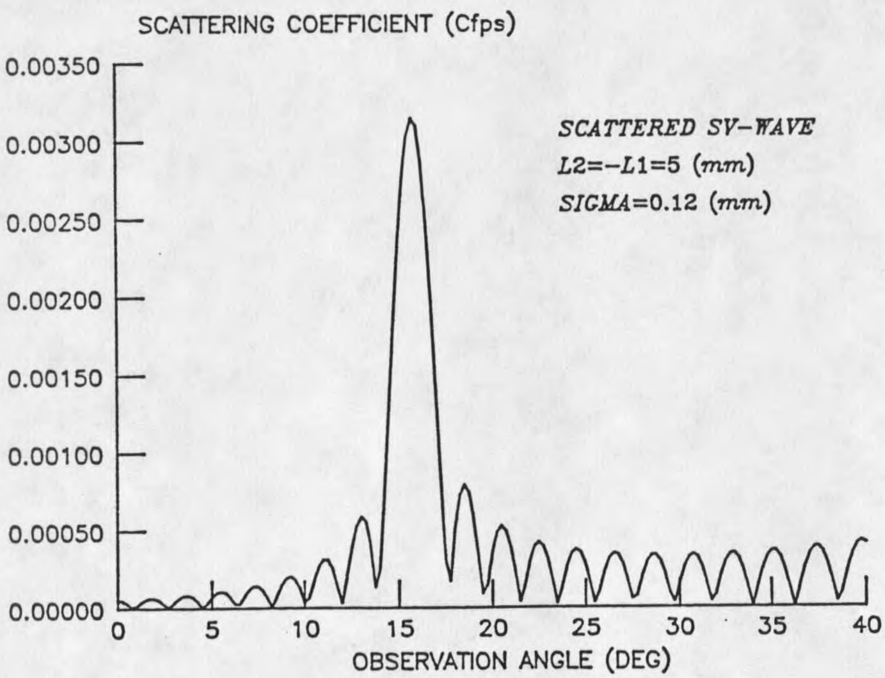

Figure 63. Scattering coefficient for scattered SV-wave in region A due to incident P-wave (L_2=-L_1=5 mm)

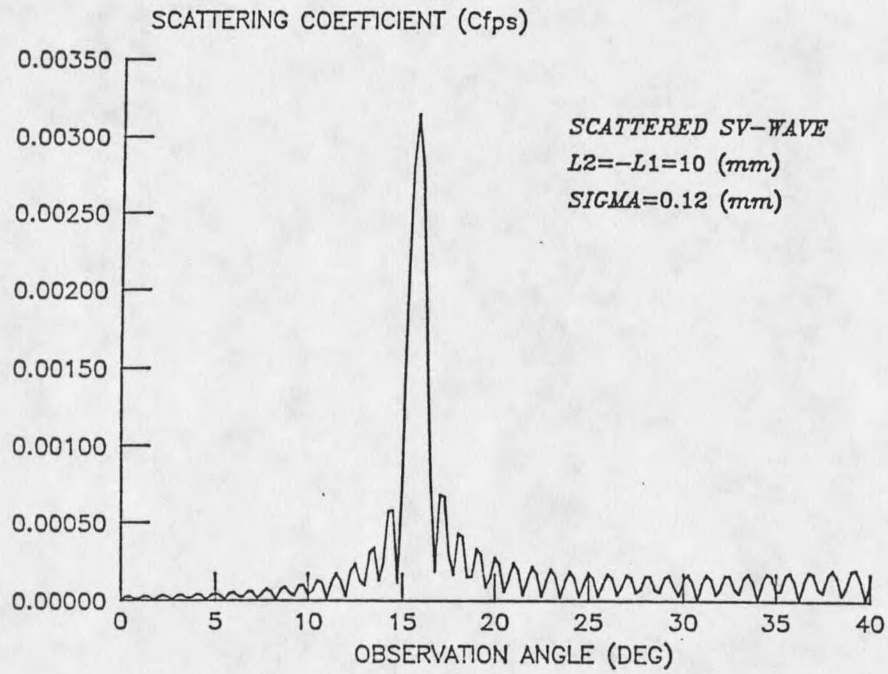

Figure 64. Scattering coefficient for scattered SV-wave in region A due to incident P-wave (L_2=$-L_1$=10 mm)

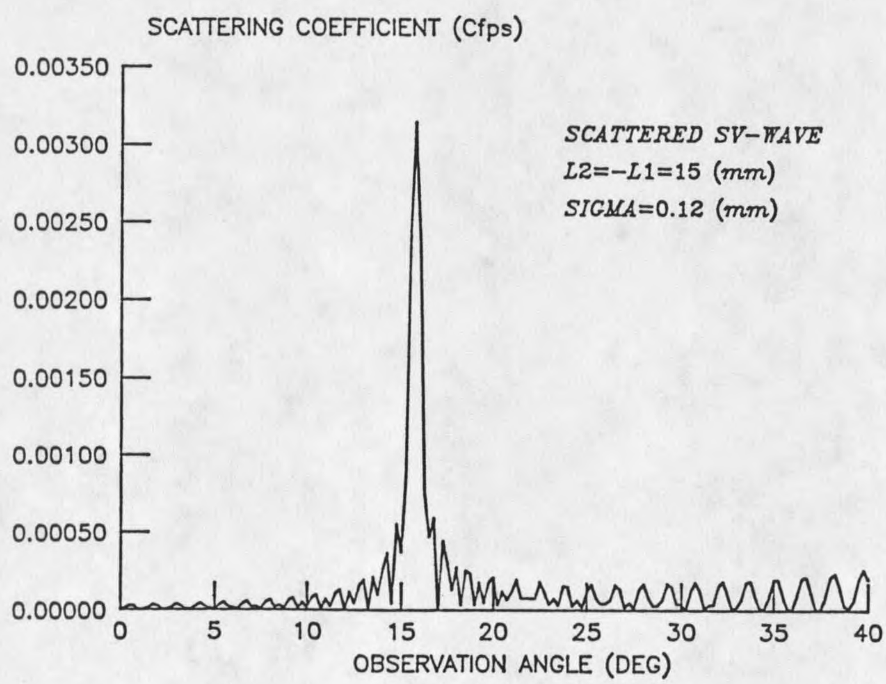

Figure 65. Scattering coefficient for scattered SV-wave in region A due to incident P-wave (L_2=$-L_1$=15 mm)

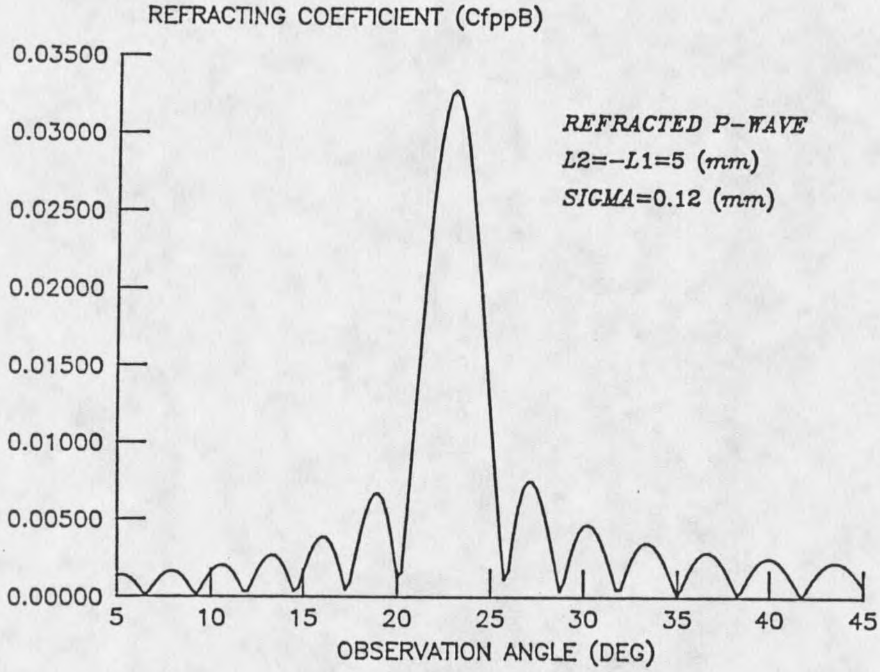

Figure 66. Scattering coefficient for refracted P-wave in region A due to incident P-wave (L_2=$-L_1$=5 mm)

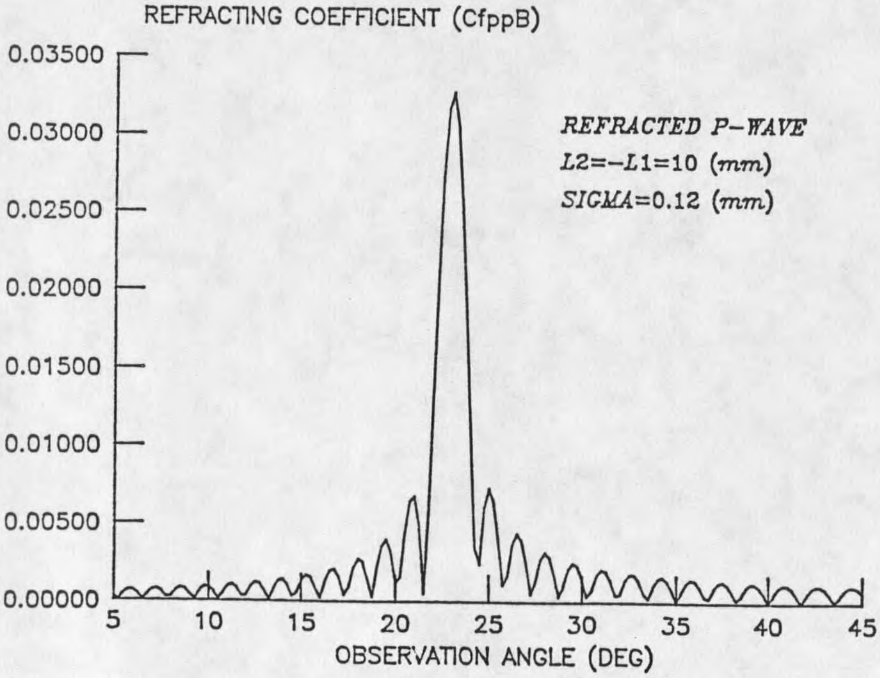

Figure 67. Scattering coefficient for refracted P-wave in region A due to incident P-wave (L_2=$-L_1$=10 mm)

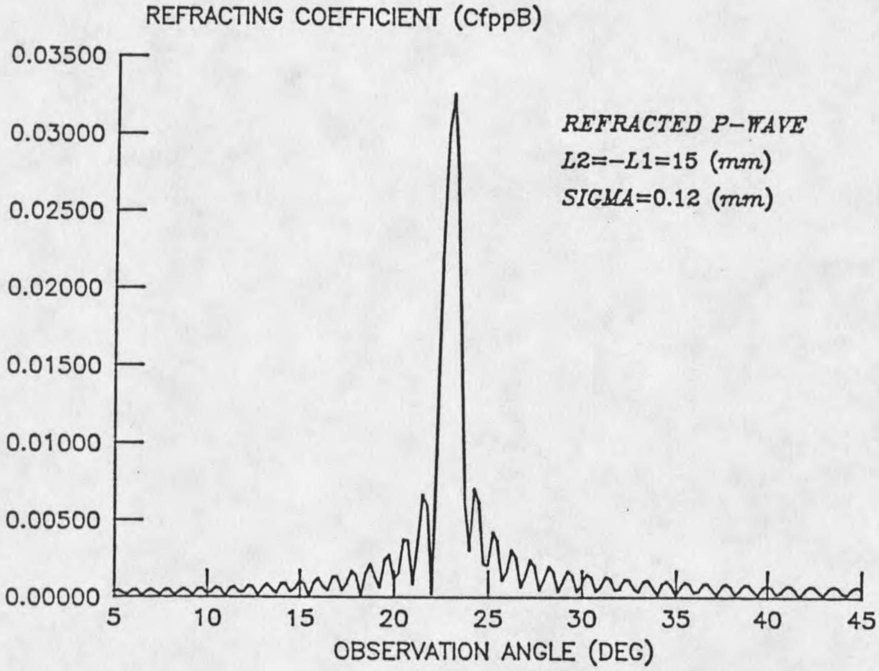

Figure 68. Scattering coefficient for refracted P-wave in region A due to incident P-wave (L_2=-L_1=15 mm)

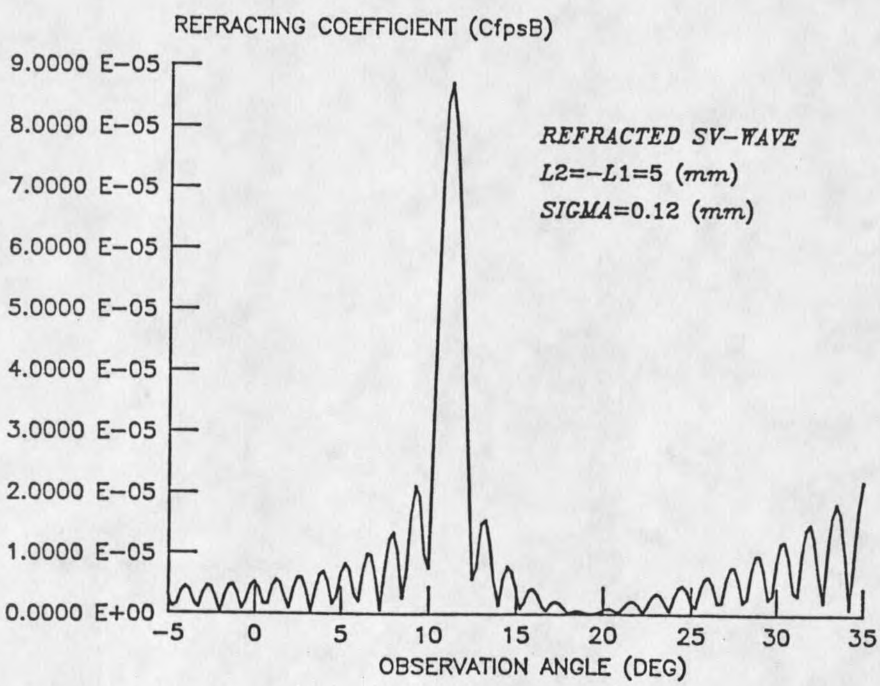

Figure 69. Scattering coefficient for refracted SV-wave in region A due to incident P-wave (L_2=-L_1=5 mm)

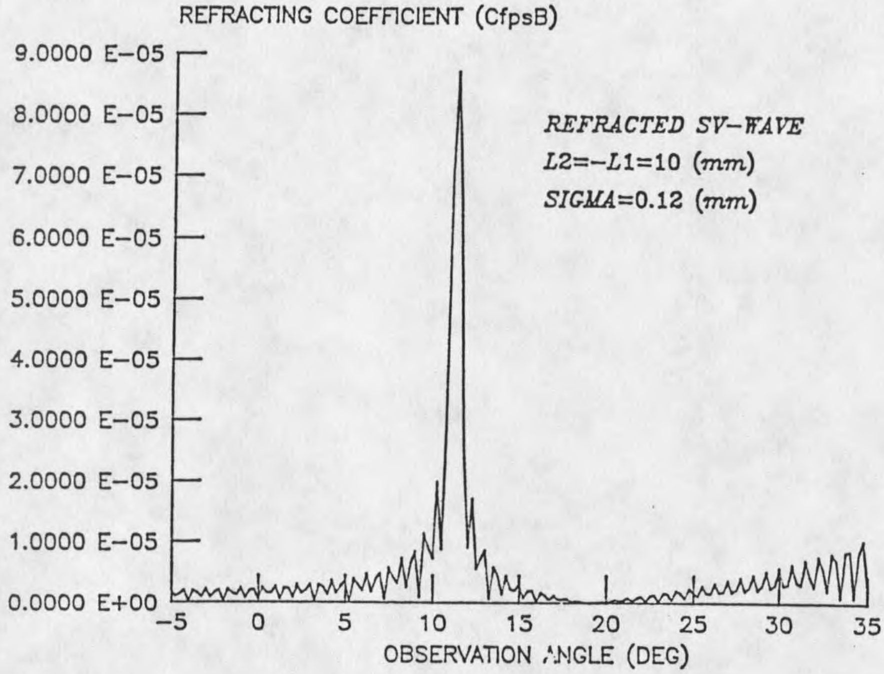

Figure 70. Scattering coefficient for refracted SV-wave in region A due to incident P-wave (L_2=-L_1=10 mm)

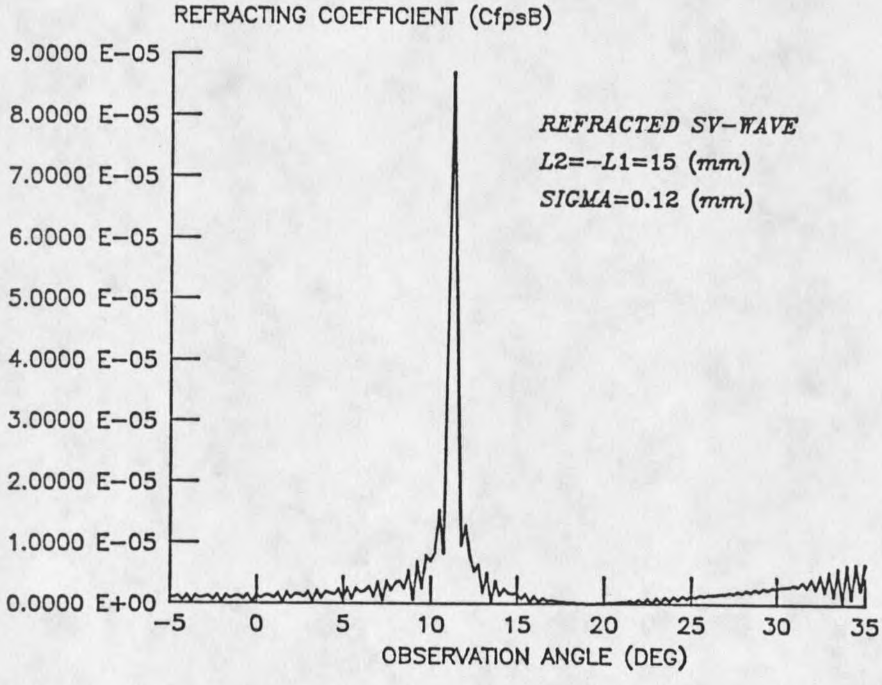

Figure 71. Scattering coefficient for refracted SV-wave in region A due to incident P-wave (L_2=-L_1=15 mm)

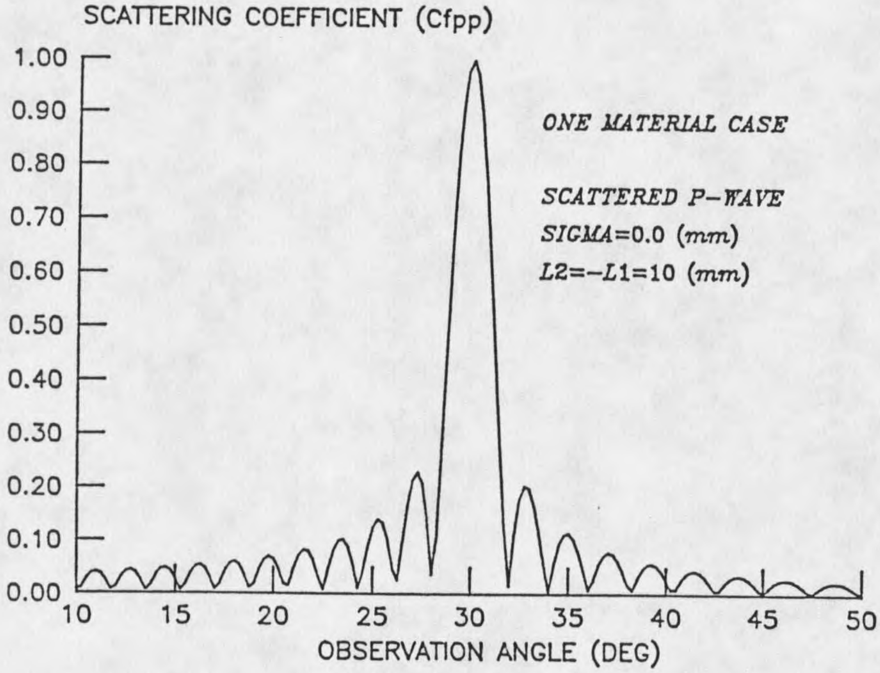

Figure 72. Scattering coefficient for scattered P-wave due to incident P-wave (one material case L_2=-L_1=10 mm)

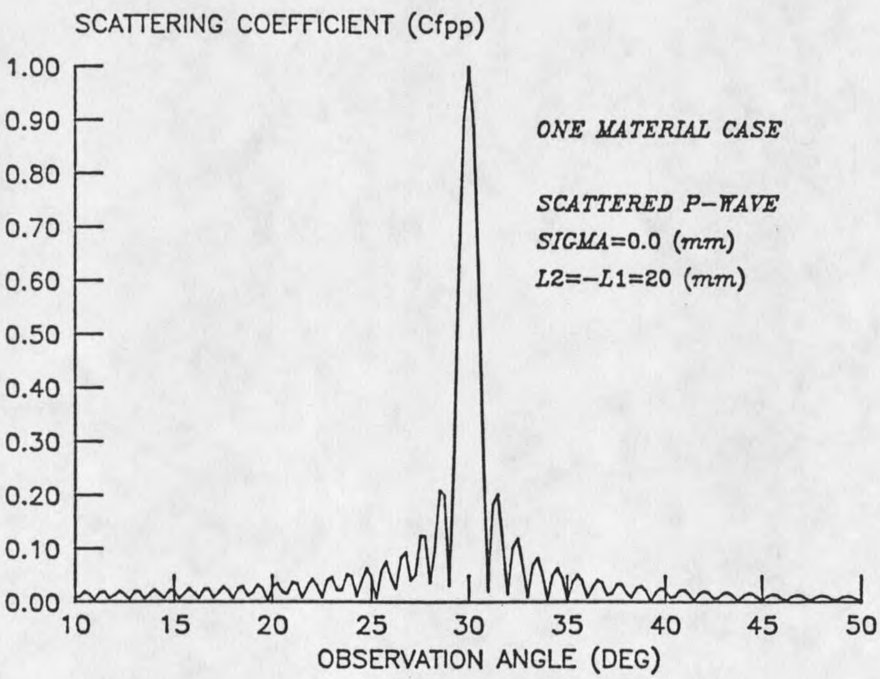

Figure 73. Scattering coefficient for scattered P-wave due to incident P-wave (one material case L_2=-L_1=20 mm)

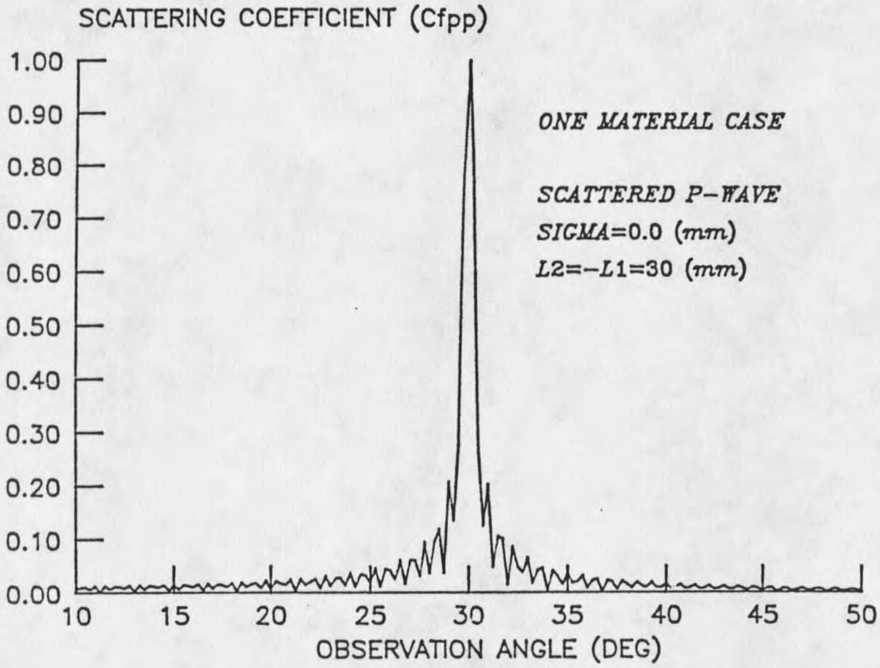

Figure 74. Scattering coefficient for scattered P-wave due to incident P-wave (one material case L_2=-L_1=30 mm)

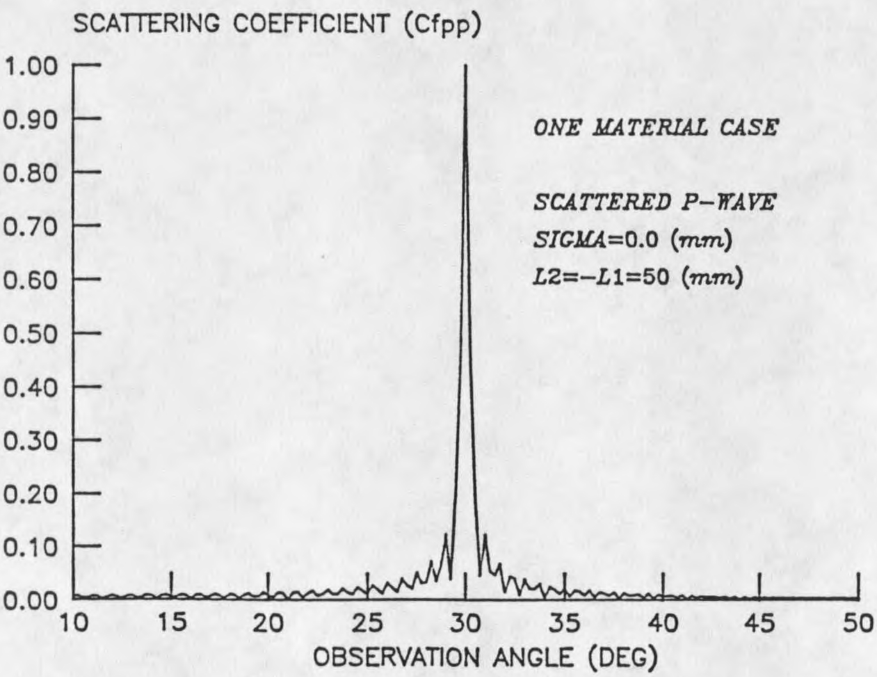

Figure 75. Scattering coefficient for scattered P-wave due to incident P-wave (one material case L_2=-L_1=50 mm)

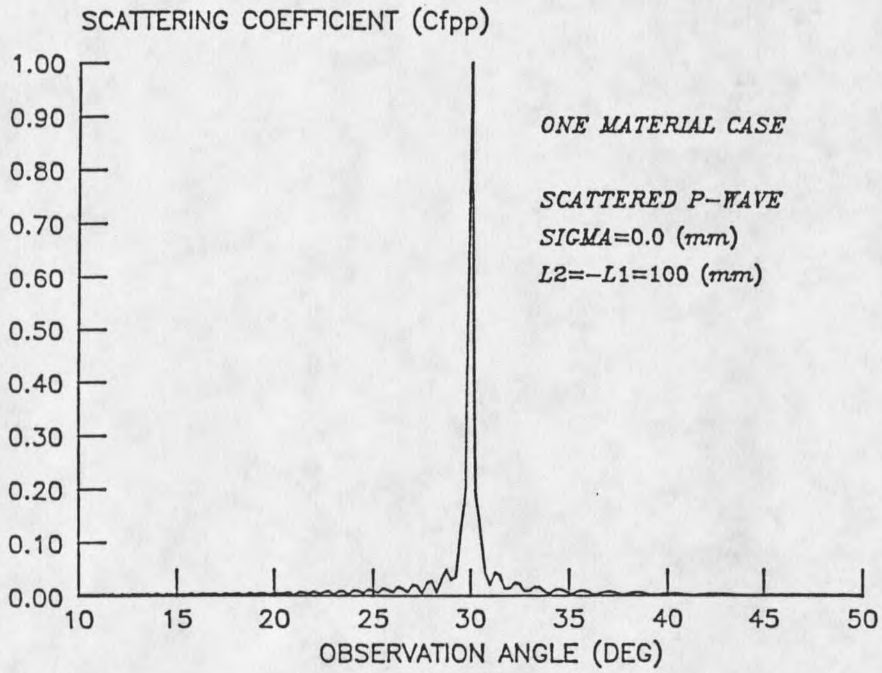

Figure 76. Scattering coefficient for scattered P-wave due to incident P-wave (one material case L_2=-L_1=100 mm)

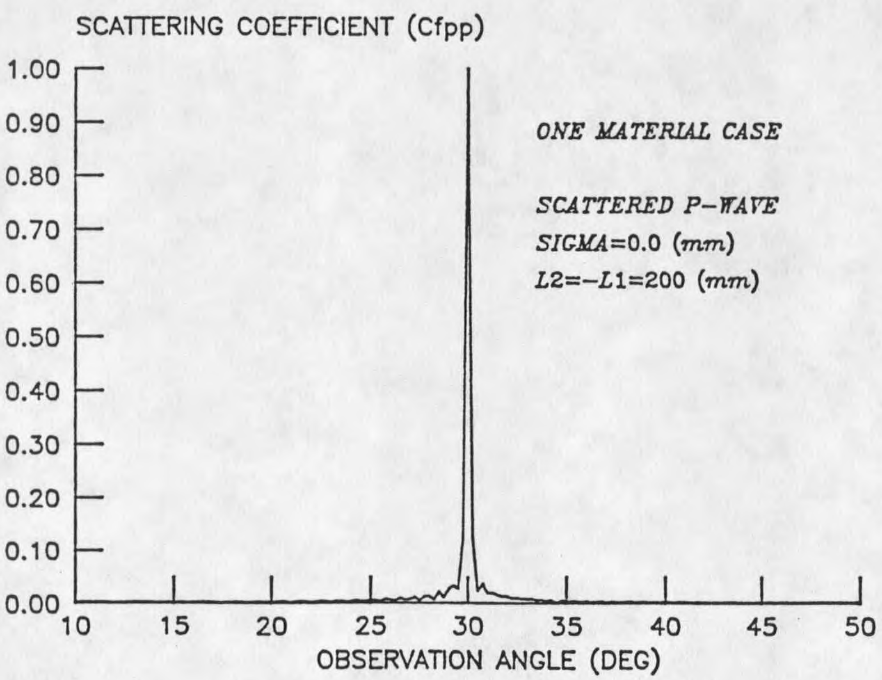

Figure 77. Scattering coefficient for scattered P-wave due to incident P-wave (one material case L_2=-L_1=200 mm)

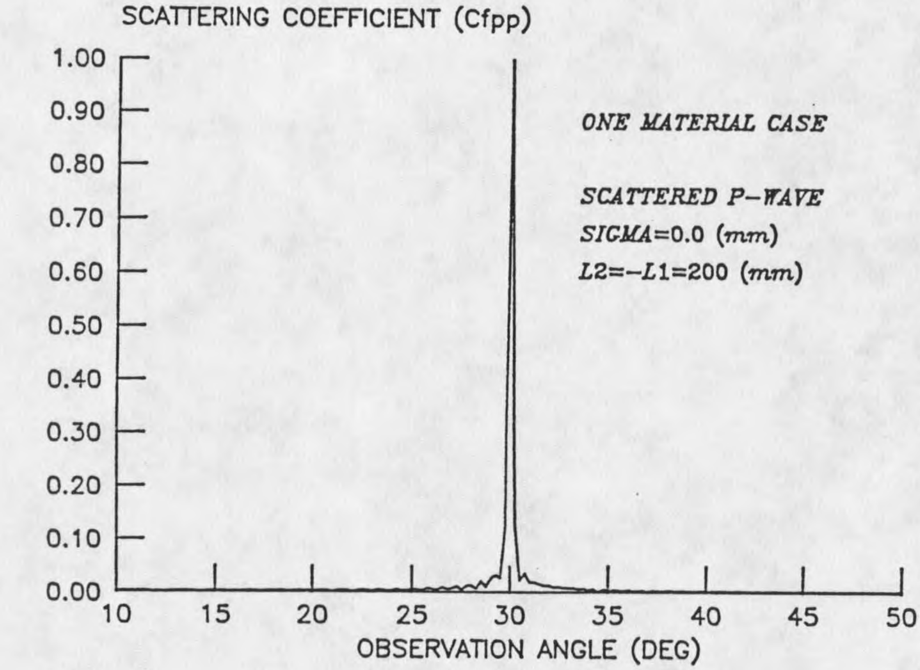

Figure 78. Scattering coefficient for scattered P-wave from large surface (one material case, σ=0.0 mm)

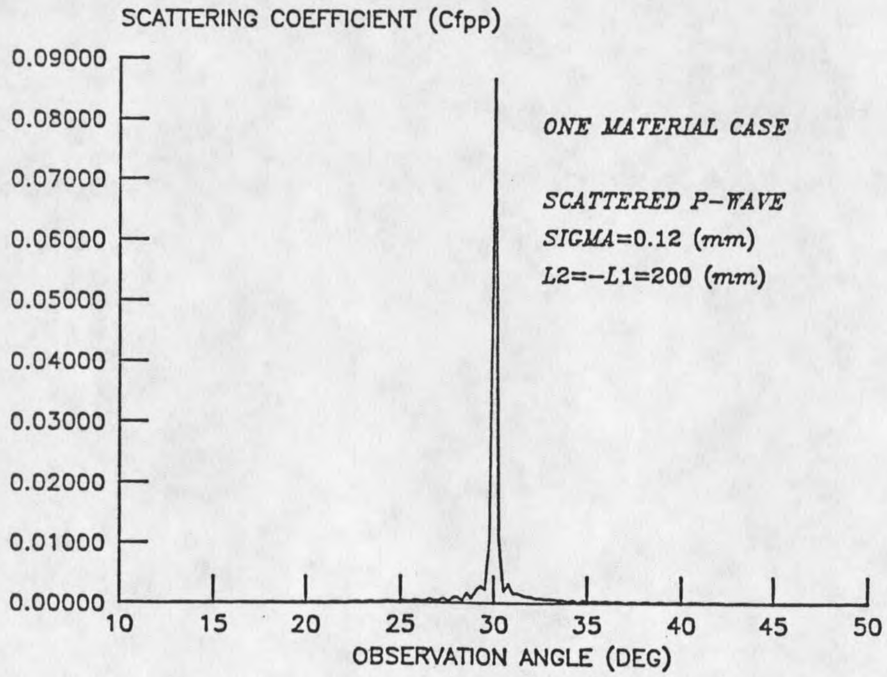

Figure 79. Scattering coefficient for scattered P-wave from large surface (one material case, σ=0.12 mm)

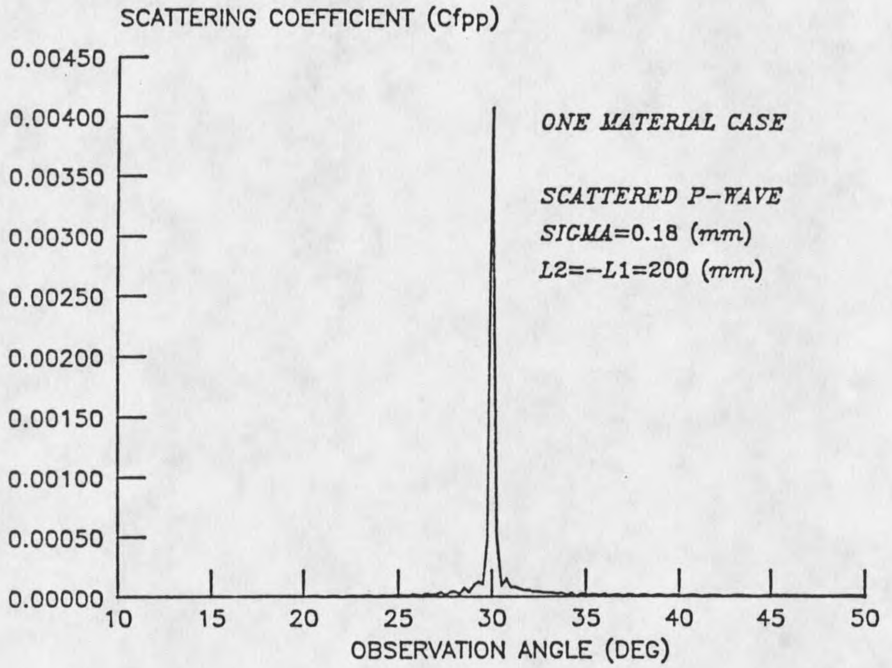

Figure 80. Scattering coefficient for scattered P-wave from large surface (one material case, σ=0.18 mm)

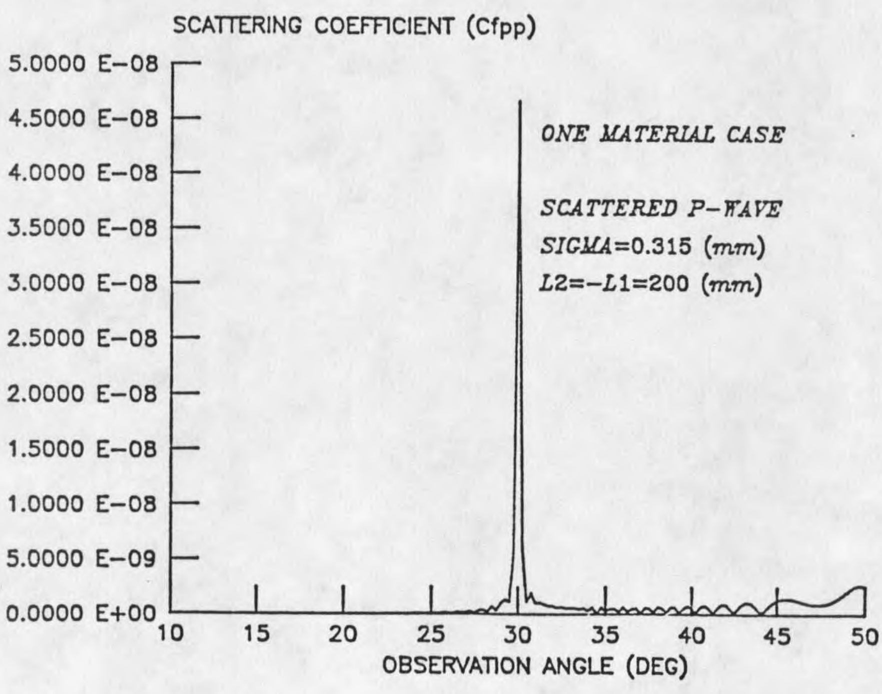

Figure 81. Scattering coefficient for scattered P-wave from large surface (one material case, σ=0.315 mm)

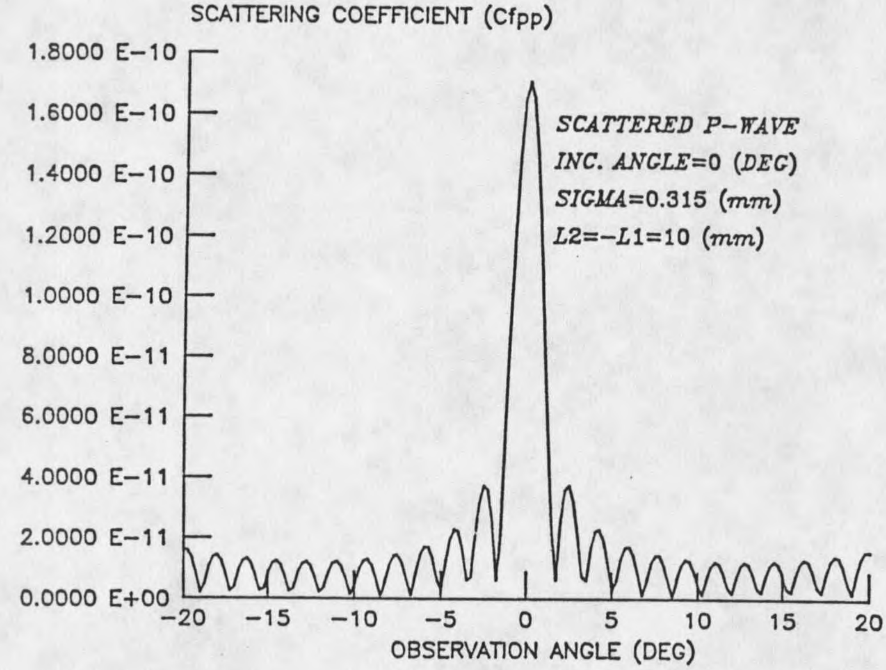

Figure 82. Scattering coefficient for scattered P-wave (incident angle $\theta_{inc}=0^{o}$, $\sigma=0.315$ mm)

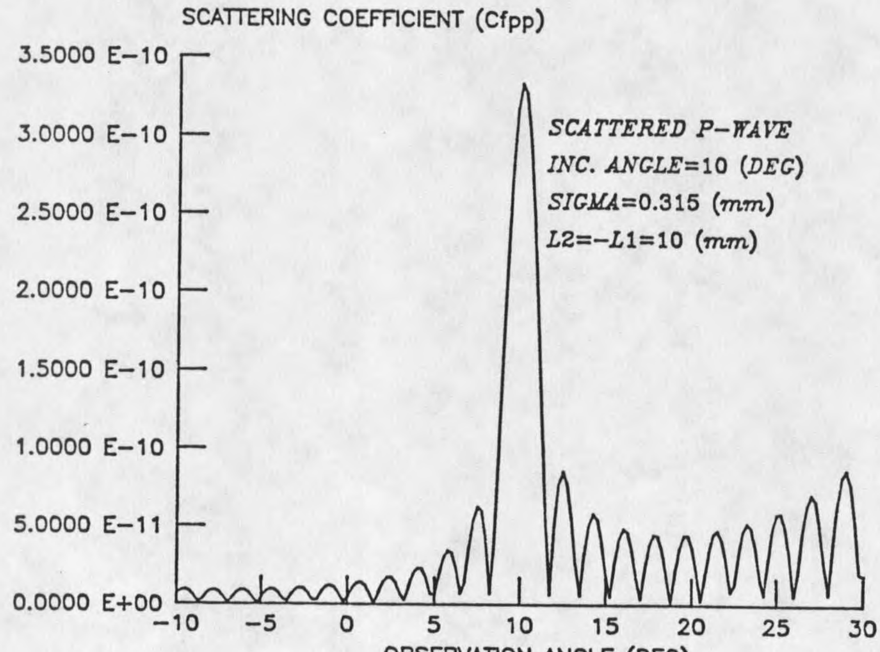

Figure 83. Scattering coefficient for scattered P-wave (incident angle $\theta_{inc}=10^{o}$, $\sigma=0.315$ mm)

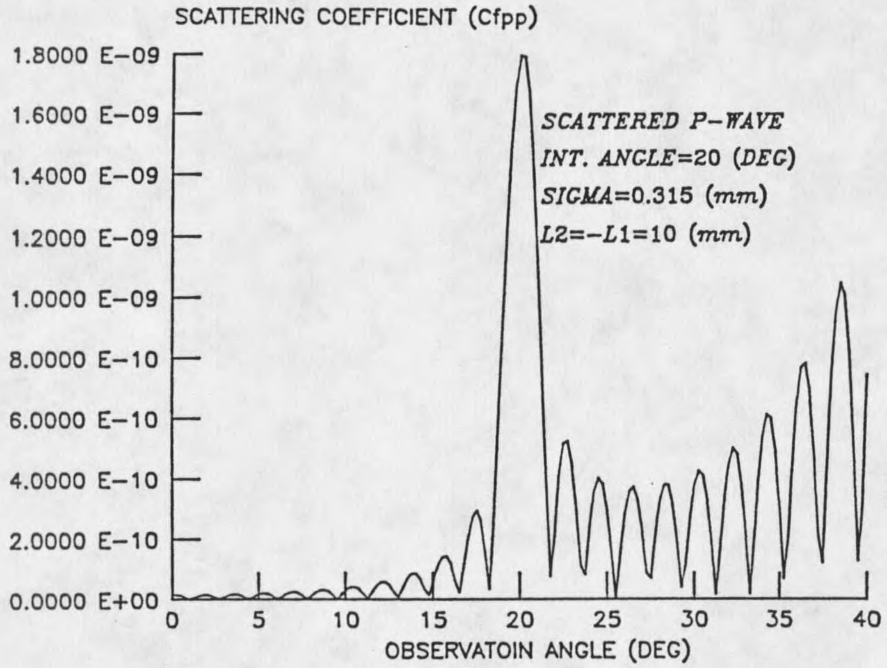

Figure 84. Scattering coefficient for scattered P-wave (incident angle θ_{inc}=20°, σ=0.315 mm)

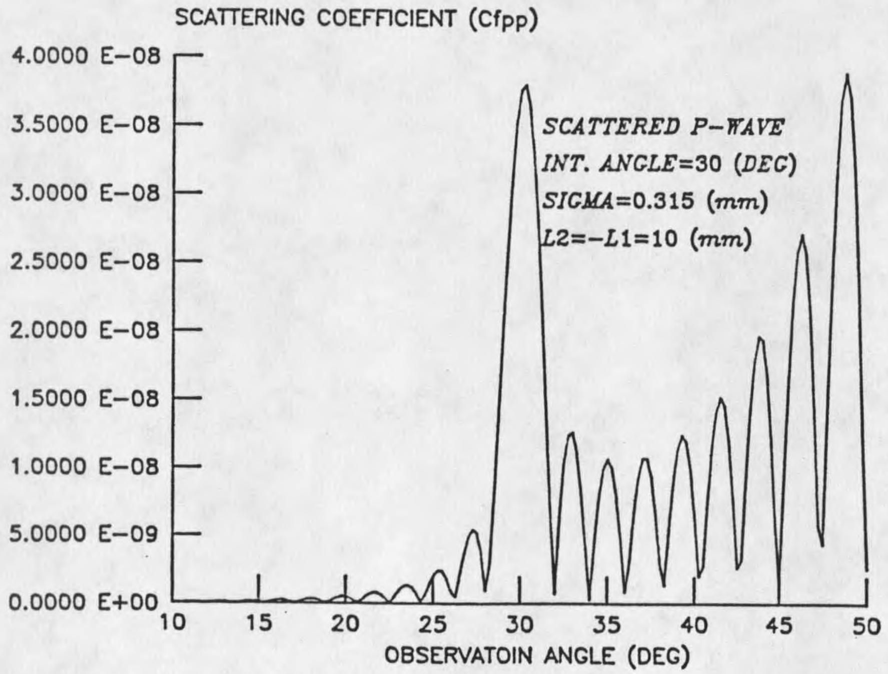

Figure 85. Scattering coefficient for scattered P-wave (incident angle θ_{inc}=30°, σ=0.315 mm)

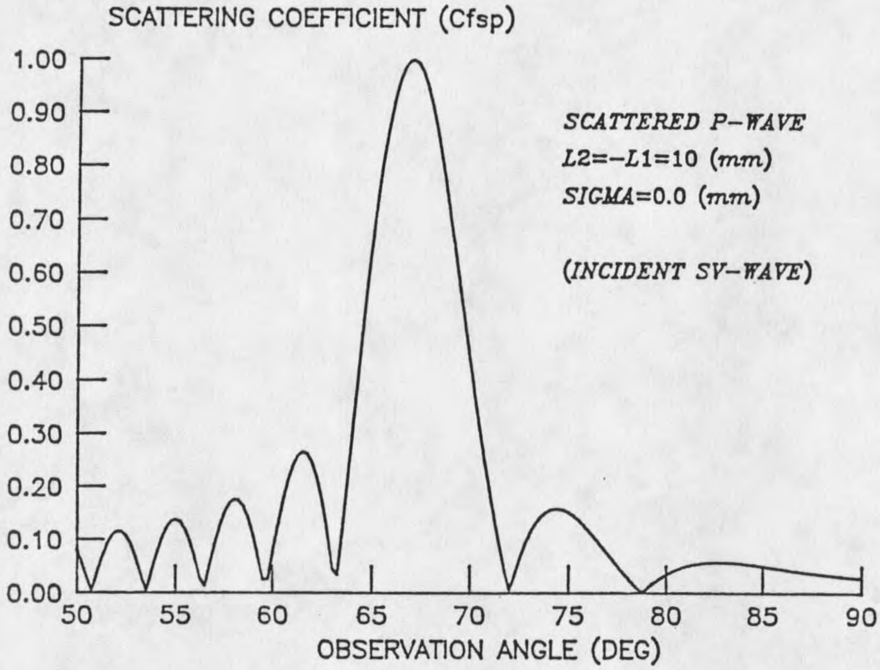

Figure 86. Scattering coefficient for scattered P-wave due to incident SV-wave (σ=0.0 mm)

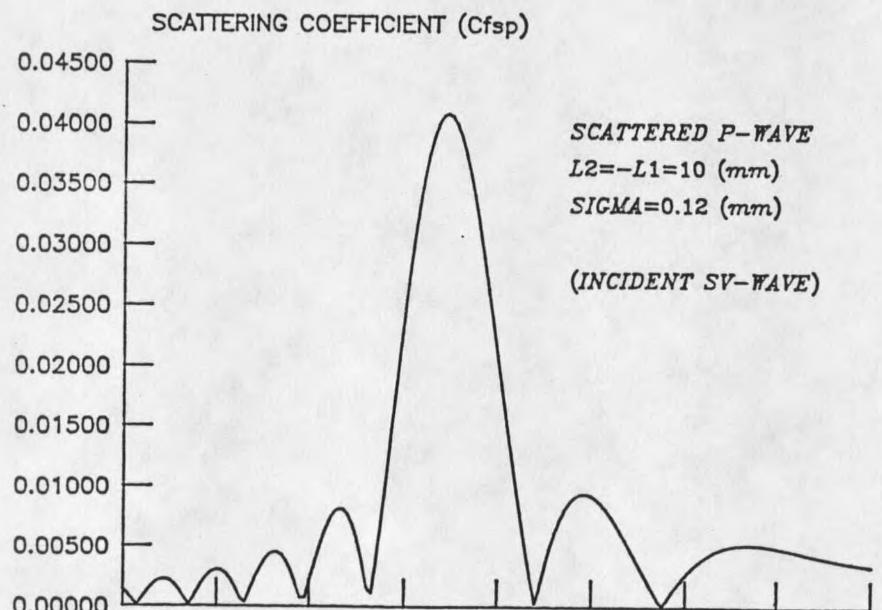

Figure 87. Scattering coefficient for scattered P-wave due to incident SV-wave (σ=0.12 mm)

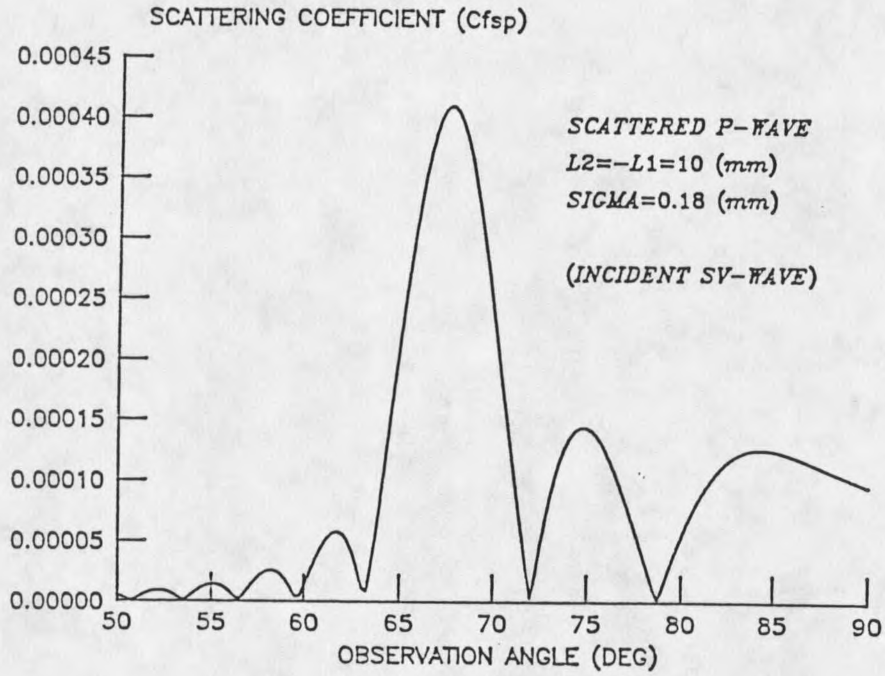

Figure 88. Scattering coefficient for scattered P-wave due to incident SV-wave (σ=0.18 mm)

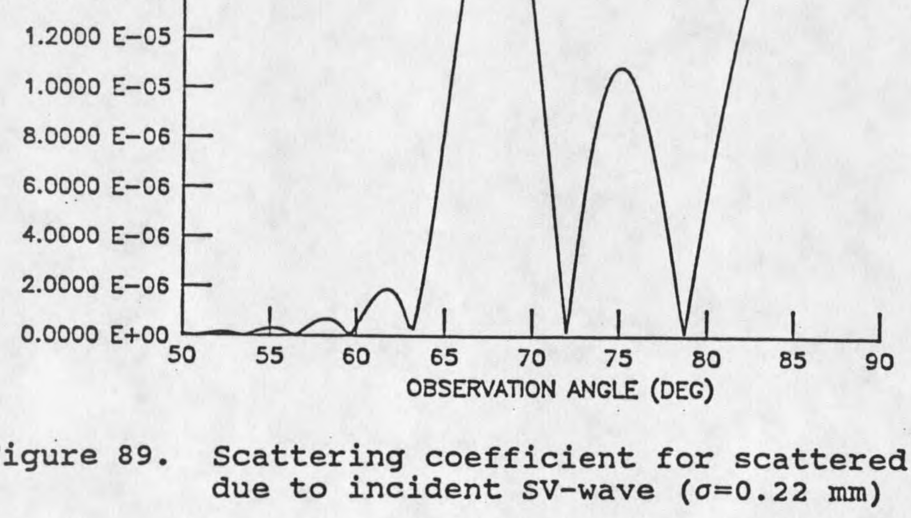

Figure 89. Scattering coefficient for scattered P-wave due to incident SV-wave (σ=0.22 mm)

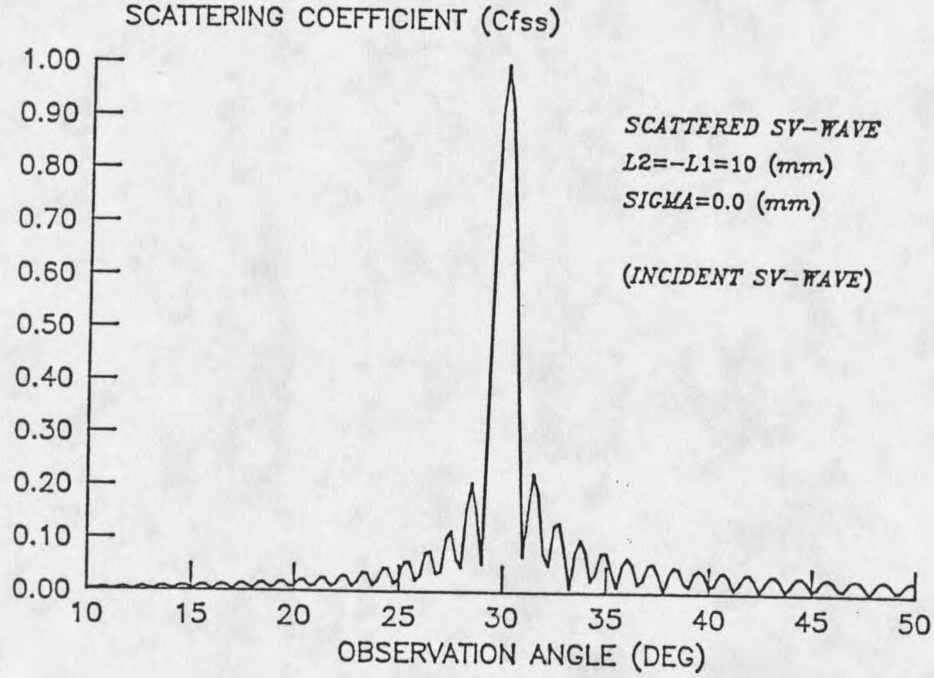

Figure 90. Scattering coefficient for scattered SV-wave due to incident SV-wave (σ=0.0 mm)

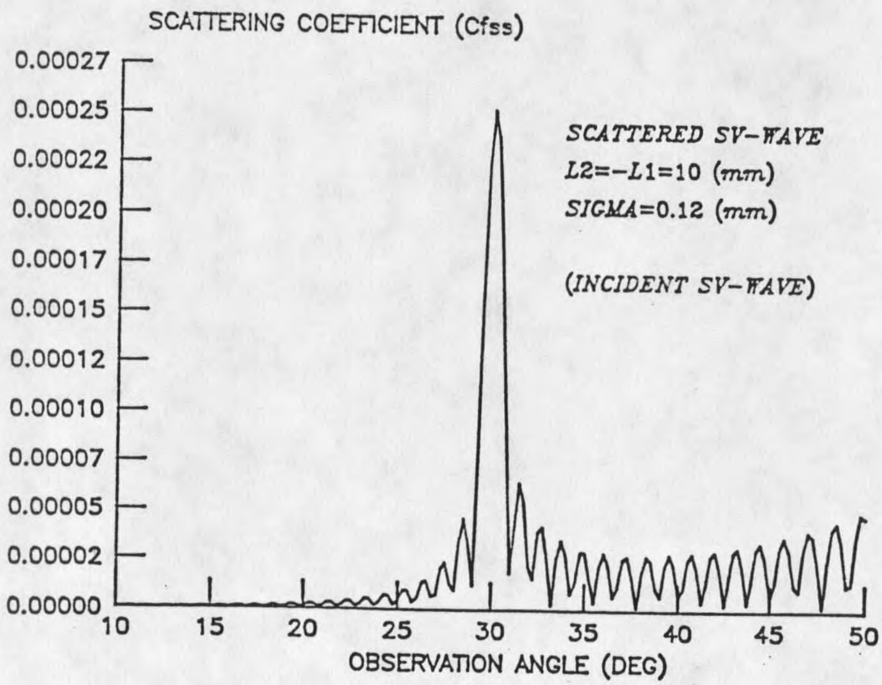

Figure 91. Scattering coefficient for scattered SV-wave due to incident SV-wave (σ=0.12 mm)

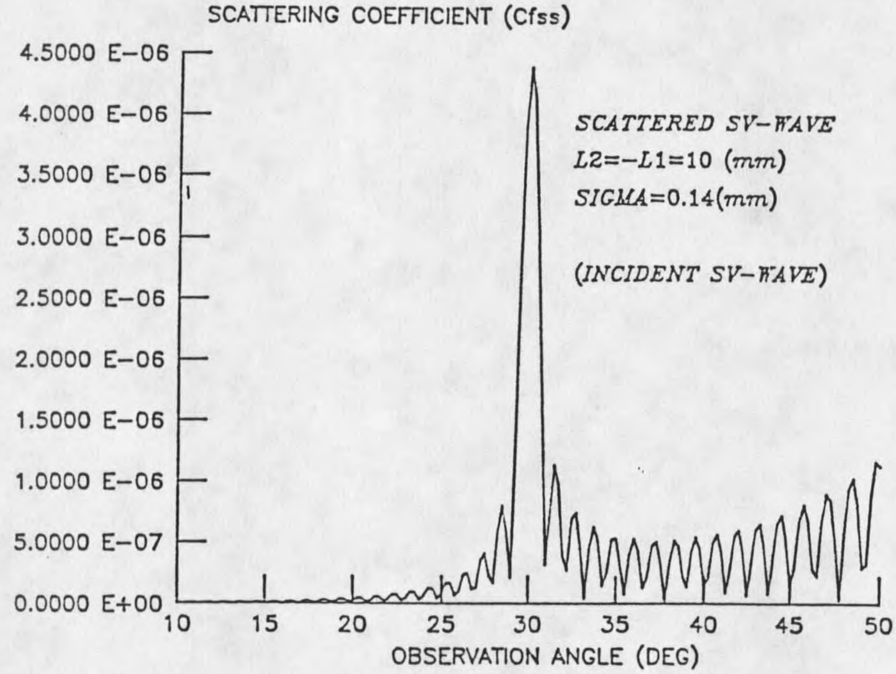

Figure 92. Scattering coefficient for scattered SV-wave due to incident SV-wave (σ=0.14 mm)

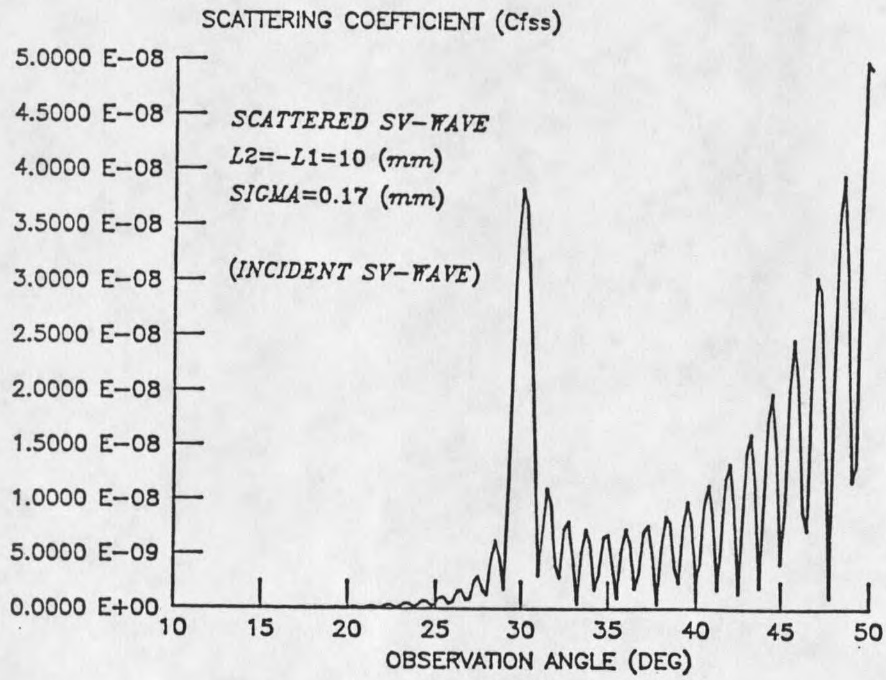

Figure 93. Scattering coefficient for scattered SV-wave due to incident SV-wave (σ=0.17 mm)

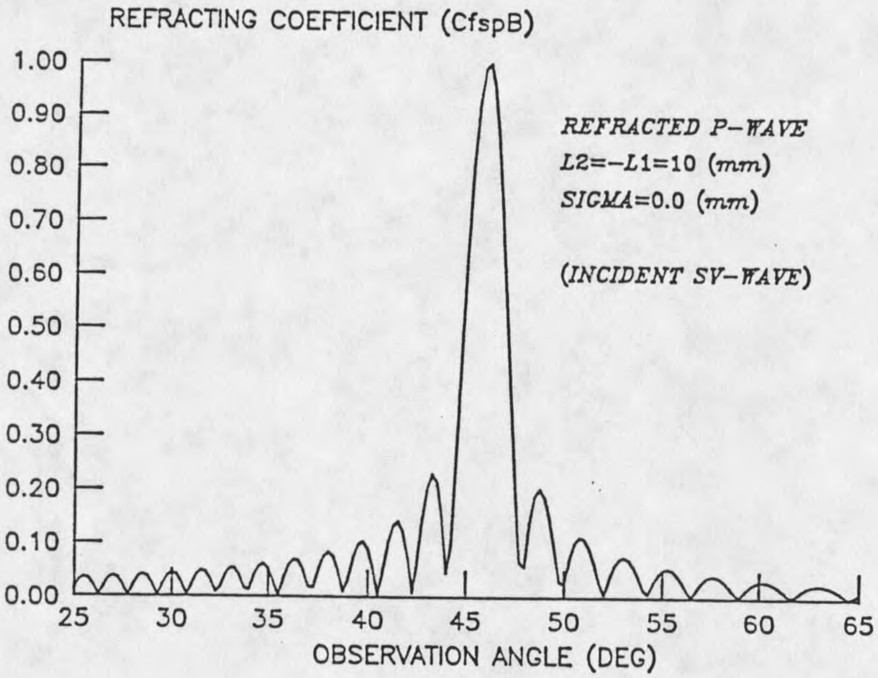

Figure 94. Scattering coefficient for refracted P-wave due to incident SV-wave (σ=0.0 mm)

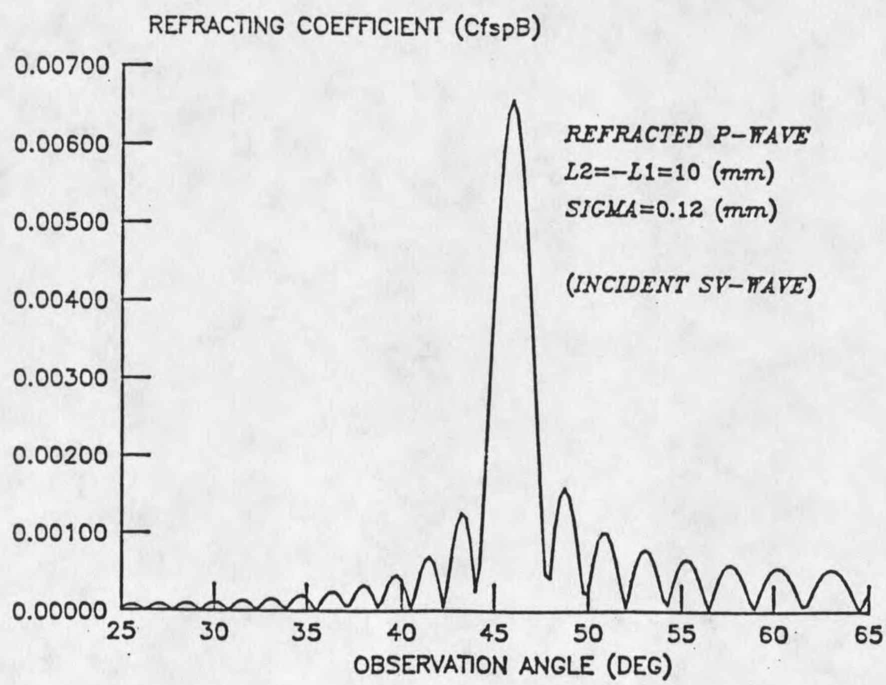

Figure 95. Scattering coefficient for refracted P-wave due to incident SV-wave (σ=0.12 mm)

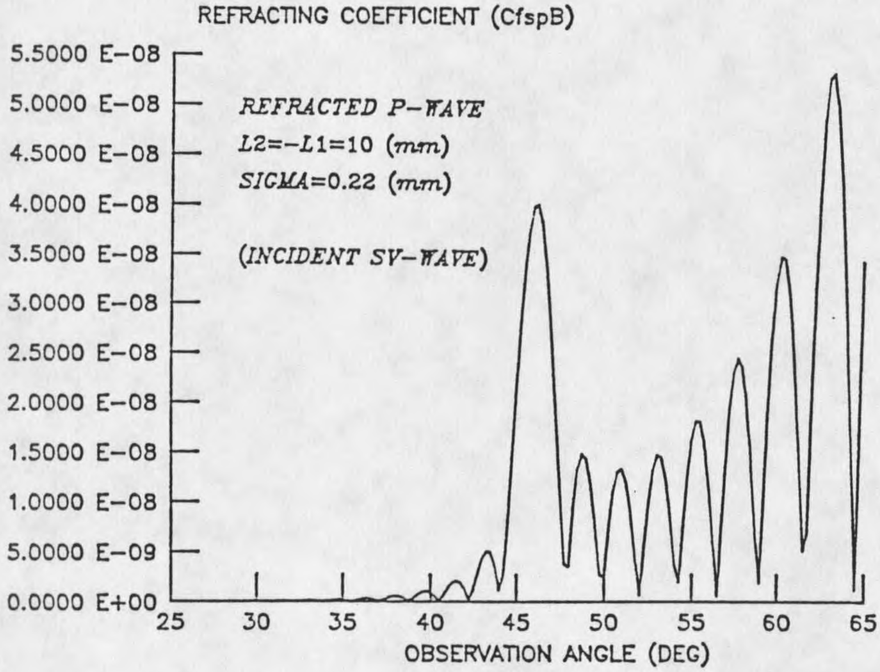

Figure 96. Scattering coefficient for refracted P-wave due to incident SV-wave (σ=0.22 mm)

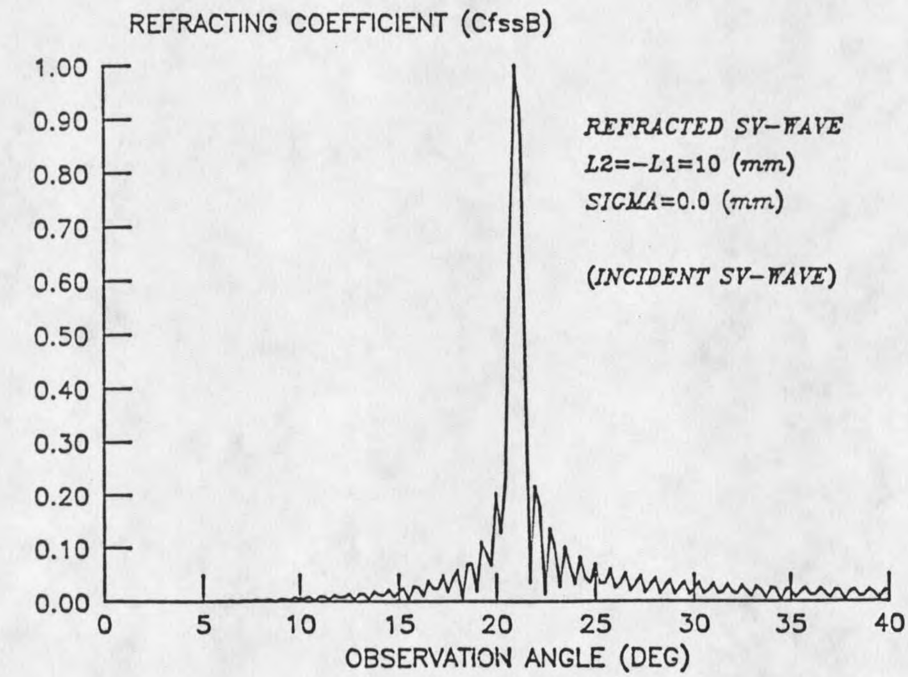

Figure 97. Scattering coefficient for refracted SV-wave due to incident SV-wave (σ=0.0 mm)

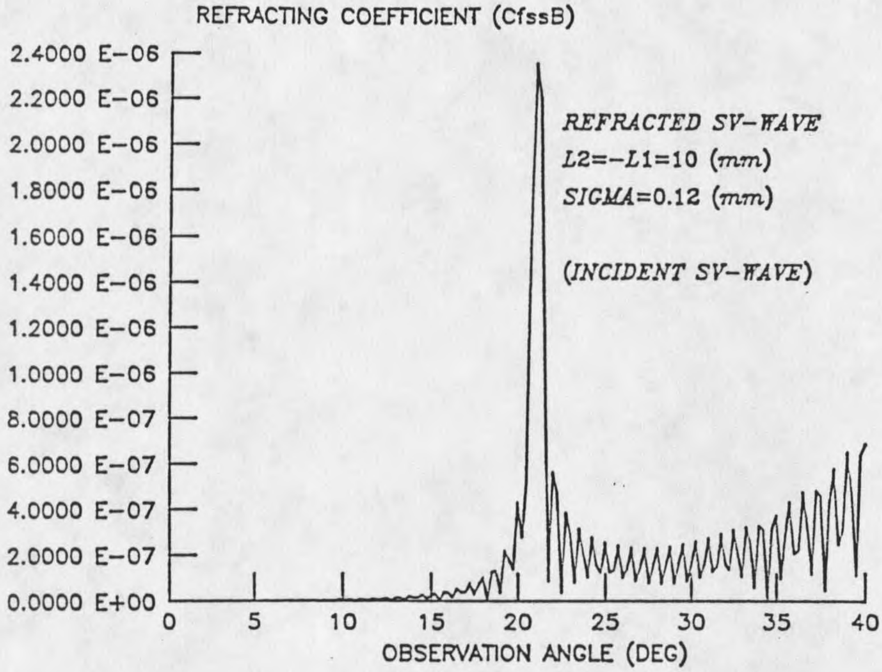

Figure 98. Scattering coefficient for refracted SV-wave due to incident SV-wave (σ=0.12 mm)

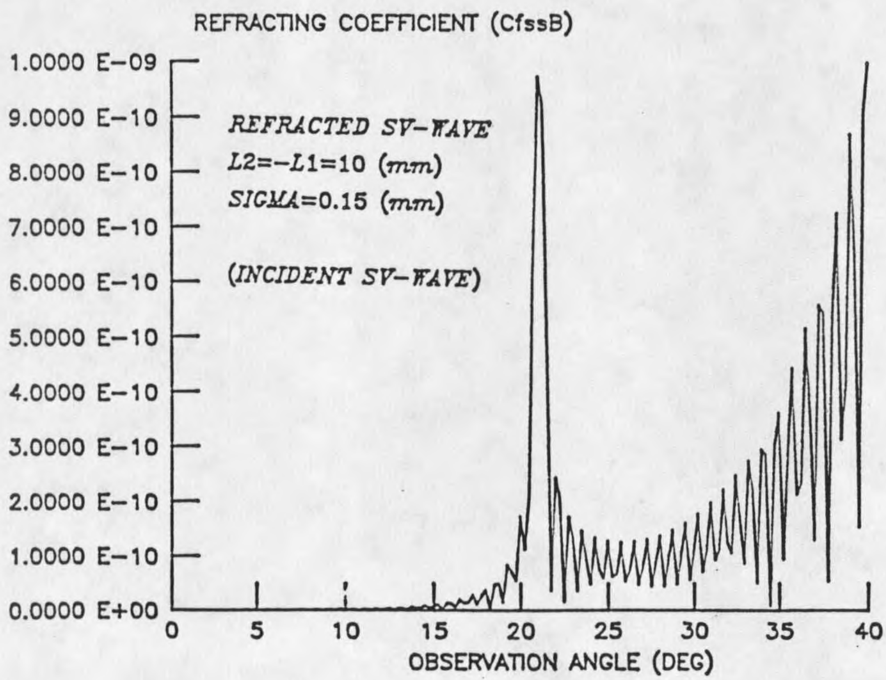

Figure 99. Scattering coefficient for refracted SV-wave due to incident SV-wave (σ=0.15 mm)

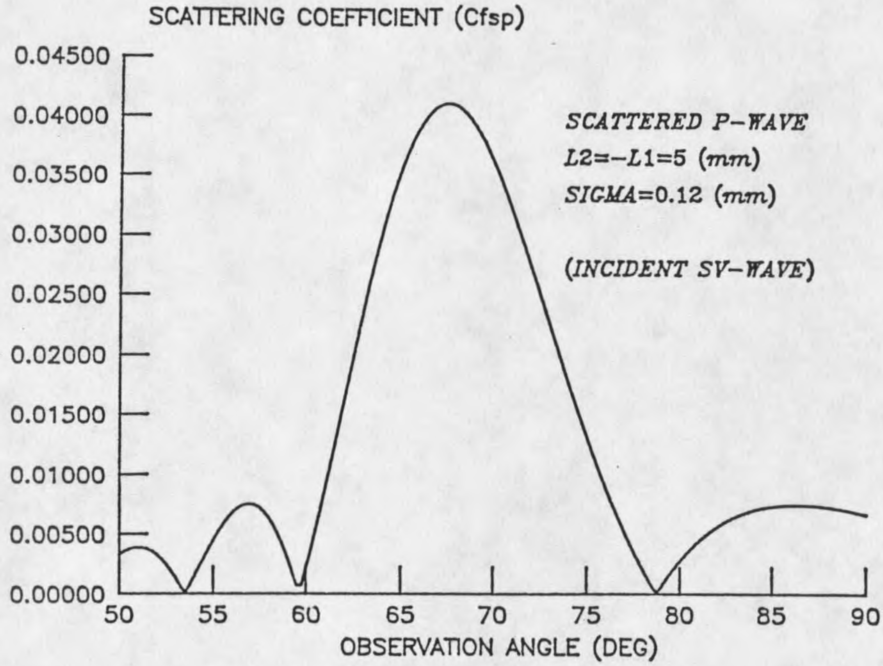

Figure 100. Scattering coefficient for scattered P-wave due to incident SV-wave (L_2=-L_1=5 mm, σ=0.12 mm)

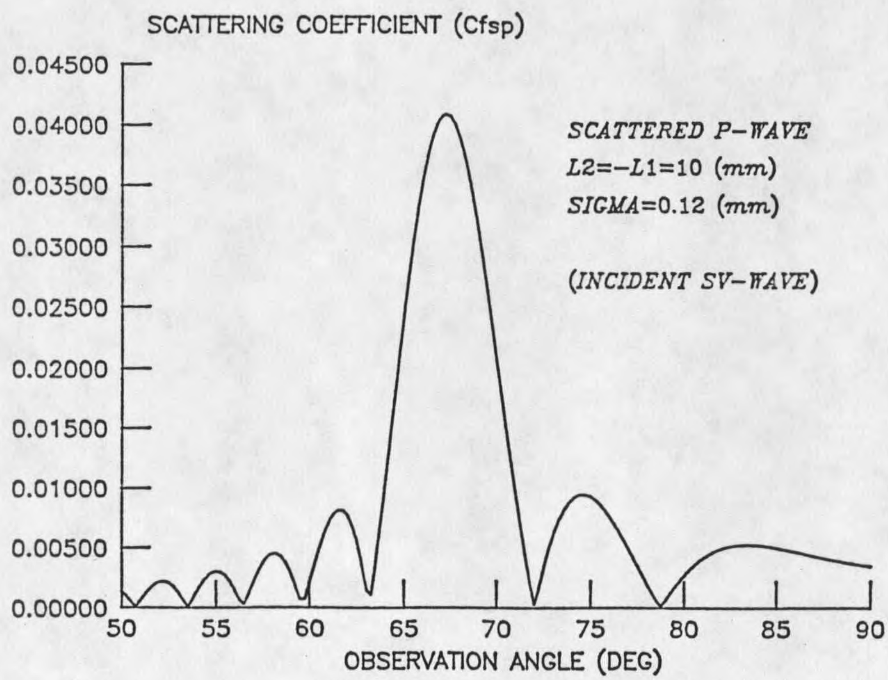

Figure 101. Scattering coefficient for scattered P-wave due to incident SV-wave (L_2=-L_1=10 mm, σ=0.12 mm)

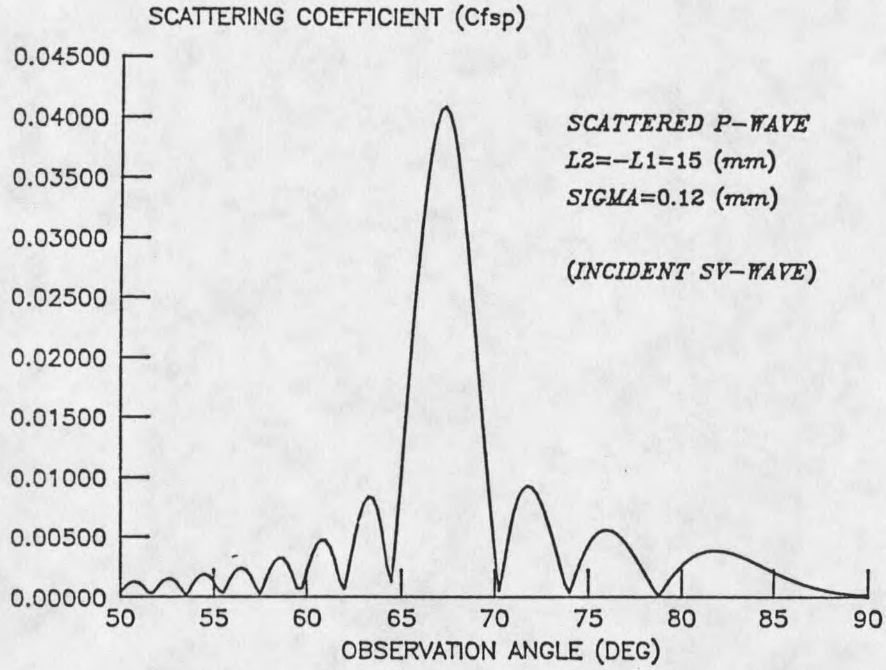

Figure 102. Scattering coefficient for scattered P-wave due to incident SV-wave (L_2=$-L_1$=15 mm, σ=0.12 mm)

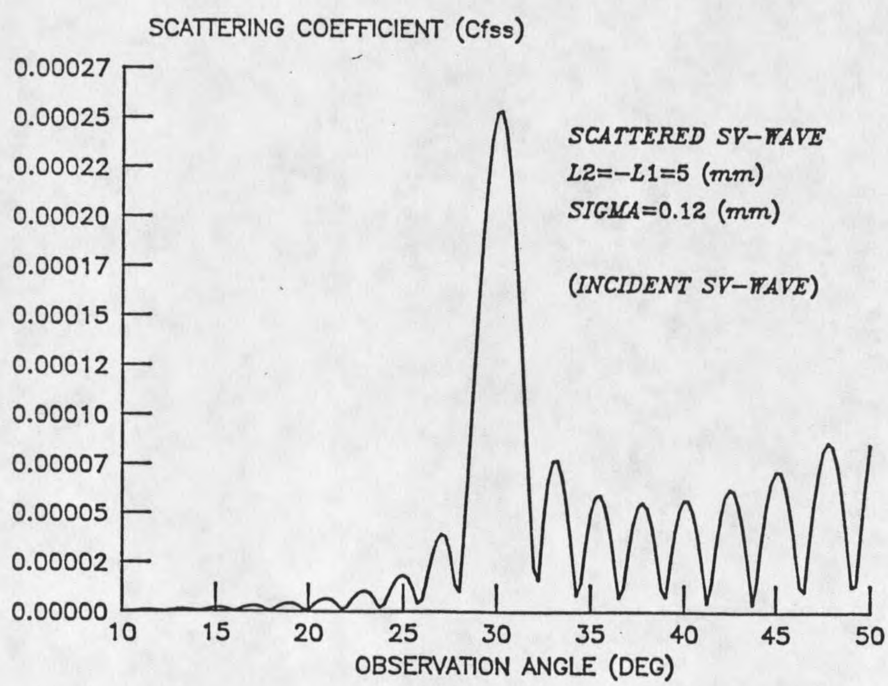

Figure 103. Scattering coefficient for scattered SV-wave due to incident SV-wave (L_2=$-L_1$=5 mm, σ=0.12 mm)

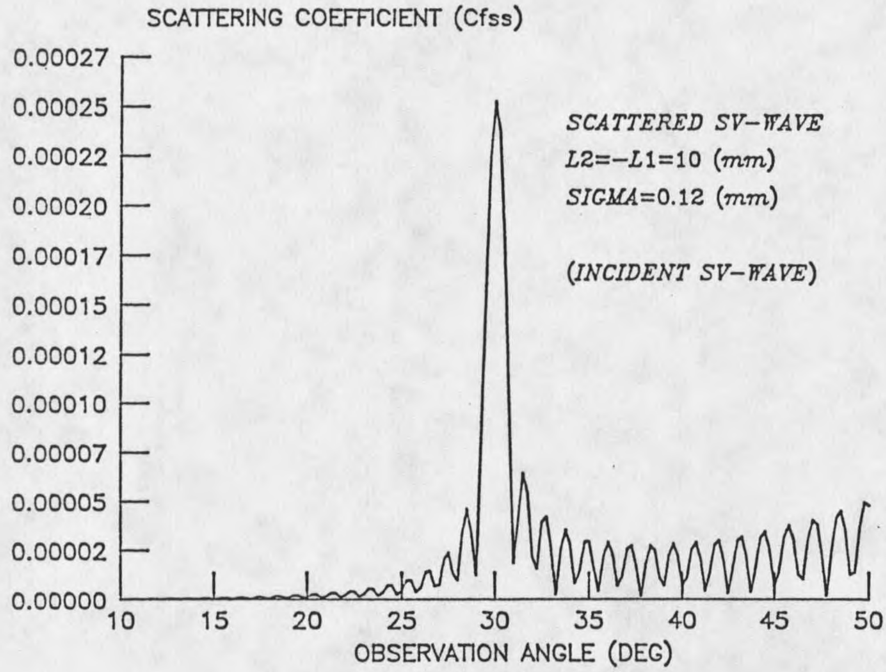

Figure 104. Scattering coefficient for scattered SV-wave due to incident SV-wave (L_2=-L_1=10 mm, σ=0.12 mm)

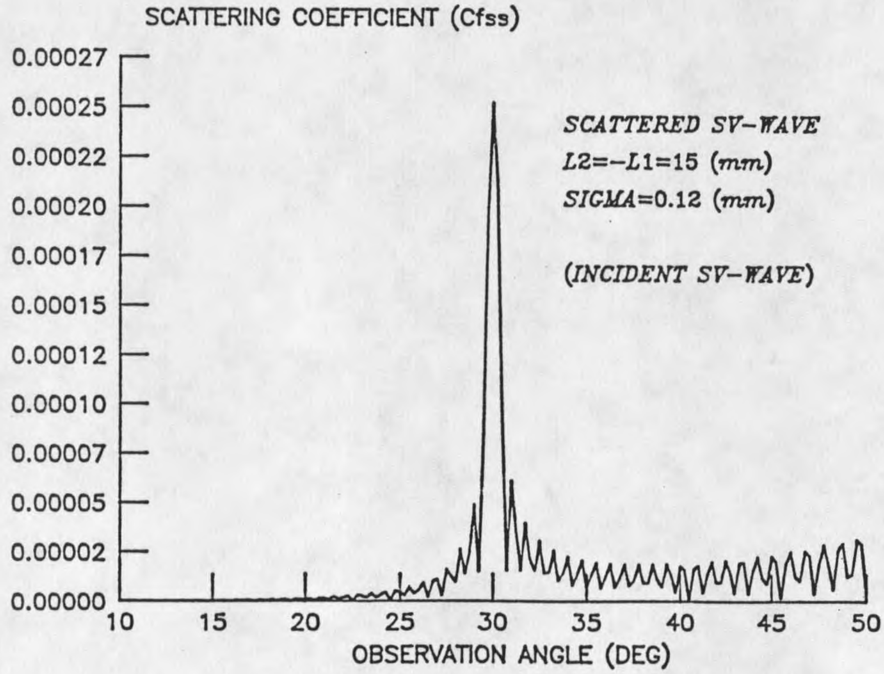

Figure 105. Scattering coefficient for scattered SV-wave due to incident SV-wave (L_2=-L_1=15 mm, σ=0.12 mm)

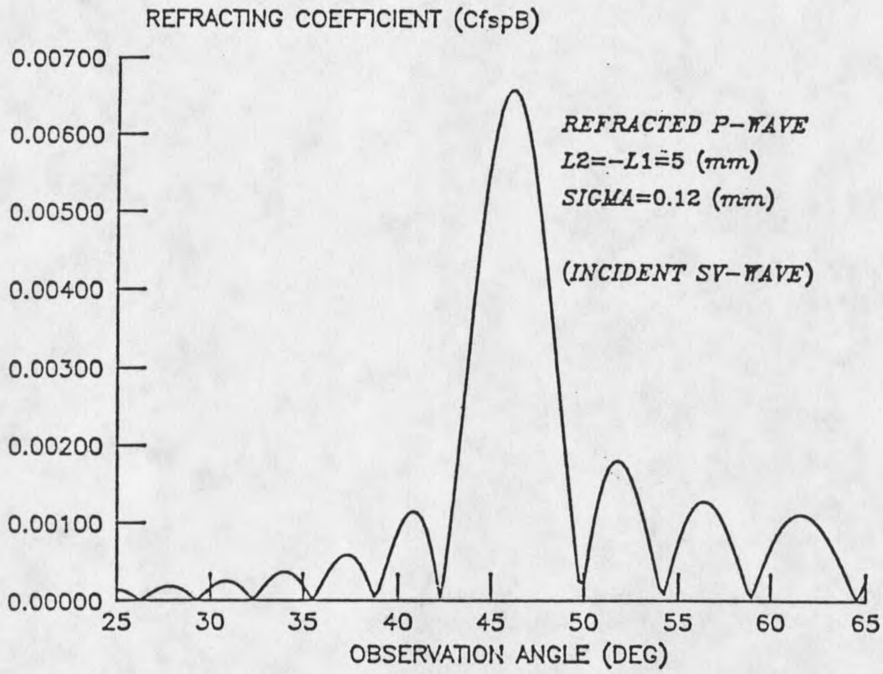

Figure 106. Scattering coefficient for refracted P-wave due to incident SV-wave (L_2=-L_1=5 mm, σ=0.12 mm)

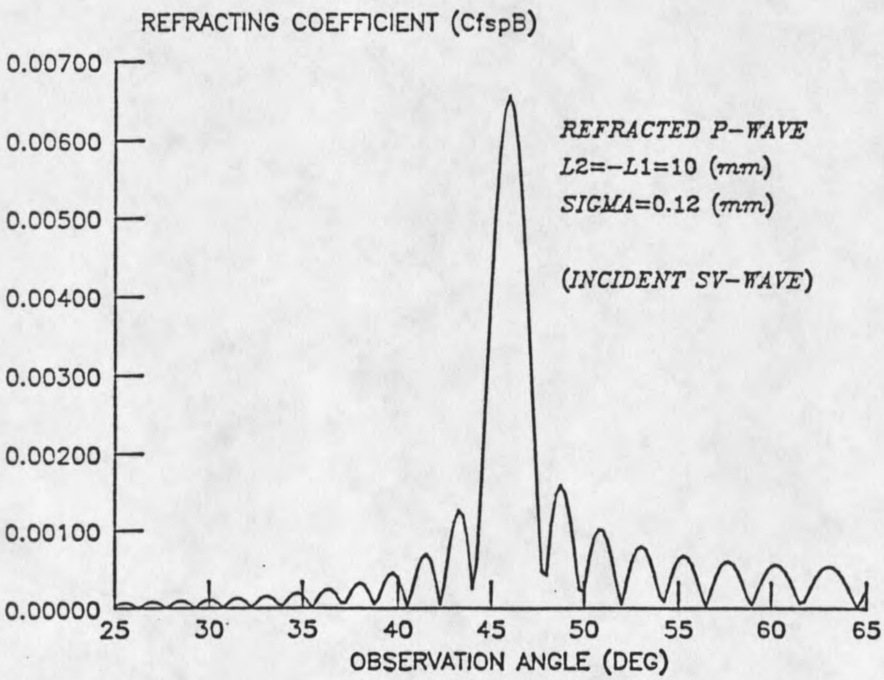

Figure 107. Scattering coefficient for refracted P-wave due to incident SV-wave (L_2=-L_1=10 mm, σ=0.12 mm)

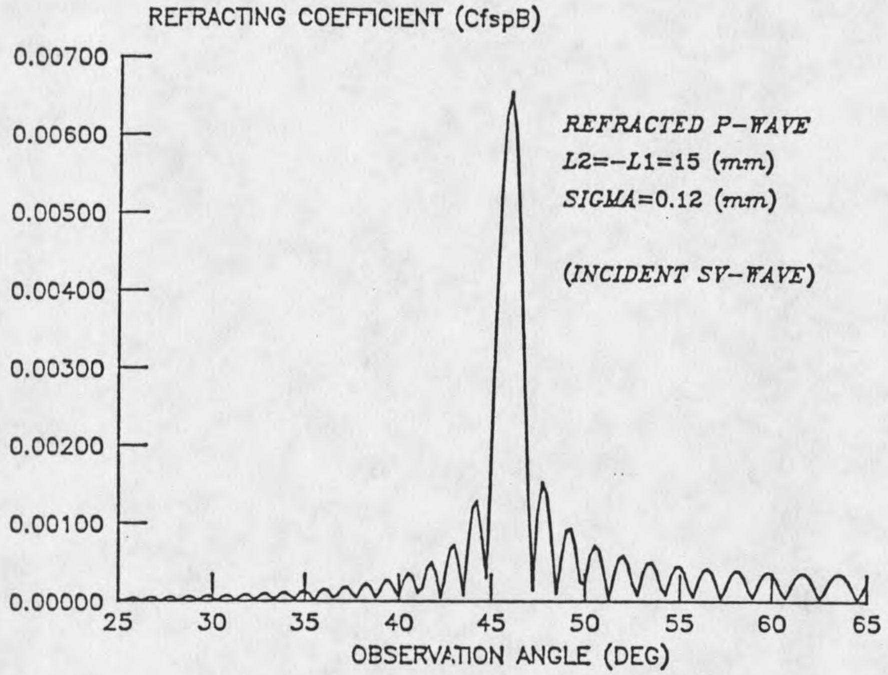

Figure 108. Scattering coefficient for refracted P-wave due to incident SV-wave (L_2=-L_1=15 mm, σ=0.12 mm)

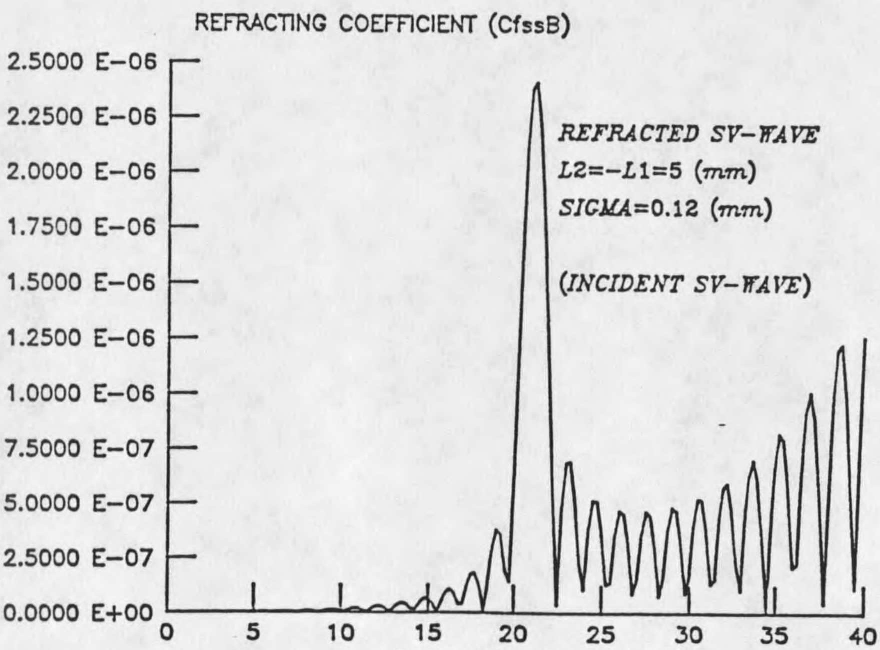

Figure 109. Scattering coefficient for refracted SV-wave due to incident SV-wave (L_2=-L_1=5 mm, σ=0.12 mm)

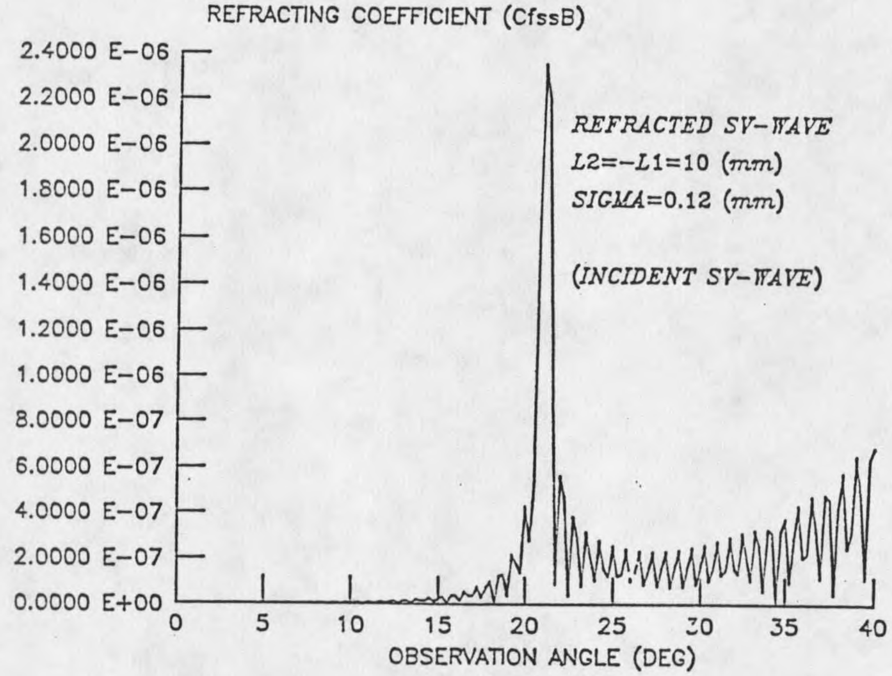

Figure 110. Scattering coefficient for refracted SV-wave due to incident SV-wave (L_2=-L_1=10 mm, σ=0.12 mm)

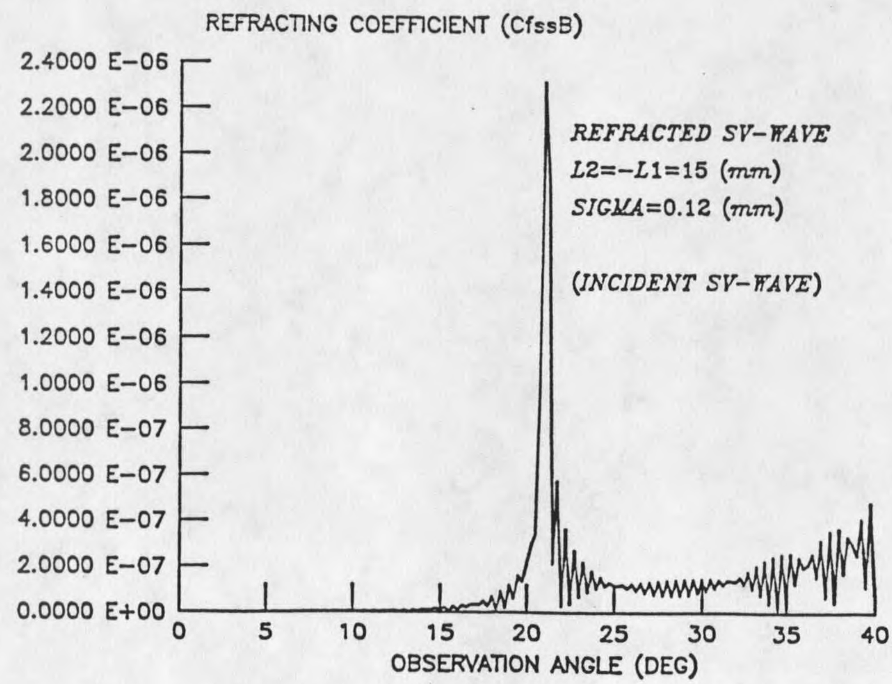

Figure 111. Scattering coefficient for refracted SV-wave due to incident SV-wave (L_2=-L_1=15 mm, σ=0.12 mm)

CHAPTER 9

SUMMARY

A theoretical investigation of elastic wave scattering from a random rough interface between two elastic solids is studied in this dissertation. This work presents a general approach for elastic wave scattering problems. Some special cases of elastic wave scattering involving simpler boundaries, for example, a free boundary, rigid boundary, or an interface with given shape, can be easily evaluated from the basic processes in this work. The formulation and evaluation of this problem result in the scattered and refracted field being expressed in terms of surface integrals which are based on the elastic reciprocal relations. The surface integrals contain elastic Green's functions and scattered fields on the rough boundary. The evaluations of the Green's functions are based on the exponential Fourier transform. The scattered and refracted fields are evaluated by applying the Kirchhoff approximation. This gives the solutions of the scattered and refracted fields on the rough boundary in terms of the incident wave and plane reflection coefficients. The application of the Kirchhoff method to this problem is a crucial step, because the unknown scattered and refracted fields on the rough boundary can be replaced by known quantities in this approximation. The Kirchhoff approximation, however, requires that the radius of curvature of the rough interface be much larger than the wavelength of the incident wave. For typical values of the surface roughness in modern industries, say, fatigue cracks or manufacturing defects, the elastic Kirchhoff approximation requires high frequency incident waves. Because the rough boundary is assumed to have a random profile, exact results of the scattered fields can not be obtained, and the average evaluations are performed numerically.

From the results, we can observe the general distributions of the scattered and refracted fields versus the observation angle, the peak values in specular directions, and the diffuse signals. These results show that the theoretical study in this work has important industrial applications in non-destructive testing (NDT) techniques. The problem involving wave scattering from a rough interface between two elastic solids can be applied to NDT for a weld joint between two metal parts. For a given sending signal, the quality of the weld joint can be investigated from the received signal. The theoretical study can also be applied to NDT for flaws inside elastic solids, which can be considered as a problem involving wave scattering from a free boundary. From the received signal, the scattered fields in the specular directions, and the general distributions of the scattered fields, the location and size of flaws inside a solid can be investigated. For example, as the location of a flaw inside a solid changes, the specular direction of the receiving signal changes, and the larger the size of the flaw, the more the scattered fields are concentrated around the specular direction.

The diffusion effects in the wave scattering problem are also observed in this work. The results show that in the case of very rough boundaries, the incident wave (either a compression wave or a shear wave) is diffusely scattered, and the maximum value of the scattered field is no longer scattered in the specular direction. A more detailed discussion about the diffusion effects for incident shear wave and the refracted fields is given in Chapter 8.

The restrictions of applying the Kirchhoff approximation show that wave scattering problems involving a rough surface with rapid change in its gradient cannot be evaluated using this method.

BIBLIOGRAPHY

BIBLIOGRAPHY

Achenbach, J. D., Gaustesen, A. K., and McMaken, H., Ray Methods for Waves in Elastic Solids, Pitman, (1982).

Achenbach, J. D., Wave Propagation in Elastic Solids, North-Holland, (1975).

Achenbach, J. D. and Gaustesen, A. K., "Geometrical Theory of Diffraction for Three-D Elastodynamics", J. Acoust. Soc. Am., Vol 61, No. 2, 413, (1977).

Adler, R.J. The Geometry of Random Fields, John Wiley & Sons, 31, (1981).

Ament, W. S., "Toward a Theory of Reflection by a Rough Surface," Proc. I.R.E., Vol. 41, 142-148, (1953).

Auld, B. A. and Ayter, S., "Perturbation Method for Analyzing the Effect on Ultrasonic Echo Returns in Material Cracks and Voids," IEEE Ultrasonics Symposium, 852, (1980).

Banaugh, R. P., "Scattering of Elastic Waves by Surfaces of Arbitrary Shape", Thesis, University of California, Livermore, California, (1962).

Banaugh, R. P., and Goldsmith, W., "Diffraction of Steady Elastic Waves by Surfaces of Arbitrary Shape", Trans. ASME, Ser. E, Vol. 30, 589, (1963).

Baltes, H. P., "A New Perturbation Expansion for Electromagnetic Scattering by Stochastic Surfaces", Proc. Ursi. Commission F 1983 Symposium, Louvain, Belgium, June (ESA SP-194) 309, (1983).

Barratt, P. J. and Collins, W. D., "The Scattering Cross-Section of an Obstacle in an Elastic Solid for Plane Harmonic Waves", Proc. Camb. Phil. Soc., Vol. 61, 969, (1965).

Bass, F. G. and Fuks, I. M., Wave Scattering from Statistically Rough Surfaces, eds., C.B. Vesecky and J.f. Vesecky, Pergamon Press, New York, (1979).

Beaumont, G. P., Probability and Random Variables, Ellis Horwood Limited, Chichester, London (1986).

Beckmann, P. and Spizzichino, A., The Scatteing of Electromagnetic Waves from Rough Surfaces, in International Series of Monographs on Electromagnetic Waves, Vol. 4, Eds. V. A. Fock and J.R. Wait, Pergamon Press Book, Macmillan Co. New York, (1963).

Beckmann, P., "Shadowing of Random Rough Surfaces", IEEE Transactions on Antennas and Propagation", Vol. 13, 384-388, (1965).

Billy, M. de, Cohen-Tenoudji, F., Quentin, G., Lewis, K., Adler, L., "Ultrasonic Evaluation of Geometrical and Surface Parameters of Rough Defects in Solids", J.N.D.E. Vol. 1 249-261, (1980).

Bird, Joseph F. and Farrell, Richard A., "Electromagnetic Scattering Theory", Johns Hopkins APL Technical Digest, Vol. 7, No. 1, (1986).

Bojarski, N. N., "The Scattering Integral Equation for Surfaces Containing Curvature Discontinuitites", J. Acous. Soc. Amer., Vol. 53, 792, (1973).

Boyd, M. L. and Deavenport, R. L., "Forward and Specular Scattering form a Rough Surface: Theory and Experiment", J. Acous. Soc. Amer., Vol. 53, 792, (1973).

Brekhouskikh, L., Wave in Layered Medium, Translated from the Russian by D. Liebermann, Translation edited by R. T. Beyer, Academic Press, Inc., New York (1960).

Brekhouskikh, L., "The Diffraction of Wave by a Rough Surface, part 1", Zh. Eksper. i Teor. Fiz. Vol. 23, 275-289 (1952).

Brockelman, R. A. and Hagfors, T., "Note on the Effect of Shadowing on the Backscattering of Waves form a Random Rough Surface", IEEE Transactions on Antennas and Propagation, Vol. AP-14 (5), (1966).

Chapman, D. M. "An Improved Kirchhoff Formula for Reflection Loss at a Rough Ocean Surface at Low Grazing Angles", J. Acoust. Soc.Amer., Vol. 73 (2), 520, (1983).

Crandall, Stephen H., et. al., Random Vibration, Technology Press of The Massachusetts Institute of Technology and John Wiley & Sons, New York, (1958).

Datta, S. K. "Scattering of Elastic Waves", Mechanics Today, Vol. 17, 149, (1978).

Davies, H., "The Reflection of Electromagnetic Waves from a Rough Surface," Proc. I.E.E., Pt. III, vol. 101, 209- 2 1 4 (1954) Discussion on above paper, Proc. I.E.E., Pt. III, Vol. 102, 148, (1955).

de Billy, M., Cohen-Tenoudj, Quentin, G., Lewis, K., and Adler, L., "Ultrasonic Evaluation of Geometrical and Surface Parameters of Rough Defects in Solids," Journal of Nondestructive Evaluation, Vol. 1 (4), 249, (1980).

DeSanto, J. A., "Scattering from a Random Rough Surface: Diagram Methods for Elastic Media", J. Math. Phys. Vol. 14 (11), 1566, (1973).

Eason, G., Fulton, J. and Sneddon, I. N., "The Generation of Waves in an Infinite Elastic Solid by Variable Body Forces", Phil. Tans. Royal Society A, Vol. 248, 71, (1956).

Eckart, C. "The Scattering of Sound from the Sea Surface", J. Accous. Sco. Amer., Vol. 25, 566-570, (1953).

Einspruch, N. G. and Truell, R. "Scattering of a Plane Longtudinal Wave by a Spherical Fluid Obstacle in an Elastic Medium", J. Acoust. Soc. Am., Vol. 32, 214, (1960).

Elliot, R. "On the Theory of Corrugated Plane Surfaces," Trans, I.R.E., Vol. AP-2, 71-81, (1954).

Ewing, W. M., Jardetzky, W. S. and Press, F., Elastic Waves in Layered Media, New York, McGraw-Hill Book Co., (1957)

Fortuin, L. "Survey of Literatire on Reflection and Scattering of Sound Waves at the Sea Surface", J. Acoust. Soc. Amer., Vol. 47, 1209, (1970).

Fung, Y. C., Foundations of Solid Mechanics, Prentice-Hall, Inc., Englewood Cliffs, New Jersey, (1965) Gaustesen, A. K., Achenbach, J. D., and McMaken, H.,"Surface-Wave Rays in Elastodynamics Diffraction by Cracks", J. Acoust. Soc. Am., Vol. 63 No. 6, 1284, (1978).

Gilert, F. and Knopoff, L. "Seismic Scattering from Topographic Irregularities", Journal of Geophysical research, Vol. 65 (10), 3437, (1960).

Gradshteyn, I.S. and Ryzhik, I.M., Table of Integrals, Series, and Products, Academic Press, New York, (1980).

Heeps, M. S., "Reflection of Plane Waves of Sound from a Sinusoidal Surface", J. Appl. Phys., Vol. 28, 815-818, (1957).

Karal, F. C. and Keller, J. B., "Elastic Wave Propagation in Homogeneous and Inhomogeneous Media," J. Acoust. Soc. Amer., Vol. 31, 694, (1959).

Karp, S., Hankin, R. B., Spinak, S., Pisa, E. J. and Barron, P. P., "Measurements of Optical Surface Roughness Using Coherent Radiation", Proc. IEEE, 54, 10, 1484-1485, (1966).

Keller, Joseph B., "Wave Propagation in Random Media",in Proc. Symp. in Appl. Math., Vol. 13 (Am. Math. Soc., Providence, RI, 227-246, 1962).

LaCasace, O, and Tamarkin, P. "Underwater Sound Reflection from a Corrugated Surface", J. Appl. Phys. Vol. 26, 138, (1956).

Li, Robert C. M., "Rayleigh-wave Reflection from Groove and Step Discontinuities", J. Acoust.Soc. Am. Vol. 55 (6), 1212, (1974).

Lippmann, B. A., "Note on the Theory of Gratings", J. Opt. Soc. Amer., Vol. 43, 408(L), (1953).

Longuet-Higgins, M. S., "Statistical Properties of an Isotropic Random Surface", Phil. Trans. A. Vol. 250, 157-174, (1957).

Maradudin, A. A. and Mills, D. L., "Attenuation of Rayleigh Surface Waves by Surface Roughness", Appl. Phys. Lett. Vol. 28 (10), 573-575, (1976).

Marsh, H. W. "Exact Solution of Wave Scattering by Irregular Surfaces", J. Acoust Soc. Amer., Vol. 33, 330-333, (1961).

McGonnagle, W. J., Nondestructive Testing, Gordon and Breach Science Publishers, New York, (1961)

Meecham, W. C., "Variational Method for the Calculation of the Distribution of Energy reflected from a Periodic Surface", J. Appl. Phys., Vol. 27 (4), 361, (1956).

Nagy, P. B. and Adler, L., "Surface Roughness Induced Attenuation of Reflected and Transmitted Ultrasonic Waves", J. Acous. Soc. Amer., Vol. 82 (1), 193, (1987).

Otto, Oberdan W., "Scattering of Rayleigh Waves from Topographic Irregularities at Oblique Incidence", J. Appl. Phys., Vol. 48 (12), (1977).

Ogilvy, J. A., "Ultrasonic wave scattering from rough defects: the elastic Kirchhoff Approximation", UKAEA Report AERE-R 11866, (1985).

Ogilvy, J. A., "An Estimate of the Accuracy of the Kirchhoff Approximations in Acoustic Wave Scattering from Rough Surfaces", J. Phys. D: Appl. Phys. Vol. 19, 2085-2113, (1986a).

Ogilvy, J. A., "Theoretical Comparison of Ultrosonic Signal Amplitudes from Smooth and Rough Defects", NDT International Vol. 19, 371, (1986b).

Ogilvy, J. A. "Wave Scattering from Rough Surfaces", Rep. Prog. Phys., Vol. 50 1553-1608, (1987).

Parkins, B. E., "Omnidirectional Scattering of Acoustic Waves by Rough, Imperfectly Reflection Surfaces", J. Acous. Soc. Amer., Vol. 41 (1), 126, (1967).

Pao, Yih-Hsing and Varatharajulu, V., "Huygens' Principle, Radiation Conditions, and Integral Formulas for the Scattering of Elastic Waves", J. Acous. Soc. Amer., Vol. 59, 1361, (1976).

Proud, J. M., Tamarkin, P., and Meecham, W. C., "Reflection of Sound from a Surface of Saw-Tooth Profile," J. Appl. Phys. Vol. 28, 1298-1301, (1957).

Rayleigh, Lord, The Theory of Sound, vol. 2, Macmillan and Co., Limited, London, 89, (1878).

Smith, Bruce G., "Geometrical Shadowing of a Random Rough Surface", IEEE Transactions on Antennas and Propagation, Vol. AP-15 (5), 668, (1967).

Stroud, A.H. and Secrest, Don, Gaussain Quadrature Formulas, Prentice-Hall, Inc., Englewood Cliffs, N.J. (1966)

Tan, T. H., "Scattering of Elastic Waves by Elastically Transparent Obstacles (Integral-Equation Method)", Appl. Sci. Res., Vol. 31, 29, (1975).

Tan, T. H, "Theorem on the Scattering and the Absorption Cross Section for Scattering of Plane, Time-Harmonic, Elastic Waves", J. Acous. Soc. Amer., Vol. 59 (6), 1265, (1976).

Tan, T. H., "Reciprocity Relations for Scattering of Plane, Elastic Waves", J. Acous. Soc. Amer., Vol. 61, 928, (1977).

Tuan, Hang-Shen and Li, Robert C.M., "Rayleigh-Wave Reflection from Groove and Step Discontinuities", J. Acous. Soc. Amer., Vol. 55 (6), 1212, (1974).

Twersky, V., "On the Non-specular Reflection of Sound from Planes with Absorbent Bosses", J. Accous. Soc. Amer., Vol. 23, 336-338, (1951).

Twersky, V., "Reflection Coefficients for Certain Rough Surfaces", J. Appl. Phys. Vol. 4, 569-660, (1953).

Wagner, R. J., "Shadowing of Randomly Rough Surfaces", J. Acous. Soc. Amer., Vol. 41 (1), 138, (1967).

Watson, John G. and Keller, Joseph B., "Reflection Scattering, and Absorption of Acoustic Waves by Rough Surfaces", J. Acous. Soc. Amer., Vol. 74 (6), 1887, (1983).

Watson, John G. and Keller, Joseph B., "Rough Surface Scattering Via the Smoothing Method", J. Acous. Soc. Amer., Vol. 75 (6), 1705, (1984).

Wenzel, Alan R., "Smoothed Boundary Conditions for Randomly Rough Surfaces", J. Math Phys., Vol. 15 (3), 317, (1974).

Whitehouse, D. J. and Archard, J. F., "The Properties of Random Surfaces for Significance in Their Contact", Proc. Roy. Socs. Vol. A345, 97, (1970).

White, R. M. "Elastic Wave Scattering at a Cylindrical Discontinuity in a Solid", J. Acoust. Soc. Am., Vol. 30, 771, (1958).

Ying, C. F. and Truell, R. " Scattering of a Plane Longtudinal Wave by a Spherical Obsticle in an Isotropically Elastic Solid", J. Appl. Phys., Vol. 27, 1086, (1956).

APPENDICES

APPENDIX A

DERIVATION OF GREEN'S FUNCTION

The elastic Green's functions of displacement and stress components are generated by a point load acting at position $\underline{r}$ measured from the origin. The procedure of determining the Green's functions is given below. First let us consider a point load which has the following form (Acnenbach, Gautesen, and McMaken 1982, P22).

$$f_i=a_i g(t)\delta(\underline{r}'-\underline{r}) \tag{A-1}$$

where f_i is the i^{th} component of the point load which acts in the direction of the unit vector $\underline{a}$; a_i is the i^{th} component of the unit vector $\underline{a}$; g(t) is the point load of time dependence.

In our problem, we consider the special case of a time-harmonic motion. Therefore the time dependence g(t) has the form

$$g(t)=F_0\exp(-i\omega t) \tag{A-2}$$

where the symbol F_o is used here to keep track of dimension. The dimension of F_o is force. The magnitude of F_o is unity.

The components of displacement and stress fields generated by the point load depend linearly on the components of the unit vector $\underline{a}$. If we introduce a tensor of rank two $u^G{}_{ik}$ for displacement, and a tensor of rank three $\tau^G{}_{ijk}$ for stress, then we have the relations

$$u_i^G = u_{ik}^G a_k \tag{A-3}$$

$$\tau_{ij}^G = \tau_{ijk}^G a_k \tag{A-4}$$

The governing equation of the Green's displacement and stress tensors is

$$(\tau_{ijk}^G)_{,j} + \rho\omega^2 u_{ik}^G = -\delta_{ik}\delta(\underline{r}' - \underline{r}) F_o \tag{A-5}$$

where u^G_{ik} is called the Green's displacement tensor which is the i^{th} displacement due to the point load component in the k^{th} direction; τ^G_{ijk} is the Green's stress tensor. The relation between the Green's displacement tensor and the Green's stress tensor is

$$\tau_{ijk}^G = c_{ijlm}(u_{lk}^G)_{,m} \tag{A-6}$$

for an isotropic material, the coefficient c_{ijlm} is constant and given by

$$c_{ijlm} = \lambda\delta_{ij}\delta_{lm} + \mu(\delta_{il}\delta_{jm} + \delta_{im}\delta_{jl}) \tag{A-7}$$

Putting (A-7) into (A-6), we have

$$\tau_{ijk}^G = \lambda\delta_{ij}(u_{rk})_{,r} + \mu[(u_{ik})_{,j} + (u_{jk})_{,i}] \tag{A-8}$$

Equation (A-5) can be solved by application of the Fourier transform with respect to the spatial coordinates. The definition of the Fourier transform is

$$\bar{f}(\underset{\sim}{\xi}) = \iiint_{-\infty}^{\infty} f(\underset{\sim}{x}) \exp(i\underset{\sim}{\xi}.\underset{\sim}{x})\, dx_1 dx_2 dx_3 \tag{A-9}$$

and the Fourier inversion is

$$f(\underset{\sim}{x}) = \frac{1}{(2\pi)^3} \iiint_{-\infty}^{\infty} \bar{f}(\underset{\sim}{\xi}) \exp(-i\underset{\sim}{\xi}.\underset{\sim}{x})\, d\xi_1 d\xi_2 d\xi_3 \tag{A-10}$$

the Fourier transform of the derivative of first order is

$$\bar{f}(\underset{\sim}{x})_{,i} = i\xi_i \bar{f}(\underset{\sim}{\xi}) \tag{A-11}$$

Taking Fourier transforms of the equations (A-5) and (A-6), we have

$$-i\xi_j \bar{\tau}^G_{ijk} + \rho\omega^2 \bar{u}^G_{ik} = -\delta_{ik} \exp(i\underset{\sim}{\xi}.\underset{\sim}{x}) F_o \tag{A-12}$$

and

$$\bar{\tau}^G_{ijk} = c_{ijlm} \bar{u}^G_{mk} (-i\xi_l) \tag{A-13}$$

Putting (A-13) into (A-12), the terms of Green's stress components in the Fourier transform are eliminated. Then we have the following equation

$$c_{ijlm}\xi_i\xi_l\overline{u}^G_{mk}-\rho\omega^2\overline{u}^G_{ik}=\delta_{ik}\exp(i\underline{\xi}.\underline{r})F_0 \tag{A-14}$$

To solve this equation, let us first simplify this equation by multiplying both sides of this equation by a_k. Then we have

$$c_{ijlm}\xi_i\xi_l\overline{u}^G_m-\rho\omega^2\overline{u}^G_i=a_i\exp(i\underline{\xi}.\underline{r})F_0 \tag{A-15}$$

where a_i is the i^{th} component of the unit vector. Introducing

$$\alpha_{im}=c_{ijlm}\xi_i\xi_l-\rho\omega^2\delta_{im} \tag{A-16}$$

with relations

$$u_i=u_m\delta_{im} \tag{A-16}$$

$$a_i=a_k\delta_{ik} \tag{A-17}$$

The equation (A-15) can further be written as a system of linear equations

$$\alpha_{im}\overline{u}^G_m=a_i\exp(i\underline{\xi}.\underline{r})F_0 \tag{A-18}$$

The solutions of this set of the algebra equations are given below (Eason et al, 1956)

$$\overline{u}_i^G = \frac{D_i}{D} \tag{A-19}$$

where

$$D = \begin{vmatrix} \alpha_{11} & \alpha_{12} & \alpha_{13} \\ \alpha_{21} & \alpha_{22} & \alpha_{23} \\ \alpha_{31} & \alpha_{32} & \alpha_{33} \end{vmatrix} \tag{A-20a}$$

$$D_1 = \begin{vmatrix} \overline{F}_1 & \alpha_{12} & \alpha_{13} \\ \overline{F}_2 & \alpha_{22} & \alpha_{23} \\ \overline{F}_3 & \alpha_{32} & \alpha_{33} \end{vmatrix} \tag{A-20b}$$

$$D_2 = \begin{vmatrix} \alpha_{11} & \overline{F}_1 & \alpha_{13} \\ \alpha_{21} & \overline{F}_2 & \alpha_{23} \\ \alpha_{31} & \overline{F}_3 & \alpha_{33} \end{vmatrix} \tag{A-20c}$$

$$D_3 = \begin{vmatrix} \alpha_{11} & \alpha_{12} & \overline{F}_1 \\ \alpha_{21} & \alpha_{22} & \overline{F}_2 \\ \alpha_{31} & \alpha_{32} & \overline{F}_3 \end{vmatrix} \tag{A-20d}$$

$$\overline{F}_i = a_i \exp(i\underline{\xi}.\underline{x}) F_0 \tag{A-21}$$

Finally the solutions of the displacement components, in terms of the Foruier transform, can be obtained from the above equations, and are written in (A-22). A similar procedure for solving the set of the linear equations can be found in work by Tan (1975).

$$\bar{u}_{ik}^{G}=\left(\frac{F_0}{\mu}\right)\left[\frac{\xi_i\xi_k}{k_s^2}\left(\frac{1}{(\xi^2-k_p^2)}-\frac{1}{(\xi^2-k_s^2)}\right)+\frac{\delta_{ik}}{(\xi^2-k_s^2)}\right]\exp(i\underline{\xi}.\underline{r}) \qquad \text{(A-22)}$$

In order to obtain the solutions of the displacement components of the elastic Green's functions, we now need to invert the equation (A-22). From the definition of the Fourier inversion, we have

$$u_{ik}^{G}=\left(\frac{F_0}{\mu}\right)(I_1+I_2+I_3) \qquad \text{(A-23)}$$

where

$$I_1=\frac{1}{(2\pi)^3}\iiint_{-\infty}^{\infty}\frac{\delta_{ik}}{\xi^2-k_s^2}\exp[-i\underline{\xi}.(\underline{r}'-\underline{r})]d\xi_1 d\xi_2 d\xi_3 \qquad \text{(A-24)}$$

$$I_2=\frac{1}{(2\pi)^3}\iiint_{-\infty}^{\infty}\frac{\xi_i\xi_k}{k_s^2}\left(\frac{1}{\xi^2-k_p^2}\right)\exp[-i\underline{\xi}.(\underline{r}'-\underline{r})]\,d\xi_1 d\xi_2 d\xi_3 \qquad \text{(A-25)}$$

$$I_3=\frac{-1}{(2\pi)^3}\iiint_{-\infty}^{\infty}\frac{\xi_i\xi_k}{k_s^2}\left(\frac{1}{\xi^2-k_s^2}\right)\exp[-i\underline{\xi}.(\underline{r}'-\underline{r})]d\xi_1 d\xi_2 d\xi_3 \qquad \text{(A-26)}$$

To carry out these integrals, let us first consider the integral (A-24). The evaluation can conveniently be achieved by a transform to spherical coordinates (ρ, θ, ϕ), where the azimuthal axis is chosen in the direction of ($\underline{r}' - \underline{r}$), and ϕ is the azimuthal angle between $\underline{\xi}$ and azimuthal axis, which is shown in Fig. 112

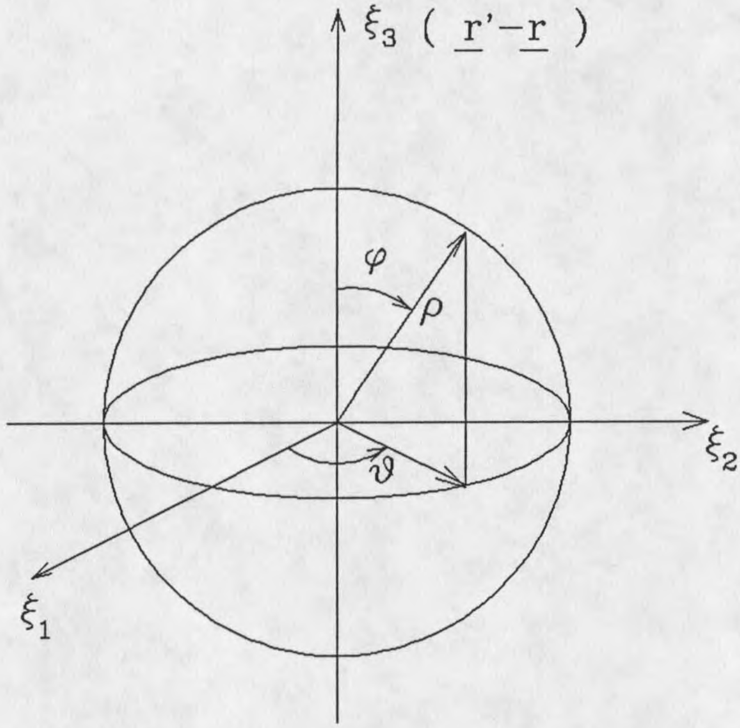

Figure 112. The transform of coordinates

Therefore, after this transform, we have the following relations

$$|\underline{\xi}|=\rho \tag{A-27}$$

$$\xi^2=\rho^2 \tag{A-28}$$

$$\underline{\xi}.(\underline{r}'-\underline{r})=\rho R\cos\phi \tag{A-29}$$

$$d\xi_1 d\xi_2 d\xi_3=\rho^2\sin\phi d\rho d\theta d\phi \tag{A-30}$$

where

$$R^2=(r'_1-r_1)^2+(r'_2-r_2)^2+(r'_3-r_2)^2 \tag{A-31}$$

From this transformation, the integral (A-24) becomes

$$I_1=\frac{\delta_{ik}}{(2\pi)^3}\int_0^\infty\int_0^\pi\int_0^{2\pi}\frac{\rho^2\sin\phi}{\rho^2-k_s^2}\exp(-i\rho R\cos\phi)\,d\rho d\theta d\phi \tag{A-32}$$

It is easy to integrate (A-32) with respect to variables θ and ϕ. This yields

$$I_1=\frac{-i\delta_{ik}}{(2\pi)^2 R}\int_0^\infty\frac{\rho}{\rho^2-k_s^2}(e^{i\rho R}-e^{-i\rho R})d\rho \tag{A-33}$$

For the second term on the right hand side in the integral (A-33), we introduce z=-ρ and dz=-dρ. Since the domain of ρ is 0→∞ , then the domain of z is 0→-∞. After changing the variable and domain, the equation (A-33) becomes

$$I_1=\frac{-i\delta_{ik}}{(2\pi)^2 R}\int_{-\infty}^{\infty}\frac{ze^{izR}}{z^2-k_s^2}dz \tag{A-34}$$

To solve this integral, a contour integration in the upper half domain of the z-plane must be considered (for the details, see Appendix B). This yields the solution of the equation (A-34) as

$$I_1 = \frac{\delta_{ik}}{4\pi R} e^{ik_s R} \tag{A-35}$$

For the integrals I_2 and I_3 in equations (A-25) and (A-26) respectively, we can use a similar procedure or apply the result in (A-35). Also we need to consider the rule that the factor $-i\xi_j$ in the ξ-space corresponds to the partial derivatives in x-space, i.e.

$$-i\xi_j \overline{F}(\xi) = \int \cdot \left\{ \frac{\partial}{\partial x_j} f(x) \right\} \tag{A-36}$$

$$(-i\xi_i)(-i\xi_j) \overline{F}(\xi) = \int \cdot \left\{ \frac{\partial}{\partial x_i} \frac{\partial}{\partial x_j} f(x) \right\} \tag{A-37}$$

This yields

$$I_2 = \frac{-1}{k_s^2} \frac{\partial}{\partial x_i} \frac{\partial}{\partial x_j} \frac{\exp(ik_p R)}{4\pi R} \tag{A-38}$$

$$I_3 = \frac{-1}{k_s^2} \frac{\partial}{\partial x_i} \frac{\partial}{\partial x_k} \frac{\exp(ik_s R)}{4\pi R} \tag{A-39}$$

Putting I_1, I_2, and I_3 together, we obtain the solution of the Green's function of the displacement as:

$$u_{ik}^{G}=\left(\frac{F_o}{\mu}\right)\left\{\delta_{ik}G(k_sR)+\frac{1}{k_s^2}[G(k_sR)-G(k_pR)]_{,ik}\right\} \tag{A-40}$$

where

$$G(k_\alpha R)=\frac{\exp(ik_\alpha R)}{4\pi R} \qquad \alpha= \mathrm{p},\ \mathrm{s} \tag{A-41}$$

Consequently we can calculate the stress tensor from the result in (A-41). Using the following relation between stress and displacement

$$\tau_{ijk}^{G}=\lambda\delta_{ij}(u_{lk}^{G})_{,l}+\mu[(u_{jk}^{G})_{,i}+(u_{ik}^{G})_{,j}] \tag{A-42}$$

and substituting (A-40) into (A-42), we can obtain the solution of the stress tensor as

$$\tau_{ijk}^{G}=F_o\left\{\frac{2}{k_s^2}[G(k_sR)-G(k_pR)]_{,ijk}+\delta_{ik}G(k_sR)_{,j}\right.$$

$$\left.+\delta_{jk}G(k_sR)_{,i}+\delta_{ij}\left(1-\frac{2k_p^2}{k_s^2}\right)G(k_pR)_{,k}\right\} \tag{A-43}$$

APPENDIX B

THE CONTOUR INTEGRATION

Let us consider the integral

$$I_1 = \frac{-i\delta_{ik}}{(2\pi)^2 R}\int_{-\infty}^{\infty}\frac{ze^{izR}}{z^2-k_s^2}dz \tag{B-1}$$

and chose a contour (see Fig. 113)

$$C = C_r \cup (-r, r) \tag{B-2}$$

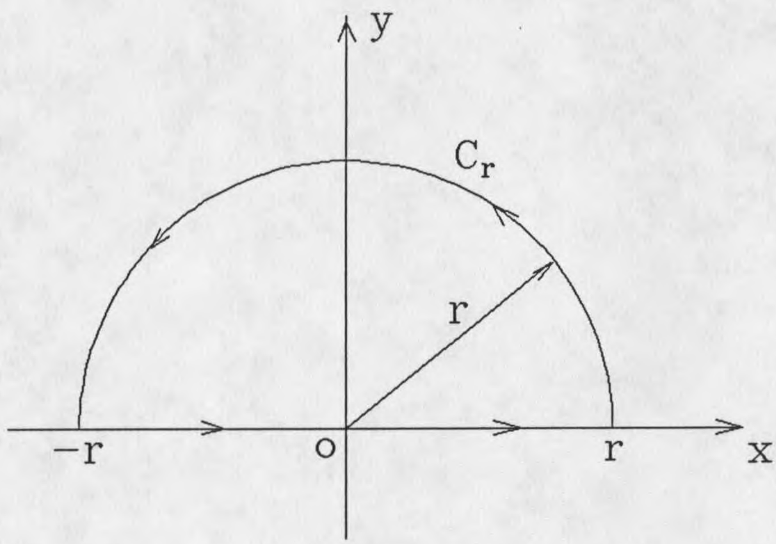

Figure 113. The contour in z-plane

By evaluating Eq. (B-1) on the contour shown in Fig. 113, we have

$$\int_{-\infty}^{\infty}\frac{ze^{izR}}{z^2-k_s^2}dz = \int_C \frac{ze^{izR}}{z^2-K_s^2}dz$$

$$-\lim_{r\to\infty}\int_{C_r}\frac{ze^{izR}}{z^2-k_s^2}dz \tag{B-3}$$

For the first term in Eq. (B-3), we have

$$\int_c \frac{ze^{iRz}}{z^2-k_s^2}dz=\int_c \frac{ze^{iRz}}{(z+k_s)(z-k_s)}dz \tag{B-4}$$

It is clear that in Eq. (B-4) k_s is the only singular point inside C. So we obtain

$$\int_c \frac{ze^{iRz}}{(z+k_s)(z-k_s)}dz=i\pi e^{iRk_s} \tag{B-5}$$

For the second term in Eq. (B-3)

$$\lim_{r\to\infty}\int_{c_r} \frac{ze^{iRz}}{z^2-k_s^2}dz \tag{B-6}$$

let

$$z=re^{i\theta}=r(\cos\theta+i\sin\theta) \tag{B-7}$$

then

$$\left|\int_{c_r} \frac{ze^{iRz}}{z^2-k_s^2}dz\right|\le\int_{c_r}\left|\frac{ze^{iRr(\cos\theta+i\sin\theta)}}{z^2-k_s^2}\right||d(re^{i\theta})| \tag{B-8a}$$

$$\le\int_0^\pi \frac{re^{-irR\sin\theta}}{|z^2|-|k_s^2|}|d(re^{i\theta})| \tag{B-8b}$$

$$=\frac{r}{r^2-k_s^2}\int_0^\pi e^{-rR\sin\theta}|ire^{i\theta}|d\theta \tag{B-8c}$$

$$=\frac{r^2}{r^2-K_s^2}\int_0^{\pi} e^{-rR\sin\theta}d\theta \tag{B-8d}$$

$$=\frac{r^2}{r^2-k_s^2}\left(\int_0^{\frac{\pi}{2}} e^{-rR\sin\theta}d\theta+\int_{\frac{\pi}{2}}^{\pi} e^{-rR\sin\theta}d\theta\right) \tag{B-8e}$$

For the second term in Eq. (B-8e), we set

$$\alpha=\pi-\theta \tag{B-9}$$

then Eq. (B-8e) becomes

$$=\frac{r^2}{r^2-k_s^2}2\int_0^{\frac{\pi}{2}} e^{-rR\sin\theta}d\theta \tag{B-10}$$

With the result:

$$\sin\theta\geq\frac{2\theta}{\pi} \qquad \text{for} \qquad 0\leq\theta\leq\frac{\pi}{2}$$

We can rewrite the Eq. (B-8a) as

$$\left|\int_{C_r}(\ldots)\,dz\right|\leq\int_0^{\frac{\pi}{2}} e^{-rR\frac{2\theta}{\pi}}d\theta \tag{B-11a}$$

$$=\frac{\pi r}{(r^2-k_s^2)R}[1-e^{-rR}] \tag{B-11b}$$

By taking a limit of Eq. (B-11b) we have

$$\lim_{r\to\infty}\left[\frac{\pi r}{(r^2-k_s^2)R}\left(1-e^{-rR}\right)\right]=0 \qquad \text{(B-12)}$$

Therefore

$$\lim_{r\to\infty}\int_{c_r}\frac{ze^{iRz}}{z^2-k_s^2}dz=0 \qquad \text{(B-13)}$$

Finally we obtain the result

$$I_1=\frac{\delta_{ik}}{4\pi R}e^{ik_sR} \qquad \text{(B-14)}$$

APPENDIX C

COMPUTER PROGRAM

Figure 114. Computer program of wave scattering

```
C**********************************************************C
C                                                          C
C        THE PROGRAM OF SOLVING  A TWO-DIMENSIONAL         C
C        WAVE SCATTERING PROBLEM (NUMERICAL METHOD)        C
C                                                          C
C                                                          C
C**********************************************************C
C
C        DESCRIPTION OF THE WAVE SCATTERING PROBLEM
C        ==========================================
C
C        THE  PROBLEM  INVOLVES  WAVE  SCATTERING  AND  WAVE
C     REFRACTING FROM A ROUGH INTERFACE BETWEEN TWO ELASTIC
C     MEDIA (REGION A AND B). AN INCIDENT WAVE PROPAGATES IN
C     REGION A TOWARD THE ROUGH INTERFACE. WHEN THE INCIDENT
C     WAVE REACHES THE ROUGH INTERFACE, TWO SCATTERED WAVES
C     (P-WAVE AND SV-WAVE) WILL GENERATED ON THE INTERFACE
C     AND PROPAGATE IN REGION A, ANTHER TWO REFRACTED WAVES
C     (P-WAVE AND SV-WAVE) WILL GENERATED ON THE INTERFACE
C     AND PROPAGATE  IN  REGION  B.  THIS  PROGRAM  IS  USED  TO
C     CALCULATE THE DISTRIBUTIONS OF THE SCATTERED AND THE
C     REFRACTED FIELDS.
C
C        INVOLVED  NAMES  OF  VARIABLES  AND  CONSTANTS  ARE
C     LISTED IN LIBRARY.
C
C     PROGRAM IS WRITTEN BY HEMIN YANG
C     --------------------------------
C
C     JUNE 1989
C
C***********************************************************
C
C        THE LIBRARY (DESCRIPTIONS OF VARIABLES)
C        ---------------------------------------
C
C     ALPHA --- INCIDENT ANGLE RELATIVE TO LOCAL NORMAL
C     ALFAP  ---  ANGLE  BETWEEN  SCATTERED  P-WAVE  AND  LOCAL
C               NORMAL
C     ALFAS  ---  ANGLE  BETWEEN  SCATTERED  SV-WAVE  AND  LOCAL
C               NORMAL
C     ALFAPB  ---  ANGLE  BETWEEN  REFRACTED  P-WAVE  AND  LOCAL
C                NORMAL
C     ALFASB  ---  ANGLE  BETWEEN  REFRACTED  SV-WAVE  AND  LOCAL
C                NORMAL
C     BETABA --- THE LOCAL NORMAL (IN DEGREE )
C     BBA --- THE LOCAL NORMAL ( IN RADIAN )
C     CP --- WAVE SPEED OF P-WAVE IN REGION A
C     CS --- WAVE SPEED OF SV-WAVE IN REGION A
C     CPB --- WAVE SPEED OF P-WAVE IN REGION B
```

```
C     CSB --- WAVE SPEED OF SV-WAVE IN REGION B
C     E  ---- YOUNG's MODULUS OF THE REGION A
C     EB ---- YOUNG's MODULUS OF THE REGION B
C     F  ---- THE FREQUENCY OF THE INCIDENT WAVE
C     KP --- WAVE NUMBER OF P-WAVE IN REGION A
C     KS --- WAVE NUMBER OF SV-WAVE IN REGION A
C     KPB --- WAVE NUMBER OF P-WAVE IN REGION B
C     KSB --- WAVE NUMBER OF SV-WAVE IN REGION B
C     L1 --- START POINT OF INTEGRATION DOMAIN
C     L2 --- END POINT OF INTEGRATION DOMAIN
C     LMDA --- ELASTIC CONSTANT OF REGION A
C     LMDAB --- ELASTIC CONSTANT OF REGION B
C     NU ---- POISSON RATIO OF THE REGION A
C     NUB --- POISSON RATIO OF THE REGION B
C     MU --- ELASTIC CONSTANT OF REGION A
C     MUB --- ELASTIC CONSTANT OF REGION B
C     ROW --- THE WEIGHT DENSITY OF REGION A
C     ROWB --- THE WEIGHT DENSITY OF REGION B
C     SIGMA --- THE ROUGHNESS OF THE INTERFACE
C     SIGMAG --- THE GRADIENT OF THE INTERFACE
C     W  ---- THE CIRCULAR FREQUENCY
C     ZETAin --- THE INCIDENT ANGLE  ( IN DEGREE )
C     Zin    --- THE INCIDENT ANGLE  ( IN RADIAN )
C     AMin --- AMPLITUDE OF THE INCIDENT WAVE
C     g --- GRAVITY
C============================================================
C
C          DECLARE VARIABLES
C          ----------------

           REAL    NU,NUB,MU,MUB,LMDA,LMDAB,KFA,KFAB,MUT,KFAT
           REAL  KP,KS,KPB,KSB,KT,KTB,LMDA,LAMDAB,LX,L1,L2
           REAL  I1,I3,I11,I33,I13,ICHK1,ICHK2
           REAL  I1B,I3B,I11B,I33B,I13B,LAMDA0
C============================================================
C
C          SET DIMENSIONS
C          -------------
C
C
           DIMENSION        X(20),A(20),F1(20),F3(22),F11(20)
           DIMENSION        F33(20),F13(20),F1B(20),F3B(20)
           DIMENSION  F11B(20),F33B(20),F13B(20)
           DIMENSION  FCHK1(20),FCHK2(20)
C============================================================
C
C          OPEN FILES OF INPUT AND OUTPUT
C          ----------------------------

           CHARACTER*20 NAME1
           CHARACTER*20 NAME2
           CHARACTER*20 NAME3
           CHARACTER*20 NAME4
```

```
      WRITE(*,*)'==== TYPE IN THE NAME OF INPUT FILE ===='
      READ(*,1) NAME1
      WRITE(*,*)'=== TYPE IN THE NAME OF OUTPUT-1 FILE ==='
      READ(*,1) NAME2
      WRITE(*,*)'=== TYPE IN THE NAME OF OUTPUT-2 FILE ==='
      READ(*,1) NAME3
      WRITE(*,*)'=== TYPE IN THE NAME OF OUTPUT-3 FILE ==='
      READ(*,1) NAME4

  1   FORMAT( A20 )

      OPEN(1,FILE=NAME1,STATUS='OLD', FORM='FORMATTED')
      OPEN(2,FILE=NAME2,STATUS='NEW', FORM='FORMATTED')
      OPEN(3,FILE=NAME3,STATUS='NEW', FORM='FORMATTED')
      OPEN(4,FILE=NAME4,STATUS='NEW', FORM='FORMATTED')
C=============================================================
C
C         GET DATA FROM INPUT FILE
C         ------------------------

      N = 15
      DO 10  I =1,N,1
        READ(1,2) X(i),A(i)
 10   CONTINUE
 2    FORMAT(2(E16.9))

C=============================================================
C
C    THE CONSTANTS     ( IN METRIC UNITS [ Kg,mm,Sec ] )
C    ----------------------------------------------------
C
C    1).  INFORMATION ABOUT THE INCIDENT WAVE
C         AND THE INTERFACE
C
      WRITE(*,*)' === PUT IN THE VALUE OF (ZETAin) === '
      WRITE(*,*)'THE INCIDENT ANGLE (ZETAin) CAN BE'
      WRITE(*,*)'CHOSEN AS 0, 10, 20, 30 (DEGREE)'

      READ(*,3) ZETAin
 3    FORMAT(F16.6)

      Zin = ZETAiN*3.141593/180.
C-----------------------------------------------------------
      WRITE(*,*) ' === PUT IN FRENQUENCY (F) ==='
      WRITE(*,*)'THE FREQUENCY (F) USED HERE IS'
      WRITE(*,*)'4E+07, 6E+07, 8E+07, OR 1E+08 (MHz)'

      READ(*,3) F

      W    = 2.*3.141593*F
      AMin = 1.
      g    = 9800.
```

```
C-------------------------------------------------------------
      WRITE(*,*)' === PUT IN VALUE OF (SIGMA) ==='
      WRITE(*,*)'THE AVERAGE VARANCE OF THE ROUGH INTERFACE'
      WRITE(*,*)'INTERFACE (SIGMA) USED HERE IS FROM 0.0 TO
      WRITE(*,*)' 0.315 (mm) ==='

      READ(*,3) SIGMA

      LMDA0 = .65
      SIGMAG= SIGMA/.65

C-------------------------------------------------------------
      WRITE(*,*)'=== PUT IN VALUE OF (L1) and (L2) ==='
      WRITE(*,*)' VALUES OF (L1) and (L2) USED HERE ARE
      WRITE(*,*)' FROM L2=-L1= 5.0  TO  200.0 (mm) ==='

      READ(*,4) L1,L2
  4   FORMAT(2(f8.2))

C-------------------------------------------------------------
C    2). INFORMATION ABOUT MATERIAL PROPERTIES OF THE FIRST
C        REGION (REGION A)
C
C     WRITE(*,*)'=== PUT IN THE VALUE OF (NU) === '
      WRITE(*,*)'THE VALUE OF (NU) IS 0.25 - 0.30 '

      READ(*,3) NU
      WRITE(*,*)'-------------------------------'

      ROW  = .785e-05
      RO   = ROW/g
      E    = .212E+05
      NU   = .2915
      MU   = E/(2.*( 1.+ NU ))
      LMDA = ( E*NU)/( (1.+NU)*(1.-2.*NU))
      CP   = SQRT( (LMDA + 2.*MU )/RO )
      CS   = SQRT( MU/RO )
      KFA  = SQRT( 2.*(1.-NU)/(1.-2.*NU) )
      KP   = W/CP
      KS   = W/CS

C-------------------------------------------------------------
C    3). INFORMATION ABOUT MATERIAL PROPERTIES OF THE SECOND
C        REGION (REGION B)
C
      WRITE(*,*)'=== DO YOU WANT TO CALCULATE THE PRBLEM FOR'
      WRITE(*,*)'ONE MATERIAL OR TWO MATERIALS (TYPE 1 OR 2)'
      WRITE(*,*)'IF YOU WANT ONE TYPE 1, ELSE TYPE 2 ==='

      READ(*,73) IRO12
 73   FORMAT(I2)
```

```
      IF ( IRO12 .EQ. 1 ) THEN
         ROWB = 0.0
      ELSE

         WRITE(*,*)'== PUT IN THE VALUE OF ROEWB =='
         WRITE(*,*)'VALUE OF ROWB IS 0.80E-05 - 0.85E-05 '

         READ(*,3) ROWB

         ROWB = .84E-05
      END IF

      IF ( ROWB .EQ. 0.E+0 ) THEN
         GO TO 11
      END IF

      ROB   = ROWB/g
      EB    = .121E+05
      NUB   = .33325
      MUB   = EB/(2.*( 1. + NUB ) )
      LMDAB= ( EB*NUB )/( (1.+NUB)*(1.-2*NUB) )
      CPB   = SQRT(   ( LMDAB+2.*MUB )/ROB)
      CSB   = SQRT( MUB/ROB )
      KFAB  = SQRT( 2.*(1.-NUB)/(1.-2.*NUB) )
      KPB   = W/CPB
      KSB   = W/CSB

C=============================================================
C
C        PRINT OUT CONSTANTS
C        -------------------
C
      WRITE(*,*)'       E               EB              NU
     $ NUB'
      WRITE(*,5) E,EB,NU,NUB
      WRITE(*,*)'       ROW             ROWB            RO
     $ ROB'
      WRITE(*,5) ROW,ROWB, RO,ROB
      WRITE(*,*)'       MU              MUB             LMDA
     $ LMDAB'
      WRITE(*,5) MU,MUB,LMDA,LMDAB
      WRITE(*,*)'       CP              CPB             CS
     $ CSB'
      WRITE(*,5) CP,CPB,CS,CSB
      WRITE(*,*)'       KFA             KFAB             f
     $ w'
      WRITE(*,5) KFA,KFAB, f, W
      WRITE(*,*) '      KP              KPB             KS
     $ KSB'
      WRITE(*,5) KP,KPB,KS,KSB
    5 FORMAT(1X,4(E12.6,3X)//)
```

```
C=============================================================
C
C          PRINT OUT HEADERS OF RESULTS
C          ----------------------------
C
C       WRITE(*,*)' SIGMAG         < U1 >            < U3 >
C     $ < U1B >             < U3B > '

   11   WRITE(*,*)' ZETAOB       USC-P        CFP       USC-SV
     $ CFS'

C     DO 20 J = 0, 100,25
C       SIGMAG = REAL (J/100.)

C=============================================================
C
C          CALCULATE THE SUB-FUNCTIONS OF THE
C     INCIDENT ANGLE ( ZETAin ) AND THE [ H'(x) ].
C     --------------------------------------------
C

         I1   = 0.0
         I3   = 0.0
         I11  = 0.0
         I33  = 0.0
         I13  = 0.0
         ICHK1= 0.0
         ICHK2= 0.0
         I1B  = 0.0
         I3B  = 0.0
         I11B = 0.0
         I33B = 0.0
         I13B = 0.0

        DEG = 180./3.141593

        DO 30 I = 1,N

        Y = X( I )

        BBA = ATAN( 1.41421*SIGMAG*Y )

        AL   = Zin - BBA
        ALP  = AL
        ALS  = ASIN( (KP/KS)*SIN(AL) )

        B  = ALP - BBA
        G  = ALS - BBA

        BETABA = BBA*DEG
        ALPHA = AL*DEG
        ALFAP = ALP*DEG
```

```
      ALFAS = ALS*DEG

      BETA = B*DEG
      GAMA = G*DEG

      IF (ROWB .EQ. 0.0 ) THEN
        GO TO 22
      END IF
C-------------------------------------
      ALPB = ASIN( (KP/KPB)*SIN(AL) )
      ALSB = ASIN( (KP/KSB)*SIN(AL) )

      BB = ALPB + BBA
      GB = ALSB + BBA

      ALFAPB= ALPB*DEG
      ALFASB= ALSB*DEG

      BETAB = BB*DEG
      GAMAB = GB*DEG

C=======================================================
C
C          CALCULATE ELEMENTS OF MATRIX  [ P1 - W4 ]
C          ---------------------------------------------
C
   22 P1  =  SIN( AL )
      Q1  =  COS( AL )
      V1  =  SIN( 2.*AL )
      W1  =  COS( 2.*ALS )

      P2  = COS( ALS )
      Q2  = SIN( ALS )
      V2  =  KFA*COS( 2.*ALS )
      W2  =  (1./KFA)*SIN( 2.*ALS )

C--------------------------------------------
      IF ( ROWB .EQ. 0.E+0 ) THEN
        D  = V1*W2 + V2*W1
        D1 = V1*W2 - V2*W1
        D2 = 2.*V1*W1
        R11 = D1/D
        R12 = D2/D
        GO TO 33
      END IF
C--------------------------------------------

      P3  = SIN( ALPB )
      Q3  = COS( ALPB )
      V3  = ( MUB/MU )*( CP/CPB )*SIN( 2.*ALPB )
      W3   =  (MUB/MU)*(CP/CPB)*((KFAB*KFAB)/(KFA*KFA))*COS(
```

```
     $ 2.*ALSB )

       P4   = COS( ALSB )
       Q4   = SIN( ALSB )
       V4   = (MUB/MU)*(CP/CSB)*COS( 2.*ALSB )
       W4   = ( 1./(KFA*KFA) )*( MUB/MU )*( CP/CSB )*SIN(
     $ 2.*ALSB )
C============================================================
C
C           CALCULATE REFLECTION AND REFRACTION
C           COEFFICIENTS ( R11, R12, R11B, R12B )
C           ------------------------------------
C
C           R11 = D1/D ,    R12 = D2/D
C           R11B = D3/D ,   R12B = D4/D
C
C-----------------------------------------------------------

       D = P1*(Q2*(V3*W4 + V4*W3)+Q3*(V2*W4 +V4*W2)
     $ +Q4*(V3*W2 - V2*W3)) +P2*(Q1*(V3*W4 + V4*W3)
     $ +Q3*(V4*W1 - V1*W4)+Q4*(V1*W3 + V3*W1))+
     $ P3*(Q1*(V2*W4 + V4*W2)+Q2*(V1*W4 - V4*W1)
     $ +Q4*(V1*W2 + V2*W1))+P4*(Q1*(V2*W3 - V3*W2)
     $ +Q2*(V1*W3 + V3*W1)+Q3*(V1*W2 + V2*W1))

       D1=-(P1*(Q2*(V3*W4+ V4*W3)+Q3*(V2*W4 + V4*W2)
     $ +Q4*(V3*W2 - V2*W3))+P2*(Q1*(-V3*W4- V4*W3)
     $ +Q3*(V1*W4 + V4*W1)+Q4*(V3*W1 - V1*W3))
     $ +P3*(Q1*(-V2*W4- V4*W2)+Q2*(-V1*W4- V4*W1)
     $ +Q4*(V2*W1 - V1*W2))+P4*(Q1*(V3*W2 - V2*W3)
     $ +Q2*(V3*W1 - V1*W3)+Q3*(V2*W1 - V1*W2)))

       D2= 2.*(P1*(Q1*(-V3*W4-V4*W3) + Q3*V1*W4 - Q4*V1*W3 )
     $ +P3*(Q1*V4*W1 + Q4*V1*W1) + P4*(Q3*V1*W1 - Q1*V3*W1))

       D3= 2.*(P1*(Q1*(V2*W4 + V4*W2) + Q2*V1*W4 + Q4*V1*W2)
     $ +P2*(Q1*V4*W1 + Q4*V1*W1) + P4*(Q1*V2*W1 + Q2*V1*W1))

       D4= 2.*(P1*(Q1*(V3*W2 - V2*W3) - Q2*V1*W3 - Q3*V1*W2)
     $ +P2*(Q1*V3*W1 - Q3*V1*W1) + P3*(Q1*V2*W1 + Q2*V1*W1))

       R11 = D1/D
       R12 = D2/D
       R11B= D3/D
       R12B= D4/D


C============================================================
C
C                PRINT OUT THE RESULTS OF THE
C           REFLECTION AND REFRACTION COEFFICIENTS
C           --------------------------------------
```

```
      WRITE(*,*)'  R11             R12              R11B
     $ R12B'
      WRITE(*,6) R11,R12,R11B,R12B
    6 FORMAT(1X, 4(E12.6,3X)/)
      WRITE(4,6) R11, R12, R11B, R12B

C=============================================================
C
C    CALCULATE FUNCTIONS OF ( BETA, GAMA, BETAB, GAMAB )
C    ------------------------------------------------
C

   33 SB   = SIN( B )
      CB   = COS( B )
      SG   = SIN( G )
      CG   = COS( G )

      IF ( ROWB .EQ. 0.0 ) THEN
        GO TO 44
      END IF

C---------------------------
     SBB = SIN( BB )
     CBB = COS( BB )
     SGB = SIN( GB )
     CGB = COS( GB )

C=============================================================
C
C         CALCULATE INTEGRALS FOR THE AVERAGE EVALUATION
C         ---------------------------------------------

  44  F1(I)   =  AMIN*( R11*SB + R12*CG)
      F3(I)   =  AMIN*( R11*CB - R12*SG)

      F11M1   = ( LMDA + 2.*MU )*SIN(Zin)*SB -
     $ LMDA*COS(Zin)*CB

      F11M2   = ( LMDA + 2.*MU )*SIN(Zin)*CG +
     $ LMDA*COS(Zin)*SG

      F11(I) = KP*AMIN*( R11*F11M1 + R12*F11M2 )

      F33(I) = KP*AMIN*( (R11*CB -
     $ R12*SG)*(-COS(Zin))*(LMDA+2.*MU)
     $ + LMDA*(R11*SB+R12*CG)*(SIN(Zin)) )

      F13(I) = KP*AMIN*MU*( (R11*SB+R12*CG)*(-COS(Zin))
     $ +(R11*CB-R12*SG)*(SIN(Zin)) )


      F1B(I) = AMIN*( R11B*SBB - R12B*CGB)
```

```
      F3B(I) = -AMIN*(R11B*CBB + R12B*SGB)
      F11B(I)= KP*AMIN*( R11B*( (LMADB +
     $ 2.*NUB)*SIN(Zin)*SBB +  LMDAB*COS(Zin)*CBB) +
     $ R12B*( LMDAB*COS(Zin)*SGB + ( LMDAB
     $ + 2.*NUB)*SIN(Zin)*SGB ))

      F33B(I)= KP*AMIN*( (LMDAB +
     $ 2.*MUB)*(R11B*CBB+R12B*SGB)*COS(Zin)
     $ + LMDAB*(R11B*SBB-R12B*CGB)*SIN(Zin) )


      F13B(I)= -KP*AMIN*MUB*( (R11B*SBB-R12B*CGB)*COS(Zin)
     $ +(R11B*CBB+R12B*SGB)*SIN(Zin) )

C==========================================================
C
C               PUT IN SOME CHECK FUNCTIONS
C               ---------------------------
C
         FCHK1(I)  =  EXP( Y )
         FCHK2(I)=(SIN( Y*(Y/2. + 1.414213 )))/1.414213

C==========================================================
C
C        CALCULATE THE INTEGRALS USING GAUSSIAN QUADRATURE
C        -------------------------------------------------
C
      I1      = I1 + A(I)*F1(I)
      I3      = I3 + A(I)*F3(I)
      I11     = I11 + A(I)*F11(I)
      I33     = I33 + A(I)*F33(I)
      I13     = I13 + A(I)*F13(I)
      ICHK1   = ICHK1 + A(I)*FCHK1(I)
      ICHK2   = ICHK2 + A(I)*FCHK2(I)
      I1B     = I1B + A(I)*F1B(I)
      I3B     = I3B + A(I)*F3B(I)
      I11B    = I11B + A(I)*F11B(I)
      I33B    = I33B + A(I)*F33B(I)
      I13B    = I13B + A(I)*F13B(I)

   30 CONTINUE

C==========================================================

      WRITE(*,7) N,ICHK1,ICHK2
      WRITE(*,*)'     I1          I3             I11
     $ I33         I13'
      WRITE(*,8) I1,I3,I11,I33,I13
      WRITE(*,*)'     I1B         I3B            I11B
     $ I33B       I13B'
      WRITE(*,30) I1B,I3B,I11B,I33B,I13B
```

```
  8    FORMAT(1X, 5( E12.6,2X)// )
  7    FORMAT( 1X,3HN =,I2,10X,7HICHK1 =, F10.6,5X,7HICHK2
     $ =, F10.6/ )

C-----------------------------------------------------------

       AU1 = I1/1.77245
       AU3 = I3/1.77245

       AU1B = I1B/1.77245
       AU3B = I3B/1.77245

       AT33 = I33/1.77245
       AT13 = I13/1.77245

       AT33B = I33B/1.77245
       AT13B = I13B/1.77245

       WRITE(*,9) SIGMAG,  AU1,AU3,AU1B,AU3B
       WRITE(*,9) SIGMAG,  AT33,AT13,AT33B,AT13B

  9    FORMAT(1X,F7.3,1X, 4(E12.6,2X) )

C-----------------------------------------------------------
C
C  20     CONTINUE

       DO 40 III = 1000,5000,25

       ZETAOB = REAL(III/100.)
       ZOB= ZETAOB*3.141593/180.

       F0 = 1.

       SOB = SIN( ZOB )
       COB = COS( ZOB )

       A11P = (F0*SOB*SOB)/(LMDA + 2.*MU)
       A11S = (F0*COB*COB)/(MU)

       A31P = (F0*SOB*COB)/(LMDA + 2.*MU)
       A31S = -(F0*SOB*COB)/(MU)

       A13P = A31P
       A13S = A31S

       A33P = (F0*COB*COB)/(LNDA + 2.*MU)
       A33S = (F0*SOB*SOB)/(MU)

       KT = (KP*KP)/(KS*KS)

       H131P = F0*KP*(2.*KT*SOB*SOB*COB)
```

```
      H131S = F0*KS*COB*(1.-2.*SOB*SOB)

      H331P = F0*KP*( (1.- 2.*KT) + 2.*KT*COB*COB )*SOB
      H331S = F0*KS*(-2.*SOB*COB*COB)

      H133P = F0*KP*(2.*KT*SOB*COB*COB)
      H133S = F0*KS*(SOB*(1.-2.*COB*COB))

      H333P = F0*KP*( (1.-2.*KT) + 2.*KT*COB*COB)*COB
      H333S = F0*KS*( 2.*COB*SOB*SOB)

      Z1P = H131P*AU1 + H331P*AU3 - A11P*AT13 - A31P*AT33
      Z1S = H131S*AU1 + H331S*AU3 - A11S*AT13 - A31S*AT33

      Z3P = H133P*AU1 + H333P*AU3 - A13P*AT13 - A33P*AT33
      Z3S = H133S*AU1 + H333S*AU3 - A13S*AT13 - A33S*AT33

      Z0P = SQRT( Z1P*Z1P + Z3P*Z3P )
      Z0S = SQRT( Z1S*Z1S + Z3S*Z3S )

      DP = KP*( SIN(Zin) - SOB )
      DS = KP*SIN(Zin) - KS*SOB
      EP = -KP*(COS(Zin) + COB )
      ES = -(KP*COS(Zin) + KS*COB )
C-----------------------------------------
C
      RP = -(SIN(KP*R))/(4.*3.141593*R)
      RS = -(SIN(KS*R))/(4.*3.141593*R)
C
C-----------------------------------------
      EEP = EXP( -(EP*EP*SIGMA*SIGMA)/2. )
      EES = EXP( -(ES*ES*SIGMA*SIGMA)/2. )

      WRITE(*,71) ZETAOB,DP,DS,EP,ES,EEP,EES
 71   FORMAT(1X, F10.4,2X, 6(E10.4,1X) )

      IF ( DP.EQ.0.0 ) THEN
        DLP = 1.
      ELSE
        DLP = ( SIN(DP*L2) - SIN(DP*L1) )/((DP)*(L2 -L1))
      END IF


      IF ( DS.EQ.0.0 ) THEN
         DLS = 1.
      ELSE
        DLS = ( SIN(DS*L2) - SIN(DS*L1) )/((DS)*(L2 -L1))
      END IF

      USC1P = EEP*Z1P*DLP
      USC1S = EES*Z1S*DLS
      USC1  = USC1P + USC1S
```

```
      USC3P = EEP*Z3P*DLP
      USC3S = EES*Z3S*DLS
      USC3  = USC3P + USC3S

      USCP = SQRT( USC1P*USC1P + USC3P*USC3P )
      USCS = SQRT( USC1S*USC1S + USC3S*USC3S )

C=============================================================

      IF ( IR012 .EQ. 1 ) THEN

         IF ( ZETAin .EQ. 30.0 ) THEN
              CFP = USCP/.169335E+02
              CFS = USCS/.355396E+02
         END IF

         IF ( ZETAin .EQ. 20.0 ) THEN
              CFP = USCP/.228258E+02
              CFS = USCS/.270755E+02
         END IF

         IF ( ZETAin .EQ. 10.0 ) THEN
              CFP = USCP/.271497E+02
              CFS = USCS/.146289E+02
         END IF

         IF ( ZETAin .EQ. 0.0 ) THEN
              CFP = USCP/.287402E+02
              CFS = USCS/1.
         END IF

    ELSE

         IF ( ZETAin .EQ. 30.0 ) THEN
              CFP = USCP/.134335E+01
              CFS = USCS/.362625E+01
         END IF

         IF ( ZETAin .EQ. 20.0 ) THEN
              CFP = USCP/.193707E+01
              CFS = USCS/.299422E+01
         END IF

         IF ( ZETAin .EQ. 10.0 ) THEN
              CFP = USCP/.241319E+01
              CFS = USCS/.168716E+01
         END IF

         IF ( ZETAin .EQ. 0.0 ) THEN
              CFP = USCP/.259521E+01
              CFS = USCS/1.
```

```
            END IF

        END IF

C==================================================================
        WRITE(*,91) ZETAOB,USCP,CFP,USCS,CFS
  91    FORMAT(1X,F8.2,2X,4(E12.6,2X) )

        WRITE(2,81) ZETAOB,CFP
        WRITE(3,81) ZETAOB,CFS

  81    FORMAT(1X, F8.2,2X, E12.6 )

  40    CONTINUE


        CLOSE(1)
        CLOSE(2)
        CLOSE(3)
        CLOSE(4)

        END
```